

UC Davis

UC Davis Electronic Theses and Dissertations

Title

Stereocontrol in the Crotylation of Imine and Allylations of Sulfonimidamides

Permalink

<https://escholarship.org/uc/item/4fp4p8tt>

Author

Gutierrez, David Alan

Publication Date

2023

Peer reviewed|Thesis/dissertation

Stereocontrol in the Crotylation of Imine and Allylations of Sulfonimidamides

By

DAVID ALAN GUTIERREZ

Dissertation

Submitted in partial satisfaction of the requirements for the degree of

DOCTOR OF PHILOSOPHY

in

Chemistry

in the

OFFICE OF GRADUATE STUDIES

of the

UNIVERSITY OF CALIFORNIA

DAVIS

Approved:

Jared T. Shaw, Chair

David Olson

Peter Beal

Committee in Charge

2023

Dedication

To my Mom, Dad, and Queenie.

“Great things are expected from me”

Our deepest fear is not that we are inadequate.
Our deepest fear is that we are powerful beyond measure.

It is our light not our darkness that most frightens us.

We ask ourselves, who am I to be brilliant, gorgeous,
talented and fabulous?

Actually, who are you not to be?

Marianne Williamson

ACKNOWLEDGEMENTS

JTS: Thank you for giving me the chance to do research in your group. A last minute email from you changed my entire trajectory of coming to UC Davis for school. A true Sliding Doors moment. You have pushed me to achieve new heights I never dreamed possible when I started, you gave me the tools to problem solve, be creative, to generate novel chemical ideas and to never hesitate to have a scientific discussion with me. You challenged my thoughts and pushed me to be a better chemist. I will always look back and appreciate the mentorship you gave me.

CRP: Giving me the chance to be the head TA of your first 231A class was an amazing experience. I appreciate every impromptu conversation in the hallway or suddenly stopping by your office.

SWL: Thank you for letting me rotate with you before you graduated. You helped me understand what I needed to do to be successful in JTS lab. I also learned what it meant to be a chemdraw wizard.

LCM: Our time overlapped briefly, and it was an amazing the leadership you exuded in the lab. The leadership qualities are skills I took to heart and tried to pass that down to younger scientists.

CAD: Thank you for helping me get started in the lab. I will never forget you looking over my shoulder in lab and seeing me working and shaking your head. You helped me develop my skills at the fume hood.

AL: Thank you for being a great friend. I respect your ability to have no fear in seminar to ask questions. Your chemical curiosity and initiative challenged me to think deeply about my own science.

NYH: Thank you for being a good lab mate and a better friend. You are someone I can talk to on a whim and feel like time never passed. You taught me so much about organization and paperwork. Thank you, the second-best listener in 378.

BDB: Thank you for being there on recruitment. Having burritos at 12 am really swayed my decision. Riding bikes to coffee or talking with you in the lab was always a joy. Thank you for being a great representative for the group.

JS: You are one of the best chemists I have ever met. If a reaction is not 95% yield, then it low yielding. More importantly you are a good friend. I am lucky to have been in the same class as you. I know you will be successful in your career. I look forward to staying connected and going on snowboarding trips.

WLC: Thank you for being a good friend during graduate school. I cherish the time we spent together climbing diablo and going to Whiskey Wednesday or just hanging out watching movies.

SND: You are the hardest working person I know. Thank you for pushing me to be a better chemist

JMR: You are a fantastic chemist and a great mentor of students. Connecting with you about Los Angeles, sports and Mexico was always a joy.

AH: I will always be grateful you joined our group. Hanging out in 303 taking the time to talk about chemistry or snowboarding or food was always fun. Keep in touch and the next time I go to Mexico I will get tequila that the custodians cannot steal.

GTW: I am so thankful to the hard work, determination, organization, and perseverance you have brought to the group. You have grown as a scientist and a leader in the group. More importantly you have been a great friend. Your friendship made lab fun. Late pizza nights to early chocolate milk runs will be memories I will have forever. Spending a week in NYC was the grad school trip of a lifetime. Finishing the NSF grant win no sleep and powered by gin and tonics in the New Jersey bar will always be an amazing memory. You have so much ability and talent. Your attention to detail, organization, selflessness and curiosity are all traits that highlight a great chemist, and you exude all of them. I know you will have success in your scientific journey and look forward to continuing our friendship in this new chapter of life.

MWD: The fastest in person in 381. I know you will make great contributions to the lab, with your small army of undergrads. Thank you for all the workplace banter.

YRO: Working with you in 378 has been a real joy. Mentoring you in the lab has been a rewarding experience. You are a lot of fun to spend time with. I will miss going to lunch and occasionally seeing you at the local breweries.

DRT: Your ability to understand chemistry is outstanding. You have so much potential to become a leader in the field of organic chemistry. Study and work hard I believe in your abilities as a scientist and a chemist.

MS: Your drive in total synthesis and understanding reactions gives you the ability to have significant contributions to the field of chemistry. I look forward to reading about your future work in the field.

LU: You have great hands in the laboratory and a great mind for organic chemistry. I enjoyed the time you rotated with me. I know you will be successful in your journey through chemistry.

Whiskey: My little boy, I know you can't read, but you still had so many good ideas on our walks. You gave me the joy in my work life balance.

Queenie Lin: You have been through my educational journey every since the day I finished my MS at USF. Your kindness, thoughtfulness, care and love has made this 5 year PhD journey possible. You uplifted my spirit in every conversation, every facetime and every IG meme. Our time together was finally a time I could stop "thinking about chemistry". Each fall snowboarding, every bike ride to winters, each weekend at the farmers market made this five year journey feel short. Thank you for always being uplifting, warm energy in my life. <°)))>< <3.

Arnold J. Gutierrez & Esther M. Gutierrez: To my parents who always believed I could achieve my dream of earning my Ph.D. The both of you have supported me through every low and every high on this journey. You supported me on my adventure to Rahway and as I start my new career in industrial chemistry. Every day I count my blessing that you are my mom and dad.

Stereocontrol in the Allylation of Imines and Sulfonimidamides

ABSTRACT OF DISSERTATION

The allylation reaction is an ambiphilic reaction depending on the nature of the allylic substituent. Depending on the allylic substituent the allyl can either be nucleophilic or electrophilic. This dissertation describes the nucleophilic crotylation of α -chiral alkoxy imines in high diastereoselectivity and the electrophilic enantioselective allylation of a prochiral heterocyclic sulfonimidamide in high enantioselectivity and yield. Chapter 1 describes the Lewis acid promoted addition of prochiral *E* and *Z* allyl nucleophiles to chiral α -alkoxy *N*-tosyl imines is described. Alkene geometry is selectively transferred to the newly formed carbon-carbon bond, resulting in stereochemical control of carbons 2 and 3, resulting in 2-alkoxy-3-*N*-tosyl-4-alkyl-5-hexene products. A computational analysis to elucidate the high selectivity is also presented. This methodology was employed in the synthesis of two naturally occurring isomers of clausenamide. Chapter 2 describes the enantioselective allylation of prochiral sulfonimidamides via a Tsuji-Trost Asymmetric Allylation reaction. Sulfonimidamides undergo prototropic tautomerization in solution. In the case where both nitrogen substituents of a disubstituted sulfonimidamide are the same, the two tautomers are also enantiomers, allowing deprotonation to generate a prochiral anion. Herein we report the first transition metal catalyzed approach to the desymmetrization of sulfonimidamides relying on commercially available palladium catalysts and ligands. The reaction leads to functionalized, enantioenriched products in high yields.

Table of Contents

1 Chapter 1: Diastereoselective Addition of Prochiral Nucleophilic Alkenes to α-Chiral <i>N</i>-Sulfonyl Imines and the Total Synthesis of (+)Cis-epi and (+)Epi-Clausenamide	1
1.1 Introduction	1
1.1.1 Overview of Closed Transition States in Nucleophilic Additions of Crotyl Boron Reagents to Aldehydes and Imines	3
1.1.2 Overview of Open Transition States in Nucleophilic Additions of Crotyl Silane Reagents to Aldehydes and Imines	14
1.1.3 Acyclic Stereocontrol of α -Chiral Imines	32
1.1.4 Overview of Completed Syntheses of Clausenamide and Epimers of Clausenamide.	39
1.1.5 Bioactivity of clausenamide	50
1.2 Acyclic Stereocontrol of α-Chiral <i>N</i>-Sulfonyl Imines with Prochiral BF₃K and Crotyl Trimethyl Silane Nucleophiles.....	51
1.2.1 Nucleophilic Addition of <i>E</i> and <i>Z</i> Crotyl BF ₃ K Nucleophilic Alkenes to α -Chiral <i>N</i> -Sulfonyl Imines.....	52
1.2.2 Results Nucleophilic Addition of <i>E</i> and <i>Z</i> Crotyl Trimethyl Silane Nucleophilic Alkenes to α -Chiral <i>N</i> -Sulfonyl Imines	57
1.3 Total Synthesis of (+)cis-epi and (+)epi-clausenamide	64

1.3.1	Retrosynthetic analysis of (+)clausenamide (+) <i>cis-epi</i> and (+) <i>epi</i> clausenamide	64
1.3.2	Preliminary Synthesis of (+)clausenamide.....	65
1.3.3	Forward synthesis of (+) <i>cis-epi</i> -clausenamide	66
1.4	Conclusion.....	68
1.5	Experimental Section.....	69
1.5.1	Materials and Instrumentation.	69
1.5.2	General Procedure A 1 mmol scale representative example	70
1.5.3	General Procedure B 1mmol scale representative example	71
1.5.4	Preparation of Imines.....	72
1.5.5	Representative Procedures for synthesis of (<i>E</i>)-BF ₃ K nucleophiles.....	83
1.5.6	Representative Procedures for synthesis of <i>Z</i> -BF ₃ K nucleophiles	84
1.5.7	Representative procedure for synthesis of (<i>E</i>)-trimethylsilane nucleophiles 88	
1.5.8	Representative procedure for synthesis of (<i>Z</i>)-trimethylsilane nucleophiles 90	
1.5.9	Representative procedure for synthesis of cyclic silane nucleophiles	91
1.5.10	Characterization Data for Isolated Compounds.....	94
1.6	References.....	123
2	Chapter 2: Enantioselective Desymmetrization of Sulfonimidamide (SIAs) Heterocycles via Tsuji-Trost-Asymmetric-Allylation	133

2.1	Introduction	133
2.1.1	Overview of Sulfonimidamides in Medicinal Chemistry	135
2.1.2	Overview of Enantioselective Syntheses of Sulfonimidamides	138
2.1.3	Overview of Enantioselective Tsuji Trost Asymmetric Allylation.....	142
2.2	Development of Enantioselective Desymmetrization of Heterocyclic Sulfonimidamides (SIAs) Methodology	146
2.2.1	High Throughput Experimentation Results	152
2.2.2	Electrophile Substrate Scope	157
2.2.3	Heterocyclic Sulfonimidamide Substrate Scope	159
2.2.4	Stereochemical model for Enantioselectivity	163
2.2.5	Functionalization Reactions of Enantioenriched Sulfonimidamides	164
2.3	Conclusion.....	167
2.4	Experimental Section.....	168
2.4.1	Materials and Instrumentation.	168
2.4.2	Synthesis of thiadiazepine Sulfonimidamides.....	168
2.4.3	Hydrogenation of 37 to yield S3.....	172
2.4.4	Synthesis of Dimethyl Acetonide SIA's.....	173
2.4.5	Synthesis of 5 and 6 membered -thiadiazine 1-oxides	176
2.4.6	Synthesis of 2-allyl Substituted Carbonates	179
2.4.7	General Procedure of Tsuji-Trost Asymmetric Allylation	189
2.4.8	High Throughput screening	211
2.5	References.....	215

1 Chapter 1: Diastereoselective Addition of Prochiral Nucleophilic Alkenes to α -Chiral *N*-Sulfonyl Imines and the Total Synthesis of (+)*Cis-epi* and (+)*Epi*-Clausenamide

1.1 Introduction

Acyclic stereocontrol of carbon-carbon bond forming reactions is a longstanding challenge in organic synthesis. The nucleophilic addition of prochiral allylic nucleophiles to α -chiral sp^2 electrophiles creates a C-C bond under mild conditions and produces two new stereogenic centers. While the crotylation of α -heteroatom-substituted electrophiles, particularly α -alkoxy aldehydes, has been studied extensively,¹ the crotylation and related nucleophilic additions to α -alkoxy imines yielding 1,2-amino alcohols are under explored.

Recently our group demonstrated a highly diastereoselective allylation of α -alkoxy *N*-tosyl imines producing either C1-C2 *anti* or *syn* homoallylic amino alcohols, by varying the reaction conditions.² Allyl BF_3K with $BF_3 \cdot OEt_2$ as a Lewis acid affords *anti* diastereoselectivity **2** and $ZnBr_2$, as Lewis acid, and allyl trimethylsilanes selectively afford *syn* products **3** (**Figure 1.1**). The diastereoselective allylation was rationalized via a polar Felkin Anh or a Cram chelate transition state. The two stereoelectronic models rationalize the observed stereoselectivity.

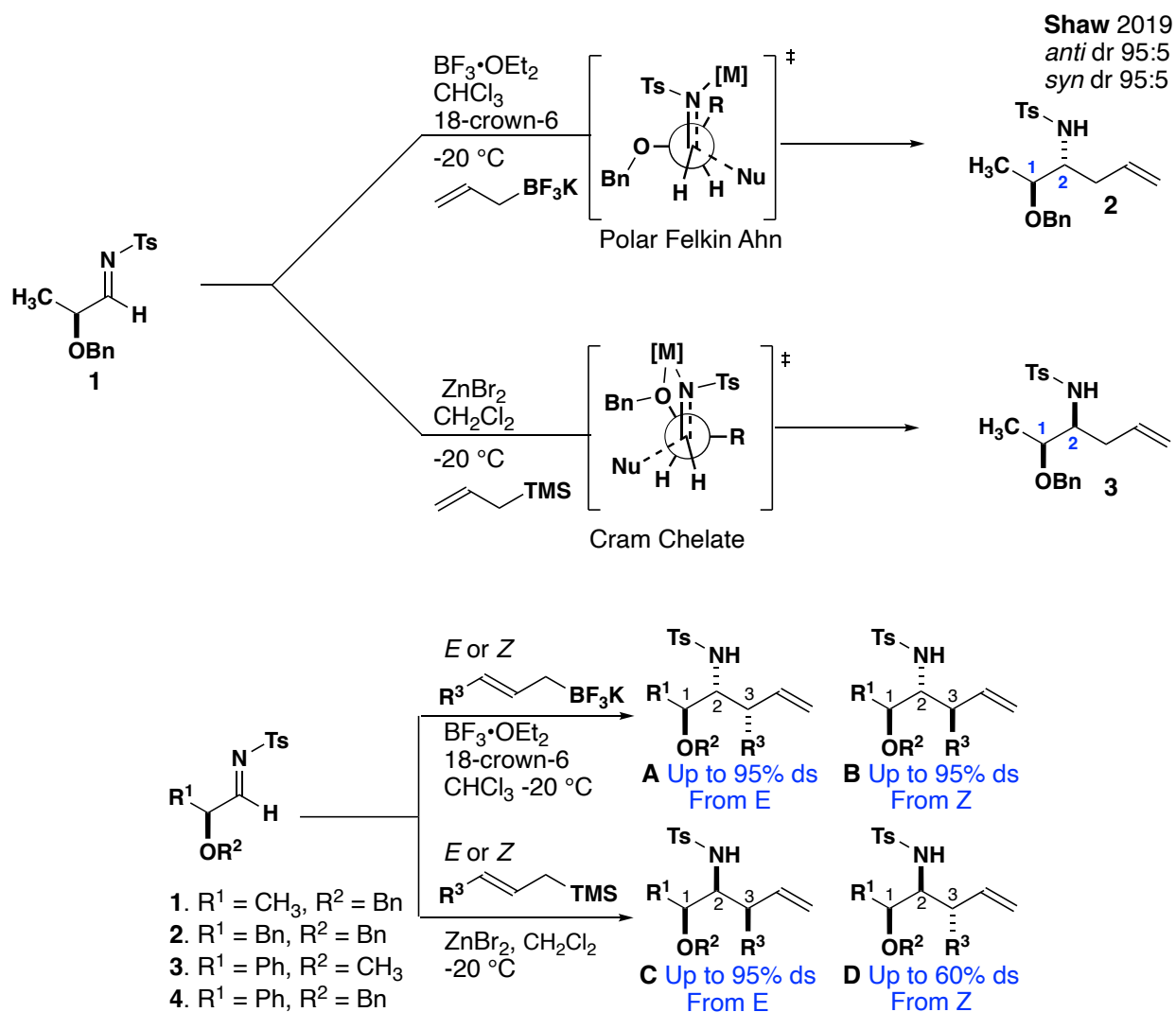


Figure 1.1 Diastereoselective allylation of α -chiral *N*-sulfonyl imines, and crotylation of α -chiral *N*-sulfonyl imines.

This chapter will describe the diastereoselective crotylation of α -alkoxy *N*-sulfonyl imines, where acyclic stereocontrol of C2 and C3 is achieved in a single step.³ The formation of two new stereogenic centers from the prochiral face of the nucleophilic alkene and the prochiral face of the imine means that a completely unselective reaction can yield four different diastereomeric products. A different stereochemical analysis of the transition state is needed to rationalize the observed diastereoselectivity of a nucleophilic crotylation reaction of an aldehyde or imine.

When analyzing the crotylation reaction of α -chiral alkoxy *N*-tosyl imines with crotyl-BF₃K and crotyl-TMS, it is imperative to understand the mechanism of how these crotyl nucleophiles react. A stereochemical analysis and mechanistic overview of crotyl BF₃K, and crotyl TMS reactions with carbonyl is provided. The unique mechanism used by these nucleophilic crotyl reagents gives an understanding for the diastereoselectivity observed in the crotylation of α -alkoxy *N*-tosyl imines. Transition states for the crotylation of α -alkoxy *N*-tosyl imines with crotyl-BF₃K and crotyl-TMS have been located and analyzed with density functional theory (B3LYP-D3/6-31G(d)) to explain the observed diastereoselectivity based on the mechanistic profiles of crotyl BF₃K and crotyl TMS. The stereocontrolled reaction was employed in a divergent synthesis of two epimers of clausenamide: (+)*epi*-clausenamide and, (+)*cis-epi*-clausenamide the latter of which has not previously been synthesized.

1.1.1 Overview of Closed Transition States in Nucleophilic Additions of Crotyl Boron Reagents to Aldehydes and Imines

Reactions of nucleophilic alkenes to aldehydes or imines can be categorized into two types. Type 1 is a rigid Zimmerman-Traxler chair like transition state structure, **5**.⁴ This is common for allyl boron, aluminum, and SnCl₃ nucleophiles (**Figure 1.2**). Type 2 transition states are open and can be best represented as reacting through a Newman projection (See section 1.1.2).⁵ This section of the overview will only focus on the crotyl boron reagents because the work embodied is focused on crotyl BF₃K.

Type 1: Rigid chair like transition state structure

-Boron, Aluminum, Stannanes

-dr reflects *E/Z* ratio of starting allyl metal

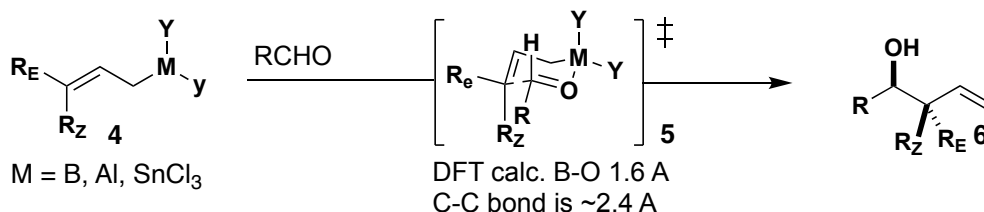


Figure 1.2 Closed Zimmerman-Traxler chair like transition state in the crotylation of aldehydes.

In Type 1 reactions the diastereoselective ratio (dr) is a direct reflection of the *E/Z* ratio of the starting allyl/crotyl metal. The high diastereoselectivity was first recognized by Hoffman and Zeiss (**Figure 1.3**).⁶ They observed the crotylation various aldehydes using crotyl pinacol borane yielded diastereomeric ratios nearly identical to the *E/Z* ratio of the starting nucleophile, **7** and **8**, respectively.

Diastereospecificity recognized by Hoffmann and Zeiss

Chair like transition state determines diastereoselectivity



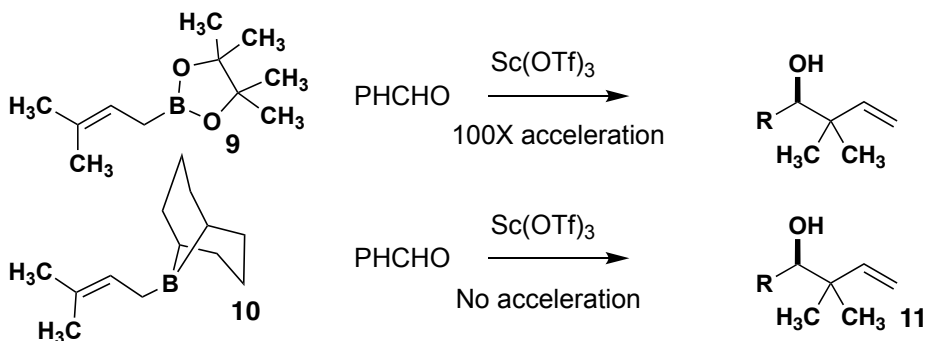
Figure 1.3: Observation by Hoffman and Zeiss that *E/Z* ratio is a direct reflection of the diastereomeric ratio of products.

A critical observation is the role of Lewis acids in the reactions of crotyl boranes. Allylic boron reagents are themselves self-activating; in that the empty p orbital of the boron is a Lewis acid site and accepts the lone pair of the reacting aldehyde or imine

(Figure 1.4). Thus, the addition of a Lewis acid to a crotylation reaction can potentially compete with carbonyl lone pairs and change the mechanism from Type 1 to Type 2 (see section 1.1.2 more information).⁵ However, allyl boronic esters in particular show an increased rate acceleration in comparison to allyl boranes.⁷⁻¹¹ This effect is probably due to the Lewis acid coordinated to the boronate oxygen and disrupting the donating effect of the oxygen lone pair to the empty p orbital of the borone **12**. Thus making the empty p orbital of the boron more electron deficient.⁴

Lewis Acid Promoted Reaction

- Allylic boron reagents are self activating
- Lewis acid can potentially compete with carbonyl, switching mechanism to Type 2
- Boronates are effectively catalyzed by LA



Coordination of the Lewis Acid to boronate and disrupts mesomeric effect making pi orbital more electron deficient

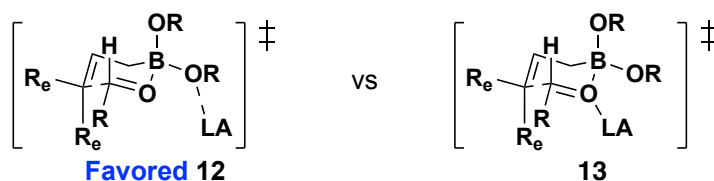


Figure 1.4: Lewis acid rate increase of boronic esters compared to boranes and favor coordination to boronic ester oxygen rather than Lewis basic aldehyde.

The general reactivity of crotyl boranes depends on the electrophilicity of the boron (Figure 1.5). Disrupting the electron donating ability increases the reactivity of crotyl boranes.¹² In general the reactivity trend for allylic boranes is: alkyl boranes reacting the

fastest as they have no resonance effect on the empty p orbital, and N -sulfonyl boronic amides reacting significantly faster than the corresponding boronic esters.¹² In general (E)-crotyl boronates react faster than (Z)-crotyl boronates.¹³

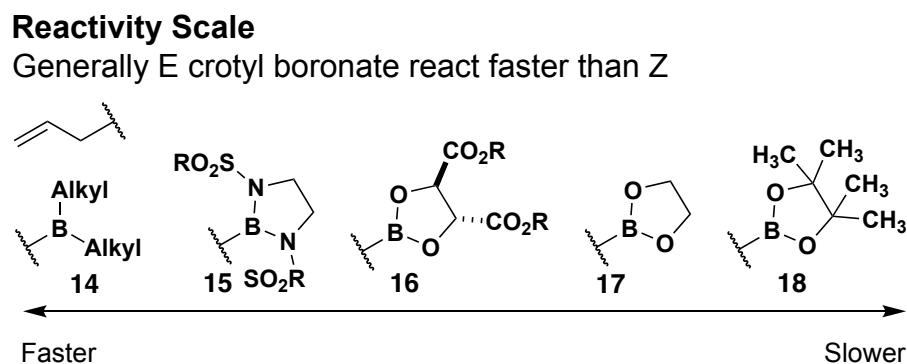


Figure 1.5: Reactivity scale for various allyl boron reagents.

A relatively new reagent that has been developed is the potassium allyl and crotyl trifluoroborates (BF_3K).¹⁴ The use of BF_3K as a boron reagent has been popularized by Molander.¹⁵ The crotyl BF_3K compounds combine bench stability with reactivity. Typically, (Z)-crotyl pinacol boranes are prone to Z to E alkene isomerization and need to be stored in cryogenic storage conditions and away from light.⁴ However, it has been demonstrated that (Z)-crotyl BF_3K shows no alkene isomerization, even at room temperature on the bench top.¹⁶ The crotyl BF_3K nucleophiles are also bench stable solids that can be easily weighed out, opposed to oils and other viscous liquids. However, because the crotyl BF_3K has no empty p orbital the reagent needs to be activated by a Lewis acid. Studies have demonstrated that the Lewis acid, abstracts a fluoride generating a highly electrophilic boron difluoride which can then self-activate the aldehyde or imine for allylation or crotylation (**Figure 1.6**).¹⁶

Trifluoroborate Salts

- Combine stability and reactivity
- No *Z* to *E* isomerization
- Reagent needs to be activated by LA

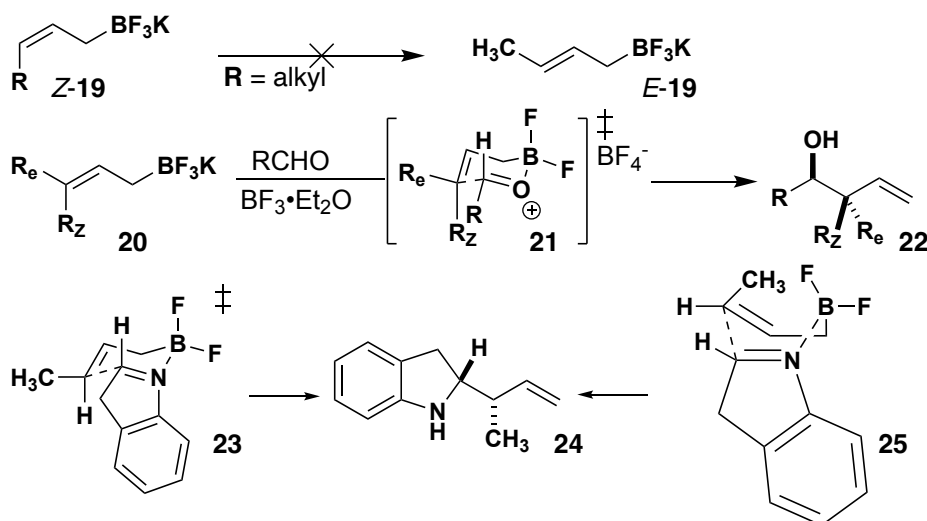


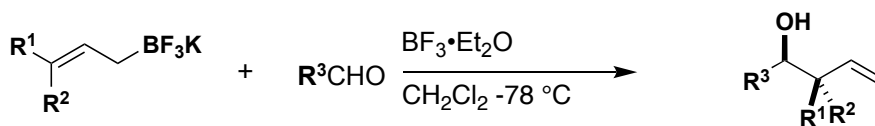
Figure 1.6: Generality of crotyl trifluoroboroate salts

1.1.1.1 Stereochemical Analysis of Nucleophilic Additions of Crotyl BF₃K Reagents to Aldehydes.

The allylation and crotylation of BF₃K nucleophiles was first reported in 1999. The reagent reacts rapidly with aldehydes using BF₃·OEt₂ as a Lewis acid (**Table 1.1**).¹⁴ The reaction is highly diastereoselective and high yielding. The high diastereoselectivity based on the geometry of the nucleophilic alkene inferred a closed Type 1 transition state.

The optimized reaction demonstrated that 2 equivalents of BF₃·OEt₂ were needed, and the reaction proceeded in 15 minutes at -78 °C. The crotylation reaction was also high yielding using 1 mol% of BF₃·OEt₂ albeit with slower reaction rates, requiring 3 hours at room temperature. In the absence of any Lewis acid no reaction occurred. The crotylation reaction with (*Z*)-crotyl BF₃K gave high selectivity to the *syn* diastereomer. While reaction with (*E*)-crotyl BF₃K gave the *anti* diastereomer. These initial results

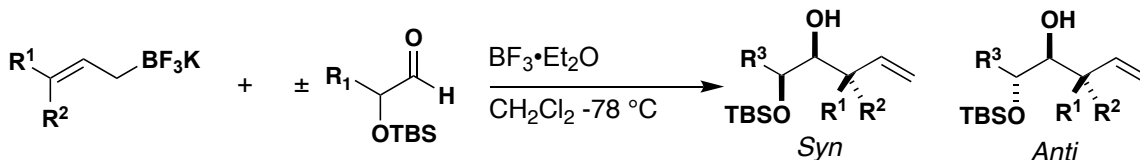
highlighted the possibility of an allylboron difluoride intermediate. Which could be generated by removal of a fluoride from the trifluoroborate by the $\text{BF}_3 \cdot \text{OEt}_2$ Lewis acid, which could then react in a Type 1 closed Zimmerman-Traxler like transition state.



Entry	R ¹	R ²	R ³	dr	Yield (%)
1	CH ₃	H	<i>n</i> -C ₇ H ₁₅	>98:2	74
2	CH ₃	H	Ph	>98:2	91
3	CH ₃	H	4-CH ₃ OC ₆ H ₄	96:4	91
4	CH ₃	H	4-O ₂ NC ₆ H ₄	>98:2	95
5	H	CH ₃	<i>n</i> -C ₇ H ₁₅	>98:2	84
6	H	CH ₃	Ph	>98:2	94
7	H	CH ₃	4-CH ₃ OC ₆ H ₄	97:3	91
8	H	CH ₃	4-O ₂ NC ₆ H ₄	>98:2	96

Table 1.1: First report using crotyl BF_3K nucleophilic alkenes.

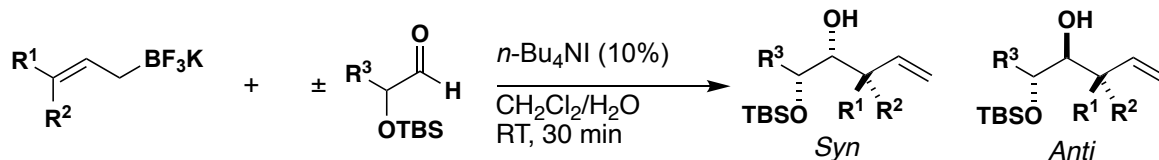
A follow up paper in 2000 demonstrated that the optimized conditions could crotylate α -chiral-siloxy aldehydes in high diastereoselectivity for the *anti* diastereomer in most cases (**Table 1.2**).¹⁷ It is noteworthy that the diastereoselectivity improves when R¹ is CH₃.



Entry	R ¹	R ²	R ³	dr	Yield (%)
1	H	H	CH ₃	30:70	69
2	H	H	Ph	35:65	91
3	CH ₃	H	CH ₃	5:95	73
4	CH ₃	H	Ph	10:90	85
5	H	CH ₃	CH ₃	75:25	72
6	H	CH ₃	Ph	10:90	82

Table 1.2: Crotylation of α -chiral-siloxy aldehydes with crotyl BF_3K nucleophiles

Biphasic reaction conditions were developed to crotylate α -chiral-siloxy aldehydes, which does not rely on $\text{BF}_3 \cdot \text{OEt}_2$ to abstract fluoride (**Table 1.3**).¹⁸ The conditions utilize tetrabutylammonium iodide (TBAI) to metathesize a fluoride ion to activate the crotyl BF_3K . The report also gave a detailed stereochemical analysis for the observed *anti* diastereoselectivity observed when using (*E*)-crotyl BF_3K .



Entry	R ¹	R ²	R ³	dr	Yield (%)
1	H	H	CH ₃	30:70	95
2	H	H	Ph	35:65	94
3	CH ₃	H	CH ₃	5:95	95
4	CH ₃	H	Ph	10:90	97
5	H	CH ₃	CH ₃	75:25	95
6	H	CH ₃	Ph	10:90	99

Table 1.3: Crotylation of α -chiral-siloxy aldehydes using TBAI

The least sterically hindered transition states accessible in reactions with (*Z*) and (*E*)-crotylboron reagents, respectively. In both **TS-4** and **TS-5** the dipole of the polar oxygen atom are anti to each other, commonly referred to as dipole disaligned also known as a Cornforth transition state (**Figure 1.7**).¹⁹ **TS-4**, lacks any significant nonbonded interactions involving the methyl group of the (*Z*)-crotyltrifluoroborate and is presumably the lowest energy transition state structure available, leading to 1,2-*anti*-2,3-*syn* **26a** as the major product.²⁰ **TS-5** experiences the fewest non-bonded (*gauche* pentane) interactions for the reaction of potassium (*E*)-crotyltrifluoroborate leading to product **26b**. **TS-6**, on the other hand, is expected to benefit from favorable Polar Felkin Anh stereoelectronic activation. The subtle differences between **TS-5** and **TS-6** perhaps may rationalize the only modest 2,3-*syn* diastereoselectivity obtained for the reaction of potassium (*E*)-crotyltrifluoroborate with α -silyloxyaldehyde (R³=CH₃)

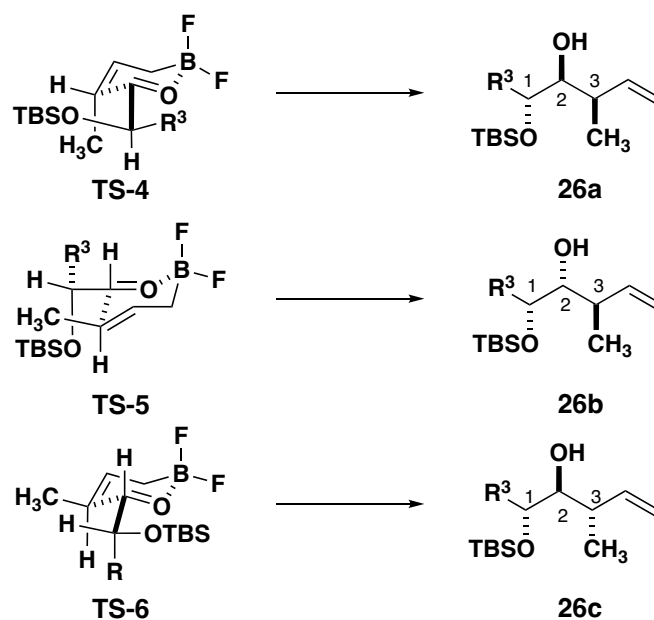


Figure 1.7: Transition states for the crotylation α -chiral-siloxy aldehydes

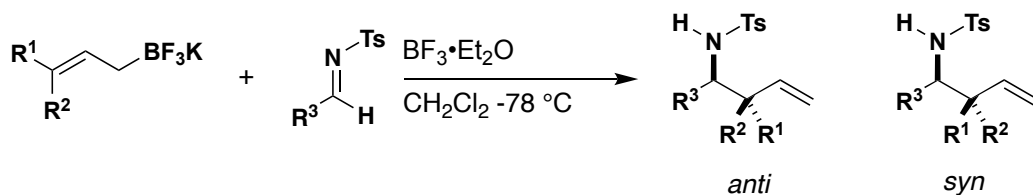
An NMR experiment was conducted using the biphasic reaction conditions to elucidate the possibility of a boron difluoride intermediate over the course of the reaction. A solution of $\text{CDCl}_3/\text{D}_2\text{O}$ with (*E*)-crotyl BF_3K showed a disappearance of signals at ^{11}B NMR (δ 4.68, q, J) 60.0 Hz) and ^{19}F NMR (δ -138.1, q, J) 60.0 Hz) as soon as TBAI was added to the mixture. In the organic layer, ^{19}F NMR showed the appearance and subsequent disappearance of both allyltrifluoroborate anion and deuterioxytrifluoroborate anion (DOBF_3^-) as the reaction proceeded. At the end of the reaction, new signals corresponding to potassium deuterioxytrifluoroborate ($\text{K}^+\text{BF}_3\text{OD}^-$) were evident in both the ^{11}B NMR (δ 0.02, q, J) 14.5 Hz) and ^{19}F NMR (δ -144.2, q, J) 14.5 Hz) spectra of the aqueous (D_2O) layer. The organic (CDCl_3) layer ^1H NMR showed full conversion of the aldehyde to homoallylic alcohol. The partitioning of the allyltrifluoroborate and deuterioxytrifluoroborate anions over the course of the reaction suggests that the allylation reaction is occurring on the organic side of the solvent interphase. However, the

NMR experiment though useful and informative did not explicitly demonstrate an allyl boron difluoride ion. The authors devised another experiment based on the “assumption” that the key step in the mechanism is the dissociation of fluoride from the crotyl BF_3K to form the crotyl BF_2 . The addition of fluoride ions to the reaction should suppress the dissociation of crotyl BF_3K into the reactive allyl/crotyl BF_2 species and lead to a slower rate of reaction via the common ion effect. This hypothesis was confirmed in the reaction of the crotyl BF_3K nucleophile (1.10 equiv) aldehyde (1.00 equiv) in CD_2Cl_2 , and added tetrabutylammonium fluoride hydrate (TBAF, H_2O , 0.5 equiv.). The exogenous fluoride ions significantly decreased the rate of the reaction. While the exact nature of the reactive species in these reactions has not been definitively established, the common ion effect exhibited by fluoride ions on the reaction is consistent with a mechanism involving crotyldifluoroborane.

1.1.1.2 Stereochemical Analysis of Closed Transition States in Nucleophilic Additions of Crotyl Boron Reagents to Imines

Crotyl BF_3K is also a competent nucleophile in the crotylation non-enolizable *N*-tosyl aldimines (**Table 1.4**).²¹ This report utilized the $\text{BF}_3\cdot\text{OEt}_2$ conditions for BF_3K activation. This report was interesting in that the observed diastereoselectivity was opposite that of in the case of aldehydes. In the crotylation of aldehydes with (*E*)-crotyltrifluoroborate the *anti* homo allylic alcohol is the major diastereomer and (*Z*)-crotyltrifluoroborate yields the *syn* diastereomer (*vide supra*). However, in the crotylation of imines with (*E*)-crotyltrifluoroborate the *syn* homo allylic amine is the major diastereomer and (*Z*)-crotyltrifluoroborate yields the *anti* diastereomer. Although not explicitly stated in

the text, the observed flip in diastereoselectivity is the result of the of the *E* imine conformation. In the case of aldehydes, the crotyldifluoroborane binds to the lone pair of the aldehyde generating the *E* aldehyde isomer. However, the imine already in the *E* geometry can only interact with the crotyldifluoroborane using the lone pair that is on the same side as the phenyl, and this changes the face of nucleophilic attack on the imine.



Entry	R ¹	R ²	R ³	dr	Yield (%)
1	CH ₃	H	Ph	3:97	94
2	CH ₃	H	4-ClC ₆ H ₄	2:98	99
3	CH ₃	H	2-furanyl	4:96	99
4	CH ₃	H	Cyhex	2:98	97
5	CH ₃	H	<i>n</i> -Bu	2:98	63
6	CH ₃	H	<i>t</i> -Bu	2:98	92
7	H	CH ₃	Ph	91:9	92
8	H	CH ₃	4-ClC ₆ H ₄	96:4	99
9	H	CH ₃	2-furanyl	95:5	98
10	H	CH ₃	Cyhex	98:2	98
11	H	CH ₃	<i>n</i> -Bu	98:2	99
12	H	CH ₃	<i>t</i> -Bu	3:1	54

Table 1.4: Crotylation of *N*-tosyl aldimines using crotyl BF₃K nucleophiles

Crotyl boronic esters can react with non-enolizable *N*-alkyl imines to generate products that give the same diastereochemical outcomes observed as aldehydes (**Figure 1.8**).^{22,23} The crotyl boronic acids cause *E* to *Z* isomerization of the *N*-alkyl aldimines. The

observed isomerization was confirmed by an NOE experiment. The results were further confirmed by B3LYP functional theory.

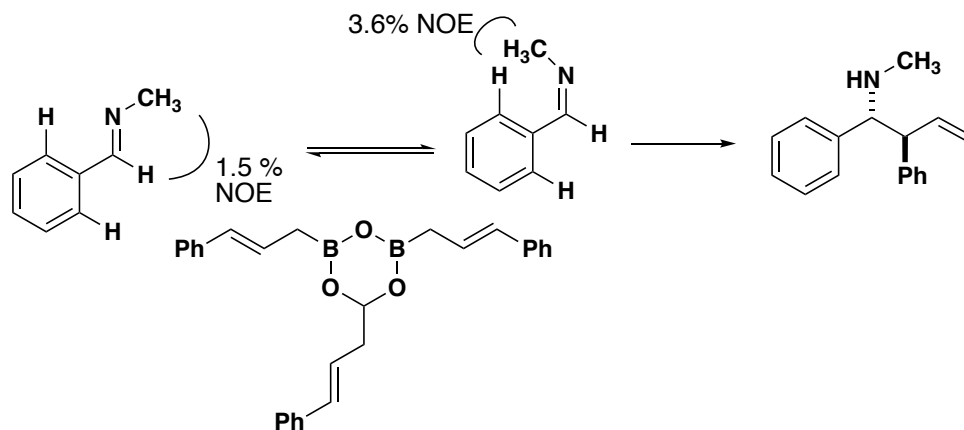


Figure 1.8: *E* to *Z* isomerization of imines.

1.1.2 Overview of Open Transition States in Nucleophilic Additions of Crotyl Silane Reagents to Aldehydes and Imines

In contrast to Type 1 nucleophiles Type 2 nucleophiles are less diastereoselective in crotylation reactions. Type 2 transition states are open and can be best represented as reacting through a Newman projection (**Figure 1.9**).⁵ In contrast to Type 1 mechanisms the nucleophilic crotylation is *syn* regardless of the *E/Z* ratio of the starting alkene. The allylic group is usually a stannane or a silane. For the purposes of the research covered in this dissertation only the mechanistic studies of silanes will be covered. In Type 2 reactions the prochiral face of the nucleophilic alkene creates three distinct transition states. The transition states orientations are anti periplanar orientation and two that are synclinal. Thus, a total of six transition states are possible, three for each prochiral face of the nucleophilic alkene. Predict the stereochemical outcome of reactions occurring through an open Type 2 mechanism is challenging, because the steric effects as well as any stereoelectronic effects between the electrophile and nucleophile must be considered.

It is also challenging to view the possible transition states and then, using only an ocular perspective predict which of the six are going to be the lowest in energy.

Type 2: Open transition state structure

- Stannanes and Silanes crotyl nucleophiles
- Reliable diastereomer prediction of Type 2 is more difficult
- Syn Selective Regardless of *E/Z* ratio

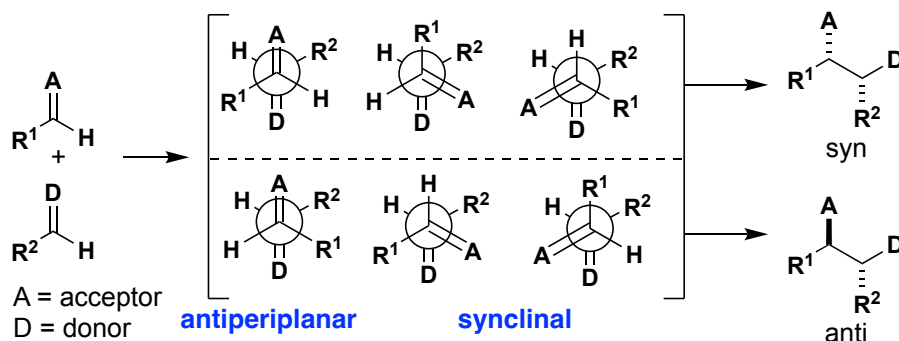


Figure 1.9: Overview of Type 2 open transition states viewed through Newman projections.

1.1.2.1 Studies to Elucidate the Anti S_E' and Syn S_E' Mechanism of Crotyl Silanes During of Nucleophilic attack of electrophiles.

Extensive experimentation and calculations to investigate the precise mechanism for the nucleophilic addition of allylsilanes have been conducted. One of the factors influencing the stereochemical outcome of the product is the *anti* S_E' or a *syn* S_E' mechanism. Because each nucleophilic face of the alkene is prochiral *anti* S_E' and *syn* S_E' give different stereochemical products (**Figure 1.10**).

Addition of the Electrophile/Acceptor

-Can either be *anti* $S_{E'}$ or *syn* $S_{E'}$

-Both additions give different stereochemical results

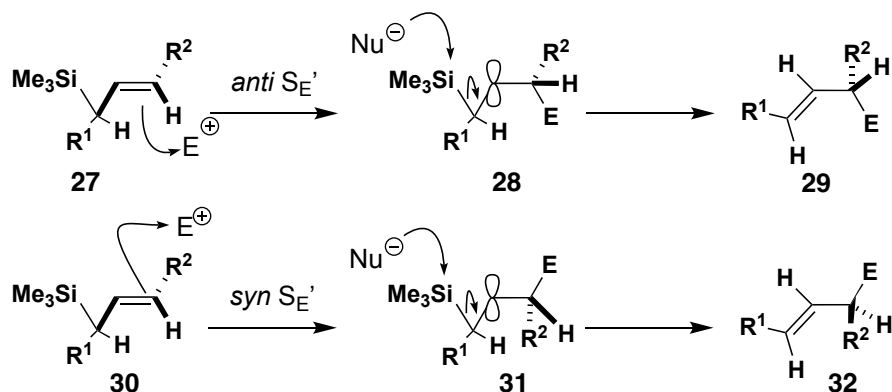


Figure 1.10: *Anti* $S_{E'}$ vs *syn* $S_{E'}$ nucleophilic attack of crotyl silane

To gain a better understanding of the *anti* $S_{E'}$ and *syn* $S_{E'}$ mechanism, Fleming calculated the energy minima for an allyl silane attacking a proton (**Figure 1.11**).²⁴ These calculations showed that **33**, **34**, and **35** were possible conformations of the allyl silane during the nucleophilic attack to yield **36**. It was determined that **33** and **34** were energy minima and **35** was an energy maxima. In **33** and **34** the allyl silane is coplanar to the p orbitals of the sp^2 carbons and the electrophile. The electrostatic potential map shows that attack of the proton electrophile is *anti* to the silane. A maximum separation of the charge is provided in conformations **33** and **34**. In this case an *anti* $S_{E'}$ is the preferred transition state for nucleophilic attack.

Calculations to determine energy minima for allyl silanes

- Determined **33** and **34** are energy minima
- Electrostatic potential map using H^+ shows attack *anti* to Si
- In **35** attack is *anti* to methyl
- Rationalized by maximum separation of developing charge

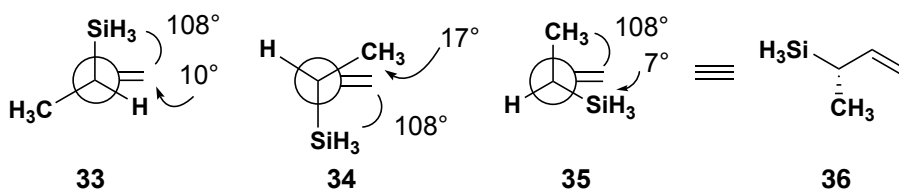


Figure 1.11: Fleming's calculations to determine energy minima for allyl silanes

Two different epimers of the cyclohexyl substrate were synthesized, **37** and **39** to elucidate the *anti* S_E' and *syn* S_E' pathway (**Figure 1.12**).²⁵ Each substrate only varies in the allylic chiral carbon. Hypothetically two different products could be isolated; one where the proton is axial and another product in which the proton is equatorial. Each product would result from *anti* S_E' and *syn* S_E' on the proton electrophile. Protonation of the allylsilane **37** was cleanly axial indicating an *anti* S_E' attack. However, the protonation of the other epimer of silane **39** gave a mixture *anti* S_E' and *syn* S_E' products. The rationalization was that the cyclohexane has axial preferences that is opposition of *anti* S_E' . The cyclohexyls axial bias does not make it a very useful model system to fully understand the *anti* S_E' and *syn* S_E' mechanism.

Model Systems to Elucidate *anti* S_{E'} or *syn* S_{E'}

-Allylsilane gives product of *anti* S_{E'} cleanly

-Diastereomer **39** is not *anti* S_{E'} selective

-Cyclohexane has an axial preference that is in opposition of *anti* S_{E'} selectivity

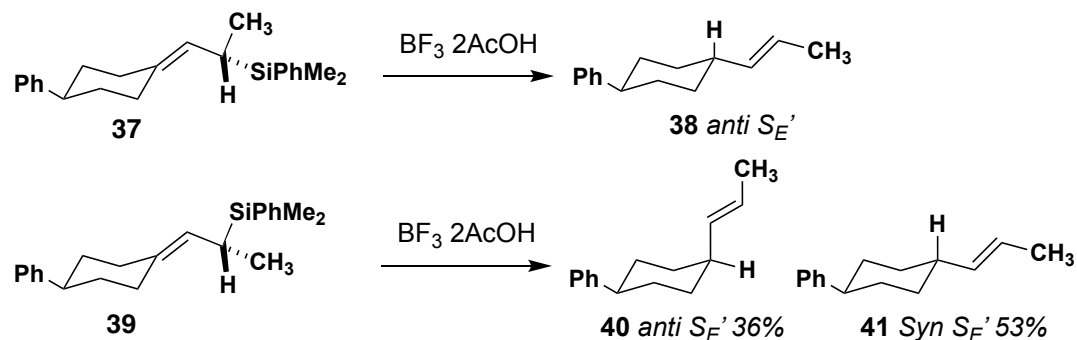


Figure 1.12: Flemings Model to elucidate *anti* S_{E'} vs *syn* S_{E'}

Kumada and Hayashi designed model system **42** and **45** to understand *anti* S_{E'} and *syn* S_{E'} mechanisms without any substrate bias as had been seen by Fleming (**Figure 1.13**).²⁶ They synthesized a chiral silane **42** in 87% ee and performed a nucleophilic crotylation reaction with various aldehydes using TiCl₄ as Lewis acid. The corresponding products were isolated in high yield and high diastereoselectivity for the *syn* product, **43**. The experiments indicate there is no erosion of ee of the crotylated *syn* product. The (*Z*) silane **45** was then subjected to the same reaction conditions and overall, the yields and diastereoselectivity were lower. However, the ee of the *syn* diastereomer **43** had nearly the same ee as the starting the (*Z*)-crotyl silane. These results strongly suggest the crotyl silane must be attacking the electrophile via an *anti* S_{E'} mechanism. Because if there was any erosion of the products ee, then that would suggest the nucleophile non-discriminately attacks the electrophile from *anti* or *syn* to the silane.

Kumada and Hayashi additions of chiral silanes

-No erosion of ee indicates that only 1 face of allyl silane is attacking

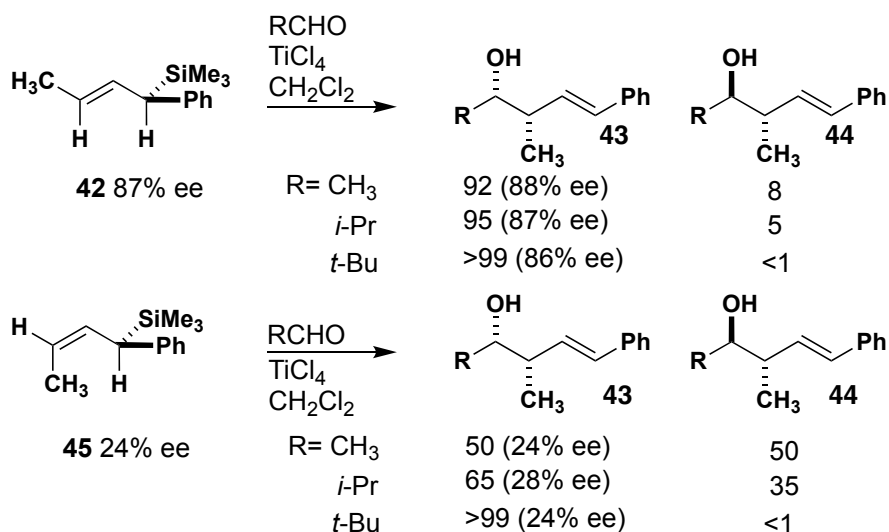


Figure 1.13 Model developed by Kumada and Hayashi to elucidate *anti* S_{E'} vs *syn* S_{E'}

Kumada and Hayashi used transition state models to rationalize the stereochemical outcomes for both geometric isomers of crotyl silane (**Figure 1.14**). The models they propose show an *anti* S_{E'} nucleophilic attack of the silane to the electrophilic aldehyde. The transition state **48** that leads to the major product with (*E*) silane **42**, shows the least number of nonbonding steric interactions. However, with (*Z*) silane **45** both transition states **50** and **51** have several have non-bonding steric interactions. This is presumably why the (*Z*) silane **45** is less diastereoselective than the (*E*) silane **42**. The assumption by Kumada and Hayashi is that the silane only prefers to attack in an antiperiplanar transition state. Neither of the synclinal orientations were considered when modeling the transition states.

These observations were rationalized by the following
 -Only antiperiplanar TS were proposed
 -Minimization of charge and sterics

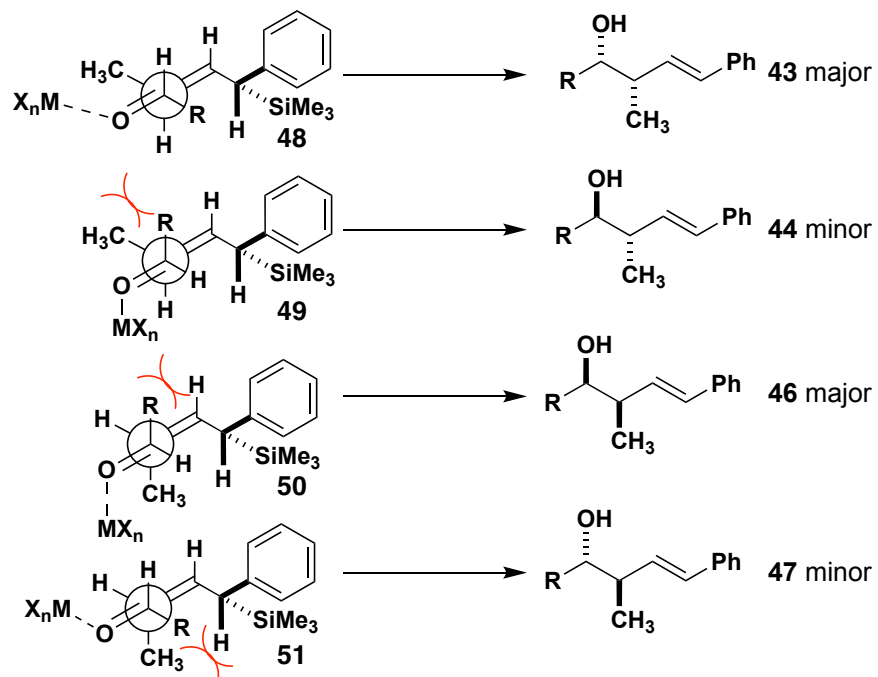


Figure 1.14: Proposed transition states for chiral silane

1.1.2.2 Studies to Elucidate Synclinal vs Antiperiplanar Orientation of Crotyl Silanes During of Nucleophilic attack of aldehydes.

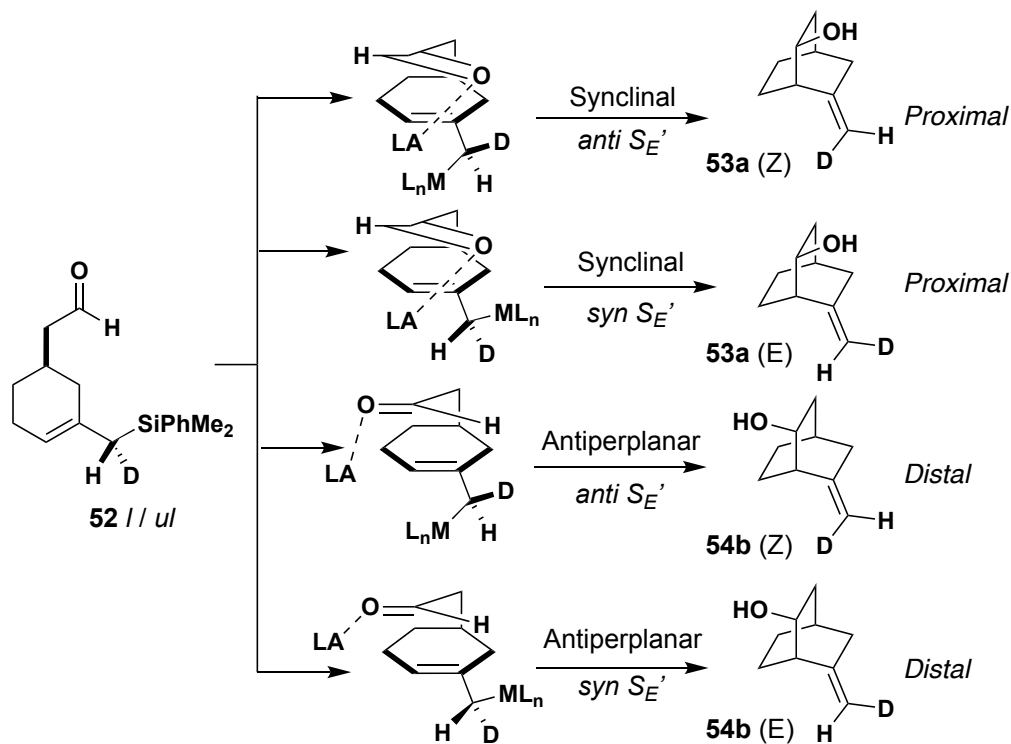
Denmark developed an updated model system to refine the transition state model for the crotylation of electrophiles with crotyl silanes.²⁷ The new model system was designed to probe *anti* S_{E'} *syn* S_{E'} and synclinal vs antiperiplanar orientation all in one substrate. Each of the transition states lead to different diastereomeric products (**Figure 1.15**). In the model Denmark uses the notation of *like* (*l*) and *unlike* (*u*) to reference the two diastereomers. The *like* indicates the stereochemistry of the hydrogen and the aldehyde are both *syn* and the *unlike* when the hydrogen and the aldehyde are *anti*.

New Model to probe *anti S_E'* or *syn S_E'* and synclinal vs antiperiplanar

-Intramolecular addition probes both *S_E'* pathway and antiperiplanar vs synclinal addition

-Model was criticized because all products are diastereomers

-Inherent bias in energy of transition structure



Lewis Acid	53a/54b	53a Z/E	54b Z/E	Proximal 53 % <i>anti S_E'</i>	Distal 54 % <i>anti S_E'</i>
1 l BF ₃ OEt ₂	75/25	94/6	94/6	100	100
1 l SnCl ₄	60/40	91/9	94/6	97	100
1 l CF ₃ SO ₃ H	95/5	93/7	94/6	99	100
1 l SiCl ₄	98/2	95/5	—	100	—
1 l n-Bu ₄ N ⁺ F ⁻	20/80	80/20	60/40	85	65
1 ul BF ₃ OEt ₂	73/27	7/93	6/94	97	100
1 ul SnCl ₄	62/38	8/92	6/94	96	100
1 ul CF ₃ SO ₃ H	94/6	7/93	—	98	—
1 ul SiCl ₄	98/2	5/95	—	100	—
1 ul n-Bu ₄ N ⁺ F ⁻	16/84	15/18	35/65	90	70

% based on 94.5% D

Figure 1.15 Denmark's model system and results.

The nucleophilic crotylation reaction was tested with various Lewis acids and the results indicate a strong preference for *anti S_E'* and for a synclinal attack of the nucleophile.

The product ratio with **a** is highest for product **53a** in the Lewis acid screen. The ratio for **53a** is highest when triflic acid is used. The reaction using fluoride (TBAF) is anomalous, in that **54b** is favored. The mechanism of attack has changes when TBAF is used to activate the silane. The fluoride ion attacks the silane first generating an anionic charge on the silane which then attacks the electrophile in a concerted manner. In contrast too, the nucleophilic alkene attacking the electrophile first generating a stabilized carbocation and then desilylation by the counter ion of the Lewis acid. The *E/Z* ratio of product **53a** is the ratio of synclinal *anti* S_{E'} and synclinal *syn* S_{E'} products. The high ratio for the *Z* isomer indicates the silane attacks the electrophile in an *anti* S_{E'} fashion. The *E* isomer would be formed by the *syn* S_{E'} attack of the silane.

Even though this model system was highly sophisticated, the model received criticism from the chemistry community; because the products are diastereomers and have differing transition state energies. The different diastereomeric transition states create an inherent bias in the system to favor one product over the another. Like Fleming, Denmark's model system was inherently flawed. Thus, a new model system was needed to account for these inherent biases.

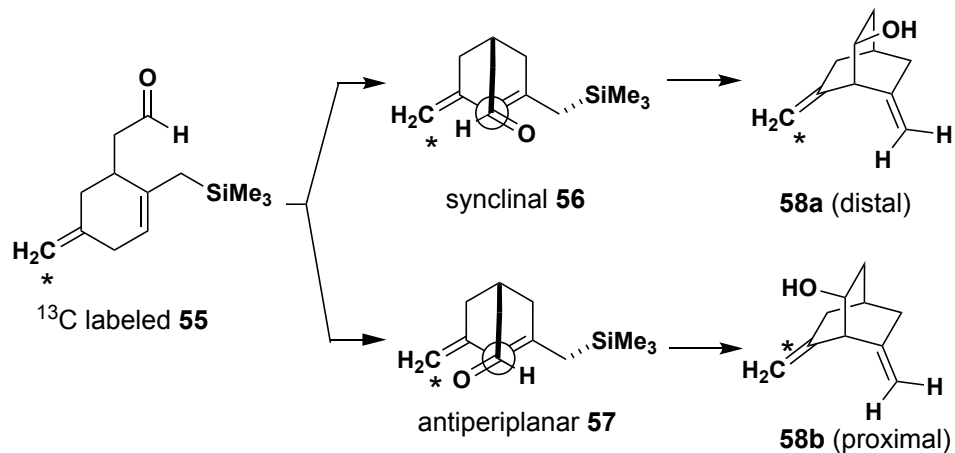
Denmark designed two new model systems to address the inherent diastereomeric bias in the original model.²⁸ Model 1 removed the diastereomeric bias by relying on an enantiomeric ratio to determine the synclinal to antiperiplanar ratio (**Figure 1.16**). The product resulting from an antiperiplanar transition state would give the enantiomer where the hydroxyl group is proximal to the ¹³C labeled carbon, **58b**. The synclinal product would orient the hydroxyl group distal to the isotopic carbon, **58a**. Model 2 was designed to

remove any steric influence the silane may enact on the synclinal vs antiperiplanar transition state, **59** (Figure 1.17). Any steric influence of the Lewis acid binding to the aldehyde would be inconsequential because the silane is below the plane of the ring. In **model 2** the proximal product would result from a synclinal transition state **62a** and the distal product would result from an antiperiplanar transition state, **62b**.

Thus a new model needed to be developed

- Two Model Systems were developed
- Model 1 removes diastereomeric bias by enantiomeric model
- Model 2 removes sterically altering trialkylsilane

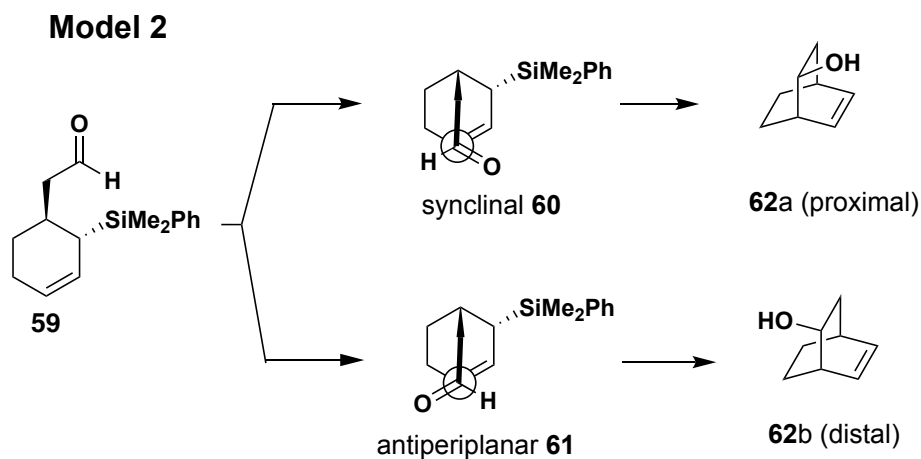
Model 1



Lewis Acid	58a/58b	$\Delta\Delta G$
BF ₃ •OEt ₂	70/30	0.34
FeCl ₃	70/30	0.34
Et ₂ AlCl	73/27	0.4
SnCl ₄	67/37	0.29
n-Bu ₄ N ⁺ F ⁻	53/47	0.05

- Results indicate there is no steric bias by LA and that synclinal transition state is more favored

Figure 1.16: Denmark's model 1 system to eliminate diastereomeric bias of the substrate.



Lewis acid	62a/62b	$\Delta\Delta G$
SnCl_4	90/10	0.85
TiCl_4	94/6	1.07
$\text{BF}_3 \cdot \text{OEt}_2$	80/20	0.54
$\text{CF}_3\text{SO}_3\text{H}$	95/5	1.14
ZrCl_4	78/22	0.49
$n\text{-Bu}_4\text{N}^+\text{F}^-$	16/84	-0.64

- Results demonstrate that Lewis acid prefers synclinal transition state
- Results of TBAF indicate another mechanism through silyl anion going through antiperiplanar transition state

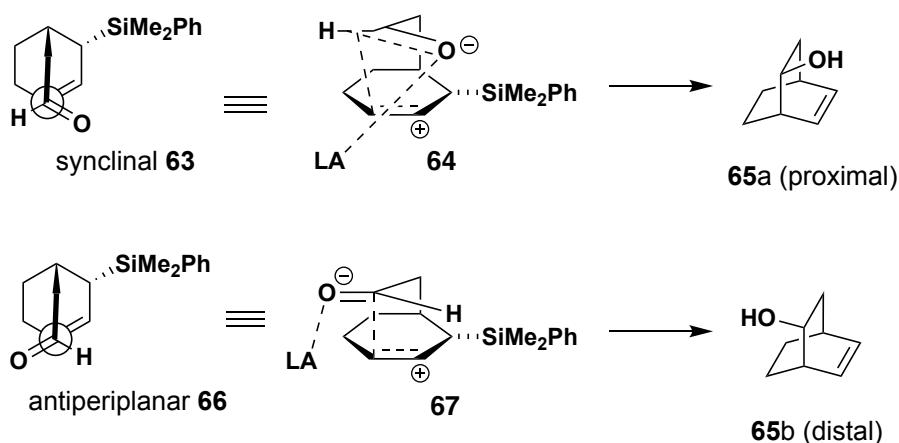
Figure 1.17: Denmark's model 2 to eliminate any steric bias of the system.

The results of the updated models reinforced the mechanism for the nucleophilic additions of allyl silanes. In model 1 using various Lewis acids the preferred enantiomer is the distal product in a 70/30 ratio. These results suggest that the synclinal orientation is preferred during the transition state. The $\Delta\Delta G$ of the synclinal to antiperiplanar orientation is ~ 0.3 kcal/mol. The data also indicates there is no steric bias by the Lewis acid in orienting the synclinal transition state. In model 2 the data demonstrates that Lewis acids strongly prefer the synclinal orientation in the transition state to the antiperiplanar transition state. The $\Delta\Delta G$ for the synclinal to the antiperiplanar transition state is >0.49 kcal/mol in a variety of Lewis acids.

Denmark used the data to rationalize the preference for a synclinal transition state. The original hypothesis of a coulombic interaction of the developing charge during the transition state. Denmark reasoned that if there was a coulombic interaction then solvent would have a critical impact on the selectivity of the ratio of synclinal products vs antiperiplanar products. However, a solvent screen had a negligible on the diastereomeric ratio (**Figure 1.18**).

Preference for Synclinal transition state

-Originally rationalized because of a coulombic interaction of developing charge



To probe this interaction a solvent effect was explored

-This screen indicates that solvent effect is negligible to dr

Lewis Acid	Solvent	65a/65b	$\Delta\Delta G$
BF ₃ •OEt ₂	CH ₂ Cl ₂	80/20	0.54
BF ₃ •OEt ₂	Hexane	82/18	0.59
BF ₃ •OEt ₂	Toluene	82/18	0.59
BF ₃ •OEt ₂	Nitropropane	90/10	0.85

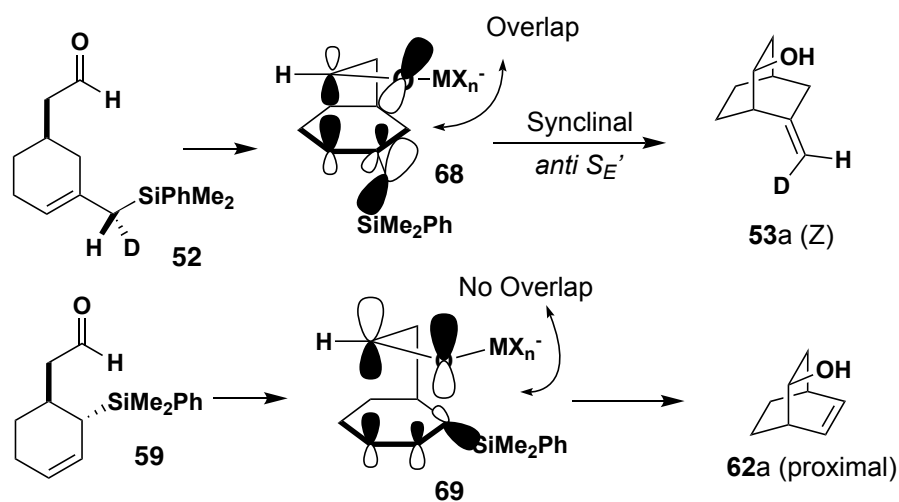
Figure 1.18: Solvent effect on model 2

Thus, it was hypothesized that the synclinal transition state is stabilized by secondary orbital overlap (**Figure 1.19**). The secondary orbital overlap overrides any

steric effect and gives synclinal transition states. In Denmark's model substrate **52** the secondary orbital overlap is argued to occur between the O lp to the allylic carbons C-Si σ^* . However, in Denmark's model substrate **59** secondary orbital overlap is precluded from happening yet the transition state prefers the synclinal transition state, suggesting other factors must still be at play. To completely understand the transition state for the nucleophilic addition to aldehydes more computational analysis is needed.

Synclinal transition state is stabilized by secondary orbital overlap

- Secondary orbital overlap over rides steric effect and gives synclinal transition state in model 2
- However in model 3 overlap is precluded from happening but still synclinal
- Thus other factors still must be at play



Computational Data Needed

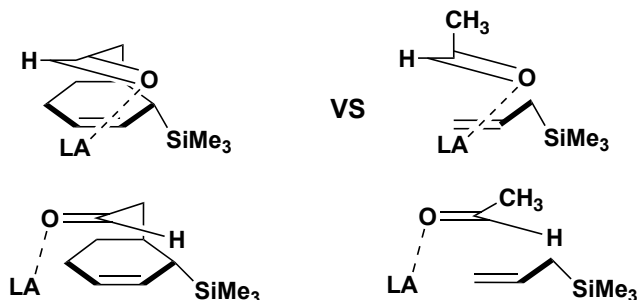


Figure 1.19: Secondary orbital overlap in various Denmark models

To gain a better understanding the stereoelectronic factors influencing synclinal vs antiperiplanar transition states a series of computational experiments were undertaken (**Figure 1.20**).²⁹ The diagram shows that the $\text{BF}_3 \cdot \text{O}(\text{CH}_3)_2$ Lewis acid chelates in an *E* orientation **A**, then the crotyl silane approaches the Lewis acid activated electrophile **B**. The transition state **C** for the C—C bond forming step is at 14.1 kcal/mol. This is the diastereoselective step of the reaction and incorporates the synclinal vs antiperiplanar transition state. The resulting carbocation is stabilized via the β -silicon effect at 12.3 kcal/mol **D**. Then a molecule of $\text{O}(\text{CH}_3)_2$ is calculated attack the silicon to desilylate the intermediate **E**. Following desilylation the compound eventually funnels down to product **G**.

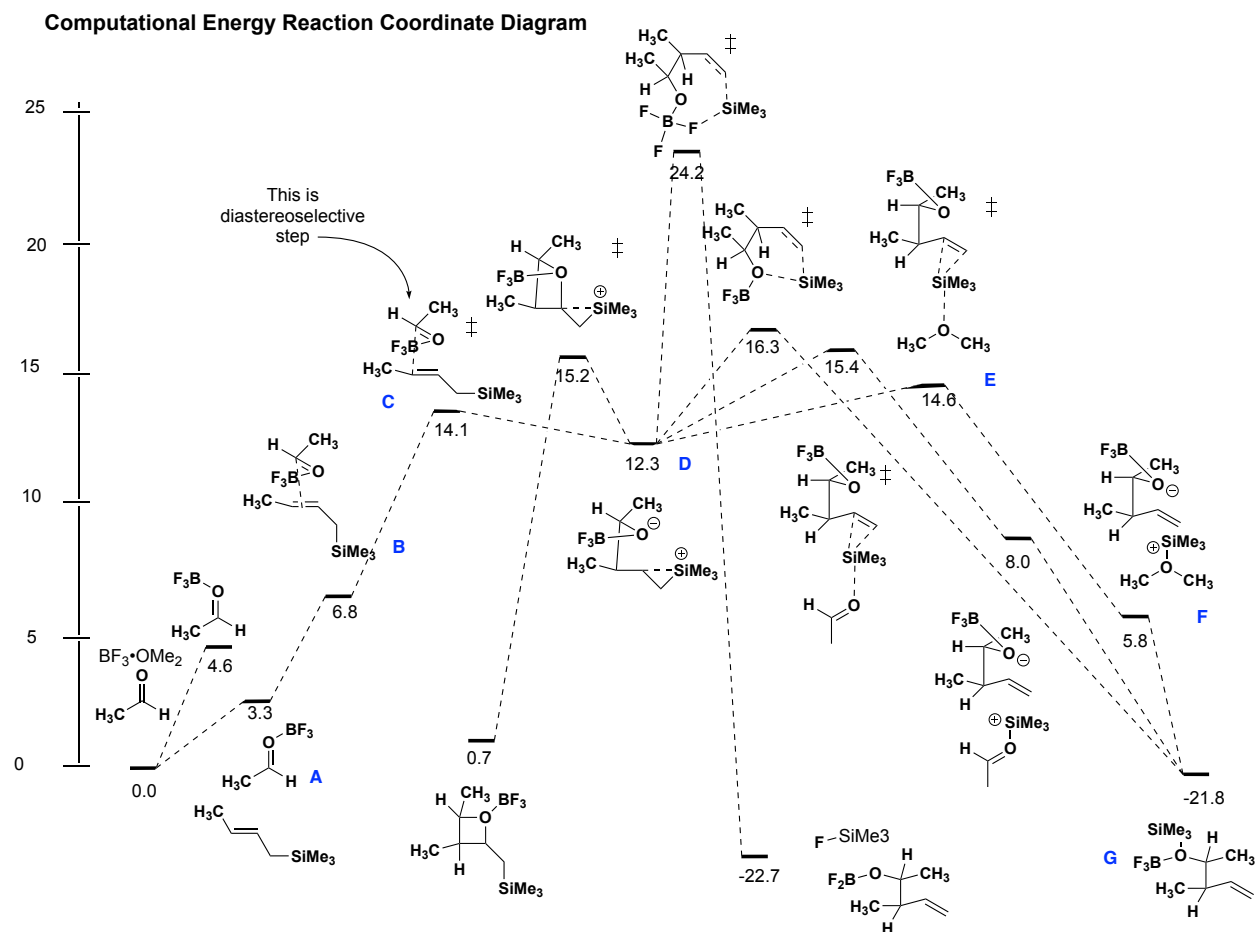
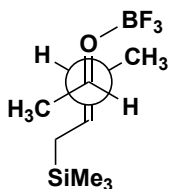


Figure 1.20: Energy coordinate diagram for the crotylation of acetylaldehyde and (*E*)-crotyl silane, calculated by Denmark in 2013.

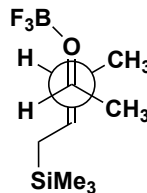
With an understanding of the reaction coordinate diagram the energies for the diastereoselective transition state were calculated. The antiperiplanar and both synclinal transition states were calculated for each prochiral face of the nucleophilic alkene (**Figure 1.21**). Overall, the ΔG^\ddagger is lowest for the **Syn-T3-L** transition state, then **Syn-T2-L** followed by **Anti-T3-L**, **Anti-T1-L**, **Anti-T2-L**, **Syn-T1-L**.

Energies for Diastereoselective Transition state

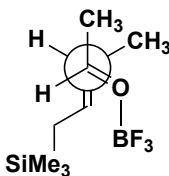
-Looking for energy minima between syn and anti
-Then using free energy, sterics, orbital interactions distortion etc. account for why syn is preferred diastereomer



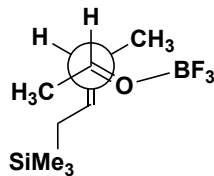
Syn-T1-L
4.2 kcal/mol



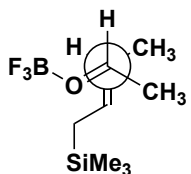
Anti-T1-L
2.0 kcal/mol



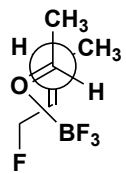
Syn-T2-L
0.8 kcal/mol



Anti-T2-L
3.0 kcal/mol



Syn-T3-L
0.0 kcal/mol



Anti-T3-L
1.0 kcal/mol

Figure 1.21: Calculated ΔG of synclinal and antiperiplanar transition states for anti and syn diastereomeric products.

The total energy ΔE_{es}^\ddagger of each transition state was broken down into to understand the relative contributions of the individual components (**Figure 1.22**). The $\Delta E_{exrep}^\ddagger$ term is for the steric repulsion in the transition state. The ΔE_{pol}^\ddagger is the interorbital mixing component. The ΔE_{disp}^\ddagger is the component that makes up the dispersion interaction. The distortion of the aldehyde and the crotylsilane are represented by $\Delta E_d^\ddagger(A)$ and $\Delta E_d^\ddagger(B)$, respectively. ΔE_{int}^\ddagger represents the interaction energy of the two components. The lowest

energy transition state leading to the *syn* product and the lowest energy transition state leading to the *anti* diastereomer, were compared to elucidate which components contribute the most to the observed selectivity $\Delta E(\text{Syn-T3-L}) - \Delta E(\text{Anti-T1-L})$ (**Figure 1.22**). The results in the graph illustrate that the largest difference and major contributor to the orientation is the steric repulsion ΔE_{exrep} . The results from the data suggest that secondary orbital interactions are negligible for the preference of synclinal over antiperiplanar. Denmark argues that if secondary orbital interactions contributed significantly then the $\Delta E_{\text{pol}}^\ddagger$ would be more significant. The $\Delta E_{\text{pol}}^\ddagger(\text{Syn-T3-L}) - \Delta E_{\text{pol}}^\ddagger(\text{Anti-T1-L})$ also favors the *anti* product. It is then suggested that the synclinal orientation is probably due to primary orbital interactions between $\pi \rightarrow \pi^*$ of the nucleophilic alkene and the aldehyde electrophile.

	ΔG^\ddagger	ΔE_{es}	ΔE_{exrep}	ΔE_{pol}	ΔE_{disp}	ΔE_d	ΔE_{int}	ΔE^\ddagger
Syn-T1-L	4.2	-34.2	120.5	-84.6	-29.6	21.8	-27.9	4.1
Syn-T2-L	0.8	-44.5	143.7	-98.2	-33.2	24.0	-32.2	-0.2
Syn-T3-L	0.0	-42.0	137.8	-96.5	-30.8	23.1	-31.5	-0.9
Anti-T1-L	2.0	-38.6	128.3	-90.1	-27.8	22.4	-29.1	1.1
Anti-T2-L	3.0	-42.9	139.7	-96	-31.3	23.9	-30.5	2.4
Anti-T3-L	1.0	-33.3	122.9	-86.4	-31.3	21.4	-28.1	1.6

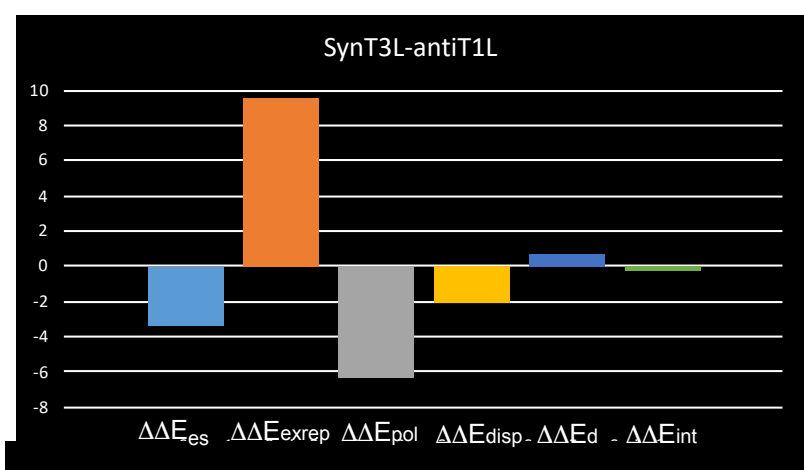
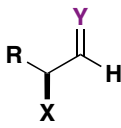


Figure 1.22 $\Delta E(\text{Syn-T3-L}) - \Delta E(\text{Anti-T1-L})$

Overall, these studies helped elucidate the transition state structure and all the components that influence that structure for the nucleophilic allylation of crotyl silanes to aldehydes. It is important to understand the mechanism and all the factors influencing these reactions because the mechanisms will be pivotal in understanding and developing stereochemical models for the crotylation of α -chiral alkoxy *N*-tosyl imines with crotyl boranes and crotyl silanes.

1.1.3 Acyclic Stereocontrol of α -Chiral Imines

Systematic studies of acyclic stereocontrol of imines are scarce, relative to aldehydes. At the time my study commenced only 170+ reports on acyclic stereocontrol had been reported. Contrast that with aldehydes where a staggering >4300 different examples of acyclic stereocontrol had been reported. The figure below is a Scifinder search illustrating how staggering the analogous imine functional group could remain underexplored (**Figure 1.23**). The major reason acyclic stereocontrol of aldehydes been explored more thoroughly is because stereocontrol was needed to synthesize many complex molecules.³⁰ Analogously new stereocontrol of imines can also lead to new retro synthetic analysis and syntheses of novel complex molecules too. Of the few reports on acyclic stereocontrol of imines the ones most relevant to this study are detailed below.

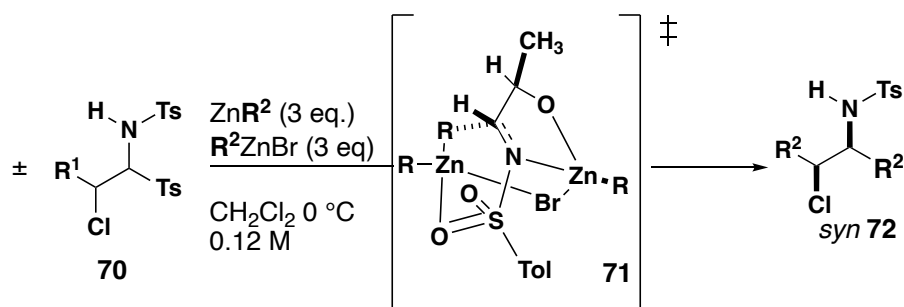
	Y	# references	
	O	>4300] acyclic stereocontrol/ stereo-electronic influence
	N-SiR ₃	1	
	N-alkyl	96	
	N-NR ₂	7	
	N-OR	0	
	N-carbonyl	0	
	N-phosphinyl	0	
	N-sulfonyl	4	
	N-*NR ₂	7] chiral auxiliary
	N-sulfinyl	63	

Scifinder *as of 2018

Figure 1.23: 2018 Scifinder search comparing acyclic stereocontrol of aldehydes to imines

1.1.3.1 Acyclic Stereocontrol in Nucleophilic Additions to α -Chiral Imines *N*-Tosyl Aldimines

A report on the acyclic stereocontrol of α -chloro *N*-tosyl imines using organozincs as nucleophiles showed high diastereoselectivity for the *syn* diastereomer (**Table 1.5**).³¹ An excess of the nucleophilic zinc was needed to deprotonate the amido sulfone and liberated the imine electrophile *in situ* and nucleophilic addition would follow. The two possible diastereomeric outcomes are *syn* and *anti*. In the report by Walsh the *syn* product was the major isomer isolated. The high diastereoselectivity was rationalized via a chelated zinc transition state, **71**. The *anti* diastereomer could never be isolated as the major product because of the zinc chelated electrophile (**Figure 1.24**).



Entry	R ¹	R ²	dr <i>syn:anti</i>	Yield (%)
1	C ₆ H ₁₃	Et	92:9	80
2	C ₆ H ₁₃	CH ₃	91:1	83
3	<i>i</i> -Pr	Et	>20:1	84
4	<i>i</i> -Pr	CH ₃	>20:1	80
5	Bn	Et	93:7	76
6	Bn	CH ₃	20:1	82
7	CH ₂ OTBDPS	Et	88:12	69
8	CH ₂ OTBDPS	CH ₃	86:14	85

Table 1.5 Walsh's acyclic stereocontrol of α -chloro imines using Zn nucleophiles.

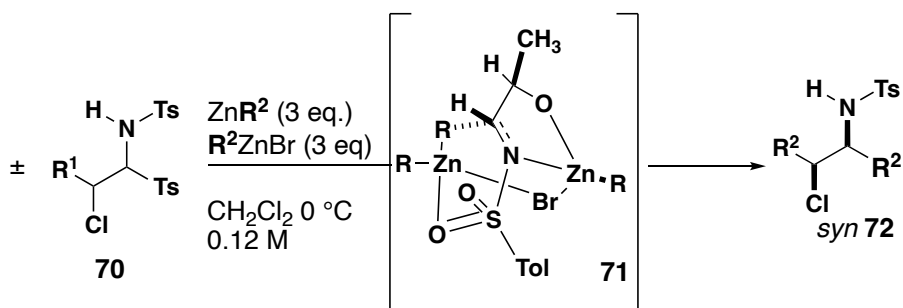


Figure 1.24: Walsh's proposed chelate transition state leading to *syn* selectivity.

Our group also published work on the acyclic stereocontrol in the additions of nucleophilic alkenes to α -chiral *N*-sulfonyl imines.² This is the only report in which *syn* and *anti* products could be isolated in high yields using the optimized reaction conditions. The *anti* diastereomer could be synthesized using BF₃•OEt₂ as a Lewis acid and allyl-BF₃K as a nucleophile **2**. In a complementary manner the *syn* diastereomer could be

synthesized using ZnBr_2 as a chelating Lewis acid and allyl trimethyl silane as a nucleophile, **3**. The investigation into acyclic stereocontrol by Moore and Lo uncovered interesting results that lead to the development of the optimized reaction conditions. They discovered that imines are more Lewis basic than their analogues aldehydes. This was discovered by the addition of $\text{BF}_3 \cdot \text{OEt}_2$ as a Lewis acid and allyl trimethyl silane as a nucleophile. The reaction was highly selective for the *syn* diastereomer. This highlighted an investigational study where the chelate of the $\text{BF}_3 \cdot \text{OEt}_2$ is the lowest in energy at -78°C , **74** and **74TS-1** (**Figure 1.25**). Nucleophilic addition of the chelated imine leads to the *syn* diastereomer. Thus to achieve high *anti* selectivity Moore and Lo raised the temperature of the reaction to -20°C to favor the formation of the di-coordinated Lewis acid complex, **76**.

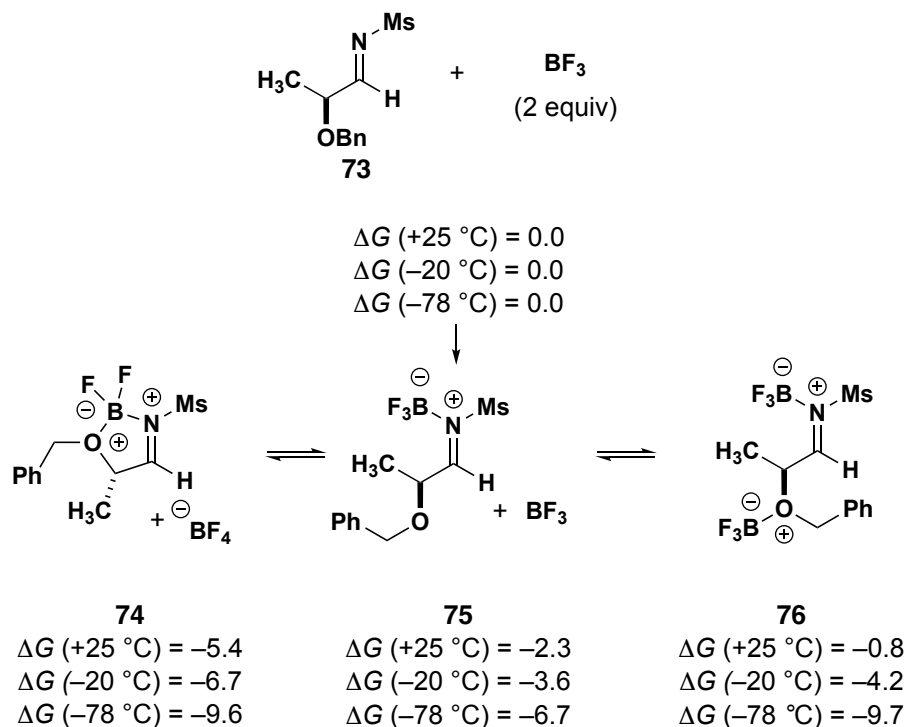
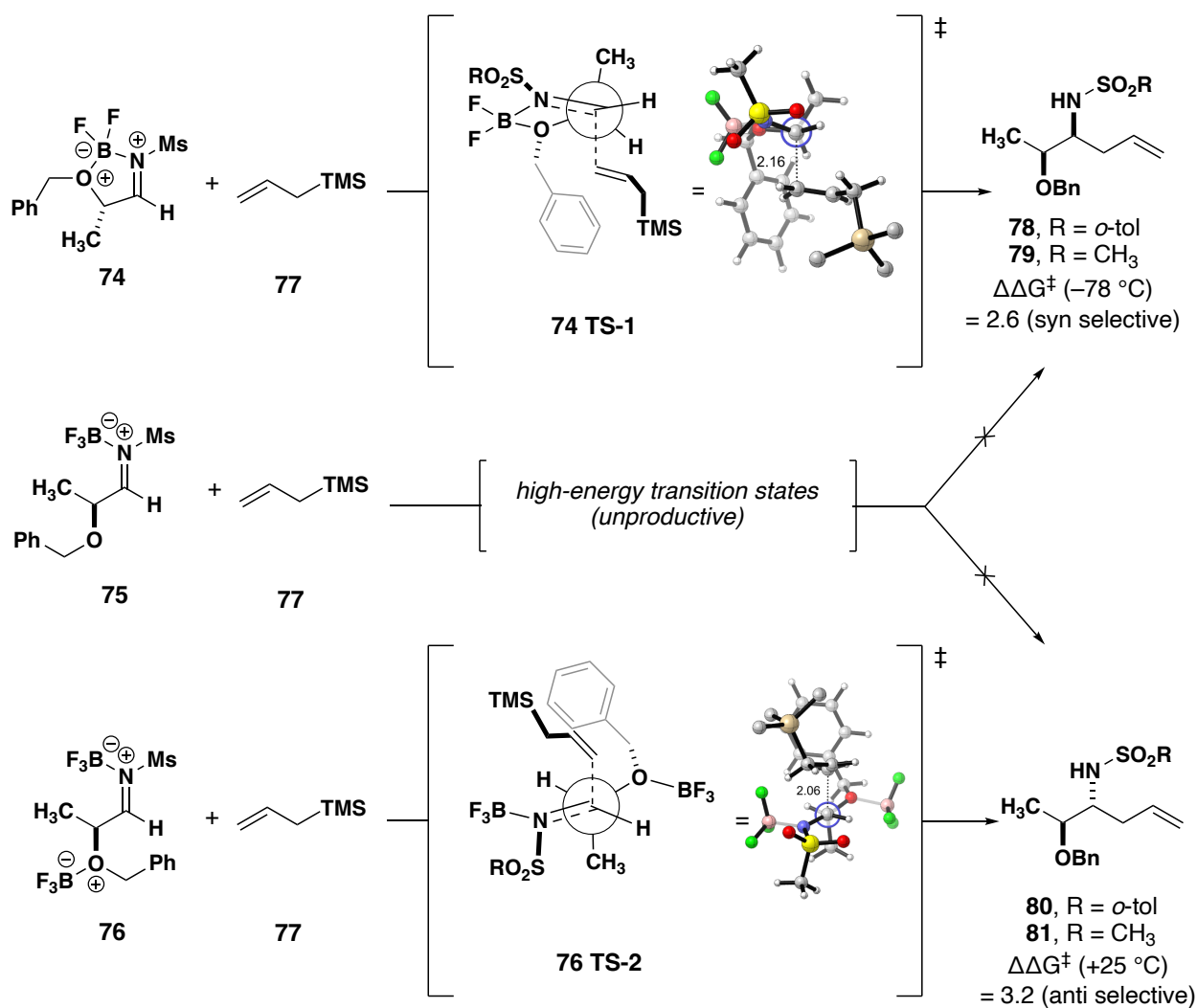


Figure 1.25: Chelate of BF_3 and imine



entry	TS	ΔG^\ddagger (-78 °C)	ΔG^\ddagger (-20 °C)	ΔG^\ddagger (+25 °C)
1	TS-1	18.7	19.7	23.5
2	TS-2	21.3	20.3	20.3

Figure 1.26: Chelation of imine with BF_3 and then allylation

1.1.3.2 Crotylation and Prenylation of α -Chiral Imines

Investigations of the crotylation reactions of α -chiral imines bearing polar heteroatoms at the time this study commenced had only been undertaken by Panek and Marek.^{32,33} Unlike the diastereoselective allylation reaction by Moore and Lo, a crotylation reaction of an α -chiral aldimine creates two new stereogenic centers; resulting in four

different diastereomeric products. In both Panek's and Marek's report only one of the possible four diastereomeric products were accessible.

Panek developed his crotylation reaction based on a synthesis of a chiral allyl silanes **85** and **86**. An enzymatic resolution of a racemic alcohol **84** and was used to make the corresponding allyl silane via an ortho-ester Claisen rearrangement (**Figure 1.27**).

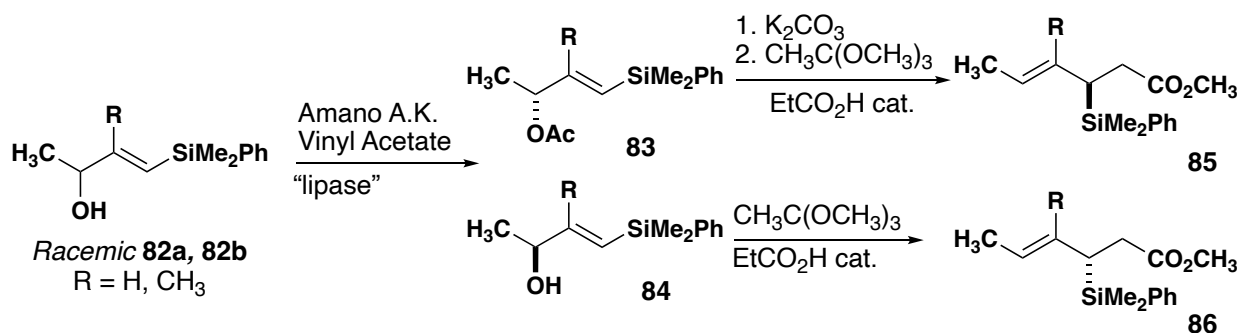


Figure 1.27: Panek's synthesis of chiral crotyl silane

The silane was used in reactions with a variety of imine electrophiles. Imine formation of alkyl aldehydes is often challenging, since these imines must be used immediately to avoid decomposition or enamine tautomerization.³⁴ To obviate this challenge, Panek used a multicomponent reaction to generate α -alkoxy *N*-carbamoyl imines *in situ*. In this case, appreciable levels of selectivity were observed with a chiral allylsilane, **88** and **89**, providing the highest selectivity when matched with the appropriate chiral aldehyde. The stereochemistry of the product was rationalized using an antiperiplanar like transition state **90**. Of all the electrophiles screened the α -chiral imine derived from ethyl lactate is the most relevant to the study presented herein (**Figure 1.28**). The transition state model proposed suggests an imine *E* to *Z* isomerization that is then

allylated. Based on the results of Moore and Lo, it is more likely the BF_2 is chelated between the imine and the alkoxy group; leading to the high *syn* diastereoselectivity.

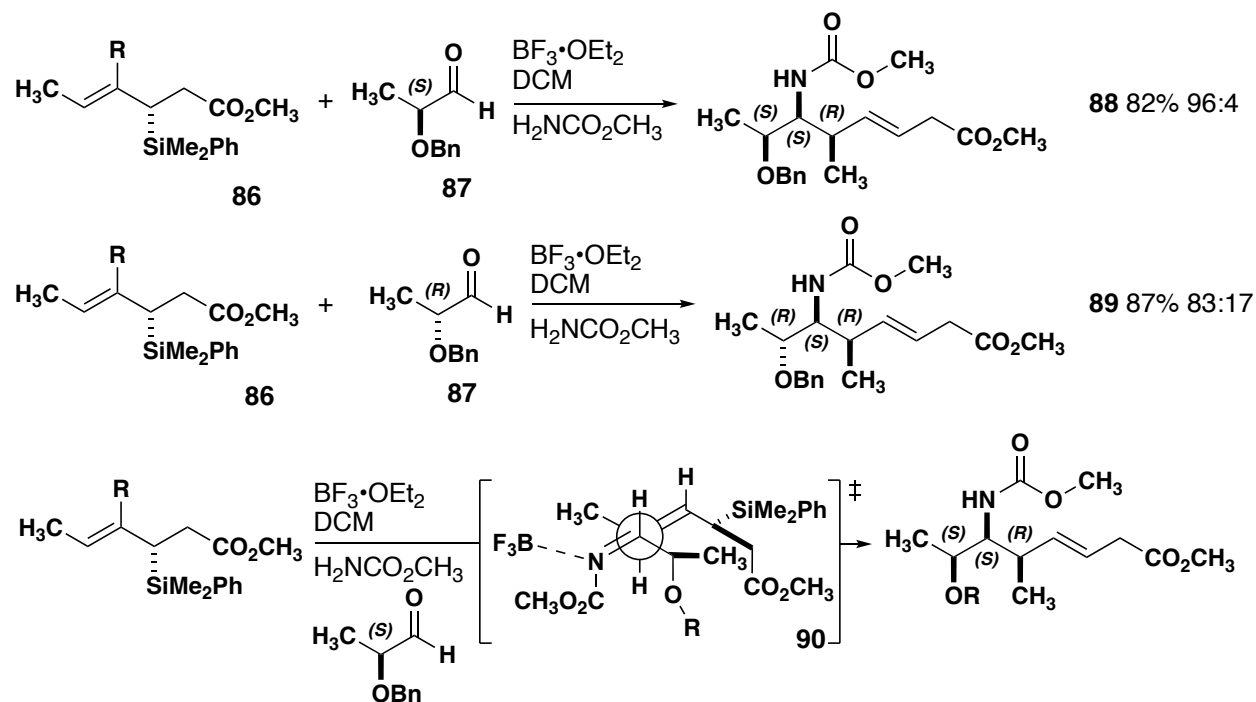
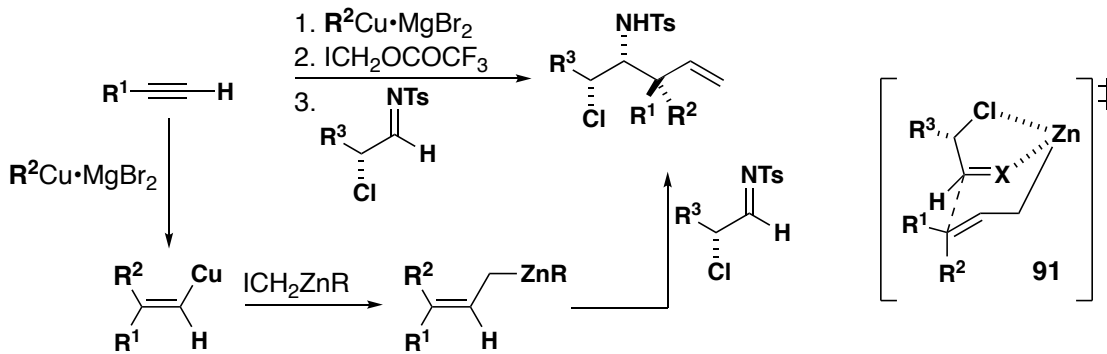


Figure 1.28: Panek's allylation of chiral imines using a multicomponent reaction to generate imines *in situ*

Marek demonstrated C1-C2 *syn* and C2-C3 *syn* stereocontrol by utilizing an amido sulfone imine precursor and a zinc nucleophile (**Table 1.6**).³³ The Zn nucleophile was generated *in situ* by adding a cuprate to a terminal alkyne generating a vinyl cuprate which react in a homologation reaction in a reaction with $\text{ICH}_2\text{ZnOCOCF}_3$. Zinc can then act as a chelatable Lewis acid and chelate the electrophile and the nucleophile generating a preorganized chair-like transition state, **91**. Marek observed very high levels of selectivity with this approach. However, Panek nor Marek was able to access all four diastereomeric products.



Entry	R ¹	R ²	R ³	dr	Yield (%)
1	Pr	Et	<i>t</i> -Bu	100:0:0:0	70
2	Hex	Et	<i>i</i> -Pr	90:10:0:0	63
3	Pr	<i>i</i> Et	<i>i</i> -Pr	85:15:0:0	60

Table 1.6: Marek's prenylation of α -chloro *N*-sulfonyl imines with prenyl zinc nucleophiles.

1.1.4 Overview of Completed Syntheses of Clausenamide and Epimers of Clausenamide.

Clausenamide is a gamma lactam that is isolated from the leaves of *Clausena lansium*. The *C. lansium* plant is native to southeast Asia, the tree is also known as the wampi.³⁵ The tree grows a grape-like fruit. The gamma lactam, clausenamide, contains four contiguous stereocenters; this means that there are 16 unique stereoisomers possible. (**Figure 1.30**). However only racemic clausenamide and racemic *neo*-clausenamide were isolated in the original isolation report. Clausenamide and *neo*-clausenamide are proposed to be a biosynthetic precursor of lansamide, another natural product amide (**Figure 1.29**).³⁶ Oxidation and then cyclization of lansamide leads to the two lactams. The full biosynthetic pathway leading to (\pm)clausenamide and (\pm)*neo*-clausenamide and has yet to be elucidated.

The complex stereochemistry decorating the gamma lactam has interested the synthetic community since the original isolation and because of its therapeutic benefits.

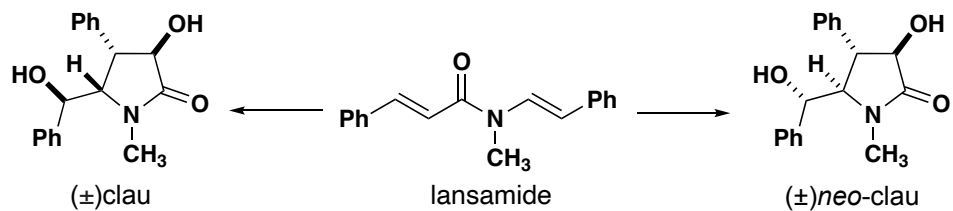


Figure 1.29: Biosynthetic intermediate leading to (±)-clausenamide and (±)-neo-clausenamide

Although there have been many syntheses of epimers of clausenamide, only a handful of the compounds have characterization data. A recent patent has claimed most of the molecules in the clausenamide family, however they only characterize the compounds by melting point and optical rotation.³⁵ The only molecule yet to be reported, prior to this work,³⁷ is *cis-epi-clausenamide*. This section will detail the original isolation of clausenamide, total and formal syntheses of this unique natural product published in chemical journals and the reported biological activity.



Clausena Lansium
(Wampi)

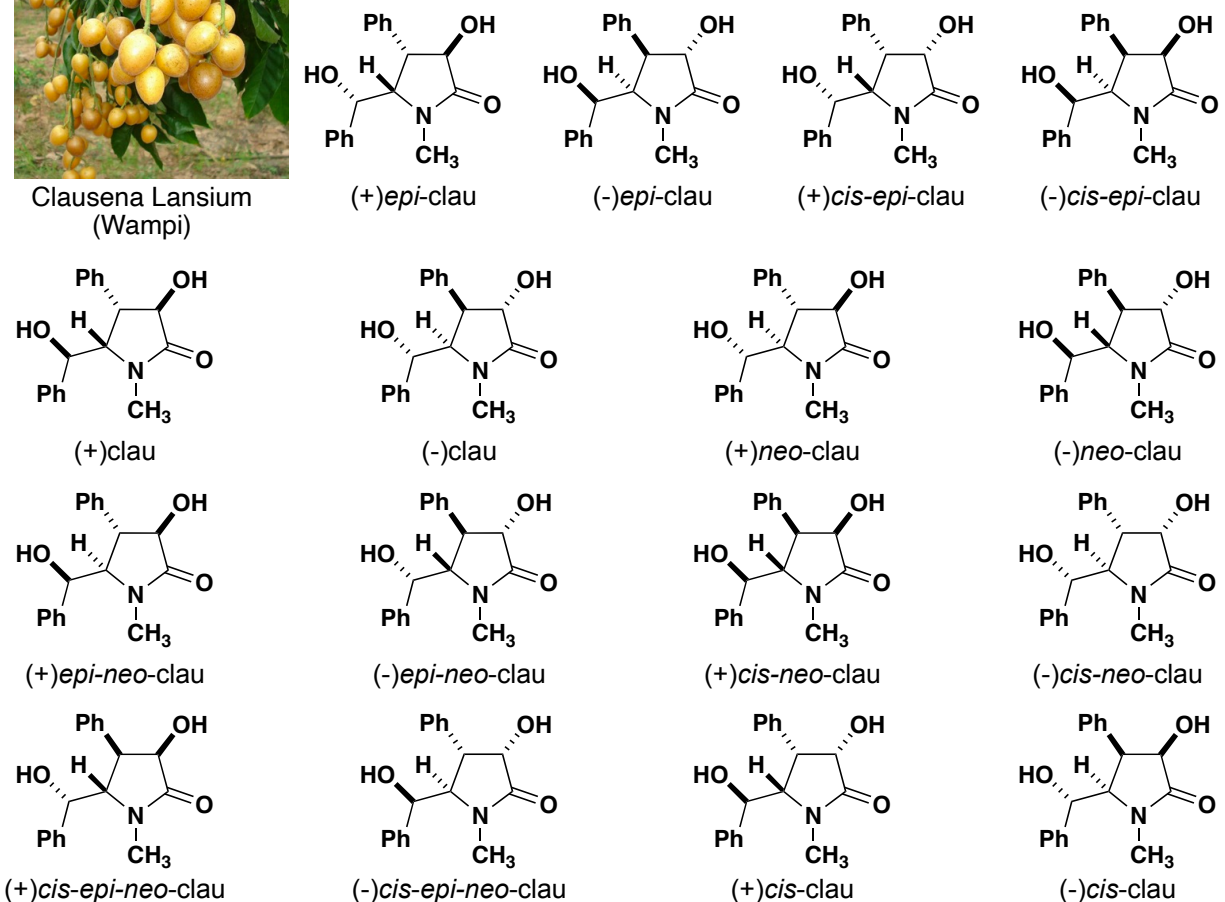


Figure 1.30: (\pm)-Clausenamide and (\pm)neo-clausenamide are the naturally occurring lactams that were originally isolated

1.1.4.1 Original Isolation of Clausenamide

The method for extraction required 80 kg of dried leaves of the *C. lansium* plant and boiled three times in water for four hours each.³⁸ Then the extracts were concentrated to yield eighteen kg of a brown residue that was dissolved in 0.06 N HCl. The supernant was then passed through a resin exchange column (H⁺ form to Na⁺ form). The resin was then washed with water and allowed to dry by evaporation. This yielded a 12.65 kg extract that was basified with 2% NH₃OH, under Soxhlet extraction for 12 hours. The

concentrated extraction yielded 118 g of a material which was chromatographed in chloroform to give 7.22 grams of clausenamide, and 0.52 grams of neo-clausenamide. The compounds were crystallized in methanol to give cubic colorless crystals. The structure elucidation of clausenamide was accomplished by IR, NMR ^1H and ^{13}C . Since clausenamide was isolated along with neo-clausenamide, the relative stereochemistry needed to be assigned. The original authors assigned the relative stereochemistry of clausenamide and neo-clausenamide by X-ray crystallography.

Dehydrocycloclausenamide was also isolated from the extraction process. This bicyclic molecule is postulated to come from the intramolecular cyclization of clausenamide through an acid mediated pathway (**Figure 1.31**).

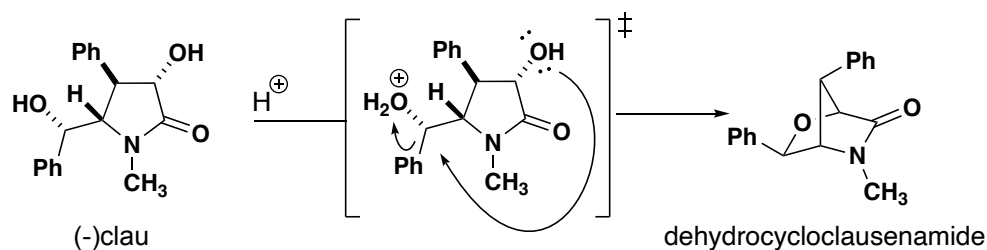


Figure 1.31: Proposed pathway for the formation of dehydrocycloclausenamide

1.1.4.2 Total and Formal Syntheses of Clausenamide and its Epimers

Shortly after the isolation of clausenamide, Wolfgang published a diastereoselective and enantioselective synthesis (**Figure 1.32**).³⁹ The enantioselective step of the synthesis begins with a conjugate addition of a heterocyclic nucleophile to *cis*-cinammic ester, to yield **93**. This compound is then hydrolyzed in concentrated HCl and treated with ammonia to generate a cyclic lactam. Methylation of the lactam leads to product **94**. The ethyl ester is subjected to a functional group interconversion by reduction to the primary alcohol and then oxidized by a modified Swern oxidation. The aldehyde is

treated with phenyl Grignard to yield the alcohol **95**. Another Swern oxidation followed by NaBH_4 reduction epimerizes the alcohol in the correct stereochemical configuration, **96**. Then the CH_2 is oxidized by enolate formation followed by treatment with $\text{P}(\text{OEt})_3$ and O_2 .

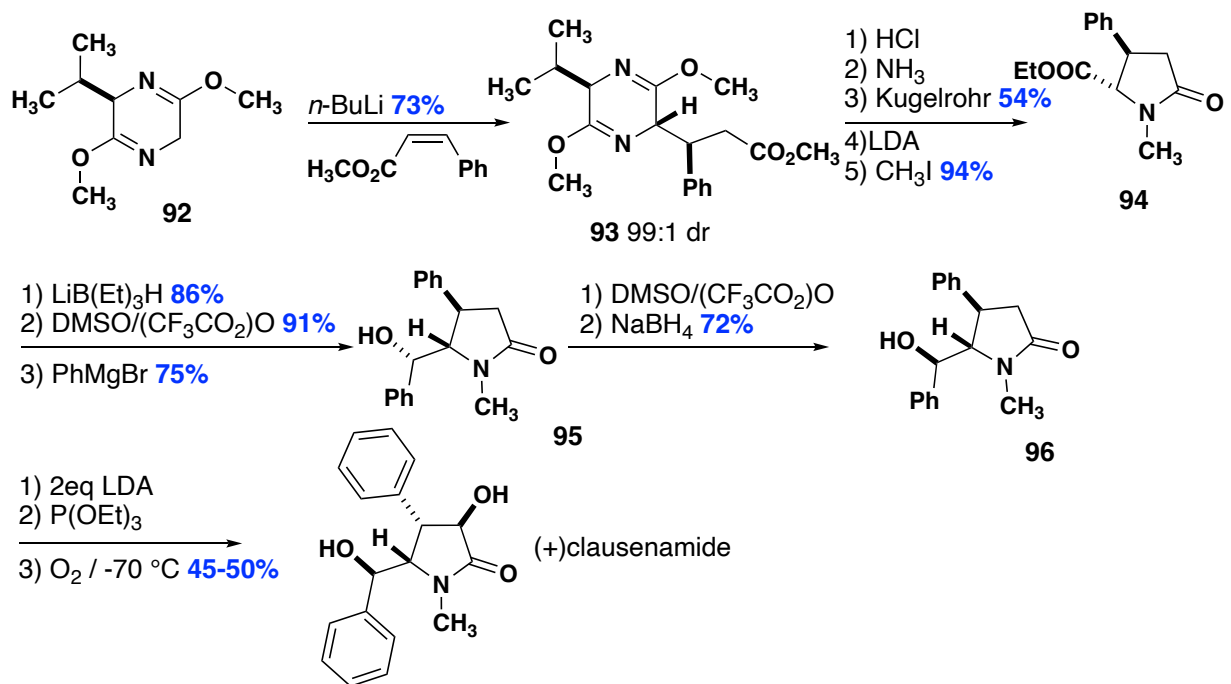


Figure 1.32: Wolfgang's enantioselective synthesis of (+)clausenamamide

A significant time had elapsed between syntheses of clausenamamide and the next reported synthesis, which was published in 2008 (**Figure 1.33**).⁴⁰ A racemic epoxide **97** bearing a cyano group is subjected to an enzymatic kinetic resolution to yield the chiral amide. This molecule is then subjected to an Ullman type coupling to attach the *Z*-vinyl bromide to the terminal NH_2 amide, **99**. The enamine then does an intramolecular epoxide ring opening to yield the lactam **100**. The lactam is selectively oxidized by Jones reagent to give the phenyl ketone, **101**. The ketone is then epimerized and then reduced with NaBH_4 to yield clausenamamide. Likewise reduction of the ketone by hydrogen palladium

on carbon yields (-)-neo-clausenamide. Overall, the synthesis is very efficient accomplishing the synthesis in 6 steps.

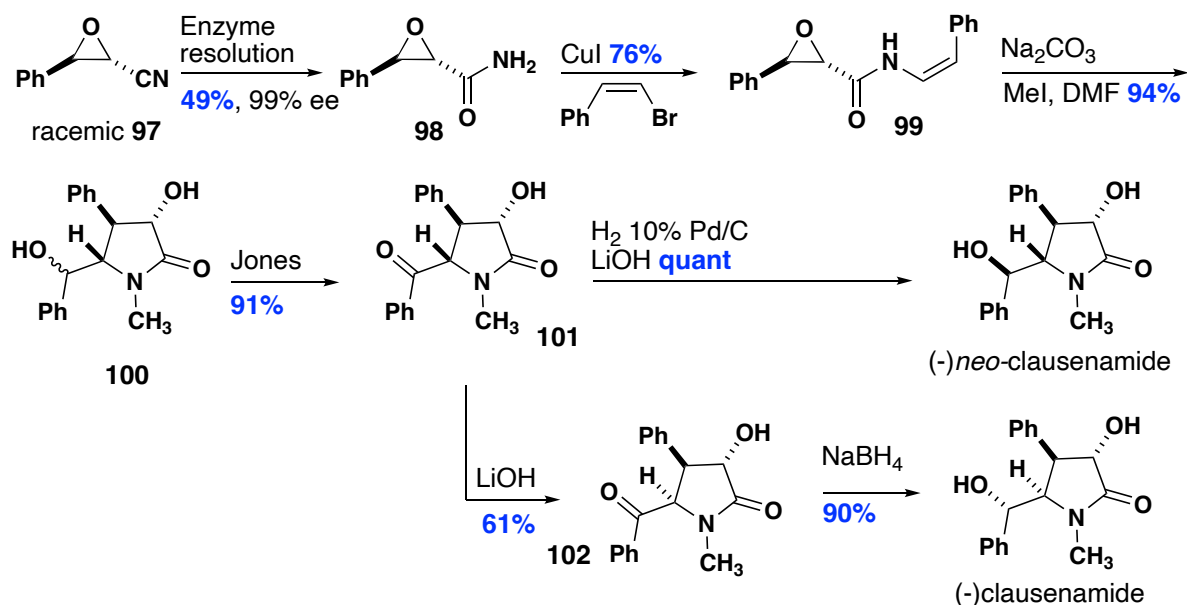


Figure 1.33: Kinetic resolution used in the synthesis of (-)-neo-clausenamide and (-)-clausenamide

The same group reported another enantioselective synthesis of clausenamide (**Figure 1.34**).⁴¹ This synthesis is built on the same concepts as the original route reported in 2008. In this synthesis an organo catalyst is used with cinnamyl aldehyde and H₂O₂ to yield epoxide **104** in 95% ee and then oxidized to the corresponding acid. Then the ester is converted to the amide with the reaction of the racemic amino alcohol, **105**. The stereochemistry of the alcohol is inconsequential because it is ablated during the oxidation with KMnO₄. Subjecting the ketone with LiOH generates and intramolecular enolate cyclization, which upon treatment with NaBH₄ yields the natural product (-)-clausenamide

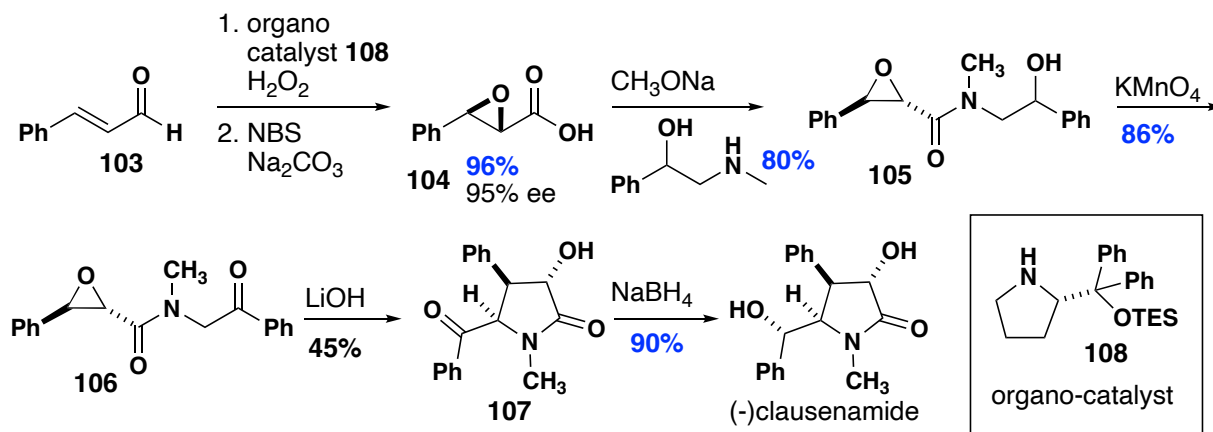


Figure 1.34 Organo-catalyst epoxidation for the synthesis of (-)-clausenamide.

The next three synthetic routes towards clausenamide have relied on the synthetic manipulation dihydroisoxazoles. The first route is an enantioselective Corey Chakovsky epoxidation followed by an nitro-enolate attack of the epoxide (**Figure 1.35**).⁴² Then a zinc reduction of the N-O ring opens the dihydroisoxazoles then recycles giving the gamma lactam, **113**. Chemoselective methylation of the amide, followed by osmium tetroxide cleavage of the alkene gives ketone precursor which can then be reduced with NaBH_4 to give (-)-cis-clausenamide.

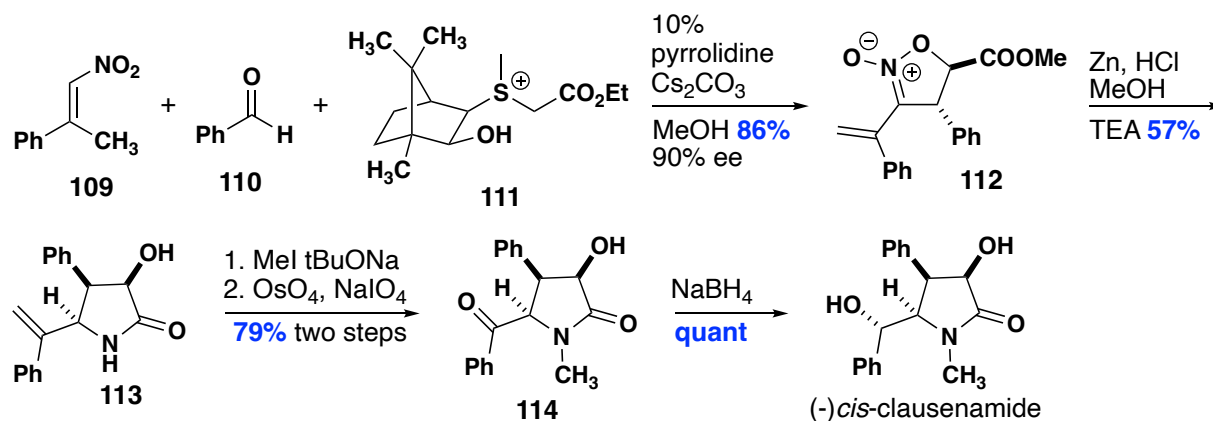


Figure 1.35: Dihydroisoxazole as key intermediate for (-)-cis-clausenamide synthesis

The next report is a formal synthesis utilizing a 3+2 dipolar cycloaddition reaction to synthesize the key dihydroisoxazole, **118** (**Figure 1.36**).⁴³ The authors retrosynthetic

analysis relies on much of the work that had previously been published: a few functional group interconversions, N-O bond cleavage, cyclization, and then a selective reduction would yield the lactam core of clausenamide. First the cyano *N*-oxide is generated in situ by treatment of the chloro oxime with ethyl Grignard followed by addition of cinnamyl alcohol. The cycloaddition product **118** is isolated in 85% yield and 75:25 dr. A stereochemical model suggest that chelation of the magnesium ions by the MOM protecting group and chelation of the N-oxide to the alkoxide ion gives the facial selectivity observed. The dihydroisoxazole is then subjected to a functional group interconversion to transform the free alcohol into ester **120**. Then methylation and selective reduction of the dihydroisoxazole to yield the reduced dihydroisoxazole. The authors did not include a comment on the observed diastereoselectivity. Then after acetyl protection the N-O bond was cleaved using Zn reduction which gives immediate cyclization, **123**. The authors employed Barton deoxygenation to give the des hydroxy lactam. The same intermediate used by Wolfgang and the final steps would have been in accordance with the scheme above.

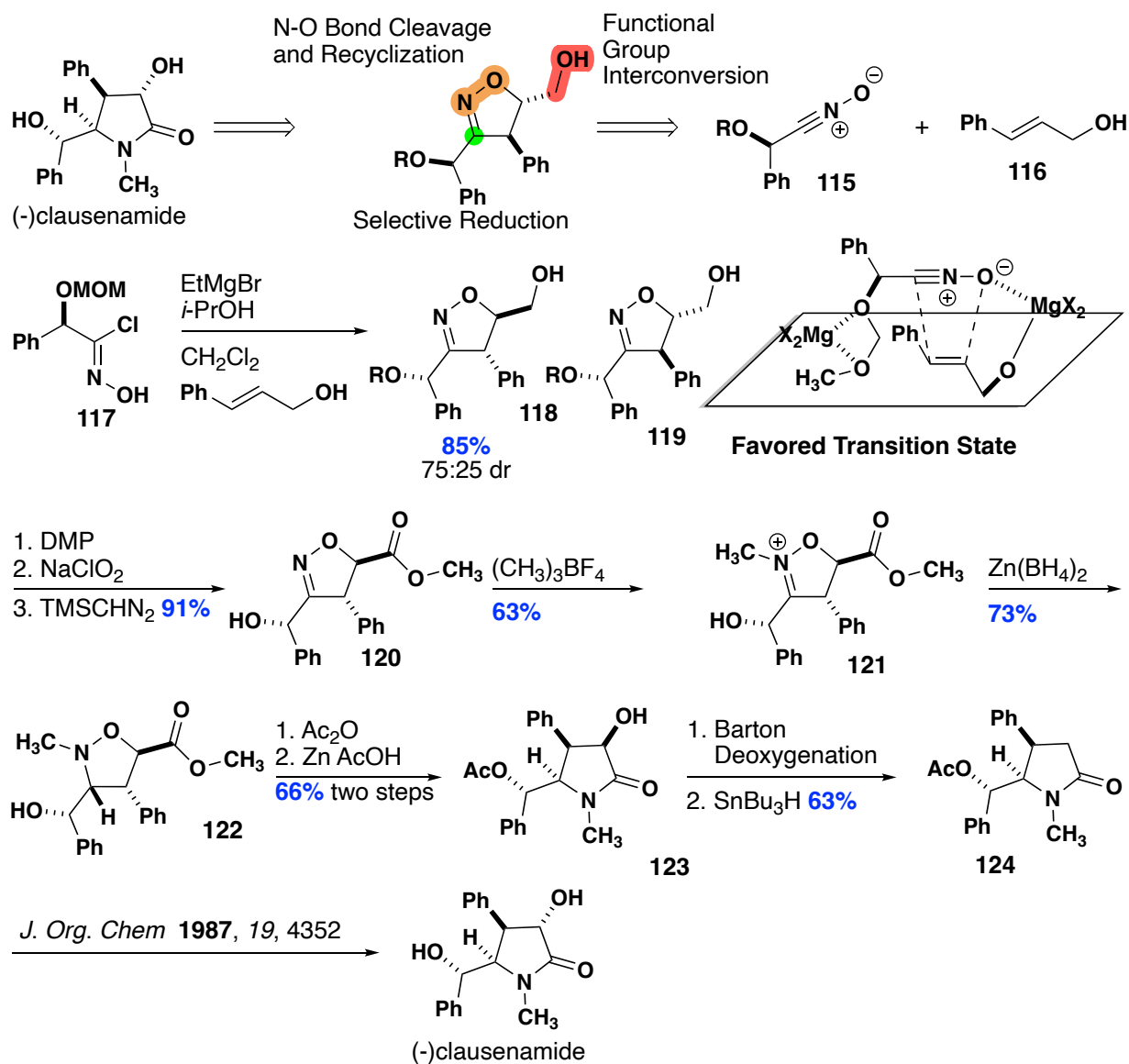


Figure 1.36: 3+2 cycloaddition as key step in formal synthesis of (-)-clausenamide

Another formal synthesis was reported in 2018 also utilizing the dihydroisoxazoles as the key intermediate.⁴⁴ This is also a formal synthesis that uses a sulfur ylide to do a conjugate addition on the α,β -unsaturated nitro alkene (**Figure 1.37**). The reaction is highly diastereoselective yielding a single detectable isomer of **127**. The authors then selectively oxidize the benzylic carbon using AgOTf and acylate the free alcohol with an

acyl chloride. The authors then reference the above synthesis to complete the route. Which is ironic considering the above synthesis is also a formal synthesis.

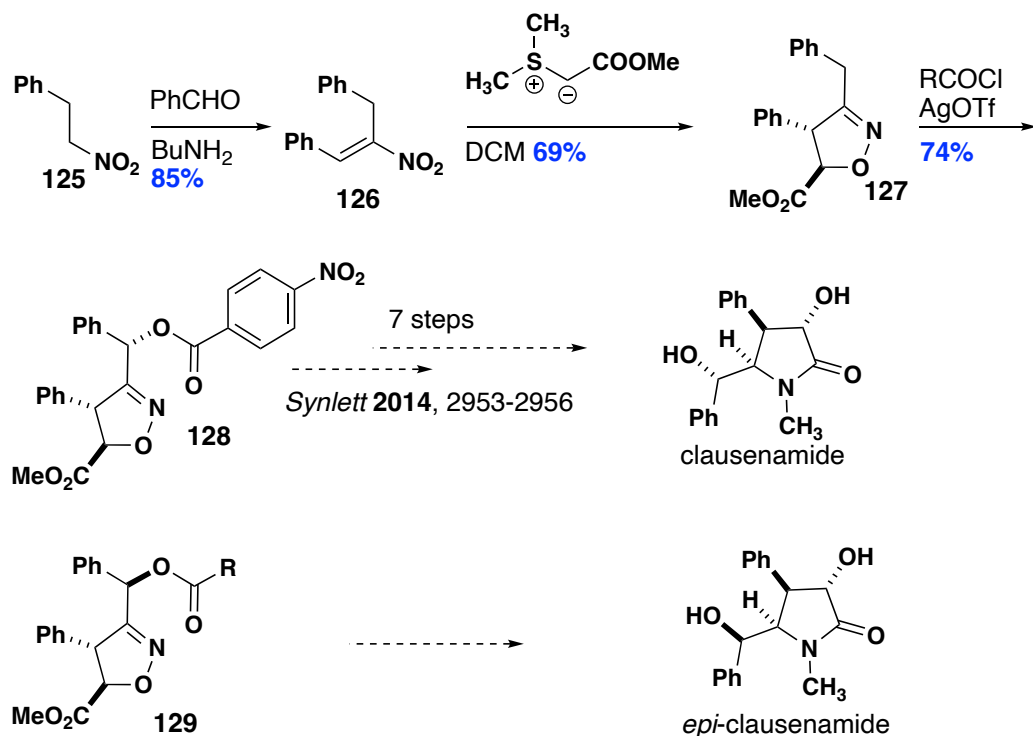


Figure 1.37: Formal synthesis of clausenamides

The last two syntheses reported do not rely on the dihydroisoxazoles. Instead the synthesis of (+)*epi*-clausenamide relies on a Suzuki coupling reaction.⁴⁵ Reacting the Boc protected amino acid with EDCI and Meldrums acid followed by tosylation yields the unsaturated lactam, **131**. This compound is then subjected to Suzuki coupling with phenyl boronic acid, **132**. Following a hydrogenation, boc deprotection and methylation yields a lactam that has been a common intermediate in most of the syntheses thus far. The primary alcohol is deprotected with TBAF and then oxidized to the aldehyde followed by treatment with phenyl Grignard. In previous syntheses this stereogeniccenter would be epimerized to the correct configuration. The oxidation of the CH₂ is performed in a similar manner to that of Wolfgang.

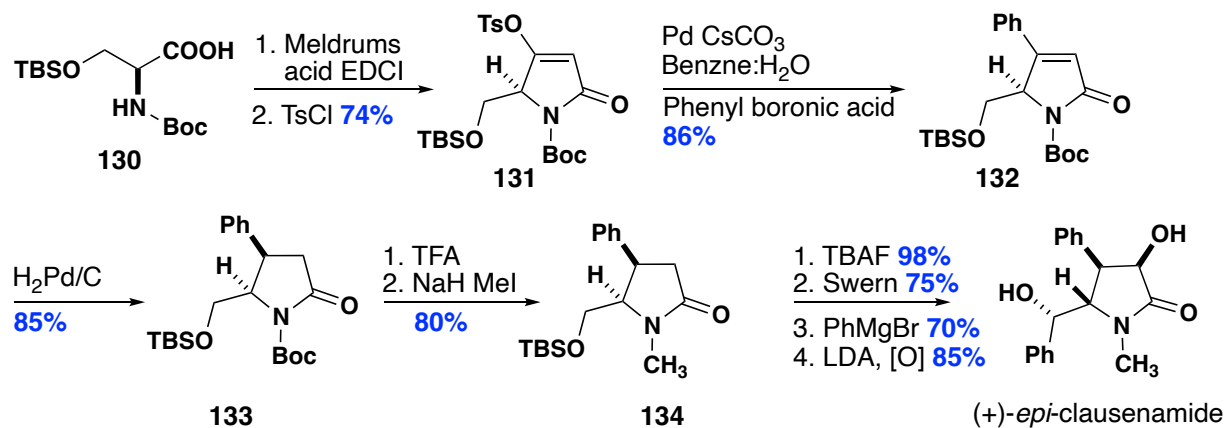


Figure 1.38: Suzuki coupling as key step for the installation of phenyl group

The formal synthesis of *epi-neo*-clausenamamide was achieved using an NHC catalyzed reaction (**Figure 1.39**).⁴⁶ The NHC catalyzed reaction gives high diastereoselectivity for the trans isomer and product **137** is highly enantioenriched. The product is a lactam like that accessed by many synthetic schemes thus far. The denosylation and then methylation yields the *N*-methyl lactam. This is a formal synthesis, and the publication references a Chinese patent which would have completed the synthesis.

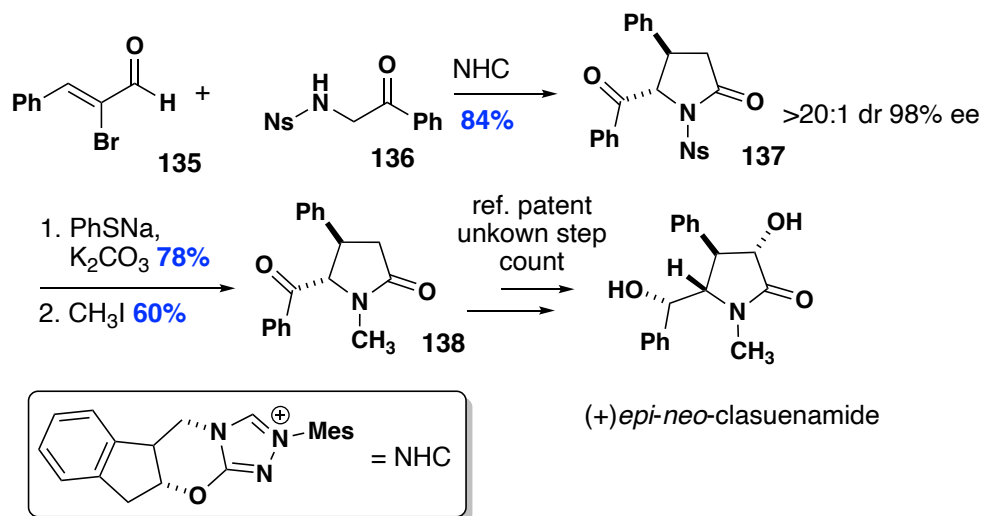


Figure 1.39: NHC catalyzed cyclization to gamma lactam

1.1.5 Bioactivity of clausenamide

Traditional Chinese Medicine (TCM) has been indirectly utilizing naturally occurring compounds for well over two thousand years.³⁵ In a modern context, efforts to isolate the natural products responsible for observed medicinal properties have become increasingly rewarding because of advances in isolation and structure determination techniques. Clausenamide (clau) was isolated in 1986, from *C. lansium*, an evergreen native to Southeast Asia.³⁶ The plant grows an edible yellow fruit resembling a grape, known as wampi, which is very popular in southern China. TCM texts detail how extracts from the leaves of *clausena lansium* can be used to treat jaundice; isolation of the extract's components yielded seven isomeric lactams containing four contiguous stereogenic centers. The parent molecule clausenamide is reported to have shown promising biological activity in the treatment of Alzheimer's disease (AD).³⁵ AD is a neurodegenerative disease characterized by a decline in cognitive function, which can be the result of senile plaques, neurofibrillary tangles, and loss of neurons and synapses.³⁶ In order to investigate the effects of clausenamide on cognitive decline. In an *in vivo* study, improvements in learning and memory were observed following the administration of 5-10 mg/kg of (-)clausenamide to mice. In an *in vivo* study, increased thickness of the cerebral cortex as well as increased synaptic density in the hippocampal region was observed. These initial results are promising, as current strategies for the treatment of Alzheimer's involve limiting synaptic loss and increasing synaptogenesis. While (-)clausenamide shows promising preliminary results, (+)clausenamide is a biologically inactive isomer. The pharmacodynamics and pharmacokinetics of (-)clausenamide and

its enantiomer have also been investigated. In a pharmacodynamic study, it was found that only 28.5% of (-)-clausenamide is protein-bound compared to 38.5% of (+)-clausenamide when added to rat plasma. In a pharmacokinetic study, it was discovered that the main metabolic pathway for the active clausenamide isomer involves hydroxylation of the *N*-methyl substituent, with subsequent demethylation.

1.2 Acyclic Stereocontrol of α -Chiral *N*-Sulfonyl Imines with Prochiral BF_3K and Crotyl Trimethyl Silane Nucleophiles.

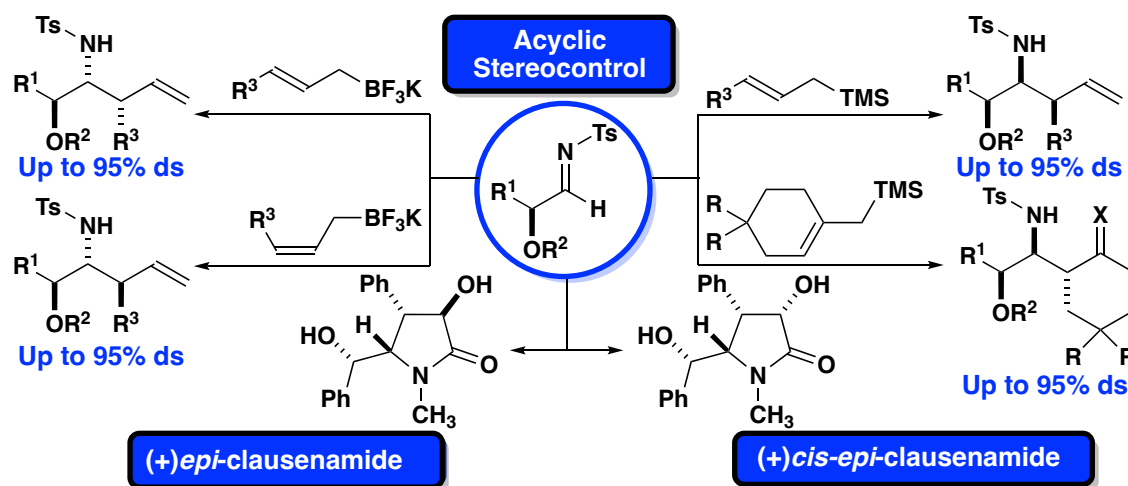


Figure 1.40: Diastereoselective crotylation of α -chiral alkoxy imines leading to all four different diastereomeric products.

The diastereoselective crotylation of α -alkoxy *N*-tosyl imines will now be described. Acyclic stereocontrol of carbons 2, and 3 is achieved in a single step and each of the four possible diastereomeric products can be isolated in high selectivity and yield. The transition states leading to the observed products have been located and analyzed with density functional theory (B3LYP-D3/6-31G(d)). The stereocontrolled reaction was then employed in a divergent synthesis of two epimers of clausenamide: (+)-*epi*-clausenamide and, (+)-*cis-epi*-clausenamide.^{35,36,45}

1.2.1 Nucleophilic Addition of *E* and *Z* Crotyl BF₃K Nucleophilic Alkenes to α -Chiral *N*-Sulfonyl Imines

The *E* and *Z* substituted nucleophilic crotyl BF₃K reagents needed to be synthesized before they could be screened. With the nucleophiles synthesized they were reacted in the optimized reaction conditions to develop an understanding of the stereochemical outcome at carbons 2 and 3.

1.2.1.1 Synthesis of *E* and *Z* Crotyl-BF₃K Nucleophile

The major synthetic challenge was the synthesis of the corresponding nucleophilic alkenes in high *E* to *Z* ratio. To solve this synthetic challenge, I used two different routes to synthesize each isomer of alkene (**Figure 1.41**).

The *E*-substituted BF₃K nucleophiles was synthesized using a palladium catalyzed borylation of the allylic alcohol. This gave the allylic borylated product in >95:5 *E* to *Z* ratio. Stirring the borylated compound in KHF₂ water and methanol would yield the BF₃K nucleophile in >95:5 *E* to *Z* ratio after crystallization in acetone. The *E* to *Z* ratio was measured using proton NMR and *J* coupling analysis of the two vinyl protons. The *E* isomer has a *J* value of 14-16 Hz and the *Z* isomer has a *J* value of 9-11 Hz. The (*Z*)-crotyl BF₃K was commercially available.

The complementary (*Z*)-BF₃K nucleophiles were synthesized in a four-step sequence. First the pentyne was iodinated using *n*-BuLi and I₂. Then alkyne was stereospecifically reduced to the (*Z*)-iodo alkene by a hydroboration protonation reaction. The vinyl iodide was then subjected to a lithium halogen exchange followed by a Matteson

reaction. This gave the *Z*-isomer in >95:5 *E* to *Z* ratio and then subjected to KHF_2 , methanol and water and was isolated in >95:5 *E* to *Z* ratio after crystallization in acetone.

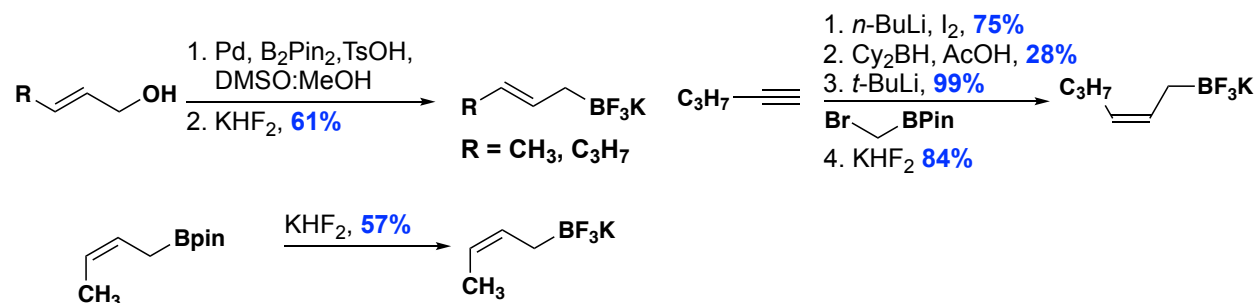


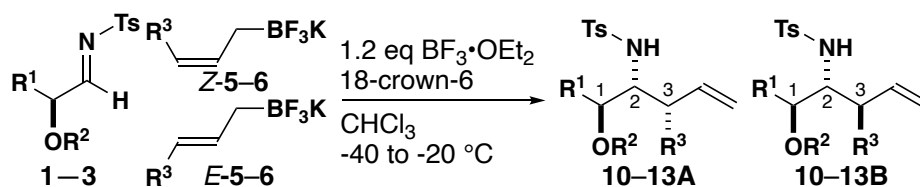
Figure 1.41: Synthesis of crotyl BF_3K nucleophiles.

1.2.1.2 Results of Nucleophilic Addition of *E* and *Z* crotyl BF_3K Nucleophilic alkenes to α -Chiral *N*-Sulfonyl Imines

Nucleophile *E*-5 was added to *N*-tosyl imine **1** to give product **10A** with >95:5 diastereoselectivity (**Table 1.7**). Compound **10A** had the expected *anti*-stereochemistry at C1 and C2 and *syn*-stereochemistry at C2 and C3. Changing the alkene geometry of the nucleophile to the *Z* configuration produced the complementary major product **10B** in 62% yield with 90% diastereoselection (entry 2, **Table 1.7**). The same *anti* selectivity at C1 and C2 is observed, but now C2 and C3 have *anti* stereochemistry. Crotyl BF_3K nucleophiles *E*-6 and *Z*-6 were also added to imine **1** and gave similar levels of stereocontrol, 95% diastereoselection for **11A**, and 91% diastereoselection for **11B** (entries 3 and 4, **Table 1.7**). While the α -stereogenic center of the electrophile completely controls the facial approach of the nucleophile, the two new stereogenic centers at C2 and C3 are largely controlled by the geometry of the alkene nucleophile.

Imines **2** and **3** were screened to determine the effect of added substitution. The addition of *E*-**6** crotyl BF₃K to imines **2** and **3** gave 95% diastereoselection for products **12A** and **13A** respectively (entries 5 and 7, **Table 1.7**)

The crotylation of imines **2** and **3** with *Z*-**6**-crotyl BF₃K gave 95% diastereoselectivity for products **12B** and **13B** respectively (entries 6 and 8, **Table 1.7**). Overall, imine substituents with a range of steric influence all undergo highly stereoselective addition reactions with substituted allyl BF₃K reagents.



Entry	R ¹	R ²	R ³	<i>E/Z</i>	Yield	A:B ^a
1	CH ₃	Bn	<i>n</i> -Pr	<i>E</i> - 5	10A ^b 56%	95:5
2	CH ₃	Bn	<i>n</i> -Pr	<i>Z</i> - 5	10B 62%	10:90
3	CH ₃	Bn	CH ₃	<i>E</i> - 6	11A 76%	95:5
4	CH ₃	Bn	CH ₃	<i>Z</i> - 6	11B 53%	9:91
5 ^c	Bn	Bn	CH ₃	<i>E</i> - 6	12A ^b 47%	95:5
6	Bn	Bn	CH ₃	<i>Z</i> - 6	12B 56%	5:95
7	Ph	CH ₃	CH ₃	<i>E</i> - 6	13A 72%	95:5
8	Ph	CH ₃	CH ₃	<i>Z</i> - 6	13B ^b 51%	5:95

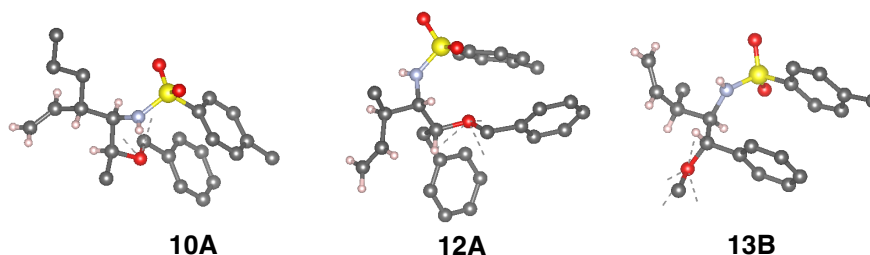


Table 1.7: Results for crotylation using BF₃K nucleophiles.

1.2.1.3 Closed Transition State Detailing Stereochemical Selectivity

The reaction characteristics of crotyl-BF₃K^{4,14,16–18,21,47,48} and crotyl trimethyl silane^{29,28} were used to develop stereochemical models for the observed selectivity in the nucleophilic additions to α -chiral alkoxy *N*-tosyl imines. In the case of highly diastereoselective additions of *E*-**6** and *Z*-**6** crotyl BF₃K salts; first, a fluoride is abstracted by BF₃•OEt₂, generating the highly electrophilic crotyl BF₂ species *E*-**22** and *Z*-**22** (**Figure 1.42**).⁴⁷ The lone pair of the (*E*)-imine coordinates to the electrophilic boron generating a chair transition state structure. The lowest energy pathway with *E*-**22** is *E*-**TS1**, leading to the observed diastereomer **24A**. In *E*-**TS1**, the methyl of *E*-**22** is pseudo equatorial and thus imposes no 1,3 diaxial interactions with the *N*-mesyl. The C2, C3 *syn* stereochemistry is dictated by the (*E*)-geometry of the imine.^{22,49,50} In each case where the imine has isomerized to the (*Z*)-geometry, *E*-**TS2** and *E*-**TS4**, C2-C3 are *anti*.²²

The *anti*-selectivity of C1 and C2 observed in **24A** and **24B** from *E*-**TS1** and *Z*-**TS2** is the result of a Cornforth orientation **25**, with the electronegative α -alkoxy group and the imine *anti*, following the dipole-dipole repulsion model proposed by Cornforth.⁵¹ The stereoelectronically favored,⁵² polar Felkin-Anh conformer **26** induces a non-bonded interaction between the α -alkyl group of the imine and the developing chair transition state.²⁰ Analysis of the stereochemical elements in the transition state explicitly details the high diastereoselectivity using crotyl BF₃K reagents.

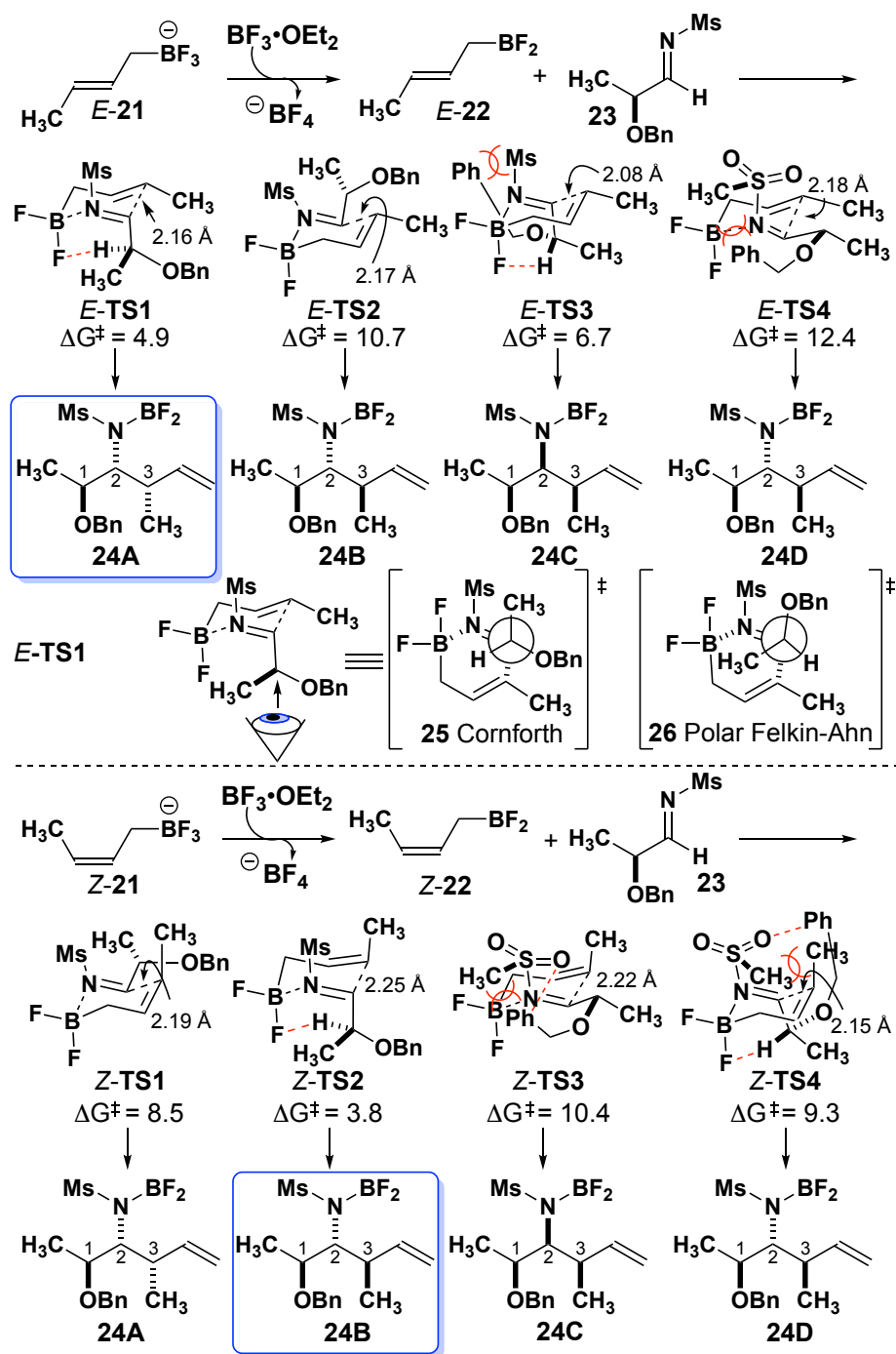


Figure 1.42: Calculated closed transition states.

1.2.1.4 Synthesis of *E* and *Z* Crotyl-TMS Nucleophiles

A series of *E* and *Z* substituted silanes were synthesized to screen in the zinc chelated reaction conditions. I reacted the allylic chloride with trichlorosilane catalytic

copper chloride and triethyl amine in diethyl ether to synthesize the (*E*)-crotyl, (*E*)-propyl and (*E*)-cinnamyl substituted nucleophilic silane. The (*Z*)-crotyl silane was synthesized from the vinyl iodide I had synthesized above and then subjected it to a Kumada coupling with (trimethylsilyl)methylmagnesium bromide. Then I subjected butadiene to palladium catalyzed hydrosilylation with trichlorosilane and then quenched with methyl magnesium bromide to synthesize the (*Z*)-crotyl trimethyl silane nucleophile. In these cases, unlike the BF₃K nucleophiles which were salts, I confirmed the *E* to *Z* geometric ratio of each of these nucleophiles by GCMS. In each of the syntheses described >100:1 selectivity was observed. The final silane nucleophile was synthesized from cyclohexanone. The enolate was trapped as the phosphonate and then subjected to a Kumada coupling using (trimethylsilyl)methylmagnesium bromide. With the nucleophilic alkenes in hand the chelate controlled reaction could now be tested

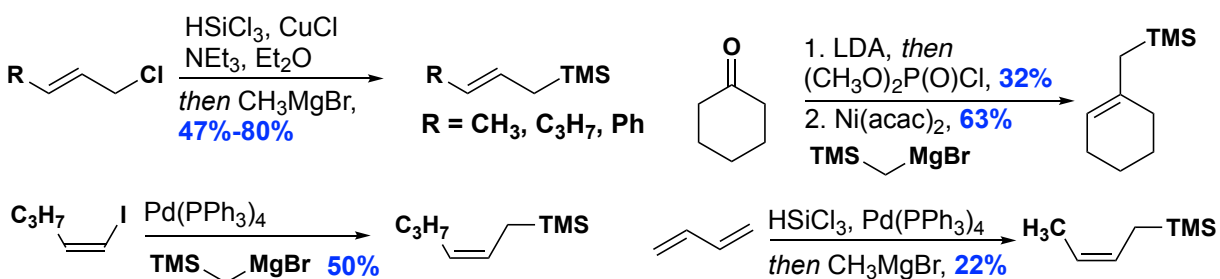


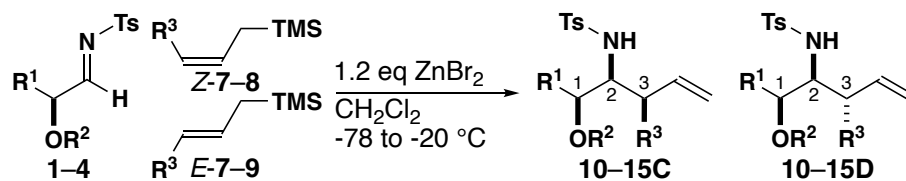
Figure 1.43: Synthesis of silane nucleophiles.

1.2.2 Results Nucleophilic Addition of *E* and *Z* Crotyl Trimethyl Silane Nucleophilic Alkenes to α -Chiral *N*-Sulfonyl Imines

Substituted allylsilanes were examined, to achieve complementary selectivity with the goal of producing isomers **C** and **D** selectively. Nucleophile *E*-7 was added to *N*-tosyl imine **1** using ZnBr₂ as Lewis acid mediator, giving **10C** in 95% diastereoselection. (entry

1, **Table 1.8**). To imine **1** was added crotyl TMS *E-8* giving **11C** in 89:11 diastereoselectivity (entry 3, **Table 1.8**). Nucleophilic addition of *E-8* to imine **2**, provided **12C** with similar diastereoselectivity 88% (entry 5, **Table 1.8**). Imine **3**, reacted with *E-8* crotyl allyl TMS and ZnBr₂ to give **13C** in 95% diastereoselection (entry 7, **Table 1.8**). The addition of (*E*)-cinnamyl trimethylsilane *E-9* to imine **3** bearing an α -methoxy was highly diastereoselective, yielding a single detectable diastereomer (entry 9, **Table 1.8**). However, addition of *E-9* to imine **4** decreased the diastereoselectivity to 86% with ZnBr₂ as the promoter. Substituting ZnCl₂ as the Lewis acid promoter increased the diastereoselectivity to 95:5 (entry 10, **Table 1.8**). In all cases, excellent facial selectivity was observed in that only isomers **C** and **D** were formed. These results are complementary to the C1-C2 facial selectivity of allylic BF₃K reagents.

In contrast (*Z*)-substituted allyl trimethylsilanes react with lower diastereoselectivity than the (*E*)-substituted counterpart. The addition of *Z-7* using ZnBr₂ was unselective, giving 60% diastereoselectivity for **10D** and 40% of **10C** (entry 2, **Table 1.8**). The addition of crotyl silane *Z-8* to imine **1** gave a small preference for the *syn* diastereomer, 67% of **11C** and 33% of **11D** (entry 4, Table 2). The addition of *Z-8* to imines **2** and **3** gave 95% diastereoselectivity for **12C** and **13C**, respectively (entries 6 and 8, **Table 1.8**), the same sense of induction is seen with *E-8* and imine **1**. In summary, **10-15C** is favored in all cases except entry 2 in Table 2.



Entry	R ¹	R ²	R ³	E/Z	Yield	C:D ^a
1	CH ₃	Bn	<i>n</i> -Pr	<i>E</i> -7	10C ^b 77%	95:5
2	CH ₃	Bn	<i>n</i> -Pr	<i>Z</i> -7	10D 11%	40:60
3	CH ₃	Bn	CH ₃	<i>E</i> -8	11C 53%	89:11
4	CH ₃	Bn	CH ₃	<i>Z</i> -8	11C nd ^e	67:33
5 ^c	Bn	Bn	CH ₃	<i>E</i> -8	12C 61%	88:12
6	Bn	Bn	CH ₃	<i>Z</i> -8	12C nd ^e	95:5
7	Ph	CH ₃	CH ₃	<i>E</i> -8	13C 75%	95:5
8	Ph	CH ₃	CH ₃	<i>Z</i> -8	13C nd ^e	95:5
9	Ph	CH ₃	Ph	<i>E</i> -9	14C 75%	95:5
10	Ph	Bn	Ph	<i>E</i> -9	15C 85%	95:5
11 ^a	CH ₃	Bn	<i>n</i> -Pr	<i>Z</i> -7	10D nd%	47:53
12 ^b	CH ₃	Bn	<i>n</i> -Pr	<i>Z</i> -7	10D 11%	25:75
13 ^c	CH ₃	Bn	<i>n</i> -Pr	<i>Z</i> -7	10D 11%	55:45
14 ^d	CH ₃	Bn	<i>n</i> -Pr	<i>Z</i> -7	10D 11%	40:60
15 ^b	CH ₃	Bn	CH ₃	<i>Z</i> -8	11C nd ^e	42:58

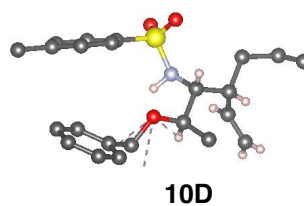
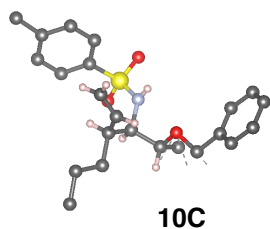


Table 1.8 ^aZnCl₂ as Lewis acid, ^bZnI₂ as Lewis acid, ^cCF₃C₆H₅ as solvent, ^dNO₂CH₃ as solvent

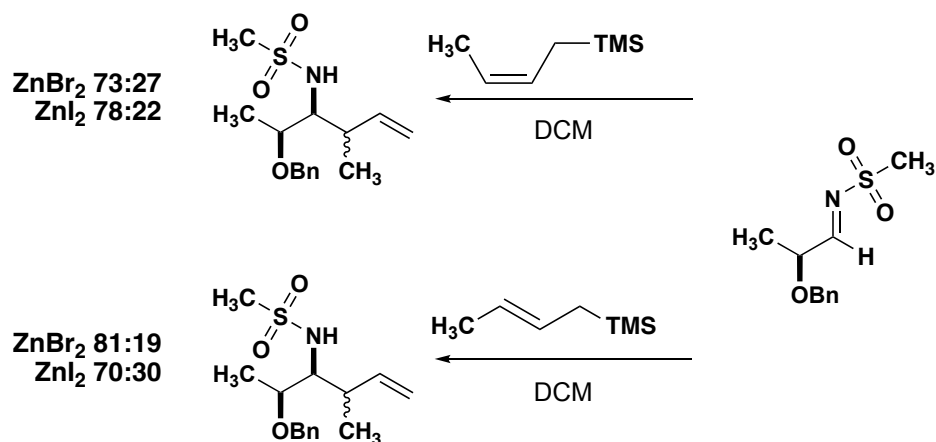


Figure 1.44: (*E*) and (*Z*)-crotyl silane additions to imine 1.

The selectivity for *Z* substituted silanes were attempted to be optimized (entries 11-15 **Table 1.8**). First other zinc salts were screened, only zinc chloride or iodide gave any reaction. Unfortunately, none of these Lewis Acids could increase the selectivity for the desired diastereomer D. Next different electronic solvents were screened to understand if the polarity of the solvent had a significant impact on the reaction. It is important to note that the solvent needed to be sufficiently polar to dissolve enough zinc into the reaction, thus non-polar solvents like hexane were not screened. However the solvent also had a negligible effect on the diastereoselectivity of the reaction.

Finally, the tosyl imine was substituted with mesyl to see if the imine substitution had any effect on the diastereoselectivity (**Figure 1.44**). To accurately assess the selectivity the imine was reacted with *E*-**8** to establish a baseline of diastereoselectivity. In this case the selectivity was diminished compared to its tosyl counterpart at 81:19 and the selectivity was even worse with ZnI_2 at 70:30. Using *Z*-**8** as the nucleophile the ratio of *syn* 2,3 to *anti* 2,3 was 73:27, and with ZnI_2 the induction was 78:22. Unfortunately the diastereoselectivity of diastereomer D could not be improved.

Cyclic allyl silanes **16** and **17** were added to imine **1** and were highly diastereoselective for the *syn* 1,2 and *anti* 2,3 product. Silanes **16** and **17** have a similar (*E*)-geometric alkene configuration to *E*-**8**. Based on observations with *E*-**8**, it was hypothesized that the major diastereomer would be analogous. That is *syn* between both C1-C2 and C2-C3. However, addition of silane **16** to imine **1**, yielded product **18** in 80:20 dr, favoring the *syn* C1-C2, *anti* C2-C3 diastereomer (**Figure 1.45**). This is the opposite result to the addition of silane *E*-**8** to imine **1** under the identical conditions. The exocyclic alkene was ozonolyzed to yield the crystalline ketone **19**. The addition of the more sterically hindered nucleophilic silane **17** gave the same stereochemical result with greater selectivity (95:5) for the formation of **20**. These results may eventually enable the design of other allylsilane nucleophiles that form isomer **D** selectively.

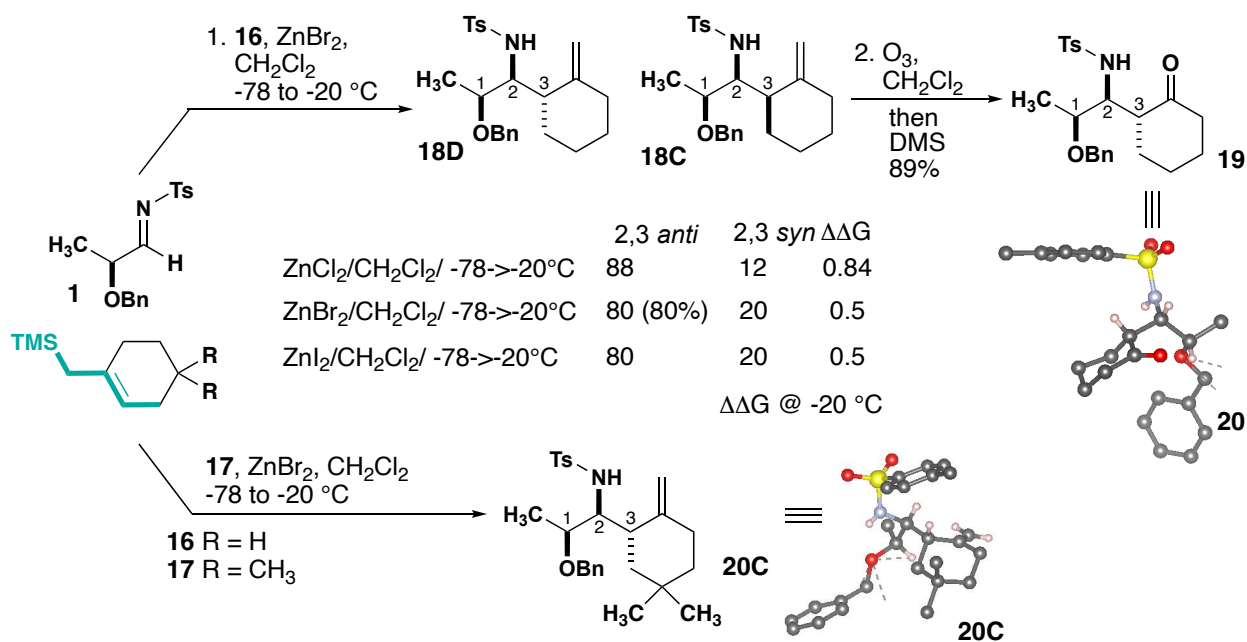


Figure 1.45 ^adr was measured using ¹H NMR of the unpurified reaction mixture. ^bThe relative stereochemistry **19** and **20C** were established by X-ray crystallography.

1.2.2.1 Open Transition State Detailing Stereochemical Selectivity

The transition states for the addition of crotyl silanes to **25** were computed as well. The zinc-chelated imine **26** positions the methyl group on the ring to create a more sterically hindered face resulting in high *syn* diastereoselectivity for C1 and C2 (**Figure 1.46**). The C2-C3 *syn* addition is set via three alignments: one antiperiplanar and two synclinal orientations. Alternatively, opposite facial attack of the allyl silane results in the C2-C3 *anti* adduct via another set of antiperiplanar and synclinal conformations. The **1-Anti-S** (antiperiplanar-*syn* product) transition state is the lowest energy conformer (5.2 kcal/mol) of the possible six transition states and leads to the experimentally observed major diastereomer **27C**. This transition state arranges the crotyl trimethyl silane *E-8* in an antiperiplanar approach to the zinc-chelated imine. The lowest energy transition state for the minor diastereomer, **27D**, is **1-Anti-A** (6.0 kcal/mol). The $\Delta\Delta G$ between the **1-Anti-A** and **1-Anti-S** is 0.8 kcal/mole in excellent agreement with the experimental results reported for **1** and *E-8* (Table 2, Entry 3). The **1-Syn1-S** (synclinal-*syn* product) transition state reorients to **1-Anti-S**. Therefore the **1-Syn1-S** transition state structure is too unstable to be a viable pathway. In all cases, synclinal orientations are higher energy than the two antiperiplanar ones.

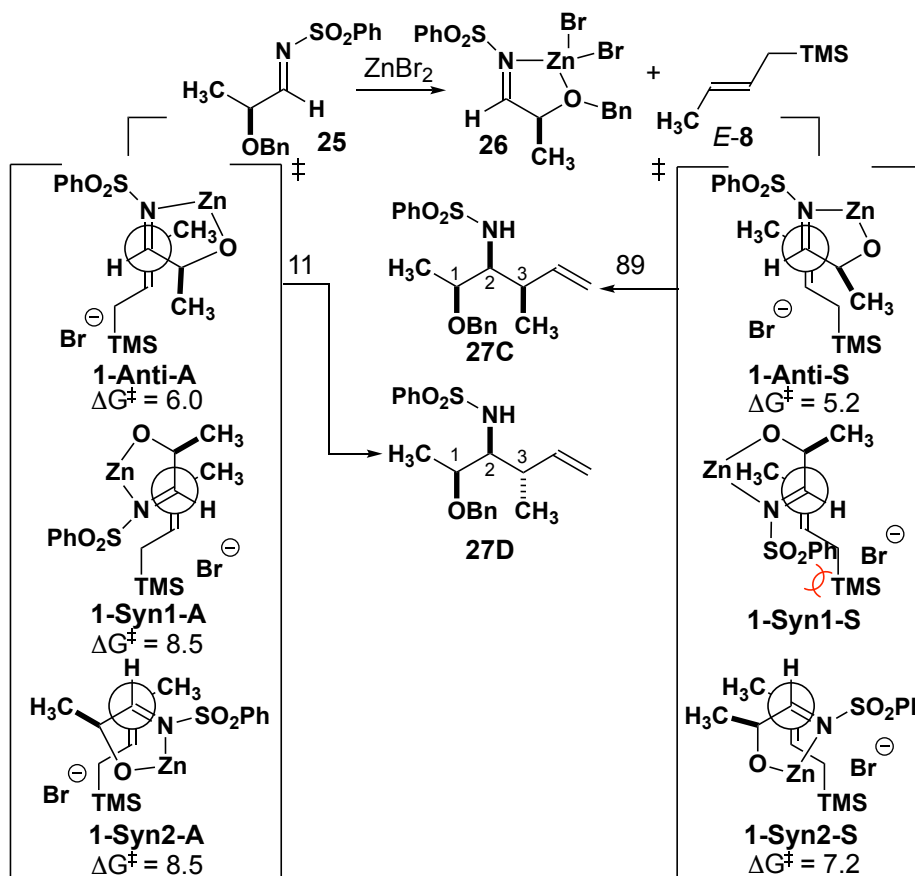


Figure 1.46: Calculated open transition states with chelate **26** and (E) -crotyl silane.

The calculated transition states for the addition of silanes **16** and **17** to chelate **26** show a change in the orientation of the prochiral nucleophile leading to opposite selectivity from the acyclic cases (**Figure 1.47**).⁵³ This change in transition state is interesting because compared to **2-Anti-A** visually **2-Anti-S** would appear to be more favorable because visually it minimizes any non bonding interactions. However **2-Anti-A** is the lowest in energy transition state. Analyzing the transition states for **17** silane nucleophile we can see now that **3-Syn1-A** is the lowest in energy and in this transition state the synclinal orientation is preferred. This indicates that simple steric analysis of the cyclic allyl silanes cannot give a predictive model on selectivity but solves the challenge of accessing the *anti* 2,3 product.

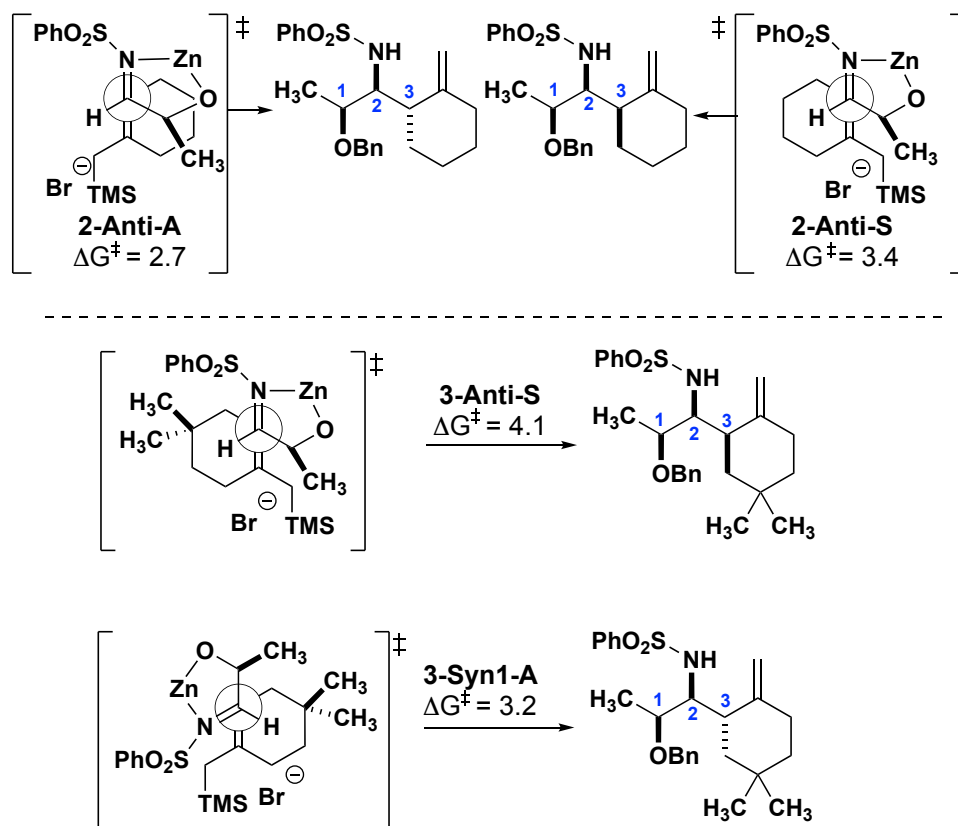


Figure 1.47: Calculated open transition states for nucleophiles **16** and **17**.

1.3 Total Synthesis of (+)*cis-epi* and (+)*epi-clausenamide*

This diastereoselective method was highlighted in the diastereoselective synthesis of (+)*cisepi* and (+)*epi-clausenamide*.

1.3.1 Retrosynthetic analysis of (+)*clausenamide* (+)*cis-epi* and (+)*epi-clausenamide*

Retro synthetically disconnecting the amide bond of *clausenamide* reveals an *anti* 1,2 *syn* 2,3 stereochemistry (**Figure 1.48**). This indicates that using *anti* 1,2 *syn* 2,3 reaction would be ideal. The alkene would then be a functional group manipulation away from becoming the target molecule. Similarly (+)*cis-epi-clausenamide* would come from an all *syn* selective reaction to yield the target molecule.

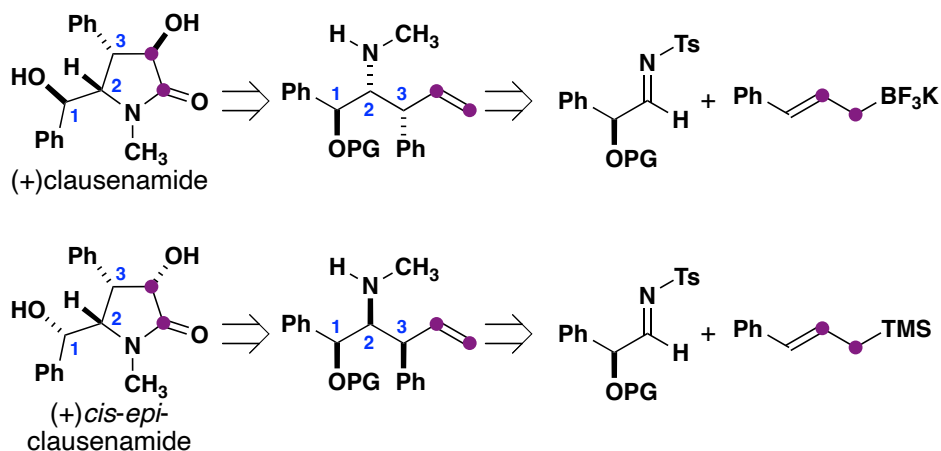


Figure 1.48: Retro Synthetic disconnection for (+)clausenamide and (+)cis-epi-clausenamide

1.3.2 Preliminary Synthesis of (+)clausenamide

To facilitate the synthesis of (+)clausenamide I needed to synthesize the corresponding cinnamyl BF₃K salt (**Figure 1.49**). Starting from the cinnamyl alcohol doing a palladium catalyzed borylation to install the allylic pinacol boronic ester was trivial. After column chromatography the boronic ester was dissolved in MeOH/H₂O and KHF₂ was added. The BF₃K was difficult to recrystallize in acetone and would often lead to other unidentifiable byproducts. The BF₃K salt was able to be isolated in 23% yield however the chemical shifts in the proton NMR of the product did not match the literature values. This was discerning, however the *anti* 1,2 *syn* 2,3 selective reactions was still set up and the reaction gave no product, and all starting material was consumed. A complex mixture of unidentifiable products was isolated after column chromatography. Ultimately this target was abandoned because of the nucleophile and no productive reaction in the key step.

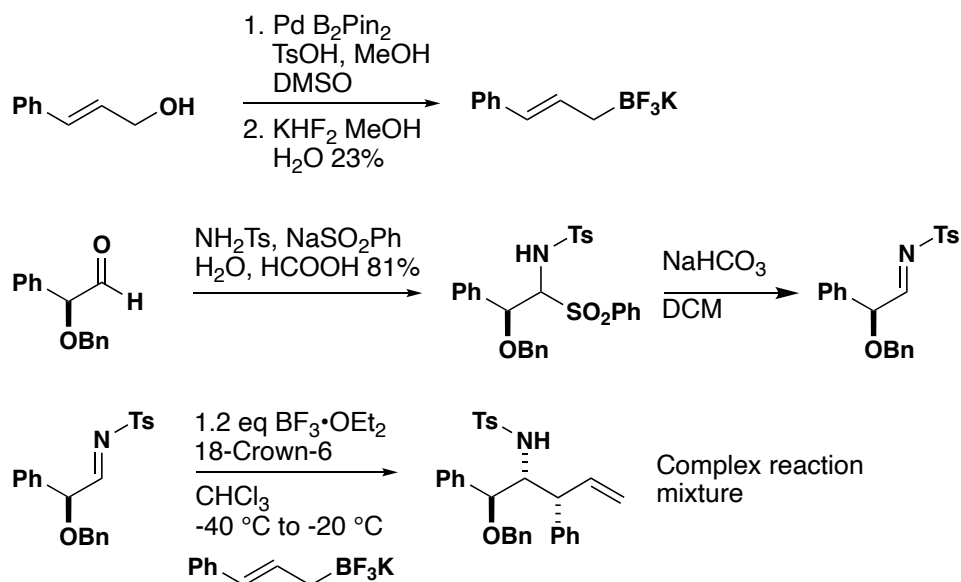


Figure 1.49: Failed route towards (+)clausenamidine

1.3.3 Forward synthesis of (+)*cis-epi*-clausenamidine

The failure to synthesize (+)clausenamidine led to a reroute in which (+)*cis-epi*-clausenamidine now became the target molecule (**Figure 1.50**). The cinnamyl silane synthesis was also trivial at this point and was synthesized in 80% isolated yield. The key step of this reaction needed to be optimized. It became apparent that ZnBr₂ led to an 86:14 mixture of diastereomers; epimeric at C3. Screening other zinc halogen salts revealed that ZnCl₂ could give 95:5 dr of the compound in 76% isolated yield. The reaction could never be scaled past 500 mg. However, at that reaction scale the reaction gave an improved isolated yield at 85%. Checking the enantiomeric purity of the product indicated a 95:5 er. The starting mandelic acid was 99:1 er indicating only a small erosion of enantiopurity of the imine during the reaction. In the *syn* selective reaction is high yielding and very reliable as a result this path towards (+)*cis-epi*-clausenamidine was continued.

Only a few key modifications were needed to synthesize the target molecule from here on. Methylation of the sulfonamide was high yielding and easily isolated. A diastereoselective dihydroxylation of the terminal alkene was attempted. Many different modifications of the AD-mix α and β were screened. However even after 20 days of stirring no reaction was observed and only starting material was recovered. Thus, the idea was conceived that this synthesis could be divergent and two different epimers of clausenamide could be synthesized in 1 route. The terminal alkene was oxidized using OsO_4 , NMO in ACN/ H_2O . Other solvents were screened to test if a solvent effect on diastereoselectivity was possible. However, the solvent screen was fruitless. At this point in the synthesis the epimeric diols could be separated by column chromatography. The diols **28A** and **28B** were subjected to a modified Pinnick oxidation. This oxidation is primary selective and yields the carboxylic acid after 7 days of stirring. The acid was then esterified using TMS-diazomethane in MeOH/DCM.

A few different tosyl deprotections were attempted however no reaction was observed. Sodium naphthalide deprotection of the sulfonamide proceeded smoothly and yielded the cyclized lactam product. At this point hydrogenation of the benzyl ether yielded the target (+)*cis-epi*-clausenamide. The other epimer of diol was carried forward in the exact manner to yield (+)*epi*-clausenamide.

While this sequence is not the shortest synthesis of clausenamide or some of its epimers, the synthetic route is the most modular in that cinnamyl silane can be modified or substituted and the imine derived from mandelic acid can be modified as well. Thus, if

one was so inclined one could use this synthetic scheme to synthesize many synthetic analogs of clausenamide.

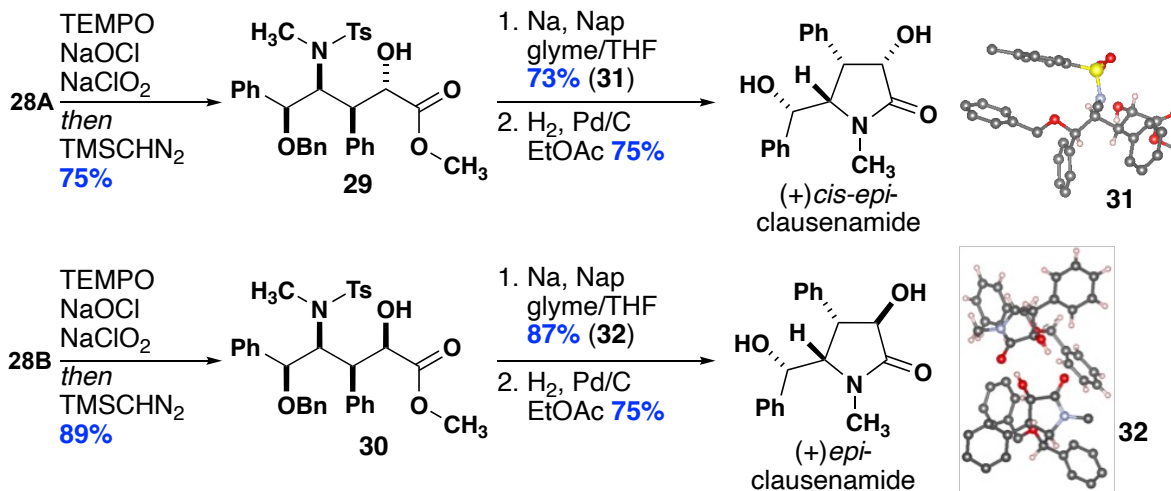
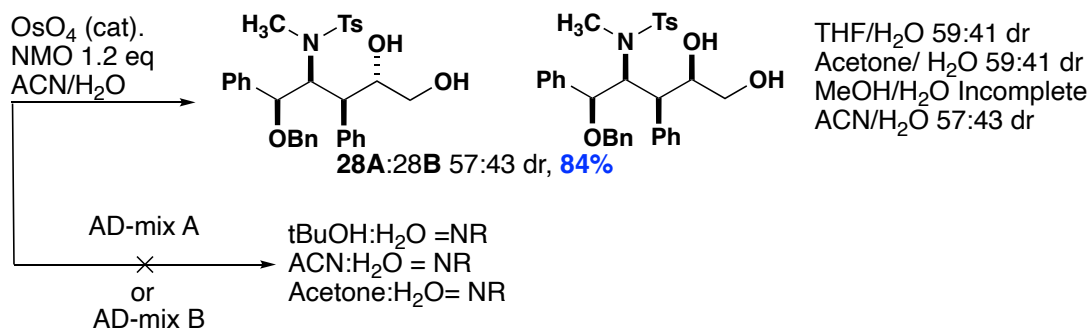
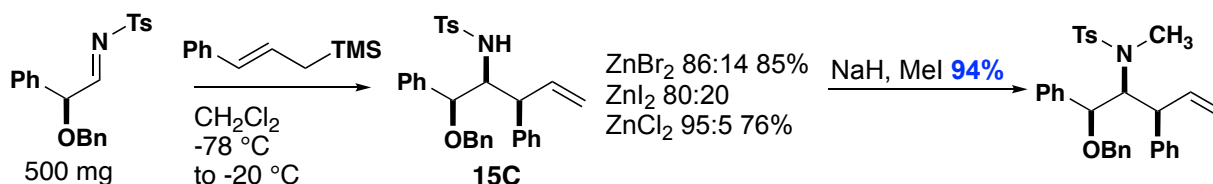


Figure 1.50 Forward synthesis of (+)*cis-epi* and (+)*epi*-clausenamide

1.4 Conclusion

In summary, we have conducted the first exhaustive study of the diastereochemical outcome of substituted nucleophilic alkenes to electron deficient imines derived from α -alkoxy aldehydes. In three out of four cases, one diastereomer out

of four dominates and is formed in >90% selectivity. Although only 65% selectivity can be achieved for the last case, a constrained cyclic analog proceeds with higher selectivity (95%). In the case of the substituted borane nucleophiles, calculations indicate that the major diastereomer is formed through a Zimmerman-Traxler like transition state. The major isomers resulting from substituted allylic silanes emerge from anti-periplanar approach of the acyclic allyl silane nucleophile to the zinc Lewis-acid-chelated imine. The observations of selectivity in the addition of substituted alkene nucleophiles to chiral α -alkoxy *N*-sulfonyl imines enabled a short, stereoselective synthesis of two diastereomers of clausenamide.

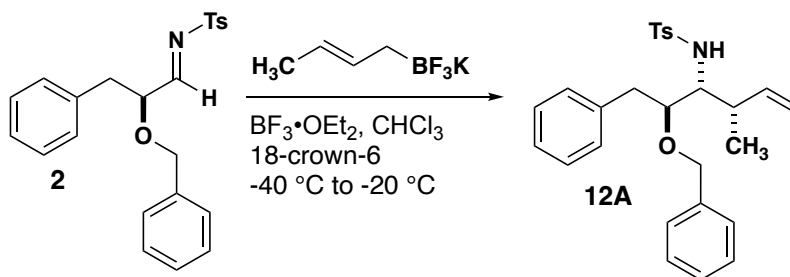
1.5 Experimental Section

1.5.1 Materials and Instrumentation.

Unless otherwise specified, all commercially available reagents were used as received. All reactions using dried solvents were carried out under an atmosphere of argon in oven-dried glassware with magnetic stirring. Dry solvent was dispensed from a solvent purification system that passes solvent through two columns of dry neutral alumina. Chloroform was passed through basic alumina and then stored over molecular sieves in a dark cool environment. ^1H and ^{13}C NMR spectra were acquired at ambient temperature using Varian-600 (600 and 151 MHz, respectively), or Bruker-400 (400 and 100 MHz, respectively) spectrometers, as indicated. The data are reported as follows: chemical shift in ppm from internal tetramethylsilane or referenced to residual solvent (^1H NMR: CDCl_3 δ 7.26. ^{13}C NMR: CDCl_3 δ 77.16) on the δ scale, multiplicity (appar = apparent, br = broad, s = singlet, d = doublet, t = triplet, q = quartet, quint = quintet, sext = sextet, m = multiplet),

coupling constants (Hz), and integration. High-resolution mass spectra (HRMS) were acquired on a Thermo Electron LTQ-Orbitrap XL Hybrid mass spectrometer on positive ESI mode. Melting points were obtained on an EZ-melting apparatus and were uncorrected. Liquid chromatography was performed using forced flow (flash chromatography) of the indicated solvent system silica gel (Fisher, 40-63 μm) packed in glass columns.

1.5.2 General Procedure A 1 mmol scale representative example



***N*-((2*S*,3*R*,4*S*)-2-(Benzyloxy)-4-methyl-1-phenylhex-5-en-3-yl)-4-methylbenzenesulfonamide **12A**.**

Imine **2** (440 mg, 1.12 mmol) was charged to a round bottom flask with stir bar and then dissolved in chloroform (5.5 mL) under argon. Then the reaction was cooled to $-40\text{ }^\circ\text{C}$ dry ice acetonitrile bath. Then $\text{BF}_3 \cdot \text{Et}_2\text{O}$ (0.164 mL, 1.34 mmol) was added to the reaction vessel and was stirred for 10 min. Then (*E*)-but-2-en-1-yltrifluoroborate (55 mg, 0.33 mmol) **E-6** and 18-crown-6 (89 mg, 0.33 mmol) were dissolved in chloroform (5.5 mL) and added in one portion. Reaction was stirred for 1h. The reaction was then transferred to the $-20\text{ }^\circ\text{C}$ freezer overnight. The reaction was quenched with 1/1/1 DCM methanol TEA solution (2.5 mL). Then filtered through silica gel plug and concentrated. The crude mixture was purified by flash chromatography (30:70 Et_2O /hexanes) to afford product **12A**

Yield: 236 mg (47%)

Physical Description: clear colorless solid **mp** 76 °C

Column Conditions: SiO₂, (10% to 30% Et₂O/Hexanes)

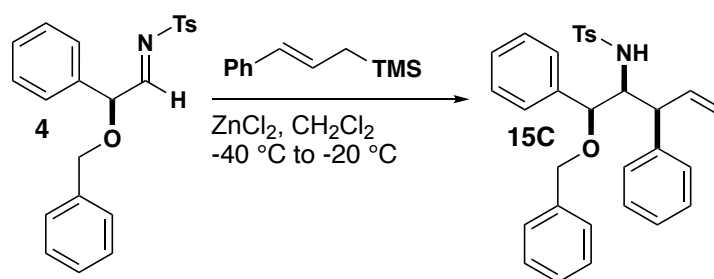
¹H NMR: (400 MHz, CDCl₃) δ 7.56 (d, *J* = 8.3 Hz, 2H), 7.36 – 7.29 (m, 4H), 7.27 – 7.22 (m, 2H), 7.17 (d, *J* = 8.0 Hz, 2H), 7.13 – 7.08 (m, 2H), 7.08 – 7.03 (m, 2H), 5.62 (ddd, *J* = 17.2, 10.3, 7.8 Hz, 1H), 5.03 – 4.88 (m, 2H), 4.60 (d, *J* = 9.4 Hz, 1H), 4.29 – 4.14 (m, 2H), 3.55 (ddd, *J* = 7.7, 6.1, 3.3 Hz, 1H), 3.37 (ddd, *J* = 8.7, 5.0, 3.3 Hz, 1H), 2.86 – 2.70 (m, 2H), 2.57 (dt, *J* = 13.1, 6.9 Hz, 1H), 2.42 (s, 3H), 1.12 (d, *J* = 6.8 Hz, 3H).

¹³C NMR: (101 MHz, CD₂Cl₂) δ 143.0, 141.3, 138.2, 138.1, 138.0, 129.4, 129.2, 128.5, 128.4, 127.6, 127.6, 127.2, 126.5, 114.6, 82.1, 72.3, 58.7, 38.5, 37.2, 21.5, 16.1

IR (neat): 2836, 1597, 1494, 1275, 1147.

AMM: (ESI) *m/z* calcd for C₂₇H₃₁NO₃SH 450.2097; Found 450.2116.

1.5.3 General Procedure B 1mmol scale representative example



N*-((1*S*,2*S*,3*S*)-1-(Benzyloxy)-1,3-diphenylpent-4-en-2-yl)-4-methylbenzenesulfonamide **15C*

Imine **4** (447 mg, 1.18 mmol) was dissolved in methylene chloride (11.8 mL) and transferred to a sealed vial under argon containing ZnCl₂ (192 mg, 1.42 mmol) that was pre-cooled to -78 °C dry ice acetone. Reaction vial was stirred for 10 min. Then silane *E*-

9 (336 mg, 1.77 mmol) was added dropwise to the reaction vessel and stirred for 1h and then transferred to a -20 °C freezer and allowed to stir overnight. The reaction was then diluted using diethyl ether and then passed through a silica plug and concentrated. A sample was taken for crude NMR for dr. The crude mixture was adsorbed onto silica gel and then purified by flash chromatography (30:70 Et₂O/hexanes) to afford product **15C**.

Yield: 501 mg (85%)

Physical Description: clear oil

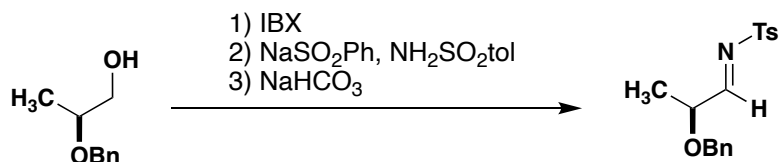
Column Conditions: SiO₂, (10% to 30% Et₂O/Hexanes)

¹H NMR: (400 MHz, CDCl₃) δ 7.37 (dq, *J* = 13.7, 7.0 Hz, 3H), 7.28 (s, 2H), 7.22 (t, *J* = 7.4 Hz, 2H), 7.20 – 7.13 (m, 4H), 7.09 (d, *J* = 7.5 Hz, 2H), 7.01 (d, *J* = 7.2 Hz, 2H), 6.97 (d, *J* = 8.0 Hz, 2H), 6.27 (dt, *J* = 17.0, 10.0 Hz, 1H), 5.19 (dt, *J* = 10.1, 1.1 Hz, 1H), 5.07 – 5.00 (m, 2H), 4.51 (s, 1H), 4.41 (d, *J* = 11.3 Hz, 1H), 4.17 (d, *J* = 11.3 Hz, 1H), 3.78 (ddd, *J* = 9.2, 6.5, 1.7 Hz, 1H), 3.69 (dd, *J* = 9.9, 6.4 Hz, 1H), 2.33 (s, 3H).

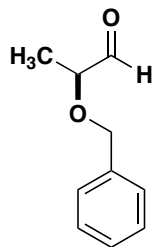
¹³C NMR: (101 MHz, CDCl₃) δ 142.2, 140.9, 138.8, 138.5, 137.4, 136.4, 129.2, 128.6, 128.5, 128.3, 128.3, 128.1, 128.0, 127.5, 126.7, 126.7, 126.4, 118.4, 78.0, 70.7, 64.1, 54.6, 21.4.;

AMM: (ESI) *m/z* : [M - OBn]⁺ Calcd for C₂₄H₂₄NO₃S 390.1528; Found 390.1543.

1.5.4 Preparation of Imines



All imines were prepared in a similar manner as described below



(S)-2-(Benzyloxy)propanal

Aldehyde 1

Was prepared according to literature procedure.⁵⁴ (S)-2-(benzyloxy)propan-1-ol (0.750 g, 4.5 mmol) was dissolved in ethyl acetate (43 mL) 0.14 M final concentration, and IBX (3.78 g, 3.00 mmol) was added. The resulting suspension was heated in an aluminum heating block to 80 °C and stirred vigorously open to the atmosphere. After 3.25 h (TLC monitoring), the reaction was cooled to 0 °C and filtered through celite and a medium glass frit. The filter cake was washed with 3 × 10 mL of ethyl acetate, and the combined filtrates were concentrated to yield the corresponding aldehyde

Yield: 738 mg (100%)

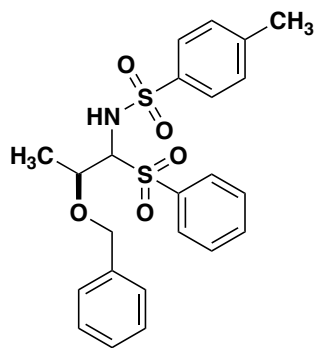
Physical Description: clear oil

Column Conditions: SiO₂, (10% to 30% Et₂O/Hexanes)

¹H NMR: (400 MHz, CDCl₃) δ 9.67 (d, *J* = 1.6 Hz, 1H), 7.41 – 7.30 (m, 5H), 4.63 (q, *J* = 11.8 Hz, 2H), 3.90 (qt, *J* = 7.0, 1.6 Hz, 1H), 1.33 (dd, *J* = 7.0, 1.2 Hz, 3H)

AMM: (ESI) *m/z* : [M - OBn]⁺ Calcd for C₂₄H₂₄NO₃S 390.1528; Found 390.1543.

Compound is in agreement with literature values⁵⁵



***N*-((2*S*)-2-(Benzyloxy)-1-(phenylsulfonyl)propyl)-4-methylbenzenesulfonamide**

Imine precursor 1

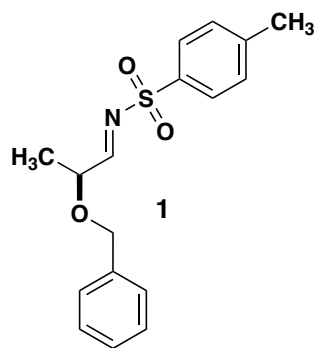
The (*S*)-2-(benzyloxy)propanal (0.738 g, 4.5 mol) was charged into a round bottom flask along with TsNH₂ (0.769 g 4.5 mol) and phenyl-sulfinate (0.885 g 5.4 mol) then formic acid (7 mL) was added. The reaction was allowed to stir until the mixture solidified. The reaction was then diluted with water and filtered. The solids were rinsed with hexanes and water and dried under vacuum. The amido sulfone was then isolated as a white powder. This imine precursor can be stored at 0 °C for many months without significant degradation.

Yield: 1.5 g (75%)

Physical Description: White Solid

¹H NMR: (600 MHz, CDCl₃) δ 7.67 – 7.63 (m, 2H), 7.58 (d, J = 8.3 Hz, 2H), 7.56 – 7.51 (m, 1H), 7.38 – 7.27 (m, 5H), 7.25 – 7.22 (m, 4H), 5.56 (d, J = 9.7 Hz, 1H), 4.61 – 4.55 (m, 3H), 4.50 (d, J = 11.0 Hz, 1H), 2.42 (s, 3H), 1.14 (d, J = 6.4 Hz, 3H).

Compound is in agreement with literature values⁵⁶



(*S,E*)-*N*-(2-(Benzyloxy)propylidene)-4-methylbenzenesulfonamide (1)

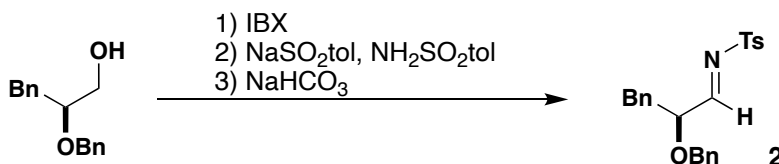
The amido sulfone (150 mg, 0.326 mmol) was then dissolved in DCM (5 mL) in a separatory funnel and then a saturated aqueous solution of NaHCO₃ (30 mL) and vigorously shaken for 60 seconds. The layers were then separated and the organic layer was dried over Na₂SO₄ and filtered and concentrated to yield the title imine as an off white oil (0.075 g 73%). Note imines are prone to decomposition after 10-15 min under vacuum. Use immediately.

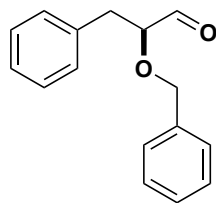
Yield: 75 mg (73%)

Physical Description: Clear Oil

¹H NMR: (400 MHz, CDCl₃) δ 8.49 (d, *J* = 4.5 Hz, 1H), 7.85 – 7.78 (m, 2H), 7.40 – 7.27 (m, 7H), 4.56 (d, *J* = 2.3 Hz, 2H), 4.27 (qd, *J* = 6.7, 4.5 Hz, 1H), 2.48 (s, 3H), 1.40 (d, *J* = 6.7 Hz, 3H).

Compound is in agreement with literature values⁵⁶





(S)-2-(Benzyloxy)-3-phenylpropanal

Aldehyde 2

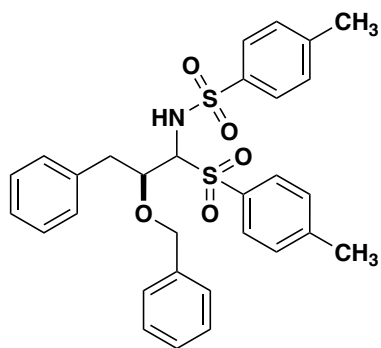
Was prepared by a similar manner as above.⁵⁴ (S)-2-(benzyloxy)-3-phenylpropan-1-ol (0.330 g, 0.002 mol) was dissolved in ethyl acetate (14 mL 0.14 M final concentration), and IBX (1.67 g, 0.006mol) was added. The resulting suspension was heated in an aluminum heating block to 80 °C and stirred vigorously open to the atmosphere. After 3.25 h (TLC monitoring), the reaction was cooled to room temperature and filtered through a medium glass frit. The filter cake was washed with 3 × 2 mL of ethyl acetate, and the combined filtrates were concentrated to yield the corresponding aldehyde.

Yield: 321 mg (98%)

Physical Description: Clear Oil

¹H NMR: (400 MHz, CDCl₃) δ 9.72 (s, 1H), 7.43 – 7.08 (m, 10H), 4.63 (d, *J* = 11.8 Hz, 1H), 4.51 (d, *J* = 11.8 Hz, 1H), 4.04 – 3.97 (m, 1H), 3.07 (dd, *J* = 14.2, 4.7 Hz, 1H), 2.97 (dd, *J* = 14.2, 8.4 Hz, 1H).

Compound is in agreement with literature values⁵⁶



***N*-((2*S*)-2-(Benzyloxy)-3-phenyl-1-tosylpropyl)-4-methylbenzenesulfonamide**

Imine Precursor 2

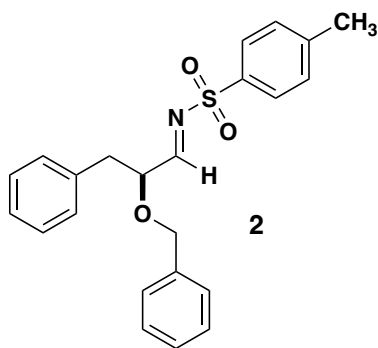
In a round bottom flask was added (S)-2-(benzyloxy)-3-phenylpropanal (0.321 g 0.0013 mol) toluenesulfonamide (0.229 g 0.0013 mol) and toluene-sulfinate (0.274 g 0.0015 mol), then a formic acid water (1:1, 0.33M) solution was added. The reaction was allowed to stir until the mixture solidified. Solids were then diluted with water and filtered and washed copiously with hexane. The solids were allowed to dry on high vac to yield the title compound as a white powder

Yield: 505 mg (68%)

Physical Description: White Solid

¹H NMR: (600 MHz, CDCl₃) δ 7.56 (d, *J* = 8.0 Hz, 2H), 7.49 (d, *J* = 7.9 Hz, 2H), 7.39 – 7.27 (m, 6H), 7.25 – 7.11 (m, 7H), 7.03 (d, *J* = 7.8 Hz, 1H), 5.79 (d, *J* = 9.6 Hz, 1H), 4.69 – 4.61 (m, 1H), 4.61 – 4.56 (m, 1H), 4.26 (d, *J* = 10.6 Hz, 1H), 2.75 (dd, *J* = 13.9, 7.2 Hz, 1H), 2.65 (dd, *J* = 13.7, 7.3 Hz, 1H), 2.44 (d, *J* = 7.3 Hz, 1H), 2.42 (s, 3H), 2.40 (s, 3H).

Compound is in agreement with literature values⁵⁶



(*S,E*)-*N*-(2-(Benzyloxy)-3-phenylpropylidene)-4-methylbenzenesulfonamide (2)

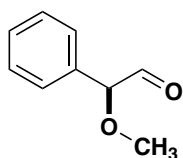
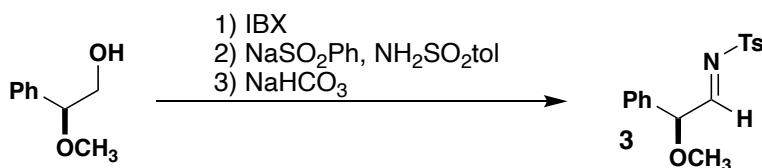
Imine was prepared in a similar manner to **1** reported above. Imine is an off-white oil

Yield: 440 mg (77%)

Physical Description: Off White Oil

¹H NMR: (600 MHz, CDCl₃) δ 8.42 (d, J = 4.7 Hz, 1H), 7.72 (d, J = 8.1 Hz, 2H), 7.33 (d, J = 8.1 Hz, 2H), 7.29 – 7.27 (m, 4H), 7.23 – 7.21 (m, 2H), 7.17 – 7.09 (m, 4H), 4.52 (d, J = 11.9 Hz, 1H), 4.42 (d, J = 11.9 Hz, 1H), 4.31 (q, J = 6.1 Hz, 1H), 3.00 (d, J = 6.5 Hz, 2H), 2.46 (s, 3H).

Compound is in agreement with literature values⁵⁶



(*S*)-2-Methoxy-2-phenylacetaldehyde

Aldehyde 3

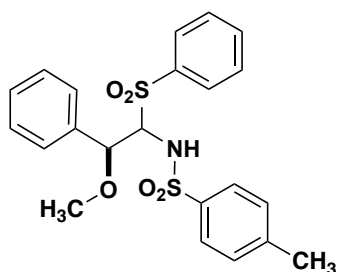
(S)-2-Methoxy-2-phenylethan-1-ol (0.396 g, 0.0026 mol) was dissolved in ethyl acetate (18 mL 0.14 M final concentration), and IBX (2.19 g, 0.0078 mol) was added. The resulting suspension was heated in an aluminum heating block to 80 °C and stirred vigorously open to the atmosphere. After 3.25 h the reaction was cooled to room temperature and filtered through a medium glass frit layered with celite. The filter cake was washed with 3 × 10 mL of ethyl acetate, and the combined filtrates were concentrated to yield aldehyde.

Yield: 390 mg (99%)

Physical Description: Clear Oil

¹H NMR: (400 MHz, CDCl₃) δ 9.70 – 9.57 (m, 1H), 7.49 – 7.35 (m, 5H), 4.67 (s, 1H), 3.48 (s, 3H).

Compound is in agreement with literature values⁵⁶



***N*-((2*S*)-2-Methoxy-2-phenyl-1-(phenylsulfonyl)ethyl)-4-methylbenzenesulfonamide**

Imine Precursor 3

In a round bottom flask was added (S)-2-(benzyloxy)-3-phenylpropanal (0.321 g, 0.0026 mol) toluenesulfonamide (0.446 g, 0.0026 mol) and toluene-sulfinate (0.274 g, 0.0015 mol), then a formic acid water (1:1, 0.33M) solution was added. The reaction was allowed to stir until the mixture solidified. Solids were then diluted with water and filtered

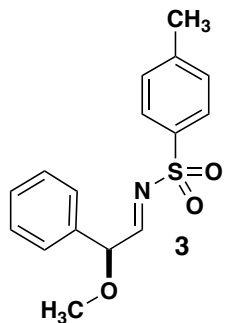
and washed copiously with hexane. The solids were allowed to dry on high vac to yield the title compound as a white powder.

Yield: 505 mg (68%)

Physical Description: White powder

¹H NMR: (600 MHz, CDCl₃) δ 7.83 – 7.78 (m, 2H), 7.66 (td, J = 7.3, 1.2 Hz, 1H), 7.54 – 7.48 (m, 2H), 7.31 – 7.27 (m, 1H), 7.26 – 7.21 (m, 2H), 7.21 – 7.16 (m, 2H), 7.12 (d, J = 7.3 Hz, 2H), 7.06 (d, J = 8.1 Hz, 2H), 5.59 (d, J = 9.8 Hz, 1H), 5.23 (s, 1H), 4.70 (dd, J = 9.7, 1.3 Hz, 1H), 3.27 (s, 3H), 2.39 (s, 3H).

Compound is in agreement with literature values⁵⁶



(*S,E*)-*N*-(2-Methoxy-2-phenylethylidene)-4-methylbenzenesulfonamide (3)

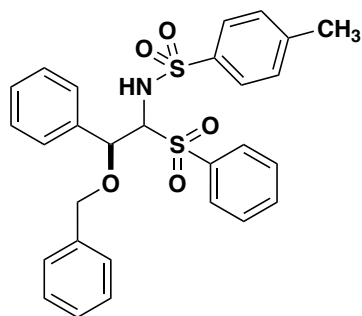
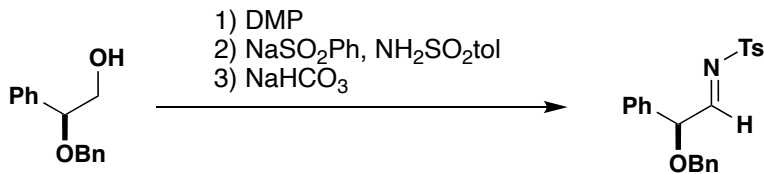
Imine was prepared in a similar manner to **1** reported above. Imine is a clear oil.

Yield: 97 mg (83%)

Physical Description: Clear Oil

¹H NMR: (600 MHz, CDCl₃) δ 8.46 (d, J = 5.0 Hz, 1H), 7.77 (d, J = 8.4 Hz, 2H), 7.42 – 7.28 (m, 7H), 4.95 (d, J = 4.9 Hz, 1H), 3.37 (s, 3H), 2.44 (s, 3H).

Compound is in agreement with literature values⁵⁶



***N*-((2*S*)-2-(Benzyloxy)-2-phenyl-1-(phenylsulfonyl)ethyl)-4-methylbenzenesulfonamide**

Imine Precursor 4

(*S*)-2-(Benzyloxy)-2-phenylethanol-1-ol was prepared in a similar method described above. This alcohol (1g 0.004 mol) was then dissolved in DCM 40 mL then cooled to 0 °C and then was added Dess Martin periodinane (2.05 g 0.0048 mol) then stirred for 1 hour. Then 10 mL of a saturated solution of thiosulfate was added and stirred for 30 min till the solution turned opaque. Then the solution was diluted with diethyl ether and the aqueous layer was extracted three times with ether and then the combined organics were washed with NaHCO₃ three times then washed three times with brine. The organic layer was dried over Na₂SO₄ and then filtered and concentrated and then immediately was added (0.750 g 0.004 mol) of tosyl sulfonamide and (0.830 g 0.005 mol) of sodium phenyl sulfinate was added then 6.6 mL of a 1:1 formic acid water solution and stirred vigorously for 24 hours. The solids were then filtered with water and hexane. To yield a white powder.

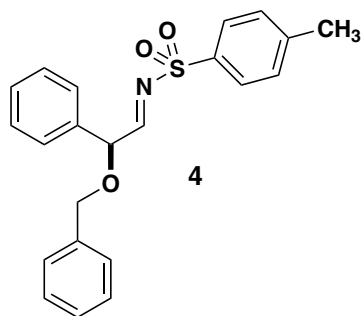
Yield: 2.0 g (86%)

Physical Description: White Powder

¹H NMR: (400 MHz, CDCl₃) δ 7.85 – 7.71 (m, 2H), 7.61 (t, *J* = 7.6 Hz, 1H), 7.44 (t, *J* = 7.7 Hz, 2H), 7.39 (dd, *J* = 13.1, 5.4 Hz, 1H), 7.34 (d, *J* = 7.3 Hz, 3H), 7.28 – 7.22 (m, 4H), 7.22 – 7.16 (m, 4H), 7.03 (d, *J* = 8.0 Hz, 2H), 5.93 – 5.77 (m, 1H), 5.49 (s, 1H), 4.75 (dd, *J* = 9.2, 2.0 Hz, 1H), 4.46 (q, *J* = 10.7 Hz, 2H), 2.37 (s, 3H).

¹³C NMR: Compound is sparingly soluble in CDCl₃, C₆D₆, CD₂Cl₂, and decomposes readily in DMSO-D₆ and (CD₃)₂CO, no ¹³C NMR was taken.;

AMM: (ESI) *m/z* : [M + Na]⁺ Calcd for C₂₈H₂₇NO₅S₂Na 544.1223; found 544.1184.



(*S,E*)-*N*-(2-(Benzyloxy)-2-phenylethylidene)-4-methylbenzenesulfonamide (4)

The following compound was prepared in a similar manner described above. Imine is an off-white oil (0. 0.447 g, 45%). Note imines are prone to decomposition after 10-15 min under vacuum. Use immediately.

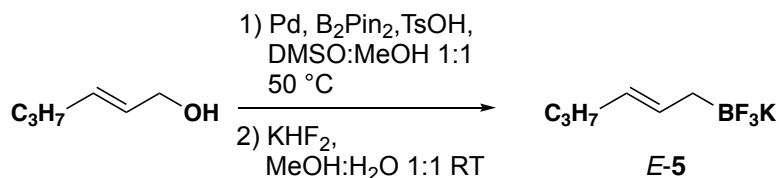
Yield: 477 mg (45%)

Physical Description: Clear Oil

¹H NMR: (400 MHz, CDCl₃) δ 8.48 (d, *J* = 5.3 Hz, 1H), 7.74 (dd, *J* = 8.4, 1.7 Hz, 2H), 7.44 – 7.25 (m, 12H), 5.12 (d, *J* = 5.2 Hz, 1H), 4.61 (d, *J* = 11.6 Hz, 1H), 4.50 (d, *J* = 11.8 Hz, 1H), 2.44 (s, 3H).

AMM: (ESI) *m/z* : [M + H]⁺ Calcd for C₂₂H₂₁NO₃SH 380.1315; found 380.1304.

1.5.5 Representative Procedures for synthesis of (*E*)-BF₃K nucleophiles



Potassium trifluoro(2-hexenyl)borate (*E*-5)

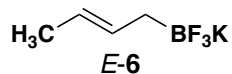
To a solution of trans-2-hexen-1-ol (400 mg, 4.00 mmol) in MeOH (10 mL) and DMSO (10 mL) was added tosic acid (19 mg, 0.10 mmol), di- μ chlorobis{2-[(dimethylamino)methyl]phenyl-C,N}dipalladium(II) (55 mg, 0.10 mmol) and B₂Pin₂ (1.12 g, 4.40 mmol), and the solution was heated in an aluminum heating block at 50 °C for 12 h. The reaction was cooled to room temperature, diluted with H₂O (25 mL), and extracted with Et₂O (3 x 25 mL), and the combined organic layers were dried, and concentrated in vacuo to leave the allyl pinacolboronic ester which was used immediately in the next step without further purification. To a solution of the above-mentioned allyl pinacolboronic ester in H₂O (15 mL) and MeOH (15 mL) was added KHF₂ (1.83 g, 24.0 mmol) and the mixture was stirred at room temperature for 2 h. The reaction was concentrated in vacuo and the resulting solid was washed with acetone (3 x 25 mL). The combined acetone washes were concentrated in vacuo. The residue was dissolved in Et₂O and the resulting suspension was filtered to leave the potassium Trifluoro(2-Hexenyl)Borate (*E*-5)

Yield: 640 mg (84%)

Physical Description: White Solid

¹H NMR: (400 MHz, Acetone-*d*₆) δ 5.54 (dt, 7.4 Hz, 15.0 Hz, 1H), 5.08 (dt, 6.8 Hz, 15.0 Hz, 1H), 1.88 (q, 7.4 Hz, 2H), 1.30 (h, 7.4 Hz, 2H), 1.02 (br, 2H), 0.85 (t, 7.4 Hz, 3H).

Compound is in agreement with literature values⁵⁷



(E)-Trifluoro(2-butenyl) (E-6) borate was synthesized in a similar manner as above and isolated as an amorphous solid.

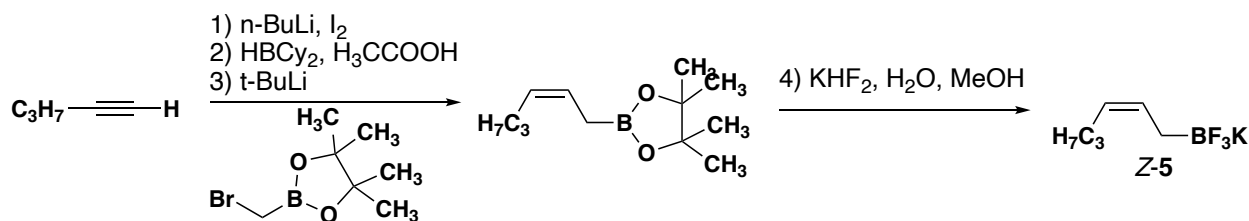
Yield: 163 mg (61%)

Physical Description: Amorphous Solid

¹H NMR: (400 MHz, acetone-D₆) δ 5.55 (dt, *J* = 15.3, 7.7 Hz, 1H), 5.02 (dq, *J* = 13.1, 6.4 Hz, 1H), 1.52 (d, *J* = 6.2 Hz, 3H), 0.98 (s, 2H).

Compound is in agreement with literature values⁵⁸⁵⁷

1.5.6 Representative Procedures for synthesis of Z-BF₃K nucleophiles



The alkyne (5 g, 49 mmol) was placed into a 250 mL flame-dried argon-filled flask sealed with a sleeve stopper and 45 mL of THF was added. The solution was cooled to -78 °C and *n*-BuLi solution in hexanes (32 mL, 1.6 M, 51 mmol) was added dropwise. The mixture was left stirring at -78 °C for 30 min, then I₂ (13.05 g, 51 mmol) solution in 45 mL of THF was slowly added via cannula. The solution was warmed to room temperature, poured into water and extracted with hexanes. The combined organic layers were washed with 10% aq. Na₂S₂O₃ solution, then with brine, dried over anhydrous Na₂SO₄ to yield the iodo alkyne

Yield: 7.09 g (75%)

Physical Description: Yellow Oil

¹H NMR: (400 MHz, CDCl₃) δ 2.36 (t, *J* = 7.0 Hz, 2H), 1.55-1.36 (m, 4H), 0.91 (t, *J* = 7.3 Hz, 3H).

Compound is in agreement with literature values⁵⁹⁵⁷

According to literature procedure.⁶⁰ Freshly prepared dicyclohexylborane was charged to a round bottom flask (0.736 g 4.1 mmol) and then pentane (4mL) was added, and the flask was placed in a 20-25 °C water bath. While this stirred, (0.725 g 3.7 mmol) of 1-iodo-1-pentyne was added dropwise via syringe. The mixture became homogeneous, and the flask was briefly shaken to wash the walls of the flask. Immediately following this, AcOH (3.3 mL, 55 mmol) was added dropwise via syringe (~5 min) while stirring. Then the mixture was directly filtered through a silica gel pad using pentane. The filtrate was then concentrated to yield the (*Z*)-iodo pentene.

Yield: 225 mg (28%)

Physical Description: Yellow Oil

¹H NMR: (400 MHz, CDCl₃) δ 6.28 – 6.13 (m, 2H), 2.15 (q, *J* = 6.8 Hz, 2H), 1.48 (p, *J* = 7.4 Hz, 2H), 0.98 (t, *J* = 7.4 Hz, 3H).

Compound is in agreement with literature values⁶¹⁵⁷

Immediately after (*Z*)-iodo-pentene (0.225 0.1 mmol) was dissolved in ether (2.3 mL) then cooled to -78°. Then butyllithium (1.2 mL 2.75 M reagent in pentane) was added and the reaction was stirred for 2 h at – 78 °C led to formation of the desired lithium reagent. The use of 2 equiv of tertbutyllithium allowed the conversion of tert-butyl iodide, the initial product of lithium halogen exchange, to the innocuous products lithium iodide and

isobutylene. α -bromoalkylboronate ester (0.365 g 1.1 mmol) and ethyl ether 2 mL to make the solution was cooled to -78 °C and (*Z*) organo lithiate was transferred directly to the reaction mixture over 3-5 min by a cold, double-ended needle. The reaction mixture was stirred at -78 °C for 10 min and warmed to room temperature where stirring was continued for 2 h. The reaction was then warmed to room temperature and then aqueous ammonium chloride was added and then the layers were separated. The aqueous layer was extracted three times with ether and the combined organics were washed with brine and the organic layer was dried with Na₂SO₄ filtered and concentrated to yield the title compound.

Yield: 241 mg (99%)

Physical Description: Yellow Oil

¹H NMR: (400 MHz, CDCl₃) δ 5.52 (t, *J* = 8.9 Hz, 1H), 5.41 (q, *J* = 8.3, 7.8 Hz, 1H), 2.02 (q, *J* = 7.4 Hz, 2H), 1.74 – 1.63 (m, 2H), 1.40 (q, *J* = 7.4 Hz, 2H), 1.27 (s, 12H), 0.92 (t, *J* = 7.4 Hz, 3H).

Compound is in agreement with literature values⁶²

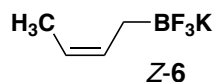
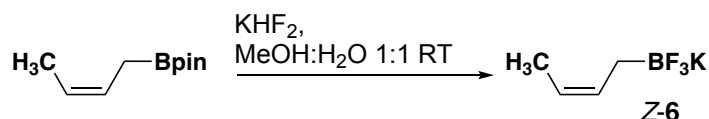
To a solution of the above-mentioned allyl pinacolboronic ester in H₂O (15 mL) and MeOH (15 mL) was added KHF₂ (1.83 g, 24.0 mmol) and the mixture was stirred at room temperature for 2 h. The reaction was concentrated in vacuo and the resulting solid was extracted with acetone (3 x 25 mL). The combined acetone extracts were filtered and concentrated in vacuo. The residue was stirred with Et₂O (10 mL) and the resulting suspension was filtered to leave the potassium allyltrifluoroborate.

Yield: 640 mg (84%)

Physical Description: White Powder

¹H NMR: (400 MHz, Acetone-*d*₆) δ 5.58 (q, *J* = 9.4 Hz, 1H), 5.03 (q, *J* = 7.7 Hz, 1H), 1.32 (dt, *J* = 14.5, 7.4 Hz, 4H), 1.05 (s, 2H), 0.89 (t, *J* = 7.3 Hz, 3H).

Compound is in agreement with literature values⁶²



(Z)-Trifluoro(2-butenyl) (Z-6)

To a solution of (*Z*)-2-buten-1-yl-boronic acid pinacol ester (0.250 g, 0.0014 mol) in MeOH (5 mL) and H₂O (5 mL) was added KHF₂ (644 mg, 0.0082 mmol) and the mixture was stirred at room temperature for 2 h. The reaction was concentrated in vacuo and azeotroped with toluene and the resulting solid dissolved in refluxing acetone filtered through a cotton pipette filter and concentrated in vacuo

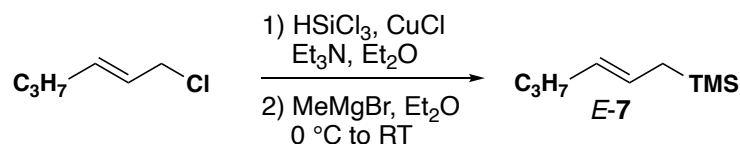
Yield: 201 mg (90%)

Physical Description: White Powder

¹H NMR: (400 MHz, CDCl₃) δ 5.53 (q, *J* = 9.1 Hz, 1H), 4.98 (q, *J* = 8.0 Hz, 1H), 1.95 (q, *J* = 7.4 Hz, 2H), 1.28 (dd, *J* = 14.7, 7.2 Hz, 3H), 1.00 (s, 2H), 0.84 (t, *J* = 8.6, 5.9, 2.2 Hz, 4H).

Compound is in agreement with literature values¹⁷

1.5.7 Representative procedure for synthesis of (*E*)-trimethylsilane nucleophiles



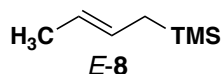
To a mixture of triethyl amine (3.8 mL, 22.0 mmol, 1.2 equiv) and CuCl (190 mg, 1.8 mmol, 0.1 equiv) in diethyl ether (16 mL) at 0 °C was slowly added a solution of 2-hexenyl chloride (3.1 mL, 18 mmol) and trichlorosilane (4.0 mL, 39 mmol, 2.2 equiv) in diethyl ether (4.0 mL). A yellow precipitate immediately formed and a slight exotherm was observed at this point. The reaction was warmed to rt and stirred overnight as judged complete by GCMS analysis. The reaction mixture was then filtered through a pad of celite, concentrated in vacuo and used without further purification. To a 2-neck round-bottom flask, equipped with a magnetic stirring bar and condenser, was charged with Et₂O (1.1 M with respect to *E* or *Z* allylic trichlorosilane as appropriate) and MeMgI (4.5 equiv, 2.4 M in Et₂O). To this solution, which was cooled to 0 °C, was added the appropriate *E* or *Z* allylic trichlorosilane. A small exotherm was observed at this point. Then after 3 hours of stirring the reaction was cooled to 0 °C then saturated aq. NH₄Cl was added. A significant amount of white solids precipitated from the solution. This mixture was diluted with water and extracted with 2 x Et₂O. The organics were washed once with brine, dried with MgSO₄, and concentrated in *vacuo*. The rotovap pressure was carefully monitored to not drop below 180 Torr since the title compounds were all slightly to moderately volatile. The title compounds were then isolated by flash chromatography in pentane.

Yield: 1.32 g (47%)

Physical Description: Yellow Oil

¹H NMR: (400 MHz, CDCl₃) δ 5.36 (ddd, *J* = 15.4, 8.6, 7.1 Hz, 1H), 5.22 (dt, *J* = 14.5, 6.8 Hz, 1H), 1.94 (q, *J* = 7.2 Hz, 2H), 1.38 (d, *J* = 7.9 Hz, 2H), 1.34 (q, *J* = 7.3 Hz, 2H), 0.87 (t, *J* = 7.4 Hz, 3H), -0.03 (s, 9H).

Compound is in agreement with literature values^{17,62}



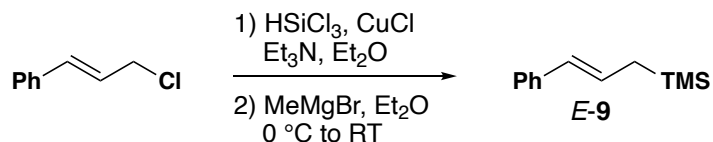
(*E*)-But-2-en-1-yltrimethylsilane was synthesized in a similar manner to that above.

Yield: 990 mg (43%)

Physical Description: Yellow Oil

¹H NMR: (400 MHz, CDCl₃) δ 5.44 – 5.33 (m, 1H), 5.28 – 5.18 (m, 1H), 1.62 (dq, *J* = 6.3, 1.4 Hz, 3H), 1.37 (d, *J* = 7.9 Hz, 2H), -0.03 (d, *J* = 1.6 Hz, 9H).

Compound is in agreement with literature values^{17,62}



(*E*)-But-2-en-1-yltrimethylsilane was synthesized in a similar manner to that above

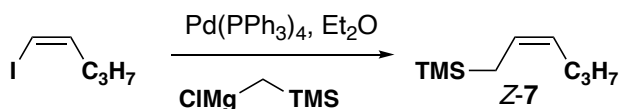
Yield: 3.5 g (80%)

Physical Description: Clear Oil

¹H NMR: (400 MHz, CDCl₃) δ 7.23 – 7.31 (m, 4H), 7.11 – 7.17 (m, 1H), 6.21 – 6.26 (m, 2H), 1.65 (m, 2H), 0.03 (s, 9H).

Compound is in agreement with literature values^{17,62,63}

1.5.8 Representative procedure for synthesis of (*Z*)-trimethylsilane nucleophiles



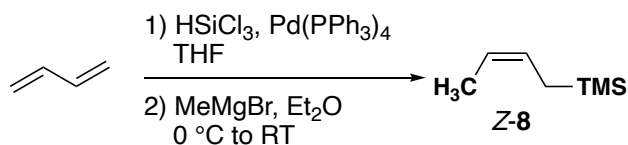
A solution of Pd(PPh₃)₄ (0.090 g, 0.07 mmol) in 15 ml of ether were added sequentially the (trimethylsilyl)methylmagnesium chloride (0.250 g 0.0017 mol) then (*E*)-1-iodo-1-pentene (0.303 g 0.0015 mol) at 0°C. After stirring the reaction mixture for 12 hr at room temperature, it was quenched with 3 N HCl and extracted with pentane. The organic layer was washed with aq NaHCO₃ followed by water and was dried over Na₂SO₄. Evaporation of volatile compounds gave the title compound.

Yield: 121 mg (50%)

Physical Description: Yellow Oil

¹H NMR: (400 MHz, CDCl₃) δ 5.42 (dt, *J* = 11.2, 8.3 Hz, 1H), 5.34 – 5.24 (m, 1H), 1.99 (q, *J* = 7.3 Hz, 2H), 1.49 (d, *J* = 8.5 Hz, 2H), 1.43 – 1.34 (m, 3H), 0.97 – 0.87 (m, 2H), 0.02 (d, *J* = 1.5 Hz, 9H).

Compound is in agreement with literature values⁶⁴



The synthesis of (*Z*)-but-2-en-1-ylchlorodimethylsilane: To a 100 mL flask was added Pd(PPh₃)₄ (0.0025 equiv., 57.7 mg) and trichlorosilane (20 mmol, 1.9 mL) in THF (10 mL) under N₂ atmosphere. The reaction was cooled to -78 °C, and 1,3-butadiene (20 mmol,

15 mL, 2 M in THF) was added. The mixture was allowed to warm to room temperature and stirred for 15 h. To this solution, which was cooled to 0 °C, was then added MeMgI (4.5 equiv, 2.4 M in Et₂O). A small exotherm was observed at this point. The reaction mixture was refluxed in an aluminum heating block overnight, cooled to 0 °C, and slowly quenched with cold, saturated aq. NH₄Cl. A significant amount of white solids precipitated from the solution. This mixture was diluted with water and extracted with 2 x Et₂O. The organics were washed once with brine, dried with MgSO₄, and concentrated in vacuo. The rotovap pressure was carefully monitored to not drop below 180 Torr since the title compounds were all slightly to moderately volatile. The title compounds were then purified via flash chromatography pentane.

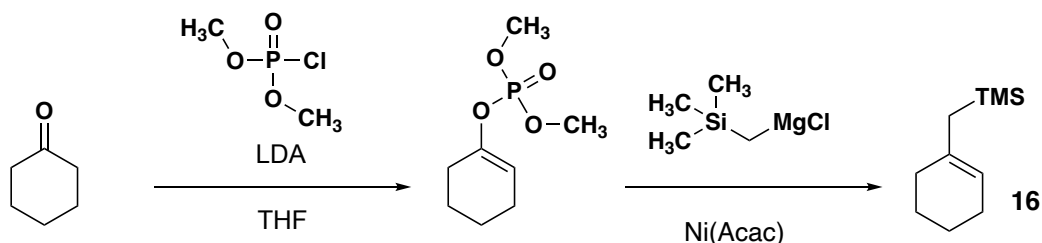
Yield: 563 mg (22%)

Physical Description: Clear Oil

¹H NMR: (600 MHz, CDCl₃) δ 5.47 – 5.40 (m, 1H), 5.39 – 5.32 (m, 1H), 1.56 (d, *J* = 6.6 Hz, 3H), 1.47 (d, *J* = 8.5 Hz, 2H), 0.00 (s, 9H).

Compound is in agreement with literature values⁶⁵

1.5.9 Representative procedure for synthesis of cyclic silane nucleophiles



The synthesis of (cyclohex-1-en-1-ylmethyl)trimethylsilane was performed according to a modified procedure of Kumada's original report. To a flame dried round bottom flask lithium diisopropylamide (0.0056 mol) in THF (20 mL) solution is cooled to -78 and the

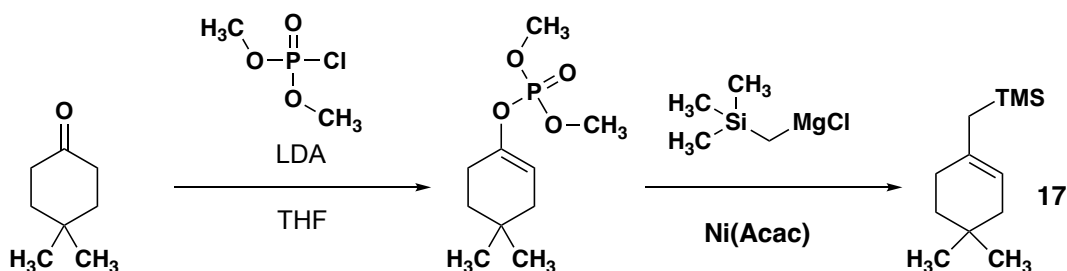
cyclohexanone (0.500 g, 0.0051 mol) is added dropwise over a period of 10 min. The mixture is stirred at -78 °C for 30 min. Dimethyl phosphorochloridate (0.882 g 0.0061 mmol) is added and the mixture is allowed to warm to RT over 1 hour. The solution is then diluted with ether and washed successively with water dilute HCl and saturated sodium carbonate solution. The ether layer is dried over sodium sulfate and concentrated to yield the phosphonate (0.340 g 28% yield). The crude material is carried forward without further purification. Then Ni(Acac)₂ (0.111 g, 0.00016 mol) was charged into a flame dried round bottom flask under Ar atmosphere. Then Et₂O (8 mL 0.2 M) is added and then phosphonate (0.340 g, 0.0016 mol) is added to the solution. The reaction is cooled to 0 °C and then ((trimethylsilyl)methyl)magnesium chloride (1M solution in THF 4.95 mL, 0.00495 mol) is added. The reaction is allowed to warm to room temperature and stirred for 20 hours. Then the solution is diluted with water and saturated ammonium chloride. The organic layer is diluted with ether and the aqueous layer is extracted 3x and the combined organics are washed with brine then dried over Na₂SO₄ and filtered and concentrated. The silane is then purified by flash column chromatography in pentane.

Yield: 90 mg (32%)

Physical Description: Yellow Oil

¹H NMR: (600 MHz, CDCl₃) δ 5.21 (s, 1H), 2.03 – 1.91 (m, 2H), 1.87 (s, 2H), 1.62 – 1.51 (m, 4H), 1.39 (s, 2H), -0.00 (s, 9H).

Compound is in agreement with literature values⁶⁶



The synthesis of ((4,4-dimethylcyclohex-1-en-1-yl)methyl)trimethylsilane was performed according to a modified procedure of Kumada's original report. To a flame dried round bottom flask lithium diisopropylamide (0.0022 mol) in THF (8 mL) solution is cooled to -78 °C and the cyclohexanone (0.250 g, 0.0020 mol) is added dropwise over a period of 10 min. The mixture is stirred at -78 C for 30 min. Dimethyl phosphorochloridate (0.343 g 0.0024 mmol) is added and the mixture is allowed to warm to RT over 1 hour. The solution is then diluted with ether and washed successively with water dilute HCl and saturated sodium carbonate solution. The ether layer is dried over sodium sulfate and concentrated to yield the phosphonate (0.460 g 98% yield). The crude material is carried forward without further purification. Then Ni(Acac)₂ (0.134 g, 0.00019 mol) was charged into a flame dried round bottom flask under Ar atmosphere. Then Et₂O (9mL 0.2 M) is added and then phosphonate (0.460 g, 0.0019 mol) is added to the solution. The reaction is cooled to 0 °C and then ((trimethylsilyl)methyl)magnesium chloride (1M solution in THF 6 mL, 0.0059 mol) is added. The reaction is allowed to warm to room temperature and stirred for 20 hours. Then the solution is diluted with water and saturated ammonium chloride. The organic layer is diluted with ether and the aqueous layer is extracted 3x and the combined organics are washed with brine then dried over Na₂SO₄ and filtered and

concentrated. The silane is then purified by flash column chromatography in pentane and isolated as a yellow oil. Compound is volatile store in fridge.

Yield: 210 mg (63%)

Physical Description: Clear Oil

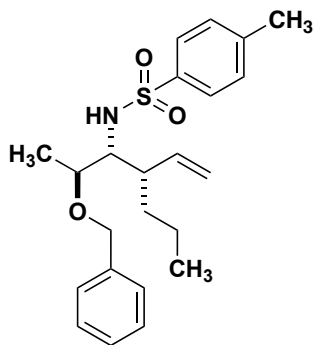
Column Conditions: SiO₂, (10% to 30% Et₂O/Hexanes)

¹H NMR: (400 MHz, CDCl₃) δ 5.10 (s, 1H), 1.89 (s, 2H), 1.76 (s, 2H), 1.54 (s, 2H), 1.32 – 1.28 (m, 6H), 0.35 (s, 2H), -0.01 (s, 9H).

¹³C NMR: (101 MHz, CD₂Cl₂) δ 134.0, 118.1, 39.7, 36.2, 29.1, 28.4, 27.8, 8.8, 1.5, -2.1.

AMM: (ESI) *m/z* calcd for C₁₂H₂₄SiH [M + H]⁺ 197.1720; Found 197.1732.

1.5.10 Characterization Data for Isolated Compounds



***N*-((2*S*,3*R*,4*S*)-2-(Benzyloxy)-4-vinylheptan-3-yl)-4-methylbenzenesulfonamide 10A.**

Prepared according to general procedure A with imine **1** and *E*-5. The crude mixture was purified by flash chromatography

Yield: 92 mg (56%)

Physical Description: Colorless Solid **mp** 97-99 °C

Column Conditions: SiO₂, (30:70 Et₂O/Hexanes)

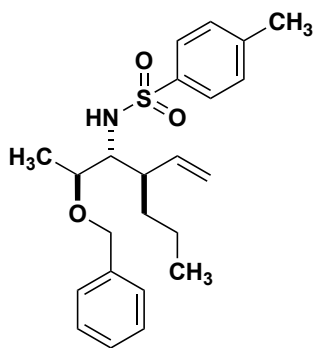
¹H NMR: (400 MHz, CDCl₃) δ 7.71 (d, *J* = 7.8 Hz, 2H), 7.30 (p, *J* = 6.9, 6.3 Hz, 3H), 7.20 (t, *J* = 6.7 Hz, 4H), 5.43 (dt, *J* = 18.2, 9.9 Hz, 1H), 5.02 – 4.87 (m, 2H), 4.57 (d, *J* = 9.3

Hz, 1H), 4.39 (d, $J = 11.8$ Hz, 1H), 4.22 (d, $J = 11.8$ Hz, 1H), 3.45 (tq, $J = 10.0, 5.3, 4.8$ Hz, 2H), 2.37 (s, 3H), 2.09 (td, $J = 9.8, 4.8$ Hz, 1H), 1.59 – 1.46 (m, 2H), 1.35 – 1.15 (m, 2H), 1.14 – 0.97 (m, 4H), 0.79 (t, $J = 7.2$ Hz, 3H).

^{13}C NMR: (101 MHz, CDCl_3) δ 142.9, 139.3, 138.7, 138.3, 129.3, 128.3, 127.5, 127.1, 116.7, 75.3, 70.5, 60.4, 46.1, 32.5, 21.5, 20.4, 15.7, 13.9.

IR (neat): 3295, 2973, 1325, 1154, 1087.

AMM: (ESI) m/z calcd for $\text{C}_{23}\text{H}_{31}\text{NO}_3\text{SH}$ [$\text{M} + \text{H}$] $^+$ 402.2097; Found 402.2104



***N*-((2*S*,3*R*,4*R*)-2-(Benzyloxy)-4-vinylheptan-3-yl)-4-methylbenzenesulfonamide **10B**.**

Prepared according to general procedure A with imine **1** and *Z*-**5**. The crude mixture was purified by flash chromatography (30:70 Et_2O /hexanes) to afford product **10B**.

Yield: 47 mg (62%)

Physical Description: White Solid mp 73 °C.

Column Conditions: SiO_2 , (30:70 Et_2O /Hexanes)

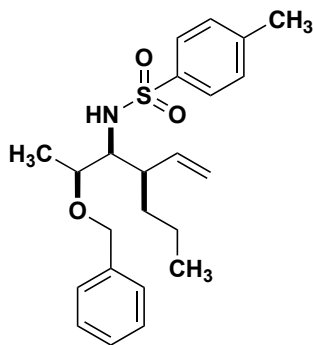
^1H NMR: (400 MHz, CDCl_3) δ 7.71 (d, $J = 7.9$ Hz, 2H), 7.38 – 7.21 (m, 7H), 5.63 (ddd, $J = 18.0, 10.7, 8.8$ Hz, 1H), 5.10 (d, $J = 10.4$ Hz, 1H), 4.93 (d, $J = 17.3$ Hz, 1H), 4.57 (d, $J = 9.6$ Hz, 1H), 4.50 (d, $J = 11.6$ Hz, 1H), 4.22 (d, $J = 11.7$ Hz, 1H), 3.40 (p, $J = 6.2$ Hz,

1H), 3.33 (ddd, $J = 9.2, 5.8, 2.9$ Hz, 1H), 2.47 (q, $J = 7.4$ Hz, 1H), 2.40 (s, 3H), 1.23 – 1.14 (m, 2H), 1.13 (d, $J = 6.2$ Hz, 3H), 1.11 – 1.02 (m, 2H), 0.73 (t, $J = 6.6$ Hz, 3H).

^{13}C NMR: (101 MHz, CDCl_3) δ 143.1, 138.8, 138.4, 137.9, 129.5, 128.3, 127.5, 127.4, 127.1, 117.2, 76.2, 70.9, 60.4, 42.4, 33.4, 21.5, 20.3, 16.3, 13.9.

IR (neat): 3310, 3063, 2954, 2870, 1313, 1186.

AMM: (ESI) m/z calcd for $\text{C}_{23}\text{H}_{31}\text{NO}_3\text{SH}$ [$\text{M} + \text{H}$] $^+$ 402.2097; Found 402.2100.



***N*-((2*S*,3*S*,4*R*)-2-(Benzyloxy)-4-vinylheptan-3-yl)-4-methylbenzenesulfonamide **10C**.**

Prepared according to general procedure B with imine **1** and *E*-7. The crude mixture was purified by flash chromatography (30:70 Et_2O /hexanes) to afford product **10C**.

Yield: 175 mg (77%)

Physical Description: Colorless Solid **mp** 61-63 °C

Column Conditions: SiO_2 , (30:70 Et_2O /Hexanes)

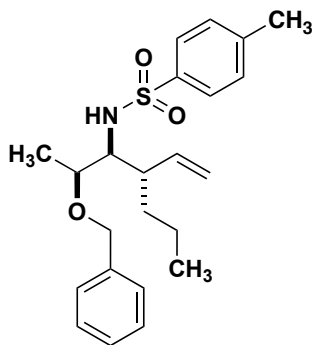
^1H NMR: (400 MHz, CDCl_3) δ 7.74 (d, $J = 7.8$ Hz, 2H), 7.37 – 7.26 (m, 7H), 5.46 (dt, $J = 16.7, 9.9$ Hz, 1H), 4.97 (dt, $J = 10.2, 1.6$ Hz, 1H), 4.86 (d, $J = 9.5$ Hz, 1H), 4.79 – 4.70 (m, 1H), 4.53 (d, $J = 11.3$ Hz, 1H), 4.27 (d, $J = 11.3$ Hz, 1H), 3.75 (q, $J = 6.3$ Hz, 1H), 3.14 (t, $J = 8.8$ Hz, 1H), 2.41 (s, 3H), 2.13 (ddd, $J = 17.7, 12.9, 7.9$ Hz, 1H), 1.24 (dtd, $J = 12.8,$

9.2, 8.3, 5.2 Hz, 2H), 1.05 (d, $J = 6.2$ Hz, 3H), 0.98 (q, $J = 9.5, 7.5$ Hz, 2H), 0.70 (t, $J = 6.7$ Hz, 3H).

^{13}C NMR: (101 MHz, CDCl_3) δ 142.9, 139.5, 139.3, 138.1, 129.4, 128.3, 127.8, 127.7, 126.9, 117.1, 72.8, 70.3, 61.9, 47.7, 33.4, 21.4, 20.3, 17.0, 13.8.

IR (neat): 3292, 2956, 2926, 1327, 1155.

AMM: (ESI) m/z calcd for $\text{C}_{23}\text{H}_{31}\text{NO}_3\text{SH}$ [$\text{M} + \text{H}$] $^+$ 402.2097; found 402.2096.



***N*-((2*S*,3*S*,4*S*)-2-(Benzyloxy)-4-vinylheptan-3-yl)-4-methylbenzenesulfonamide **10D**.**

Prepared according to general procedure B with imine **1** and *Z*-**7**. The crude mixture was purified by flash chromatography (30:70 Et_2O /hexanes) to afford product **10D** (175 mg, 82% for both diastereomers 11% for syn, anti diastereomer).

Yield: 175 mg (82%)

Physical Description: clear solid **mp** 33-35 $^\circ\text{C}$

Column Conditions: SiO_2 , (30:70 Et_2O /Hexanes)

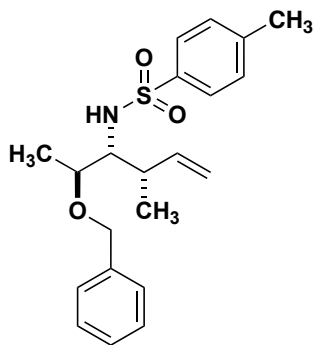
^1H NMR: (400 MHz, CDCl_3) δ 7.71 (d, $J = 8.0$ Hz, 2H), 7.33 (q, $J = 6.5, 5.9$ Hz, 4H), 7.24 (d, $J = 8.0$ Hz, 3H), 5.37 (dt, $J = 18.5, 9.8$ Hz, 1H), 4.94 – 4.86 (m, 2H), 4.79 (d, $J = 8.8$ Hz, 1H), 4.50 (d, $J = 11.4$ Hz, 1H), 4.30 (d, $J = 11.4$ Hz, 1H), 3.61 (d, $J = 6.8$ Hz, 1H),

3.22 (t, $J = 7.3$ Hz, 1H), 2.40 (s, 3H), 2.26 – 2.14 (m, 1H), 1.34 – 1.09 (m, 4H), 1.05 (d, $J = 6.2$ Hz, 3H), 0.76 (t, $J = 7.0$ Hz, 3H).

^{13}C NMR: (101 MHz, CDCl_3) δ 142.9, 139.0, 138.1, 129.3, 128.3, 127.9, 127.7, 127.1, 126.9, 116.8, 74.0, 70.5, 61.3, 59.5, 46.9, 38.1, 31.2, 29.7

IR (neat): 3290, 2956, 2927, 2870, 1158.

AMM: (ESI) m/z calcd for $\text{C}_{23}\text{H}_{31}\text{NO}_3\text{SH}$ [$\text{M} + \text{H}$] $^+$ 402.2097; Found 402.2098.



***N*-((2*S*,3*R*,4*S*)-2-(Benzyloxy)-4-methylhex-5-en-3-yl)-4-methylbenzenesulfonamide**

11A. Prepared according to general procedure A with imine **1** and *E*-**6**. The crude mixture was purified by flash chromatography (30:70 Et_2O /hexanes) to afford product **11A**.

Yield: 27 mg (76%)

Physical Description: Colorless Oil

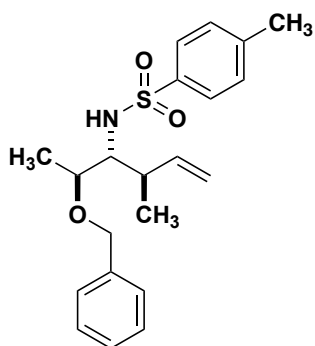
Column Conditions: SiO_2 , (30:70 Et_2O /Hexanes)

^1H NMR: (600 MHz, CDCl_3) δ 7.69 (d, $J = 8.3$ Hz, 2H), 7.35 – 7.27 (m, 3H), 7.24 – 7.16 (m, 4H), 5.58 (ddd, $J = 17.1, 10.2, 7.8$ Hz, 1H), 4.92 (dt, $J = 17.2, 1.4$ Hz, 1H), 4.84 (ddd, $J = 10.3, 1.7, 0.9$ Hz, 1H), 4.61 (d, $J = 9.5$ Hz, 1H), 4.42 (d, $J = 11.7$ Hz, 1H), 4.18 (d, $J = 11.7$ Hz, 1H), 3.46 (qd, $J = 6.3, 4.5$ Hz, 1H), 3.38 (dt, $J = 9.4, 4.7$ Hz, 1H), 2.44 (q, $J = 6.8$ Hz, 1H), 2.38 (s, 3H), 1.12 (d, $J = 6.3$ Hz, 3H), 1.02 (d, $J = 7.0$ Hz, 3H).

¹³C NMR: (151 MHz, CDCl₃) δ 143.0, 141.2, 138.6, 138.3, 129.4, 128.3, 127.6, 127.5, 127.1, 114.6, 75.7, 70.8, 60.7, 38.7, 21.5, 15.8, 15.8.

IR (neat): 3285, 2920, 2852, 1153.

AMM: (ESI) *m/z* calcd for C₂₁H₂₇NO₃SH [M + H]⁺ 374.1784; Found 374.1774.



***N*-((2*S*,3*R*,4*R*)-2-(Benzyloxy)-4-methylhex-5-en-3-yl)-4-methylbenzenesulfonamide**

11B. Prepared according to general procedure A with imine **1** and *Z*-**6**. The crude mixture was purified by flash chromatography (30:70 Et₂O/hexanes) to afford product **11B**.

Yield: 27 mg (53%)

Physical Description: Colorless Oil

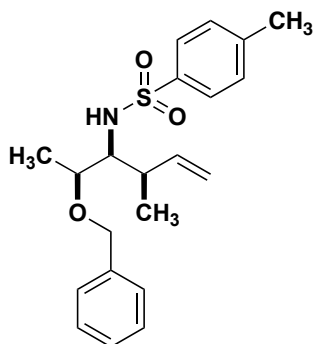
Column Conditions: SiO₂, (30:70 Et₂O/Hexanes)

¹H NMR: (400 MHz, CDCl₃) δ 7.72 (d, *J* = 8.3 Hz, 2H), 7.39 – 7.30 (m, 3H), 7.28 – 7.23 (m, 4H), 5.84 (ddd, *J* = 17.3, 10.5, 6.7 Hz, 1H), 5.10 (dt, *J* = 10.6, 1.4 Hz, 1H), 5.00 (dt, *J* = 17.4, 1.6 Hz, 1H), 4.54 (dd, *J* = 12.5, 10.3 Hz, 2H), 4.24 (d, *J* = 11.6 Hz, 1H), 3.44 (p, *J* = 6.2 Hz, 1H), 3.30 (ddd, *J* = 9.2, 5.8, 3.3 Hz, 1H), 2.77 (s, 1H), 2.43 (s, 3H), 1.16 (d, *J* = 6.3 Hz, 3H), 0.88 (d, *J* = 7.0 Hz, 3H).

¹³C NMR: (101 MHz, CDCl₃) δ 143.1, 138.8, 138.8, 138.4, 129.5, 128.4, 127.6, 127.5, 127.0, 116.2, 76.1, 71.0, 61.8, 36.5, 21.5, 17.1, 16.4.

IR (neat): 3290, 2972, 2870, 1325, 1156.

AMM: (ESI) m/z calcd for $C_{21}H_{27}NO_3SH$ $[M + H]^+$ 374.1784; Found 374.1788.



***N*-((2*S*,3*S*,4*R*)-2-(Benzyloxy)-4-methylhex-5-en-3-yl)-4-methylbenzenesulfonamide**

11C. Prepared according to general procedure B with imine **1** and *E*-**8**. The crude mixture was purified by flash chromatography (30:70 Et₂O/hexanes) to afford product **11C** (101 mg, 53%) as a clear colorless oil.

Yield: 101 mg (53%)

Physical Description: Colorless Oil

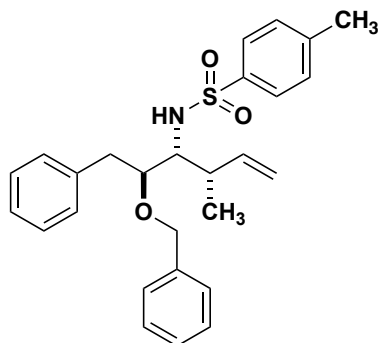
Column Conditions: SiO₂, (30:70 Et₂O/Hexanes)

¹H NMR: (800 MHz, CDCl₃) δ 7.77 (d, J = 8.3 Hz, 2H), 7.38 – 7.35 (m, 2H), 7.33 – 7.29 (m, 5H), 5.72 – 5.60 (m, 1H), 4.95 (ddd, J = 10.3, 1.8, 0.7 Hz, 1H), 4.90 (dt, J = 9.6, 2.8 Hz, 1H), 4.86 (ddt, J = 17.1, 1.7, 0.9 Hz, 1H), 4.54 (d, J = 11.3 Hz, 1H), 4.30 (d, J = 11.3 Hz, 1H), 3.75 (qd, J = 6.3, 1.5 Hz, 1H), 3.13 (ddd, J = 9.7, 8.3, 1.4 Hz, 1H), 2.44 (s, 3H), 2.43 – 2.39 (m, 1H), 1.01 (d, J = 6.3 Hz, 3H), 0.92 (dd, J = 7.0, 1.0 Hz, 3H).

¹³C NMR: (101 MHz, CDCl₃) δ 142.9, 141.0, 139.3, 138.1, 129.4, 128.4, 127.9, 127.7, 126.9, 115.4, 72.9, 70.5, 63.0, 41.8, 21.5, 18.0, 17.0.

IR (neat): 3295, 2973, 1325, 1154.

AMM: (ESI) m/z calcd for $C_{21}H_{27}NO_3SH$ $[M + H]^+$ 374.1784; Found 374.1786.



***N*-((2*S*,3*R*,4*S*)-2-(Benzyloxy)-4-methyl-1-phenylhex-5-en-3-yl)-4-**

methylbenzenesulfonamide 12A. Prepared according to general procedure A with imine **2** and *E*-**6**. The crude mixture was purified by flash chromatography (30:70 Et₂O/hexanes) to afford product **12A**.

Yield: 60 mg (56%)

Physical Description: Clear Solid **mp** 75-76 °C

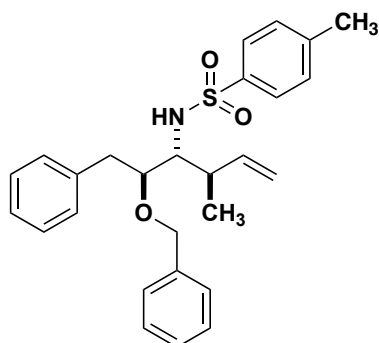
Column Conditions: SiO₂, (30:70 Et₂O/Hexanes)

¹H NMR: (400 MHz, CDCl₃) δ 7.56 (d, J = 8.3 Hz, 2H), 7.36 – 7.29 (m, 4H), 7.27 – 7.22 (m, 2H), 7.17 (d, J = 8.0 Hz, 2H), 7.13 – 7.08 (m, 2H), 7.08 – 7.03 (m, 2H), 5.62 (ddd, J = 17.2, 10.3, 7.8 Hz, 1H), 5.03 – 4.88 (m, 2H), 4.60 (d, J = 9.4 Hz, 1H), 4.29 – 4.14 (m, 2H), 3.55 (ddd, J = 7.7, 6.1, 3.3 Hz, 1H), 3.37 (ddd, J = 8.7, 5.0, 3.3 Hz, 1H), 2.86 – 2.70 (m, 2H), 2.57 (dt, J = 13.1, 6.9 Hz, 1H), 2.42 (s, 3H), 1.12 (d, J = 6.8 Hz, 3H).

¹³C NMR: (101 MHz, CDCl₃) δ 143.0, 141.3, 138.2, 138.1, 138.0, 129.4, 129.2, 128.5, 128.4, 127.6, 127.6, 127.2, 126.5, 114.6, 82.1, 72.3, 58.7, 38.5, 37.2, 21.5, 16.1.

IR (neat): 3271, 1496, 1453, 1319, 1156.

AMM: (ESI) m/z calcd for $C_{27}H_{31}NO_3SH$ $[M + H]^+$ 450.2097; Found 450.2116



***N*-((2*S*,3*R*,4*R*)-2-(Benzyloxy)-4-methyl-1-phenylhex-5-en-3-yl)-4-**

methylbenzenesulfonamide 12B. Prepared according to general procedure A with imine **2** and *Z*-**6**. The crude mixture was purified by flash chromatography (30:70 Et₂O/hexanes) to afford product **12B**.

Yield: 61 mg (56%)

Physical Description: Clear Oil

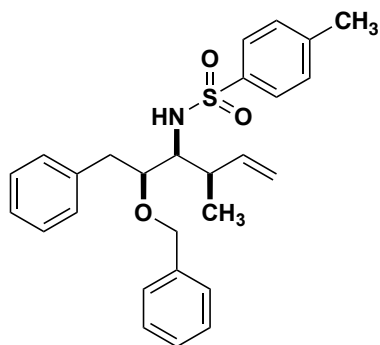
Column Conditions: SiO₂, (30:70 Et₂O/Hexanes)

¹H NMR: (400 MHz, CDCl₃) δ 7.56 – 7.51 (m, 2H), 7.37 – 7.29 (m, 5H), 7.25 (d, J = 7.4 Hz, 1H), 7.21 (d, J = 7.9 Hz, 2H), 7.16 (dd, J = 7.8, 1.7 Hz, 2H), 7.12 – 7.07 (m, 2H), 6.00 (ddd, J = 17.2, 10.5, 6.5 Hz, 1H), 5.21 – 4.98 (m, 2H), 4.62 (d, J = 9.0 Hz, 1H), 4.36 – 4.18 (m, 2H), 3.59 (td, J = 7.1, 3.8 Hz, 1H), 3.20 (dt, J = 9.0, 3.5 Hz, 1H), 2.89 (dd, J = 13.8, 7.4 Hz, 1H), 2.82 – 2.70 (m, 2H), 2.44 (s, 3H), 0.86 (d, J = 6.9 Hz, 3H).

¹³C NMR: (151 MHz, CDCl₃) δ 143.1, 139.0, 138.2, 138.0, 138.0, 129.5, 129.2, 128.5, 128.3, 127.6, 127.5, 127.1, 126.5, 116.1, 82.7, 72.8, 59.3, 38.0, 36.0, 21.5, 17.1

IR (neat): 3255, 1453, 1316, 1148.

AMM: (ESI) m/z calcd for $C_{27}H_{31}NO_3SH$ $[M + H]^+$ 450.2097; Found 450.2121.



***N*-((2*S*,3*S*,4*R*)-2-(Benzyloxy)-4-methyl-1-phenylhex-5-en-3-yl)-4-**

methylbenzenesulfonamide 12C. Prepared according to general procedure B with imine **2** and *E*-**8**. The crude mixture was purified by flash chromatography (30:70 Et₂O/hexanes) to afford product **12C**.

Yield: 44 mg (61%)

Physical Description: Clear Oil

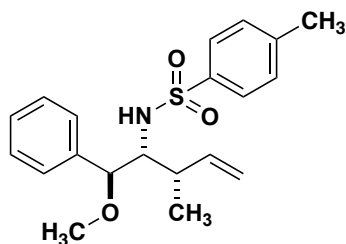
Column Conditions: SiO₂, (30:70 Et₂O/Hexanes)

¹H NMR: (600 MHz, CDCl₃) δ 7.8 (d, *J* = 6.5 Hz, 2H), 7.4 – 7.2 (m, 10H), 7.1 (d, *J* = 7.5 Hz, 2H), 5.6 – 5.5 (m, 1H), 5.1 (d, *J* = 9.2 Hz, 1H), 4.9 (d, *J* = 10.3 Hz, 1H), 4.8 (d, *J* = 17.1 Hz, 1H), 4.4 – 4.3 (m, 2H), 3.7 (t, *J* = 6.9 Hz, 1H), 3.2 (t, *J* = 8.4 Hz, 1H), 2.8 (dd, *J* = 13.8, 5.7 Hz, 1H), 2.6 – 2.5 (m, 1H), 2.4 (s, 3H), 2.3 (h, *J* = 7.1 Hz, 1H), 0.8 (dd, *J* = 6.9, 1.6 Hz, 3H).

¹³C NMR: (151 MHz, CDCl₃) δ 143.1, 140.5, 139.2, 138.0, 137.8, 129.6, 129.5, 128.5, 128.4, 128.1, 127.9, 127.1, 126.4, 115.5, 78.6, 72.1, 59.8, 41.8, 38.0, 21.5, 17.6.

IR (neat): 3265, 1457, 1321, 1150.

AMM: (ESI) *m/z* calcd for C₂₇H₃₁NO₃SH [M + H]⁺ 450.2097; Found 450.2115.



***N*-((1*S*,2*R*,3*S*)-1-Methoxy-3-methyl-1-phenylpent-4-en-2-yl)-4-**

methylbenzenesulfonamide 13A. Prepared according to general procedure A with imine **3** and *E*-**6**. The crude mixture was purified by flash chromatography (30:70 Et₂O/hexanes) to afford product **13A**

Yield: 71 mg (72%)

Physical Description: Clear Oil

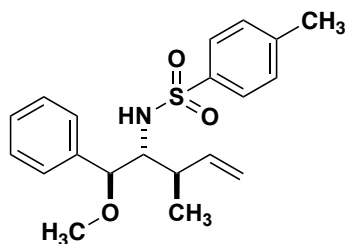
Column Conditions: SiO₂, (30:70 Et₂O/Hexanes)

¹H NMR: (600 MHz, CDCl₃) δ 7.73 (d, *J* = 7.9 Hz, 2H), 7.35 – 7.23 (m, 5H), 7.08 (d, *J* = 7.5 Hz, 2H), 5.62 – 5.53 (m, 1H), 4.85 (d, *J* = 6.1 Hz, 1H), 4.82 (dd, *J* = 13.3, 1.6 Hz, 1H), 4.61 (d, *J* = 9.9 Hz, 1H), 4.12 (d, *J* = 4.3 Hz, 1H), 3.54 (dt, *J* = 9.7, 4.6 Hz, 1H), 3.05 (s, 3H), 2.41 (s, 3H), 2.12 (q, *J* = 6.6 Hz, 1H), 1.01 (d, *J* = 6.8 Hz, 3H).

¹³C NMR: (101 MHz, CDCl₃) δ 143.1, 141.6, 138.7, 137.6, 129.4, 128.5, 127.9, 127.2, 126.9, 114.7, 84.5, 61.7, 57.3, 38.1, 21.5, 15.9.

IR (neat): 3235, 1457, 1318, 1152.

AMM: (ESI) *m/z* calcd for C₂₀H₂₅NO₃SNa [M + Na]⁺ 382.1447; Found 382.1470.



***N*-((1*S*,2*R*,3*R*)-1-Methoxy-3-methyl-1-phenylpent-4-en-2-yl)-4-**

methylbenzenesulfonamide 13B. Prepared according to general procedure A with imine **3** and *Z*-**6**. The crude mixture was purified by flash chromatography (30:70 Et₂O/hexanes) to afford product **13B**.

Yield: 52 mg (51%)

Physical Description: Clear Colorless Solid **mp** 56-57 °C

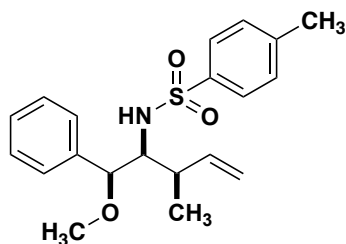
Column Conditions: SiO₂, (30:70 Et₂O/Hexanes)

¹H NMR: (600 MHz, CDCl₃) δ 7.65 (d, *J* = 6.6 Hz, 1H), 7.27 (dd, *J* = 8.1, 6.4 Hz, 3H), 7.27 – 7.21 (m, 5H), 7.16 – 7.11 (m, 2H), 5.96 (dddd, *J* = 17.2, 10.5, 6.5, 1.6 Hz, 1H), 5.09 (dd, *J* = 10.6, 1.7 Hz, 1H), 4.96 (dd, *J* = 17.5, 1.8 Hz, 1H), 4.67 (d, *J* = 9.7 Hz, 1H), 4.04 – 4.00 (m, 1H), 3.43 (ddt, *J* = 7.6, 5.3, 2.5 Hz, 1H), 3.08 (d, *J* = 1.6 Hz, 3H), 2.42 (t, *J* = 6.9 Hz, 4H), 0.81 (dd, *J* = 7.0, 1.7 Hz, 3H).

¹³C NMR: (151 MHz, CDCl₃) δ 143.0, 138.9, 138.6, 138.2, 129.5, 128.5, 127.7, 126.9, 126.8, 115.9, 85.1, 62.4, 57.6, 35.6, 21.5, 17.3.

IR (neat): 3247, 1496, 1310, 1156.

AMM: (ESI) *m/z* calcd for C₂₀H₂₅NO₃SNa [M + Na]⁺ 382.1447; Found 382.1470.



***N*-((1*S*,2*S*,3*R*)-1-Methoxy-3-methyl-1-phenylpent-4-en-2-yl)-4-**

methylbenzenesulfonamide 13C. Prepared according to general procedure B with imine **3** and *E*-**8**. The crude mixture was purified by flash chromatography (30:70 Et₂O/hexanes) to afford product **13C**

Yield: 72 mg (75%)

Physical Description: Clear Colorless Oil

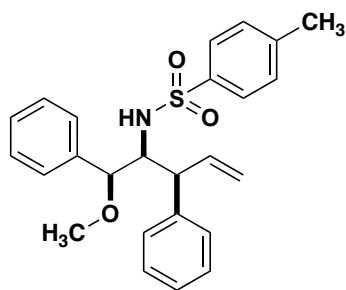
Column Conditions: SiO₂, (30:70 Et₂O/Hexanes)

¹H NMR: (600 MHz, CDCl₃) δ 7.33 (d, *J* = 7.5 Hz, 2H), 7.10 (dd, *J* = 7.5, 1.5 Hz, 3H), 7.03 – 6.98 (m, 4H), 5.88 – 5.78 (m, 1H), 5.10 – 5.01 (m, 2H), 4.90 (d, *J* = 9.0 Hz, 1H), 4.31 – 4.26 (m, 1H), 3.35 (ddd, *J* = 9.0, 7.1, 1.9 Hz, 1H), 3.14 (d, *J* = 1.3 Hz, 3H), 2.56 (h, *J* = 7.2 Hz, 1H), 2.34 (s, 3H), 1.06 (dd, *J* = 7.0, 1.4 Hz, 3H).

¹³C NMR: (101 MHz, CDCl₃) δ 142.2, 140.8, 139.1, 138.8, 129.2, 128.3, 127.3, 126.5, 126.4, 115.6, 81.0, 64.3, 56.9, 42.2, 21.4, 17.4.

IR (neat): 3293, 1447, 1331, 1160, 1097

AMM: (ESI) *m/z* calcd for C₂₀H₂₅NO₃SNa [M + Na]⁺ 382.1447; Found 382.1468.



***N*-((1*S*,2*S*,3*S*)-1-Methoxy-1,3-diphenylpent-4-en-2-yl)-4-methylbenzenesulfonamide**

14C

Prepared according to general procedure B with imine **3** and *E*-**9**. The crude mixture was purified by flash chromatography (30:70 Et₂O/hexanes) to afford product **14C**

Yield: 72 mg (75%)

Physical Description: Clear Colorless Oil

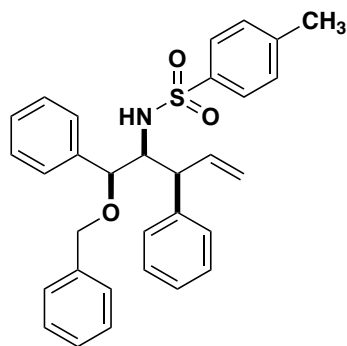
Column Conditions: SiO₂, (30:70 Et₂O/Hexanes)

¹H NMR: (600 MHz, CDCl₃) δ 7.31 – 7.25 (m, 4H), 7.21 (dd, *J* = 14.0, 7.3 Hz, 3H), 7.15 (d, *J* = 7.7 Hz, 3H), 6.99 (d, *J* = 8.0 Hz, 2H), 6.95 (d, *J* = 7.0 Hz, 2H), 6.32 (dt, *J* = 18.2, 9.9 Hz, 1H), 5.24 (d, *J* = 10.1 Hz, 1H), 5.12 (d, *J* = 17.0 Hz, 1H), 4.95 (d, *J* = 9.5 Hz, 1H), 4.24 (s, 1H), 3.77 (t, *J* = 7.9 Hz, 1H), 3.70 (t, *J* = 8.2 Hz, 1H), 3.15 (d, *J* = 2.4 Hz, 3H), 2.33 (d, *J* = 2.4 Hz, 3H).

¹³C NMR: (101 MHz, CDCl₃) δ 142.2, 140.9, 138.7, 138.5, 136.4, 129.2, 128.7, 128.2, 128.2, 127.4, 126.8, 126.5, 126.5, 118.5, 80.6, 63.9, 56.6, 54.4, 21.4.

IR (neat): 3316, 1440, 1333, 1158, 1087.

AMM: (ESI) *m/z* calcd for C₂₄H₂₄NO₃S [M - OCH₃]⁺ 390.1528; Found 390.1550.



N*-((1*S*,2*S*,3*S*)-1-(Benzyloxy)-1,3-diphenylpent-4-en-2-yl)-4-methylbenzenesulfonamide **15C*

Prepared according to general procedure B with imine **4** and *E*-**9** with the ZnCl₂ as a Lewis acid. The crude mixture was purified by flash chromatography (30:70 Et₂O/hexanes) to afford product **15C**.

Yield: 501 mg (85%)

Physical Description: Clear Colorless Oil

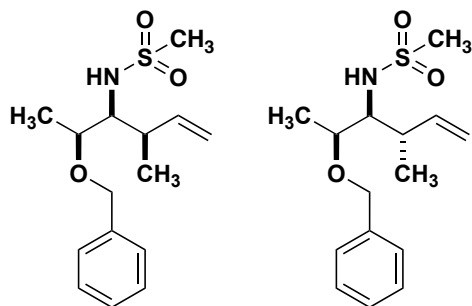
Column Conditions: SiO₂, (30:70 Et₂O/Hexanes)

¹H NMR: (600 MHz, CDCl₃) δ 7.37 (dq, *J* = 13.7, 7.0 Hz, 3H), 7.28 (s, 2H), 7.22 (t, *J* = 7.4 Hz, 2H), 7.20 – 7.13 (m, 4H), 7.09 (d, *J* = 7.5 Hz, 2H), 7.01 (d, *J* = 7.2 Hz, 2H), 6.97 (d, *J* = 8.0 Hz, 2H), 6.27 (dt, *J* = 17.0, 10.0 Hz, 2H), 5.19 (dt, *J* = 10.1, 1.1 Hz, 1H), 5.07 – 5.00 (m, 2H), 4.51 (s, 1H), 4.41 (d, *J* = 11.3 Hz, 1H), 4.17 (d, *J* = 11.3 Hz, 1H), 3.78 (ddd, *J* = 9.2, 6.5, 1.7 Hz, 1H), 3.69 (dd, *J* = 9.9, 6.4 Hz, 1H), 2.33 (s, 3H).

¹³C NMR: (101 MHz, CDCl₃) δ 142.2, 140.9, 138.8, 138.5, 137.4, 136.4, 129.2, 128.6, 128.5, 128.3, 128.3, 128.1, 128.0, 127.5, 126.7, 126.7, 126.4, 118.4, 78.0, 70.7, 64.1, 54.6, 21.4.

IR (neat): 3329, 1454, 1339, 1155, 1083.

AMM: (ESI) m/z calcd for $C_{24}H_{24}NO_3S$ [M - OBn]⁺ 390.1528; Found 390.1543.



***N*-((2*S*,3*S*,4*R*)-2-(Benzyloxy)-4-methylhex-5-en-3-yl)methanesulfonamide SI-1C**

***N*-((2*S*,3*S*,4*S*)-2-(Benzyloxy)-4-methylhex-5-en-3-yl)methanesulfonamide SI-1D**

Prepared according to general procedure B. The crude mixture was purified by flash chromatography (30:70 Et₂O/hexanes) to afford product **SI-1C** and **SI-1D**.

Yield: 268 mg (72%)

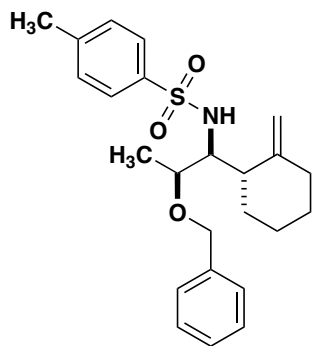
Physical Description: white solid **mp** 102 °C

Column Conditions: SiO₂, (30:70 Et₂O/Hexanes)

¹H NMR: (600 MHz, CDCl₃) δ 7.40 – 7.26 (m, 7H), 5.69 (ddd, $J = 17.1, 10.4, 8.6$ Hz, 1H), 5.05 – 4.93 (m, 2H), 4.59 (d, $J = 11.4$ Hz, 1H), 4.34 (t, $J = 10.4$ Hz, 1H), 3.79 (qd, $J = 6.3, 1.9$ Hz, 1H), 3.20 (ddd, $J = 10.0, 8.4, 1.8$ Hz, 1H), 3.00 (s, 3H), 2.51 (h, $J = 7.5$ Hz, 1H), 1.29 (d, $J = 6.1$ Hz, 3H), 1.10 (d, $J = 6.9$ Hz, 3H)

¹³C NMR: (101 MHz, CDCl₃) δ 141.1, 138.1, 128.4, 127.9, 127.8, 115.7, 73.1, 70.6, 63.2, 42.9, 41.6, 17.8, 17.3.

AMM: (ESI) m/z calcd for $C_{15}H_{23}NO_3SNa$ [M + Na]⁺ 320.1291; Found 320.1312.



***N*-((1*S*,2*S*)-2-(benzyloxy)-1-((*S*)-2-methylenecyclohexyl)propyl)-4-**

methylbenzenesulfonamide 18. Prepared according to general procedure B. The crude mixture was purified by flash chromatography (30:70 Et₂O/hexanes) to afford product **18**.

Yield: 49 mg (80%)

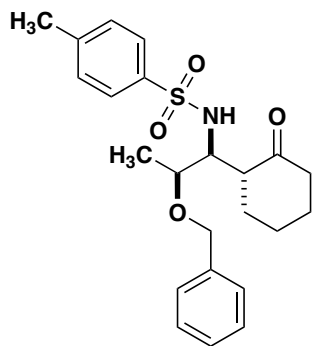
Physical Description: clear colorless oil

Column Conditions: SiO₂, (30:70 Et₂O/Hexanes)

¹H NMR: (600 MHz, CDCl₃) δ 7.67 (d, *J* = 6.5 Hz, 2H), 7.36 – 7.31 (m, 2H), 7.31 – 7.24 (m, 3H), 7.22 (d, *J* = 7.9 Hz, 2H), 4.65 (d, *J* = 7.3 Hz, 1H), 4.57 (d, *J* = 11.5 Hz, 1H), 4.47 (s, 1H), 4.41 (s, 1H), 4.38 (d, *J* = 11.5 Hz, 1H), 3.86 (q, *J* = 6.4 Hz, 1H), 3.60 (td, *J* = 8.2, 7.4, 2.0 Hz, 1H), 2.40 (s, 4H), 2.35 (t, *J* = 4.6 Hz, 1H), 1.80 (q, *J* = 6.8, 4.9 Hz, 1H), 1.79 – 1.71 (m, 1H), 1.68 (dt, *J* = 13.8, 4.5 Hz, 1H), 1.59 – 1.48 (m, 3H), 1.40 (tdd, *J* = 13.8, 9.5, 3.8 Hz, 2H), 1.31 (d, *J* = 11.7 Hz, 1H), 1.25 (s, 1H), 1.13 (dd, *J* = 6.3, 1.6 Hz, 3H).

¹³C NMR: (101 MHz, CDCl₃) δ 149.5, 142.8, 138.7, 138.3, 129.2, 128.4, 128.0, 127.8, 127.7, 127.1, 109.8, 73.7, 70.6, 56.9, 45.7, 32.8, 28.9, 28.1, 22.3, 21.5, 16.1.

AMM: (ESI) *m/z* calcd for C₂₄H₃₁NO₃SNa [M + Na]⁺ 436.1917; Found 436.1936.



***N*-((1*S*,2*S*)-2-(benzyloxy)-1-((*R*)-2-oxocyclohexyl)propyl)-4-**

methylbenzenesulfonamide 19. The corresponding olefin (11 mg 0.0266 mmol) was dissolved in 5 ml of dichloromethane and then cooled to -78 °C and then purged with ozone till the solution was blue and then stirred for 2 hours at -78° then dimethyl sulfide was added to the mixture until the solution turned clear ~0.3 ml. Then the solution was concentrated and the crude mixture was purified by flash chromatography (30:70 Et₂O/hexanes) to afford product **19**

Yield: 9 mg (89%)

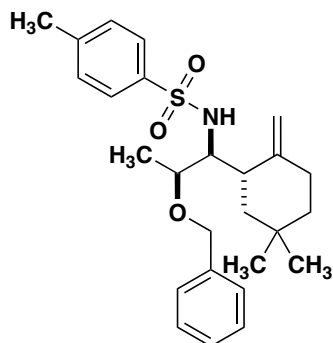
Physical Description: Clear Colorless Solid **mp** 103-105 °C

Column Conditions: SiO₂, (30:70 Et₂O/Hexanes)

¹H NMR: (600 MHz, CDCl₃) δ 7.70 (d, *J* = 7.4 Hz, 2H), 7.31 (td, *J* = 7.2, 1.7 Hz, 2H), 7.30 – 7.26 (m, 1H), 7.22 (d, *J* = 7.9 Hz, 2H), 7.18 (d, *J* = 7.4 Hz, 2H), 5.54 (d, *J* = 8.3 Hz, 1H), 4.40 (d, *J* = 11.6 Hz, 1H), 4.20 (d, *J* = 11.6 Hz, 1H), 3.59 – 3.54 (m, 2H), 2.75 – 2.70 (m, 1H), 2.38 (s, 3H), 2.36 – 2.19 (m, 2H), 2.13 – 2.07 (m, 1H), 2.01 (d, *J* = 11.8 Hz, 1H), 1.83 (d, *J* = 10.3 Hz, 1H), 1.57 (t, *J* = 10.9 Hz, 1H), 1.51 (s, 1H), 1.50 – 1.40 (m, 1H), 0.86 (dd, *J* = 6.1, 1.7 Hz, 3H).

¹³C NMR: (101 MHz, CDCl₃) δ 213.0, 143.0, 138.3, 138.0, 129.5, 128.3, 127.7, 127.6, 127.0, 74.6, 70.4, 57.3, 53.2, 42.6, 30.3, 27.6, 25.1, 21.5, 16.8.

AMM: (ESI) *m/z* calcd for C₂₃H₂₉NO₄SH [M + H]⁺ 416.1890; Found 416.1903.



***N*-((1*S*,2*S*)-2-(Benzyloxy)-1-((*S*)-5,5-dimethyl-2-methylenecyclohexyl)propyl)-4-methylbenzenesulfonamide **20**.** Prepared according to general procedure B. The crude mixture was purified by flash chromatography (30:70 Et₂O/hexanes) to afford product **20**.

Yield: 37 mg (80%)

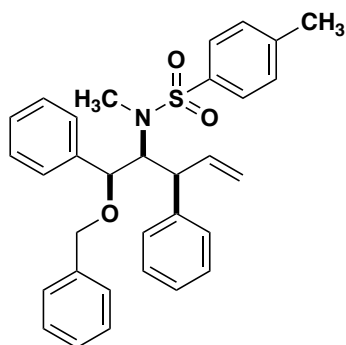
Physical Description: Clear Colorless Solid mp 102-103°C

Column Conditions: SiO₂, (30:70 Et₂O/Hexanes)

¹H NMR: (600 MHz, CDCl₃) δ 7.73 (d, *J* = 7.8 Hz, 2H), 7.33 (dt, *J* = 16.3, 7.3 Hz, 3H), 7.26 (d, *J* = 6.3 Hz, 4H), 5.22 (d, *J* = 7.9 Hz, 1H), 4.68 (s, 1H), 4.48 (d, *J* = 10.9 Hz, 1H), 4.28 – 4.21 (m, 2H), 3.77 (q, *J* = 6.5 Hz, 1H), 3.64 (q, *J* = 3.4 Hz, 1H), 2.40 (s, 3H), 2.27 (d, *J* = 12.5 Hz, 1H), 2.08 – 2.02 (m, 2H), 1.55 (d, *J* = 4.9 Hz, 1H), 1.36 (d, *J* = 13.1 Hz, 1H), 1.18 (q, *J* = 9.8 Hz, 1H), 1.05 (d, *J* = 6.3 Hz, 4H), 0.88 (s, 3H), 0.76 (s, 3H).

¹³C NMR: (101 MHz, CDCl₃) δ 150.2, 142.9, 138.9, 137.8, 129.5, 128.4, 128.1, 127.8, 127.0, 105.9, 72.4, 70.4, 58.0, 43.2, 40.8, 40.4, 32.8, 32.2, 30.6, 24.5, 21.5, 17.0.

AMM: (ESI) m/z calcd for $C_{26}H_{35}NO_3SNa$ $[M + Na]^+$ 464.2230; Found 464.2248.



N*-((1*S*,2*S*,3*S*)-1-(Benzyloxy)-1,3-diphenylpent-4-en-2-yl)-*N*,4-dimethylbenzenesulfonamide **SI-2*

Sodium hydride 60 wt% in mineral oil (0.50 grams, 0.0013 mol) was added to flame dried flask under argon then suspended in THF (10.5 mL 0.1M) solvent. Then the suspension was cooled to 0 °C and sulfonamide **15C** (0.524 grams 0.001 mol) was added to the suspension then stir for 5 min. Then added methyl iodide was added in one portion. Stir overnight then dilute with water and ether and then wash organic layer with brine 3x dried Na_2SO_4 and filtered then purified by flash chromatography 30% to 50% ether in hexane to isolate the product **SI-2** as a gum.

Yield: 511 mg (74%)

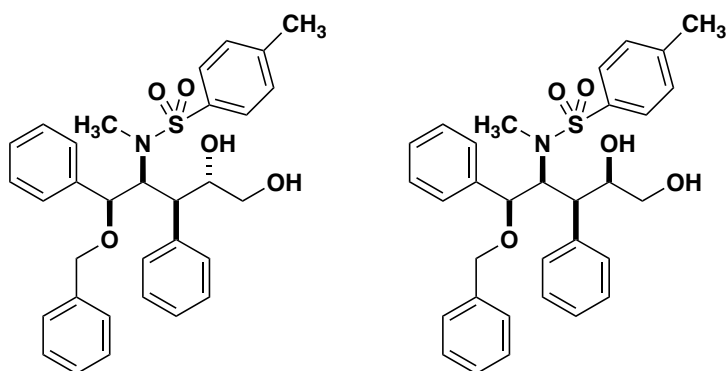
Physical Description: Gum

Column Conditions: SiO_2 , (30:70 Et_2O /Hexanes)

1H NMR: (600 MHz, $CDCl_3$) δ 7.37 (d, $J = 12.9$ Hz, 7H), 7.31 (q, $J = 6.9$ Hz, 7H), 7.28 – 7.23 (m, 2H), 6.84 (d, $J = 7.9$ Hz, 2H), 6.65 (d, $J = 8.0$ Hz, 2H), 6.21 (dt, $J = 16.8, 9.8$ Hz, 1H), 5.20 – 5.08 (m, 2H), 4.93 – 4.84 (m, 2H), 4.46 (d, $J = 11.2$ Hz, 1H), 4.19 (d, $J = 11.2$ Hz, 1H), 4.07 (t, $J = 9.9$ Hz, 1H), 2.75 (s, 3H), 2.27 (s, 3H).

¹³C NMR: (101 MHz, CDCl₃) δ 141.9, 141.2, 139.6, 139.0, 138.2, 136.1, 128.8, 128.7, 128.7, 128.5, 128.4, 127.7, 127.6, 127.6, 127.4, 127.2, 127.0, 116.5, 82.6, 71.6, 65.6, 51.5, 31.0, 21.3.

AMM: (ESI) *m/z* calcd for C₃₂H₃₃NO₃SH [M + H]⁺ 512.2254; Found 512.2271



N*-((1*S*,2*S*,3*S*,4*S*)-1-(Benzyloxy)-4,5-dihydroxy-1,3-diphenylpentan-2-yl)-*N*,4-dimethylbenzenesulfonamide **28A*

N*-((1*S*,2*S*,3*S*,4*R*)-1-(Benzyloxy)-4,5-dihydroxy-1,3-diphenylpentan-2-yl)-*N*,4-dimethylbenzenesulfonamide **28B*

A round bottom flask was charged with the corresponding olefin **SI-2** then (0.511 grams 0.001 mol) dissolved with acetonitrile / H₂O (9:1, 10 mL). NMO (0.176 grams, 0.0015 mol) was added to the reaction mixture. OsO₄ in t-butanol (1 mol%) was added, and the reaction mixture was stirred overnight at rt. The reaction was quenched by the addition of saturated sodium sulfite and extracted with EtOAc (3x). The combined organic layers were washed with brine, dried over anhydrous Na₂SO₄, filtered, and concentrated. Then purified by flash chromatography 50% ethyl acetate/hexane 84% combined yield of diols, separated 0.260 grams of (1*S*,2*S*,3*S*,4*S*) **28A** 47% as a clear oil and 0.200 grams of (1*S*,2*S*,3*S*,4*R*) **28B** 37% as a clear oil diastereomeric ratio 57:43 of diols.

***N*-((1*S*,2*S*,3*S*,4*S*)-1-(Benzyloxy)-4,5-dihydroxy-1,3-diphenylpentan-2-yl)-*N*,4-dimethylbenzenesulfonamide 28A**

Yield: 260 mg (47%)

Physical Description: Clear Oil

Column Conditions: SiO₂, (30:70 Et₂O/Hexanes)

¹H NMR: (600 MHz, CDCl₃) δ 7.73 – 7.66 (m, 2H), 7.55 (dd, *J* = 8.0, 6.6 Hz, 2H), 7.48 (dt, *J* = 7.9, 1.9 Hz, 3H), 7.41 – 7.29 (m, 5H), 7.25 – 7.18 (m, 1H), 7.17 – 7.09 (m, 2H), 6.94 (d, *J* = 8.1 Hz, 2H), 6.70 – 6.63 (m, 2H), 4.98 (dd, *J* = 10.5, 1.5 Hz, 1H), 4.42 (dddd, *J* = 10.4, 7.5, 5.1, 2.9 Hz, 1H), 4.34 (dd, *J* = 5.2, 1.2 Hz, 1H), 4.06 (d, *J* = 10.5 Hz, 1H), 3.84 (d, *J* = 10.8 Hz, 1H), 3.71 (d, *J* = 10.8 Hz, 1H), 3.28 – 3.15 (m, 1H), 2.96 (ddd, *J* = 11.2, 7.2, 3.6 Hz, 1H), 2.37 (dt, *J* = 8.8, 1.5 Hz, 1H), 2.31 (s, 3H), 2.27 (s, 3H), 2.13 – 2.04 (m, 1H).

¹³C NMR: (101 MHz, CDCl₃) δ 142.9, 138.3, 136.9, 136.7, 134.5, 129.2, 129.1, 129.0, 128.8, 128.7, 128.5, 128.4, 128.3, 127.9, 127.5, 127.5, 80.3, 70.8, 70.0, 64.4, 61.6, 48.7, 31.9, 21.6.

AMM: (ESI) *m/z* calcd for C₃₂H₃₅NO₅SH [M + H]⁺ 546.2309; Found 546.2331

***N*-((1*S*,2*S*,3*S*,4*R*)-1-(Benzyloxy)-4,5-dihydroxy-1,3-diphenylpentan-2-yl)-*N*,4-dimethylbenzenesulfonamide 28B**

Yield: 200 mg (37%)

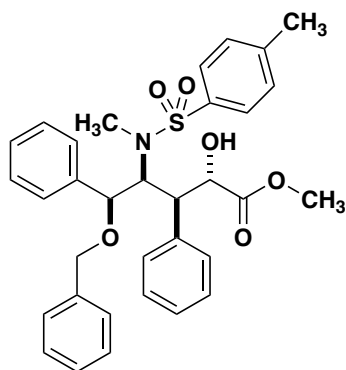
Physical Description: Clear Oil

Column Conditions: SiO₂, (30:70 Et₂O/Hexanes)

¹H NMR: (600 MHz, CDCl₃) δ 7.50 – 7.42 (m, 4H), 7.39 (s, 3H), 7.31 (dt, *J* = 6.3, 4.3 Hz, 7H), 7.07 (dd, *J* = 10.0, 5.9 Hz, 4H), 6.90 (d, *J* = 8.1 Hz, 2H), 4.98 (t, *J* = 6.6 Hz, 1H), 4.74 (d, *J* = 6.3 Hz, 1H), 4.33 (d, *J* = 11.3 Hz, 1H), 4.13 (s, 1H), 4.07 (d, *J* = 11.3 Hz, 1H), 3.46 (ddd, *J* = 10.8, 7.0, 3.6 Hz, 1H), 3.08 (dt, *J* = 21.3, 5.8 Hz, 2H), 2.49 (s, 1H), 2.42 (s, 3H), 2.29 (s, 3H).

¹³C NMR: (101 MHz, CDCl₃) δ 142.2, 138.7, 137.4, 137.0, 135.8, 130.3, 129.0, 128.8, 128.5, 128.4, 128.3 (benzene), 128.3, 128.2, 128.0, 127.8, 127.7, 127.5, 81.6, 71.9, 71.0, 65.5, 63.1, 47.5, 31.0, 21.4.

AMM: (ESI) *m/z* calcd for C₃₂H₃₅NO₅SH [M + H]⁺ 546.2309; Found 546.2338



Methyl (2S,3S,4S,5S)-5-(benzyloxy)-4-((N,4-dimethylphenyl)sulfonamido)-2-hydroxy-3,5-diphenylpentanoate 29

Diol **28A** (0.260 grams 0.00047 mol) was dissolved in toluene 4.5 ml and then TEMPO (0.007 grams 0.000047 mol) was added, and the solution turned pink. Then added pH 6.8 phosphate buffer, followed by chlorite solution (5M 0.48 mL) and then bleach (279 μ L 0.000047 mol). Stirred for 91 hours at room temperature and then rinsed into a separatory funnel using Et₂O and extract organic layer 3x with 1N NaOH solution. Then the basic aqueous layer was acidified to pH 2.1 using 1N HCl and extracted with Et₂O 3x and the

combined organics were washed 3x with brine. Dried organic layer with Na₂SO₄. Filter and concentrate. Then the hydroxy acid in DCM/MeOH 2:1 (5.5 mL) was cooled to 0 °C and was added TMS Diazomethane then stirred for till the solution was yellow and quenched with acetic acid till the solution went clear and no gas evolution was observed and then concentrated. Purified by flash chromatography.

Yield: 218 mg (81%)

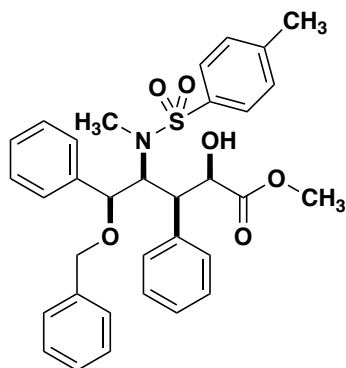
Physical Description: white powder

Column Conditions: SiO₂, (30:70 Et₂O/Hexanes)

¹H NMR: (600 MHz, CDCl₃) δ 7.48 (t, *J* = 7.4 Hz, 2H), 7.45 – 7.38 (m, 5H), 7.29 (q, *J* = 6.4, 5.4 Hz, 5H), 7.21 (dd, *J* = 8.2, 6.4 Hz, 1H), 7.17 (t, *J* = 7.4 Hz, 2H), 6.91 (d, *J* = 8.0 Hz, 2H), 6.80 (d, *J* = 7.3 Hz, 2H), 5.00 (dd, *J* = 8.8, 3.8 Hz, 1H), 4.77 (t, *J* = 7.9 Hz, 1H), 4.32 (d, *J* = 8.8 Hz, 1H), 3.98 (d, *J* = 11.1 Hz, 1H), 3.82 (d, *J* = 11.0 Hz, 1H), 3.58 (d, *J* = 7.4 Hz, 1H), 3.40 (s, 3H), 2.98 (dd, *J* = 8.5, 3.8 Hz, 1H), 2.38 (s, 3H), 2.25 (s, 3H).

¹³C NMR: (101 MHz, CDCl₃) δ 172.6, 142.6, 138.2, 137.0, 135.8, 135.0, 130.3, 129.1, 128.9, 128.8, 128.6, 128.3, 128.3, 128.1, 128.1, 127.8, 127.6, 80.7, 71.9, 70.3, 61.2, 51.8, 49.8, 31.5, 21.5.

AMM: (ESI) *m/z* calcd for C₃₃H₃₅NO₃SH [M + H]⁺ 574.2258; Found 574.2281



Methyl (2*R*,3*S*,4*S*,5*S*)-5-(benzyloxy)-4-((*N*,4-dimethylphenyl)sulfonamido)-2-hydroxy-3,5-diphenylpentanoate 30

Diol **28B** (0.200 grams 0.00037 mol) was dissolved in toluene 4.5 ml and then TEMPO (0.005 grams 0.000037 mol) was added, and the solution turned pink. Then added pH 6.8 phosphate buffer (3 mL), followed by chlorite solution (5M 0.48 mL) and then bleach (220 uL 0.000037 mol). Stirred for 91 hours at room temperature and then rinsed into a separatory funnel using Et₂O and extract organic layer 3x with 1N NaOH solution. Then the basic aqueous layer was acidified to pH 2.1 using 1N HCl and extracted with Et₂O 3x and the combined organics were washed 3x with brine NaCl. Dried organic layer with Na₂SO₄. Filter and concentrate. Then the hydroxy acid in DCM/MeOH 2:1 (5.5 mL) was cooled to 0 °C and was added TMS Diazomethane then stirred for till the solution was yellow and quenched with acetic acid till the solution went clear and no gas evolution was observed and then concentrated. Purified by flash chromatography

Yield: 165 mg (79%)

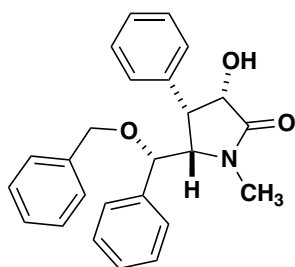
Physical Description: white powder

Column Conditions: SiO₂, (30:70 Et₂O/Hexanes)

¹H NMR: (600 MHz, CDCl₃) δ 7.48 (t, *J* = 7.4 Hz, 2H), 7.45 – 7.38 (m, 5H), 7.29 (q, *J* = 6.4, 5.4 Hz, 5H), 7.21 (dd, *J* = 8.2, 6.4 Hz, 1H), 7.17 (t, *J* = 7.4 Hz, 2H), 6.91 (d, *J* = 8.0 Hz, 2H), 6.80 (d, *J* = 7.3 Hz, 2H), 5.00 (dd, *J* = 8.8, 3.8 Hz, 1H), 4.77 (t, *J* = 7.9 Hz, 1H), 4.32 (d, *J* = 8.8 Hz, 1H), 3.98 (d, *J* = 11.1 Hz, 1H), 3.82 (d, *J* = 11.0 Hz, 1H), 3.58 (d, *J* = 7.4 Hz, 1H), 3.40 (s, 3H), 2.98 (dd, *J* = 8.5, 3.8 Hz, 1H), 2.38 (s, 3H), 2.25 (s, 3H).

¹³C NMR: (101 MHz, CDCl₃) δ 172.6, 142.6, 138.2, 137.0, 135.8, 135.0, 130.3, 129.1, 128.9, 128.8, 128.6, 128.3, 128.3, 128.1, 128.1, 127.8, 127.6, 80.7, 71.9, 70.3, 61.2, 51.8, 49.8, 31.5, 21.5.

AMM: (ESI) *m/z* calcd for C₃₃H₃₅NO₃SH [M + H]⁺ 574.2258; Found 574.2281



(3S,4S,5S)-5-((S)-(Benzyloxy)(phenyl)methyl)-3-hydroxy-1-methyl-4-phenylpyrrolidin-2-one 31

In an oven dried round bottom flask was dissolved naphthene (0.603 grams 0.0047 mol) in glyme 9 mL 0.5M solution and then stirred for 15 min under argon. Fresh cut sodium metal (0.108 grams 0.0047 mol) was cleaned with hexane, then added in 1 portion and sonicated for 1 hour. Then the methyl ester **29** was dissolved in benzene and rotovaped 3 times and put on high vac for 45 min. Then the starting material was dissolved in THF (15 mL) and cooled to -78 °C and then the naphthalide solution was added dropwise to solution for 45 min. Then sat. NaHCO₃ was added while the reaction was at -78 then extracted with ethyl acetate 3x dried organic with brine then dried with Na₂SO₄ and filtered and concentrated. Purified by flash chromatography

Yield: 46 mg (76%)

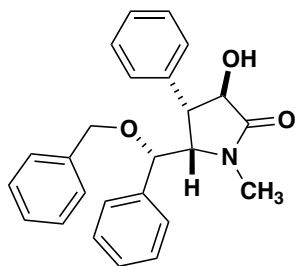
Physical Description: Clear Oil

Column Conditions: SiO₂, (100% EtOAc)

¹H NMR: (600 MHz, CDCl₃) δ 7.34 – 7.23 (m, 9H), 7.17 (d, *J* = 6.6 Hz, 2H), 7.05 (d, *J* = 7.2 Hz, 2H), 6.96 (d, *J* = 7.3 Hz, 2H), 4.44 (t, *J* = 7.5 Hz, 1H), 4.36 (d, *J* = 6.6 Hz, 1H), 4.24 (t, *J* = 6.4 Hz, 1H), 4.20 (d, *J* = 10.7 Hz, 1H), 3.97 (d, *J* = 10.7 Hz, 1H), 3.35 (t, *J* = 6.6 Hz, 1H), 2.97 (dd, *J* = 8.0, 4.1 Hz, 1H), 2.89 (s, 3H).

¹³C NMR: (101 MHz, CDCl₃) δ 175.3, 136.8, 136.7, 134.7, 129.5, 128.5, 128.5, 128.4, 128.2, 128.2, 128.1, 127.9, 127.6, 80.2, 72.1, 70.5, 66.0, 47.8, 30.4.

AMM: (ESI) *m/z* calcd for C₂₅H₂₅NOH [M + H]⁺ 388.1907; Found 388.1925



(3*R*,4*S*,5*S*)-5-((*S*)-(Benzyloxy)(phenyl)methyl)-3-hydroxy-1-methyl-4-phenylpyrrolidin-2-one 32

In an oven dried round bottom flask was dissolved naphthene (0.643 grams 0.0050 mol) in glyme 10 mL 0.5M solution and then stirred for 15 min under argon. Fresh cut sodium metal (0.116 grams 0.0050 mol) was cleaned with hexane, then added in 1 portion and sonicated for 1 hour. Then the methyl ester **30** (0.096 grams 0.00016 mol) was dissolved in benzene and rotovaped 3 times and put on high vac for 45 min. Then the starting material was dissolved in THF (16 mL) and cooled to -78 °C and then the naphthalide solution was added dropwise to solution for 45 min. Then sat. NaHCO₃ was added while

the reaction was at -78 then extracted with ethyl acetate 3x dried organic with brine then dried with Na₂SO₄ and filtered and concentrated. Purified by flash chromatography.

Yield: 57 mg (87%)

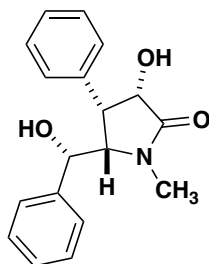
Physical Description: clear colorless solid **mp** 119-120 °C

Column Conditions: SiO₂, (100% EtOAc)

¹H NMR: (600 MHz, CDCl₃) δ 7.40 (q, *J* = 7.5 Hz, 5H), 7.34 (dt, *J* = 17.5, 8.3 Hz, 5H), 7.27 (q, *J* = 6.8, 5.8 Hz, 5H), 5.25 (dd, *J* = 10.5, 2.6 Hz, 1H), 4.22 (d, *J* = 11.2 Hz, 1H), 4.13 (s, 1H), 3.98 (dd, *J* = 8.1, 2.2 Hz, 1H), 3.80 – 3.71 (m, 1H), 3.60 (d, *J* = 11.1 Hz, 1H), 3.02 (d, *J* = 2.9 Hz, 1H), 2.37 (s, 3H).

¹³C NMR: (101 MHz, CDCl₃) δ 175.8, 138.7, 137.7, 136.0, 128.8, 128.8, 128.5, 128.0, 127.9, 127.6, 127.4, 127.1, 126.3, 78.6, 70.8, 69.9, 68.8, 52.4, 31.8.

AMM: (ESI) *m/z* calcd for C₂₅H₂₅NOH [M + H]⁺ 388.1907; Found 388.1931



(3S,4S,5S)-3-Hydroxy-5-((S)-hydroxy(phenyl)methyl)-1-methyl-4-phenylpyrrolidin-2-one (+) *cis-epi-clausenamide*

A round bottom flask was flame dried and purged with argon and a solution of ethyl acetate (4 mL) with starting benzylated material **31** (0.017 grams 0.00044 mol) was transferred to round bottom and then head space was purged with argon. Then palladium on carbon was added in 1 portion and a balloon with hydrogen was purged into the flask.

Reaction was stirred for 30 min. Then reaction was purged with argon and the solution was filtered through a pipette filter with cotton sand and then cellite. The filtrate was concentrated and to yield the title compound

Yield: 11 mg (85%)

Physical Description: white amorphous solid **mp** 198-199 °C

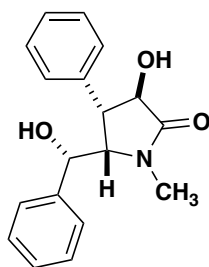
Column Conditions: SiO₂, (100% EtOAc)

¹H NMR: (600 MHz, CDCl₃) δ 7.37 – 7.27 (m, 8H), 7.17 (d, *J* = 7.2 Hz, 2H), 4.71 (s, 1H), 4.49 (d, *J* = 5.9 Hz, 1H), 4.21 (dt, *J* = 7.0, 3.1 Hz, 2H), 3.55 (t, *J* = 7.0 Hz, 1H), 3.34 (d, *J* = 9.9 Hz, 1H), 2.71 (d, *J* = 2.9 Hz, 3H).

¹³C NMR: (101 MHz, CDCl₃) δ 174.8, 141.0, 134.6, 129.7, 128.6, 128.5, 127.9, 127.7, 126.0, 71.7, 70.6, 68.7, 47.8, 30.8.

AMM: (ESI) *m/z* calcd for C₁₈H₁₉NOH [M + H]⁺ 298.1438; Found 298.1447

Optical Rotation: 26 degrees *c* 0.26 at 22 °C.



(3*R*,4*S*,5*S*)-3-Hydroxy-5-((*S*)-hydroxy(phenyl)methyl)-1-methyl-4-phenylpyrrolidin-2-one (+) *epi*-clausenamide

A round bottom flask was flame dried and purged with argon and a solution of ethyl acetate (4 mL) with starting benzylated material **32** (0.017 grams 0.00044 mol) was

transferred to round bottom and then head space was purged with argon. Then palladium on carbon was added in 1 portion and a balloon with hydrogen was purged into the flask. Reaction was stirred for 30 min. Then reaction was purged with argon and the solution was filtered through a pipette filter with cotton sand and then celite. The filtrate was concentrated and to yield the title compound.

Yield: 11 mg (85%)

Physical Description: white amorphous solid **mp** 199 °C

Column Conditions: SiO₂, (100% EtOAc)

¹H NMR: (600 MHz, CDCl₃) δ 7.51 (d, *J* = 7.6 Hz, 2H), 7.43 (t, *J* = 7.8 Hz, 2H), 7.32 (t, *J* = 7.9 Hz, 3H), 7.26 (t, *J* = 4.7 Hz, 3H), 5.25 (d, *J* = 10.4 Hz, 1H), 4.54 (s, 1H), 4.01 (d, *J* = 8.3 Hz, 1H), 3.75 (t, *J* = 9.6 Hz, 1H), 3.49 (d, *J* = 2.7 Hz, 1H), 2.38 (d, *J* = 2.7 Hz, 3H), 1.99 (s, 1H).

¹³C NMR: (101 MHz, CDCl₃) δ 175.8, 141.8, 136.1, 129.0, 128.6, 128.1, 127.6, 127.5, 125.0, 70.6, 70.3, 68.3, 52.4, 31.5.

AMM: (ESI) *m/z* calcd for C₁₈H₁₉NOH [M + H]⁺ 298.1438; Found 298.1446

Optical Rotation: 202 degrees *c* 0.66 at 22 °C.

Corresponds to previously reported literature.⁴⁵

1.6 References

- (1) Eppe, G.; Didier, D.; Marek, I. Stereocontrolled Formation of Several Carbon–Carbon Bonds in Acyclic Systems. *Chem. Rev.* **2015**, *115* (17), 9175–9206.
- (2) Moore, L. C.; Lo, A.; Fell, J. S.; Duong, M. R.; Moreno, J. A.; Rich, B. E.; Bravo, M.; Fettinger, J. C.; Souza, L. W.; Olmstead, M. M.; et al. Acyclic Stereocontrol in the

- Additions of Nucleophilic Alkenes to A-Chiral N -Sulfonyl Imines. *Chem. – A Eur. J.* **2019**, *25* (52), 12214–12220.
- (3) Lo, A.; Gutierrez, D. A.; Toth-Williams, G.; Fettinger, J. C.; Shaw, J. T. 1,3-Asymmetric Induction in Diastereoselective Allylations of Chiral N-Tosyl Imines. *J. Org. Chem.* **2022**, *87* (5), 2773–2778.
- (4) Lachance, H.; Hall, D. G. Allylboration of Carbonyl Compounds. In *Organic Reactions*; Major Reference Works; John Wiley & Sons, Inc.: Hoboken, NJ, USA, 2009; pp 1–574.
- (5) Denmark, S. E.; Weber, E. J. On the Stereochemistry of Allylmetal-Aldehyde Condensations. Preliminary Communication. *Helv. Chim. Acta* **1983**, *66* (6), 1655–1660.
- (6) Hoffmann, R. W.; Zeiss, H.-J. Diastereoselective Synthesis of β -Methyl Homoallyl Alcohols. *Angew. Chemie Int. Ed. English* **1979**, *18* (4), 306–307.
- (7) Kennedy, J. W. J.; Hall, D. G. Dramatic Rate Enhancement with Preservation of Stereospecificity in the First Metal-Catalyzed Additions of Allylboronates. *J. Am. Chem. Soc.* **2002**, *124* (39), 11586–11587.
- (8) Ishiyama, T.; Ahiko, T.; Miyaura, N. Acceleration Effect of Lewis Acid in Allylboration of Aldehydes: Catalytic, Regiospecific, Diastereospecific, and Enantioselective Synthesis of Homoallyl Alcohols. *J. Am. Chem. Soc.* **2002**, *124* (42), 12414–12415.
- (9) Kennedy, J. W. J.; Hall, D. G. Lewis Acid Catalyzed Allylboration: Discovery, Optimization, and Application to the Formation of Stereogenic Quaternary Carbon

- Centers. *J. Org. Chem.* **2004**, *69* (13), 4412–4428.
- (10) Lachance, H.; Lu, X.; Gravel, M.; Hall, D. G. Scandium-Catalyzed Allylboration of Aldehydes as a Practical Method for Highly Diastereo- and Enantioselective Construction of Homoallylic Alcohols. *J. Am. Chem. Soc.* **2003**, *125* (34), 10160–10161.
- (11) Hiersemann, M. Synthesis of α -Allyloxy-Substituted α,β -Unsaturated Esters via Aldol Condensation. Convenient Access of Highly Substituted Allyl Vinyl Ethers. *Synthesis (Stuttg.)* **2000**, *2000* (09), 1279–1290.
- (12) Omoto, K.; Fujimoto, H. Theoretical Study of the Effects of Structure and Substituents on Reactivity in Allylboration. *J. Org. Chem.* **1998**, *63* (23), 8331–8336.
- (13) Hoffmann, R. W.; Kemper, B. Acyclic Stereocontrol in the Addition of γ -Alkylthio-Allylboronates to Aldehydes. *Tetrahedron* **1984**, *40* (12), 2219–2224.
- (14) Batey, R. A.; Thadani, A. N.; Smil, D. V. Potassium Allyl- and Crotyltrifluoroborates: Stable and Efficient Agents for Allylation and Crotylation. *Tetrahedron Lett.* **1999**, *40* (23), 4289–4292.
- (15) Molander, G. A.; Ham, J. Synthesis of Functionalized Organotrifluoroborates via Halomethyltrifluoroborates. *Org. Lett.* **2006**, *8* (10), 2031–2034.
- (16) Wallner, O. A.; Szabó, K. J.; Beveridge, R. E.; Batey, R. A. Potassium Trifluoro-2-Propenylborate. In *Encyclopedia of Reagents for Organic Synthesis*; American Cancer Society, 2015; pp 1–10.
- (17) Batey, R. A.; Thadani, A. N.; Smil, D. V.; Lough, A. J. Diastereoselective Allylation and Crotylation Reactions of Aldehydes with Potassium Allyl- and

- Crotyltrifluoroborates under Lewis Acid Catalysis. *Synthesis (Stuttg)*. **2000**, 2000 (07), 990–998.
- (18) Thadani, A. N.; Batey, R. A. Diastereoselective Allylations and Crotylations under Phase-Transfer Conditions Using Trifluoroborate Salts: An Application to the Total Synthesis of (–)-Tetrahydrolipstatin. *Tetrahedron Lett.* **2003**, 44 (44), 8051–8055.
- (19) Roush, W. R. Concerning the Diastereofacial Selectivity of the Aldol Reactions of α -Methyl Chiral Aldehydes and Lithium and Boron Propionate Enolates. *J. Org. Chem.* **1991**, 56 (13), 4151–4157.
- (20) Roush, W. R.; Adam, M. A.; Walts, A. E.; Harris, D. J. Stereochemistry of the Reactions of Substituted Allylboronates with Chiral Aldehydes. Factors Influencing Aldehyde Diastereofacial Selectivity. *J. Am. Chem. Soc.* **1986**, 108 (12), 3422–3434.
- (21) Li, S.-W.; Batey, R. A. Allylation and Highly Diastereoselective Syn or Anti Crotylation of N-Toluenesulfonylimines Using Potassium Allyl- and Crotyltrifluoroborates. *Chem. Commun.* **2004**, No. 12, 1382–1383.
- (22) Alam, R.; Das, A.; Huang, G.; Eriksson, L.; Himo, F.; Szabó, K. J. Stereoselective Allylboration of Imines and Indoles under Mild Conditions. An in Situ E/Z Isomerization of Imines by Allylboroxines. *Chem. Sci.* **2014**, 5 (7), 2732–2738.
- (23) Solin, N.; Wallner, O. A.; Szabó, K. J. Palladium Pincer-Complex Catalyzed Allylation of Tosylimines by Potassium Trifluoro(Allyl)Borates. *Org. Lett.* **2005**, 7(4), 689–691.
- (24) Kahn, S. D.; Pau, C. F.; Chamberlin, A. R.; Hehre, W. J. Modeling Chemical

- Reactivity. 4. Regiochemistry and Stereochemistry of Electrophilic Additions to Allylic Double Bonds. *J. Am. Chem. Soc.* **1987**, *109* (3), 650–663.
- (25) Fleming, I.; Terrett, N. K. The Stereochemistry of Some SE₂' Reactions of Allyl- and Allenylsilanes. *Tetrahedron Lett.* **1983**, *24* (38), 4153–4156.
- (26) Hayashi, T.; Konishi, M.; Kumada, M. Optically Active Allylsilanes. 2. High Stereoselectivity in Asymmetric Reaction with Aldehydes Producing Homoallylic Alcohols. *J. Am. Chem. Soc.* **1982**, *104* (18), 4963–4965.
- (27) Denmark, S. E.; Almstead, N. G. Stereochemical Studies on the Addition of Allylsilanes to Aldehydes: The SE' Component. *J. Mex. Chem. Soc.* **2009**, *53*, 174–192.
- (28) Denmark, S. E.; Weber, E. J.; Almstead, N. G.; Wolf, L. M. On the Stereochemical Course of the Addition of Allylsilanes to Aldehydes. *Tetrahedron* **2012**, *68* (37), 7701–7718.
- (29) Wolf, L. M.; Denmark, S. E. A Theoretical Investigation on the Mechanism and Stereochemical Course of the Addition of (E)-2-Butenyltrimethylsilane to Acetaldehyde by Electrophilic and Nucleophilic Activation. *J. Am. Chem. Soc.* **2013**, *135* (12), 4743–4756.
- (30) Evans, D. A.; Siska, S. J.; Cee, V. J. Resurrecting the Cornforth Model for Carbonyl Addition: Studies on the Origin of 1,2-Asymmetric Induction in Enolate Additions to Heteroatom-Substituted Aldehydes. *Angew. Chemie.* **2003**, *115* (15), 1803–1807.
- (31) Stanton, G. R.; Norrby, P.-O.; Carroll, P. J.; Walsh, P. J. Chelation-Controlled Addition of Organozincs to α -Chloro Aldimines. *J. Am. Chem. Soc.* **2012**, *134* (42),

17599–17604.

- (32) Schaus, J. V.; Jain, N.; Panek, J. S. Asymmetric Synthesis of Homoallylic Amines and Functionalized Pyrrolidines via Direct Amino-Crotylation of In Situ Generated Imines. *Tetrahedron* **2000**, *56* (52), 10263–10274.
- (33) Vabre, R.; Island, B.; Diehl, C. J.; Schreiner, P. R.; Marek, I. Forming Stereogenic Centers in Acyclic Systems from Alkynes. *Angew. Chemie Int. Ed.* **2015**, *54* (34), 9996–9999.
- (34) Petrini, M. α -Amido Sulfones as Stable Precursors of Reactive N-Acylimino Derivatives. *Chem. Rev.* **2005**, *105* (11), 3949–3977.
- (35) Chu, S.; Zhang, J. Recent Advances in the Study of (–)Clausenamide: Chemistry, Biological Activities and Mechanism of Action. *Acta Pharm. Sin. B* **2014**, *4* (6), 417–423.
- (36) Chu, S.; Liu, S.; Duan, W.; Cheng, Y.; Jiang, X.; Zhu, C.; Tang, K.; Wang, R.; Xu, L.; Wang, X.; et al. The Anti-Dementia Drug Candidate, (-)-Clausenamide, Improves Memory Impairment through Its Multi-Target Effect. *Pharmacol. Ther.* **2016**, *162*, 179–187.
- (37) Gutierrez, D. A.; Fetting, J.; Houk, K. N.; Ando, K.; Shaw, J. T. Diastereoselective Addition of Prochiral Nucleophilic Alkenes to α -Chiral N-Sulfonyl Imines. *Org. Lett.* **2022**, *24* (5), 1164–1168.
- (38) Ming-He, Y.; Yan-Yong, C.; Liang, H. Studies on the Chemical Constituents of (Clausena Lansium) (Lour.) Skeels II: The Isolation and Structural Elucidation of Neoclausenamide and Dehydrocycloclausenamide. *Acta Chim. Sin. English Ed.*

- 1987**, 5 (3), 267–272.
- (39) Hartwig, W.; Born, L. Diastereoselective and Enantioselective Total Synthesis of the Hepatoprotective Agent Clausenamide. *J. Org. Chem.* **1987**, 52 (19), 4352–4358.
- (40) Yang, L.; Wang, D. X.; Zheng, Q. Y.; Pan, J.; Huang, Z. T.; Wang, M. X. Highly Efficient and Concise Synthesis of Both Antipodes of SB204900, Clausenamide, Neoclausenamide, Homoclausenamide and ζ -Clausenamide. Implication of Biosynthetic Pathways of Clausena Alkaloids. *Org. Biomol. Chem.* **2009**, 7 (12), 2628–2634.
- (41) Xuan, Y.; Lin, H.-S.; Yan, M. Highly Efficient Asymmetric Synthesis of α,β -Epoxy Esters via One-Pot Organocatalytic Epoxidation and Oxidative Esterification. *Org. Biomol. Chem.* **2013**, 11 (11), 1815.
- (42) Worch, C.; Atodiresei, I.; Raabe, G.; Bolm, C. Synthesis of Enantiopure Sulfonimidamides and Elucidation of Their Absolute Configuration by Comparison of Measured and Calculated CD Spectra and X-Ray Crystal Structure Determination. *Chem. - A Eur. J.* **2010**, 16 (2), 677–683.
- (43) Tanda, K.; Toyao, A.; Watanabe, A.; Sakamoto, M.; Yamasaki, T. Magnesium-Coordinated Chelation Control in 1,3-Dipolar Cycloaddition of Chiral α -Alkoxyethyl Ether Nitrile Oxide: Application to the Synthesis of (-)/(-)- Cis - Clausenamide. *Synlett* **2014**, 25 (1), 1–4.
- (44) Kokuev, A. O.; Antonova, Y. A.; Dorokhov, V. S.; Golovanov, I. S.; Nelyubina, Y. V.; Tabolin, A. A.; Sukhorukov, A. Y.; Ioffe, S. L. Acylation of Nitronates: [3,3]-

- Sigmatropic Rearrangement of in Situ Generated N -Acyloxy, N -Oxyenamines. *J. Org. Chem.* **2018**, *83* (18), 11057–11066.
- (45) Zhang, L.; Zhou, Y.; Yu, X. Suzuki-Miyaura Coupling Based Enantioselective Synthesis of (+)-Epi- Clausenamide and the Enantiomer of Its 3-Deoxy Analogue. *Synlett* **2012**, *23* (08), 1217–1220.
- (46) Hu, Z.; Zhu, Y.; Fu, Z.; Huang, W. Asymmetric Synthesis of Enantioenriched 6-Hydroxyl Butyrolactams Promoted by N-Heterocyclic Carbene. *J. Org. Chem.* **2019**, *84* (16), 10328–10337.
- (47) Thadani, A. N.; Batey, R. A. A Mild Protocol for Allylation and Highly Diastereoselective Syn or Anti Crotylation of Aldehydes in Biphasic and Aqueous Media Utilizing Potassium Allyl- and Crotyltrifluoroborates. *Org. Lett.* **2002**, *4* (22), 3827–3830.
- (48) Nowrouzi, F.; Batey, R. A. Regio- and Stereoselective Allylation and Crotylation of Indoles at C2 Through the Use of Potassium Organotrifluoroborate Salts. *Angew. Chemie.* **2013**, *125* (3), 926–929.
- (49) Yamamoto, Y.; Komatsu, T.; Maruyama, K. Diastereofacial Selectivity in the Reaction of Allylic Organometallic Compounds with Imines. Stereoelectronic Effect of Imine Group. *J. Org. Chem.* **1985**, *50* (17), 3115–3121.
- (50) Yamamoto, Y.; Maruyama, K.; Komatsu, T.; Ito, W. Very High 1,2- and 1,3-Asymmetric Induction in the Reactions of Allylic Boron Compounds with Chiral Imines. *J. Am. Chem. Soc.* **1986**, *108* (24), 7778–7786.
- (51) Cornforth, J. W.; Cornforth, R. H.; Mathew, K. K. 24. A General Stereoselective

- Synthesis of Olefins. *J. Chem. Soc.* **1959**, No. 0, 112–127.
- (52) Houk, K. N. Perspective on “Theoretical Interpretation of 1-2 Asymmetric Induction. The Importance of Antiperiplanarity.” *Theor. Chem. Acc.* **2000**, *103* (3), 330–331.
- (53) See Supplemental Information. No Title.
- (54) More, J. D.; Finney, N. S. A Simple and Advantageous Protocol for the Oxidation of Alcohols with O-Iodoxybenzoic Acid (IBX). *Org. Lett.* **2002**, *4* (17), 3001–3003.
- (55) Li, F.; Good, S.; Tulchinsky, M. L.; Whiteker, G. T. Efficient Stereoselective Synthesis of a Key Chiral Aldehyde Intermediate in the Synthesis of Picolinamide Fungicides. *Org. Process Res. Dev.* **2019**, *23* (10), 2253–2260.
- (56) Moore, L. C. Diastereoselective Additions of Anhydride Enolates and Nucleophilic Alkenes to Chiral Aldehyde-Derived N-Tosyl Imines. University of California, Davis 2019.
- (57) Olsson, V. J.; Sebelius, S.; Selander, N.; Szabó, K. J. Direct Boronation of Allyl Alcohols with Diboronic Acid Using Palladium Pincer-Complex Catalysis. A Remarkably Facile Allylic Displacement of the Hydroxy Group under Mild Reaction Conditions. *J. Am. Chem. Soc.* **2006**, *128* (14), 4588–4589.
- (58) Selander, N.; Szabó, K. J. Performance of SCS Palladium Pincer Complexes in Borylation of Allylic Alcohols. Control of the Regioselectivity in the One-Pot Borylation–Allylation Process. *J. Org. Chem.* **2009**, *74* (15), 5695–5698.
- (59) Barentsen, H. M.; van Dijk, M.; Zuilhof, H.; Sudhölter, E. J. R. Thermal and Photoinduced Polymerization of Thin Diacetylene Films. 1. Phthalimido-Substituted Diacetylenes. *Macromolecules* **2000**, *33* (3), 775–780.

- (60) Brown, H. C.; Blue, C. D.; Nelson, D. J.; Bhat, N. G. Vinylic Organoboranes. 12. Synthesis of (Z)-1-Halo-1-Alkenes via Hydroboration of 1-Halo-1-Alkynes Followed by Protonolysis. *J. Org. Chem.* **1989**, *54* (26), 6064–6067.
- (61) Stille, J. K.; Simpson, J. H. Stereospecific Palladium-Catalyzed Coupling Reactions of Vinyl Iodides with Acetylenic Tin Reagents. *J. Am. Chem. Soc.* **1987**, *109* (7), 2138–2152.
- (62) Evans, D. A.; Aye, Y.; Wu, J. Asymmetric, Anti-Selective Scandium-Catalyzed Sakurai Additions to Glyoxyamide. Applications to the Syntheses of N-Boc d-Alloisoleucine and d-Isoleucine. *Org. Lett.* **2006**, *8* (10), 2071–2073.
- (63) Terao, J.; Jin, Y.; Torii, K.; Kambe, N. Reaction Pathways of Zirconocene-Catalyzed Silylation of Alkenes with Chlorosilanes. *Tetrahedron* **2004**, *60* (6), 1301–1308.
- (64) Negishi, E.; Luo, F.-T.; Rand, C. L. Stereo- and Regioselective Routes to Allylic Silanes. *Tetrahedron Lett.* **1982**, *23* (1), 27–30.
- (65) Tietze, L. F.; Hölsken, S.; Adrio, J.; Kinzel, T.; Wegner, C. Facial-Selective Allylation of Methyl Ketones for the Asymmetric Synthesis of Tertiary Homoallylic Ethers. *Synthesis (Stuttg)*. **2004**, *2004* (13), 2236–2239.
- (66) Hayashi, T.; Fujiwa, T.; Okamoto, Y.; Katsuro, Y.; Kumada, M. Cross-Coupling of Enol Phosphates with Trimethylsilylmethylmagnesium Halides Catalyzed by Nickel or Palladium Complexes; A Selective Synthesis of Allylsilanes. *Synthesis (Stuttg)*. **1981**, *1981* (12), 1001–1003.

2 Chapter 2: Enantioselective Desymmetrization of Sulfonimidamide (SIAs) Heterocycles *via* Tsuji-Trost-Asymmetric-Allylation

2.1 Introduction

Sulfonimidamides (SIAs) are the aza substituted variants of the sulfonamide functional group that were initially discovered in the 1950's (**Figure 2.1**).⁶⁷ SIAs contain a stereogenic, configurationally stable, tetrahedral sulfur atom.^{42,67,68} The sulfonimidamide functional group has become an emerging class of organic compounds that have proven crucial in drug discovery, materials science, and related fields.⁶⁹⁻⁷² The additional basic nitrogen adds a new vector in three-dimensional space that can act as both a hydrogen bond donor/acceptor while simultaneously providing a synthetic handle for further chemical transformations. Furthermore, *N*-acylated SIAs have been shown to be bioisosteres of carboxylic acids.^{67,73,74} As a result of these properties, the introduction of the SIA functional group into biologically active compounds has become an increasingly attractive target to medicinal chemists in the last two decades. More specifically, heterocyclic SIAs have emerged as an important structural motif in medicinally relevant molecules.

Introduction to Sulfonylimidamides (SIAs)

First reported 1962

- SIA is useful functional group in drug discovery
- Features a basic nitrogen for further synthetic manipulation
- Offers new hydrogen bond donor/acceptor interactions
- Acylated SIAs are bioisostere for COOH (low efflux ratios)
- Introduces new IP space
- Major challenge is synthesizing enantioenriched SIA (chiral sulfur)

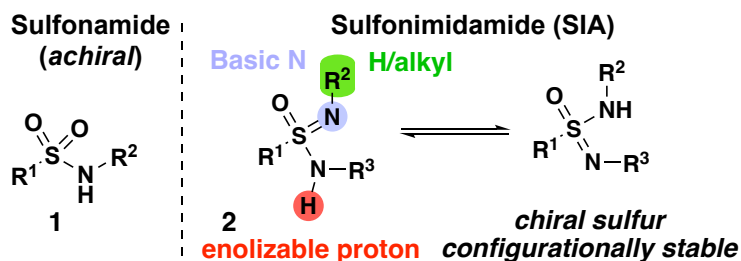


Figure 2.1: Overview of the benefits of sulfonylimidamides in medicinal chemistry

Despite displaying promising potential for potent bioactivity, synthetic reports of enantioenriched SIA heterocycles are rare.^{75,76} The synthesis of chiral sulfur functional groups is still an unmet synthetic challenge in the synthetic chemists toolbox. This notable absence in the literature is due to the fact that, until recently, methods to access SIAs containing enantiopure sulfur centers were extremely limited. Classical methods were inefficient, involving separation of diastereomers via crystallization or the use of chiral auxiliaries.^{42,77–79}

Herein, I will describe the development of a desymmetrization reaction of heterocyclic SIAs. High throughput screening was utilized for ligand and solvent optimization, leading to high enantioselectivities and yields for a variety of allylic electrophiles and SIA substrates. Additionally, I will demonstrate how these compounds are amenable to other synthetic transformations, providing access to a novel class of enantioenriched tricyclic sulfonylimidamides.

2.1.1 Overview of Sulfonimidamides in Medicinal Chemistry

The first report of the biological activity of sulfonimidamides was in 1979.⁸⁰ A series of sulfonimidamide analogues was prepared based on the known hyperglycemic agent tolbutamide and the antibacterial agent sulfadiazine (**Figure 2.2**). However, none of the sulfonimidamide compounds retained the biological activity of the parent sulfonamide. All compounds were inactive in an anti-diabetic screen, and none of the analogues exhibited sufficient activity to be of interest as an anti-bacterial.

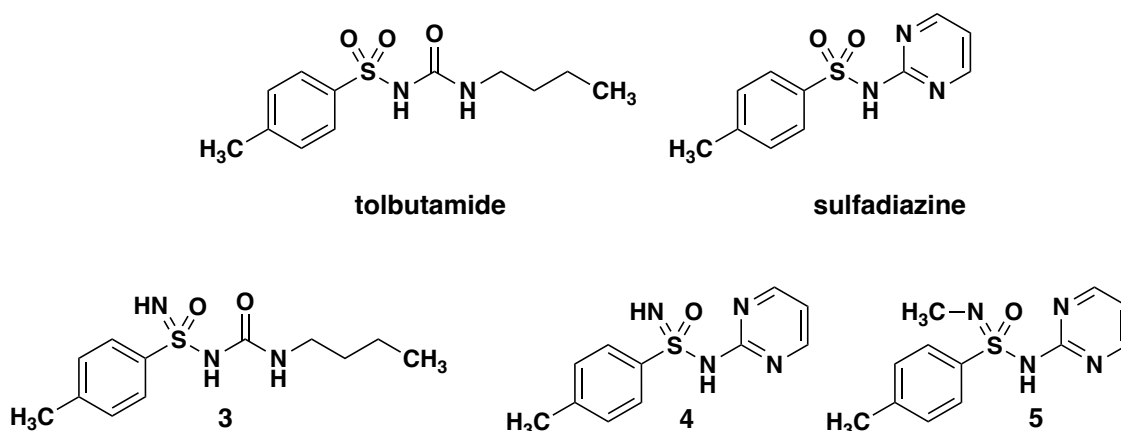


Figure 2.2: Analogs of tolbutamide and sulfadiazine in initial screening of SIAs in biological relevant molecules

Even though the screening of sulfonimidamides did not show any *in vitro* activity, the sulfonimidamide has been recognized as a suitable bioisostere. Carboxylic acids often exhibit poor ADME properties and can be metabolized to reactive acyl glucuronides or CoA esters; consequently, multiple carboxylic acid bioisosteres have been developed.⁶⁸ Two popular bioisosteres for carboxylic acids in medicinal chemistry are acyl sulfonamides and tetrazoles.^{74,81} Researchers have designed and synthesized aryl substituted cyclic sulfonimidamides as novel chiral heterocyclic carboxylic acid bioisosteres.⁸² The biological activities of these cyclic sulfonimidamide compounds were

not reported, but the biophysical properties and membrane permeability were compared to tetrazoles. The chiral cyclic sulfonimidamide scaffold was less acidic (pKa 6) than the corresponding carboxylic acid isostere (pKa 4) and were found to have higher cell permeabilities and lower efflux ratios (ERs).

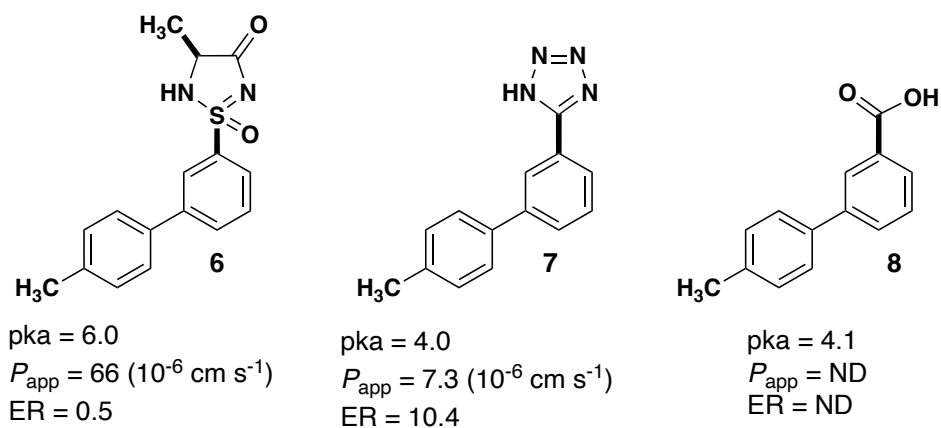
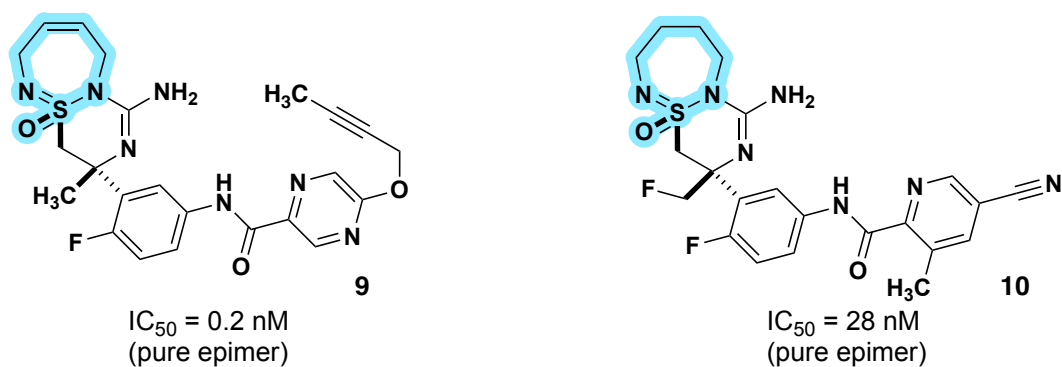


Figure 2.3: SIA as a bioisostere of carboxylic acid and comparison to tetrazoles. P_{app} Caco-2 permeabilities and ER efflux ratios.

Two reported BACE1 inhibitors are based on a seven membered bicyclic sulfonimidamide scaffold (**Figure 2.4**). β -Amyloid plaques are found in diseased brains of people who suffer from Alzheimer's disease and inhibition of the β -secretase enzyme (BACE1) has long been considered key for a disease modifying treatment. The BACE1 enzyme is involved in the cleaving the amyloid precursor protein that eventually leads to the plaques.⁸³ The stereo chemistry at both the C atom and the stereogenic S center had a significant influence on the potency of the compounds. A significant portion of the compounds tested were mixtures of diastereomers with the configuration at sulfur unknown. Only a handful of the most potent compounds were separated as pure epimers and tested. This highlights the unmet challenge of stereocontrol at chiral sulfur centers.



BACE1 Inhibitor Hoffmann-La Roche

Figure 2.4: Hoffman-La Roche's SIA BACE 1 inhibitor.

More bioactive compounds containing sulfonimidamides continue to be developed and continue to gain traction in the medicinal chemistry community. This is exemplified by the NLRP3 inflammasome inhibitor developed by Novartis and the nAChR agonist that has been developed by BASF (**Figure 2.5**).^{84,85} The explosion of the functional group is exhibited by a Scifinder patent search which shows that from 2000-2017 there had not been a significant number of reports of sulfonimidamides in the patent literature. However, in 2018 to 2020 there is a sudden burst of this unique functional group featured in the patent literature (**Figure 2.6**).

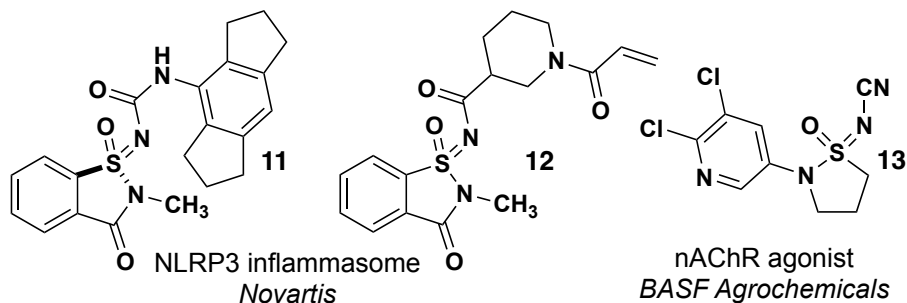


Figure 2.5: NLRP3 inflammasome compound by *Novartis* and nAChR agonist *BASF Agrochemicals*

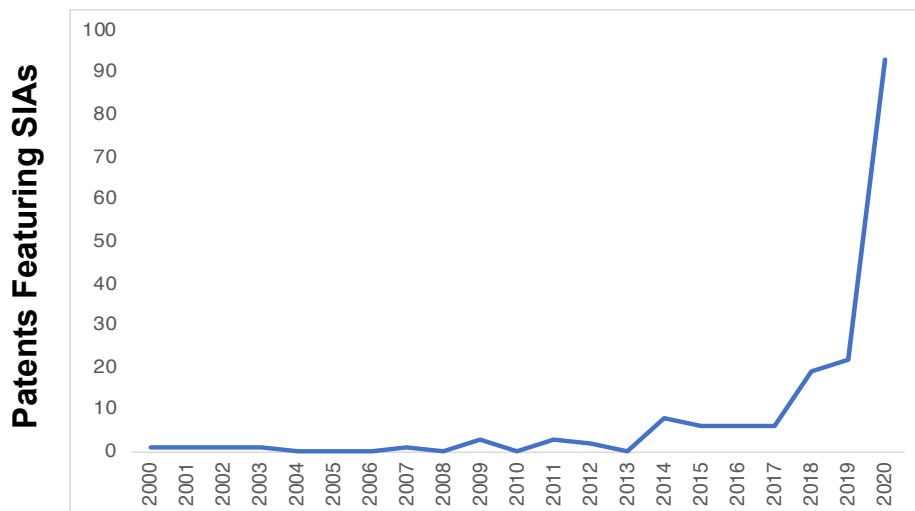
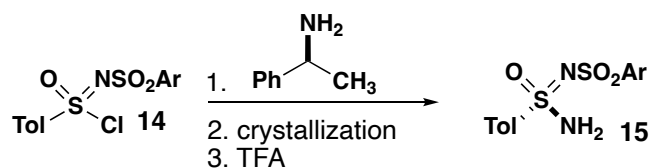


Figure 2.6: Scifinder patent search featuring sulfonimidamides from 2000-2020.

2.1.2 Overview of Enantioselective Syntheses of Sulfonimidamides

Until recently, the enantioselective synthesis of sulfonimidamides has relied on resolutions via a diastereomeric crystallization or the use of menthol as a chiral auxiliary (**Figure 2.7**).^{42,77-79} Another chiral auxiliary method has been the use of Ellman's sulfinamide to do a stereospecific nitrene insertion to yield an enantiomerically pure sulfonimidamide.

Separation by crystallization



Chiral Auxiliary

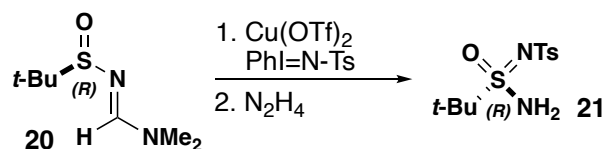
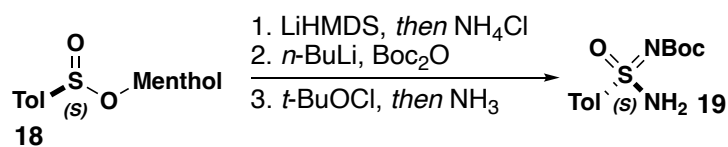
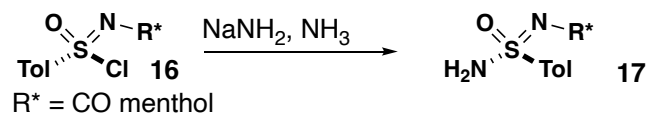


Figure 2.7: Methods to synthesize enantioenriched sulfonimidamides.

Only two catalytic synthetic methods to access enantioenriched SIAs have been developed to date. One strategy for the synthesis of enantioenriched SIAs involves the generation of enantiopure sulfonimidoyl chlorides via chiral phosphoric acid catalysis followed by a stereospecific amination reaction.⁸⁶ In this report the authors desymmetrize aza-dichlorosulfonium by an enantioselective hydrolysis (**Figure 2.8**). The enantioselective hydrolysis then generates an enantiomerically enriched sulfonimidoyl chloride which can then be stereospecifically attacked by an amine to yield enantiomerically enriched sulfonimidamides (**Figure 2.9**).

Enantioselective Hydrolysis

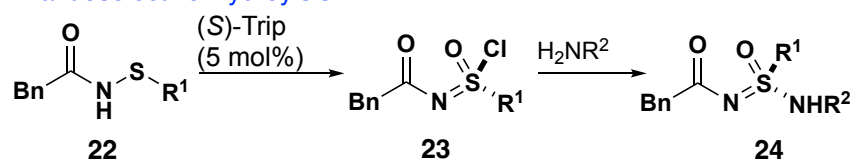


Figure 2.8: Enantioselective hydrolysis for the synthesis of enantioenriched sulfonimidamides

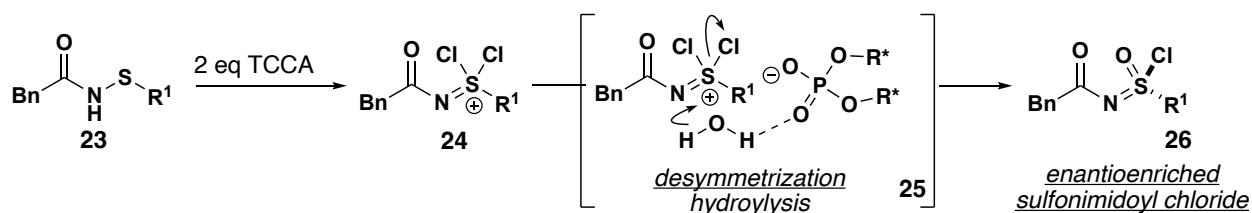


Figure 2.9: Proposed sequence for enantioenriched sulfonimidoyl chloride synthesis

The second report of a catalytic enantioselective reaction desymmetrizes a di-benzyl substituted SIA.⁸⁷ The Willis group recognized that symmetrically disubstituted SIAs tautomerize between their *R/S* enantiomers and that the ions generated from deprotonation or protonation are prochiral. A bis-quaternized cinchona alkaloid is employed as a phase transfer catalyst that facilitated the reaction of a prochiral anionic SIA with an alkyl halide electrophile, yielding a variety of enantioenriched *N*-alkyl SIAs in good yields and modest enantioselectivity.

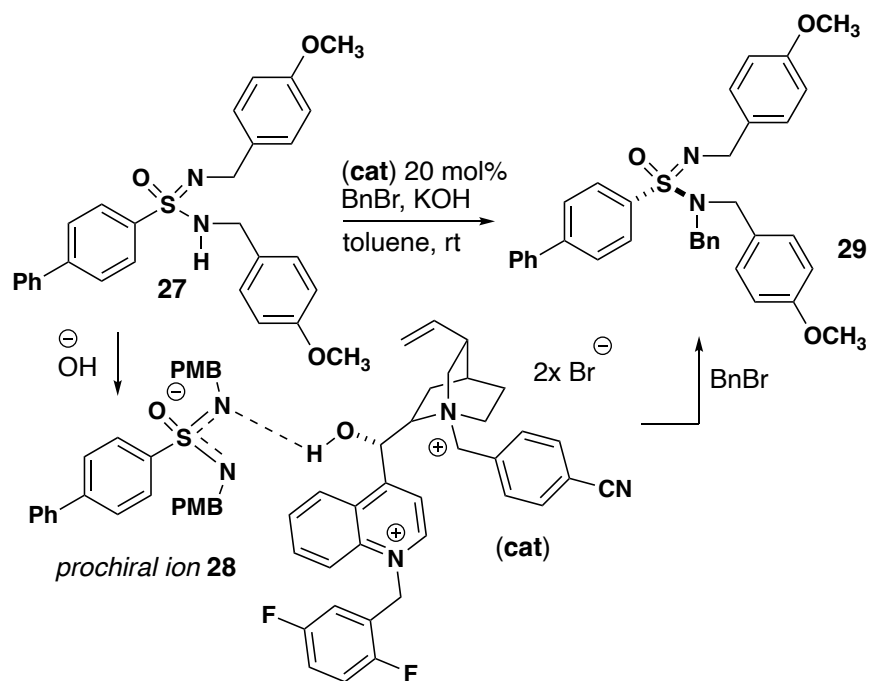


Figure 2.10: Willis' desymmetrization of disubstituted sulfonimidamides

The prototropic tautomerization exhibited by sulfonimidamides makes them uniquely suited for desymmetrization processes. In the case where both nitrogen substituents of a disubstituted sulfonimidamide are the same, the two tautomers are also enantiomers, allowing deprotonation or protonation to generate a prochiral anion or cation. A crystal structure of a protonated sulfonimidamide showed the S-N had the same bond lengths, 1.58 Å confirming that the ion is prochiral (**Figure 2.11**).

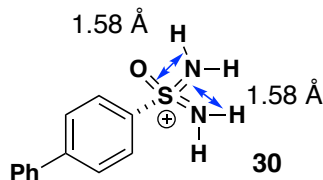


Figure 2.11: Bond lengths for protonated N-H sulfonimidamide cation **30**, from X-ray crystal structure.

These are the only known methods to synthesize enantioenriched sulfonimidamides. The lack of methods demonstrates the unmet synthetic challenge to synthesize sulfur six molecules.

2.1.3 Overview of Enantioselective Tsuji Trost Asymmetric Allylation

The first example of an enantioselective palladium catalyzed allylic substitution reaction with a stabilized nucleophile was reported in 1977.⁸⁸ However only until 1997 have these reactions developed into processes where high enantioselectivities may be realized with a wide range of substrates in a predictable fashion.⁸⁹ The problem in the developing a robust enantioselective reaction stems from the stereochemical requirements of the chiral ligand. The ligand must be able to transmit chiral information across the plane of the allyl fragment to induce asymmetry. The design and synthesis of new chiral phosphine ligands in the 21st century has rapidly advanced the ability for a transition metal catalyzed allylic alkylation to impart high levels of enantioselectivity.

The allylic alkylation reaction can impart enantioselectivity in a variety of ways when palladium is coordinated to a chiral phosphine ligand. The sources of induction include: ionization of the enantiotopic faces of the olefin, ionization of the enantiotopic leaving groups, ionization of the enantiotopic faces of the allyl group, or the nucleophilic attack on the enantiotopic termini of allyl group, and distinguishing between the enantiotopic faces of a nucleophile (**Figure 2.12**).⁸⁹ For the present study the main focus will be on the enantiotopic faces of nucleophiles for imparting enantioselectivity.

Sources of Enantioselectivity in TTA

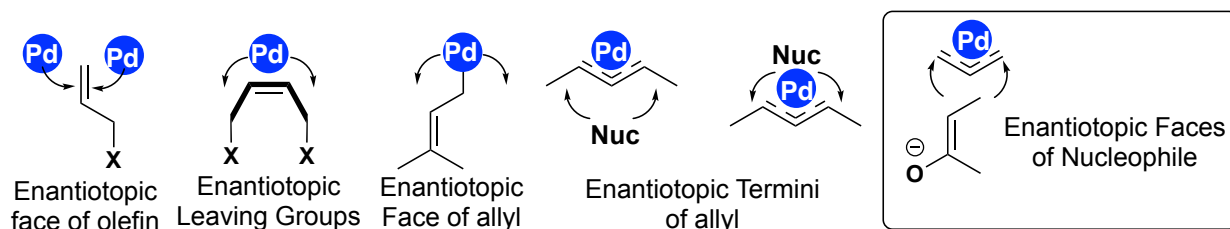


Figure 2.12: Sources of enantioselectivity in Tsuji Trost Asymmetric Allylation

The mechanistic pathway for the asymmetric allylation is usually determined by the pK_a of the nucleophile. In general, any pK_a 17 or greater is considered hard in the metal catalyzed allylation reaction. A hard nucleophile is typically an unstabilized anion. An example of a hard nucleophile is the reaction *o*-methyl pyridine (**Figure 2.13**). The methyl group is deprotonated forming an unstabilized anion that can react with the π -allyl complex.⁸⁹ Another example of a hard nucleophile is diphenylmethane which has a pK_a of 33. Soft Nucleophiles on the other hand are resonance stabilized anions such as malonates, ketoesters, amines, sulfonamides, enolates or weakly basic amines.⁹⁰

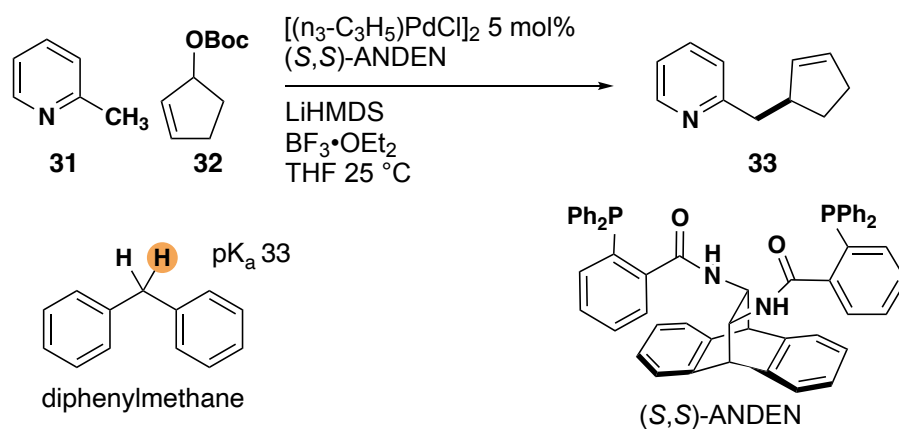


Figure 2.13: Example of hard nucleophile is Tsuji-Trost Asymmetric Alkylation

Soft nucleophiles have been demonstrated to undergo asymmetric induction more frequently than hard nucleophiles because hard and soft nucleophiles react with the π -allyl complex differently and impact the ability for the ligand to impart enantioinduction. A

hard nucleophile will typically attack the palladium and then reductively eliminate to form the allylated product. It is difficult for the ligand to transfer any chiral information to the product, through this mechanism. The attack of the hard nucleophile to the palladium causes ligand dissociation away from the metal making it difficult for the ligand to transfer the chiral information to the product. Soft nucleophiles on the other hand react in an entirely different fashion. The palladium complexes the ligand, and then complexes to the allyl group determining if the chiral metal and the face of the allyl are suitable match. If so, then the metal ionizes the leaving group and forming the reactive π allyl complex. Then the nucleophile will attack the carbon of the π -allyl complex not the metal. Finally the palladium and ligand will decomplex leaving the allylated product.⁹¹ The most common ligand in asymmetric allylation reactions is the DACH Trost ligand highlighted below (Figure 2.14).

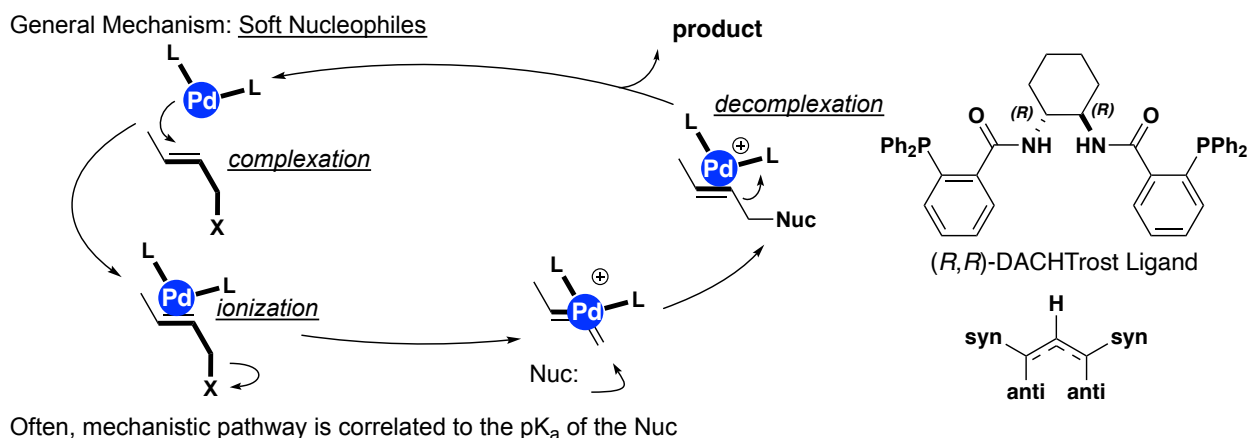


Figure 2.14: Mechanism for soft nucleophiles in asymmetric allylation reaction, DACH-phenyl ligand structure, allyl nomenclature.

Understanding the preferred trajectory of the nucleophile in the alkylation reaction provides a working model for the induced asymmetry of the ligand. The geometry of the leaving group in the ionization reaction is useful because it is the microscopic reverse of

the nucleophilic addition. Based on the Hammond postulate, the structure of the transition state can be inferred from the stable structure on either side of the transition state that lies closest in energy to the transition state. The nucleophilic attack step wherein charge on carbon is neutralized is presumably exothermic, the transition state most likely resembles the π -allyl intermediate. The transition state for ionization the process is endothermic because a charge on carbon is created and thus the transition state should resemble the π -allyl intermediate. Since these processes are, the microscopic reverse of each other, the factors which influence one will do so to the other.

It is important to note that the metal does not sit directly above the allyl but is canted 5-15° moving the anti substituents away from the metal (**Figure 2.15**). This allows for better overlap with the metal dxy orbital. In systems bearing achiral ligands, there are two possible trajectories as depicted. The two pathways differ in their orientation relative to the π -allyl. In one approach, the nucleophile comes in from the side of the **R** substituents of the π -allyl (exo), and in the other approach from the side which bears the **H** of the π -allyl (endo) (**Figure 2.15**). In nucleophilic displacement reactions (S_N2), the preferred trajectory is one that places the leaving group at an angle of 180° to the approaching nucleophile. The same stereoelectronic arguments are argued to be true in the allylic alkylation reaction. If palladium(0) is the nucleophile in the ionization and palladium(+2) the leaving group in the alkylation reaction, then both ionization and nucleophilic attack should occur at an angle that closely approaches 180°. Thus it is reasonable to propose the preferred trajectory for ionization and nucleophilic attack is via the exo mode.

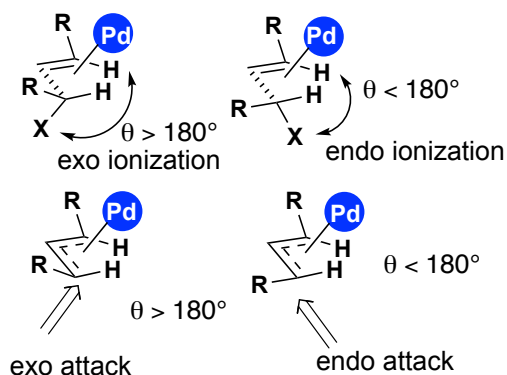


Figure 2.15: Exo versus endo attack of nucleophiles on π -allyl complex

The nucleophile should approach the π -allyl unit with an exo trajectory and through an open quadrant of ligand structure. There are four possible transition states for the nucleophilic attack. However, the two endo attacks can be ignored (*vide infra*). In the **Exo 2** approach nucleophile enters under a raised flap, while, in the **Exo 1** mode, the nucleophile encounters a lowered flap (**Figure 2.16**). Therefore, some of the difference in the transition state energies come from the steric requirements for approach of the nucleophile.

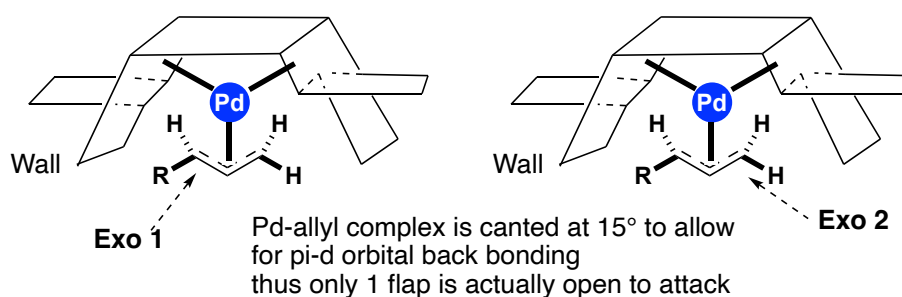
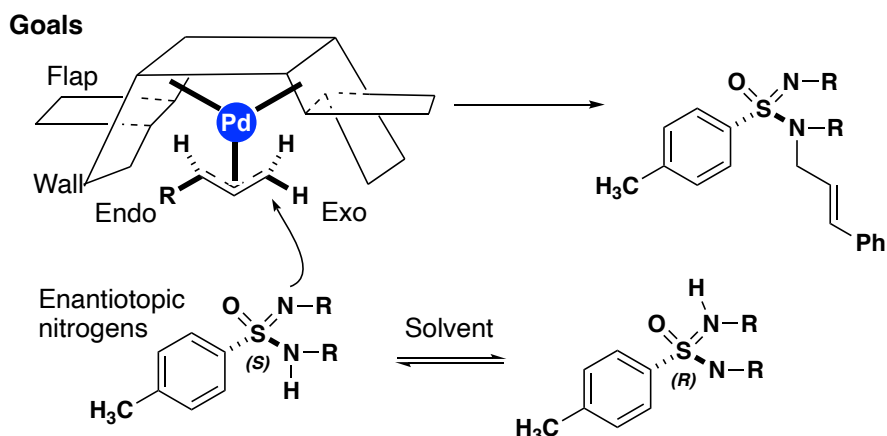


Figure 2.16: Cartoon of chiral ligand model depicting exo attack π -allyl complex

2.2 Development of Enantioselective Desymmetrization of Heterocyclic Sulfonimidamides (SIAs) Methodology

It was envisioned that a Tsuji-Trost asymmetric allylation would be an ideal candidate reaction that could lead to high enantioselectivity in the desymmetrization of

SIAs. Sulfonamides are well known to be competent nucleophiles in these reactions,^{92–97} which led hypothesis that SIAs would be capable nucleophiles as well.



The success of **L1**, **L2**, **BINAP**, **SEGFHOS**, and **DIOP**, in palladium-catalyzed asymmetric allylation reactions with sulfonamides prompted a ligand screen using sulfonimidamides as nucleophiles. (**Figure 2.17**).^{92–97} The initial rounds of screening used the di-PMB substituted sulfonimidamide **33** because of the success in Willis's desymmetrization. Josi Phos 1 and 2 (60:40 er) gave some enantioinduction, but DIOP gave a reasonably higher enantiomeric ratios (65:35 er) (**Table 2.1**). Many variables were screened to improve the selectivity. Palladium salts Pd(OAc)₂, PdCl₂, [PdCl(C₃H₅)]₂, Pd(NO₃)₂, Pd₂dba₃ and Pd(TFA)₂, were screened. A variety of polar and non polar solvents were screened in the reaction and a range of temperatures were tried to improve the enantioinduction. However, all these attempts were fruitless. Every ligand seemingly has an infinite number of possible variations when solvent and pallidum sources are considered.

Chiral Ligands Screened

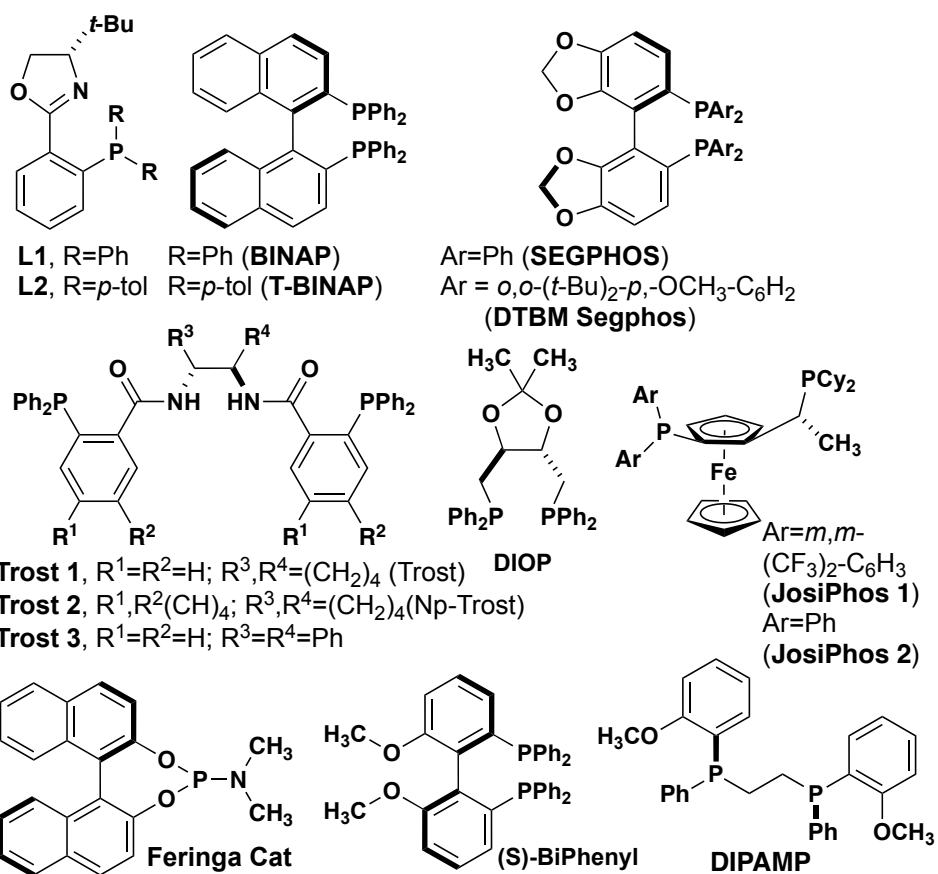
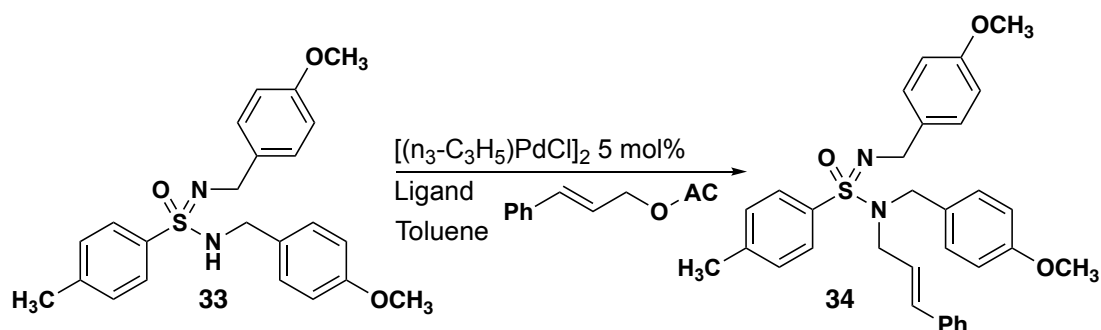


Figure 2.17: Chiral phosphine ligands available at UC Davis Chemistry Department



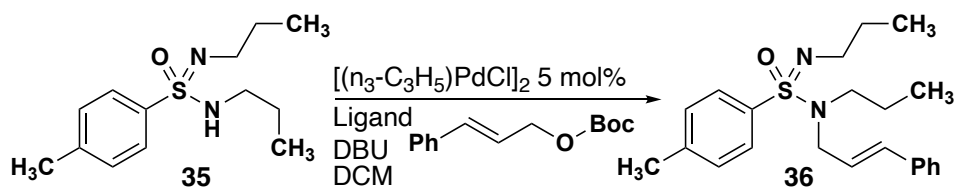
Ligand	ER
L1	NR
L2	NR
BINAP	51:49
SEGPPOS	49:51
Trost1	NR
Trost2	NR
Trost3	NR
(S)-T-BINAP	55:45
DTBM-SEG	48:52
DIOP	65:35
Feringa Cat	NR
DTBM Garphos	48:52
Josi Phos1	60:40
Josi Phos2	60:40
(S)-BiPhenyl	52:48
DIPAMP	57:43

Table 2.1: Screening of ligands with di-PMB SIA

At this point in the investigation I began to consider how the substrate is interacting with the ligand structure. My initial hypothesis was that the benzyl groups was too large for the chiral ligand to differentiate between the two enantiotopic nitrogens. The benzyl groups could clash into the ligand and the two nitrogens look identical in their steric profile.

I hypothesized that I need a to design a substrate that would make the tolyl group of the sulfur the rudder that steers the enantioinduction of the ligand.

I synthesized the di-*n*-propyl substituted SIA and reacted this substrate in a ligand screen (**Table 2.2**). The DIOP ligand loses its ability to enact any induction (50:50 er). The Josiphos ligands are also negligible in their ability to give any enantioselectivity. I revised my hypothesis, thinking that the *n*-propyl group has too many rotatable bonds and there are even more conformations the ligand needs to distinguish between. I then began thinking about locking the propyl groups into a ring. This would limit the number of conformations and force the toyl to steer enantioselectivity.

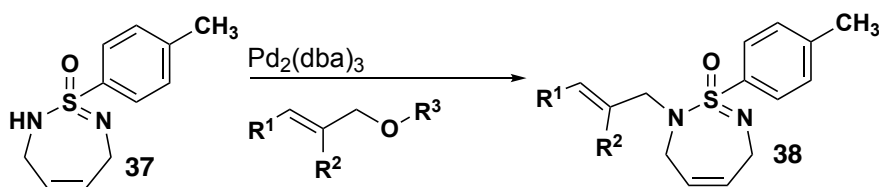


Ligand	ER
L1	47:53
L2	47:53
BINAP	51:49
SEGPPOS	46:54
Trost1	NR
Trost2	NR
Trost3	53:47
(S)-T-BINAP	48:52
DTBM-SEG	48:52
DIOP	50:50
Feringa Cat	NR
DTBM Garphos	48:52
Josi Phos1	51:49
Josi Phos2	45:55
(S)-BiPhenyl	52:48
DIPAMP	57:43

Table 2.2: Screening of ligands di-propyl SIA

The SIA heterocycle showed improved enantioselectivity in the ligand screen immediately (**Table 2.3**). The Trost ligand (*R,R*)-DACH-Ph was the most successful ligand in giving any induction. First a variety of **R**³ leaving groups was screened. The three acetate leaving groups gave no reaction however the *t*-butyl carbonate gave a good level of induction and reactivity. Then a solvent screen was undertaken. Etheral solvents performed best in the reaction in terms of reactivity and MTBE gave the highest of

enantiomeric ratio (78:22). Switching from the linear cinnamyl carbonate to the branched 2-phenyallyl carbonate gave a similar enantiomeric ratio (80:20), and experienced essentially no change when cooled to -78 °C (83:17). Switching to the (*R,R*)-DACH-naphthyl ligand gave the highest enantioselectivity of all the reactions screened to this point at 96:4. At this point in time it seemed like the optimized conditions had been established.



Ligand	R ¹ ,R ²	Solvent	R ³	ER
(<i>R,R</i>)-DACH-Ph	Ph,H	Glyme	Boc	67:33
(<i>R,R</i>)-DACH-Ph	Ph,H	Glyme	Bz	NR
(<i>R,R</i>)-DACH-Ph	Ph,H	Glyme	4-MeOBz	NR
BINAP	Ph,H	Toluene	Ac	51:48
(<i>R,R</i>)-DACH-Ph	Ph,H	Dioxane	Boc	73:27
(<i>R,R</i>)-DACH-Ph	Ph,H	THF	Boc	54:46
(<i>R,R</i>)-DACH-Ph	Ph,H	Et ₂ O	Boc	68:32
(<i>R,R</i>)-DACH-Ph	Ph,H	MeTHF	Boc	69:31
(<i>R,R</i>)-DACH-Ph	Ph,H	MTBE	Boc	78:22
(<i>R,R</i>)-DACH-Ph	H,Ph	MTBE	Boc	80:20
(<i>R,R</i>)-DACH-Ph -78 °C	H,Ph	MTBE	Boc	83:17
(<i>R,R</i>)-DACH-Nap	H,Ph	MTBE	Boc	96:4

Table 2.3: Screening of ligands with heterocyclic SIA.

2.2.1 High Throughput Experimentation Results

A collaboration was established with Merck to run a high throughput screening assay to test a larger library of Trost ligands and solvents. The high throughput screening

(HTS) study focused on the desymmetrization of a heterocyclic SIA **37**. Six different commercially available Trost-type ligands, **L1** through **L6**, were screened against eight different solvents in a 96 well plate. A variety of solvents were chosen so as to ensure a sufficient representation of chemical space: ethereal solvents MTBE, THF and CPME, halogenated DCE, aromatic toluene, polar aprotic acetonitrile and ethyl acetate, and finally polar protic *t*-amyl alcohol.⁸⁹ The entire plate was further subdivided in half for electrophiles *t*-butyl cinnamyl carbonate **E1** and *t*-butyl (2-phenylallyl) carbonate **E2**.⁹⁰

A heat map measuring both the conversion and enantioselectivity for each reaction was constructed based on UV traces from the chiral UPLC data (**Figure 2.18**). The yellow outer ring of the graph indicates percent conversion of starting material to allylated product. The inner green ring of the graph is the enantiomeric excess (ee) of the product formed. Thus a reaction with 100% conversion and 100% ee would have a full yellow band and a solid green ring. The absolute value of ee was used to normalize for the different enantiomers of catalyst used. Reactions with electrophile **E1** generally gave low conversion and low ee; even the most optimal result with **E1**, **L6** in MTBE, led to only modest ee. On the other hand, reactions with electrophile **E2** generally led to higher percent conversions as well as higher ee. Ligand **L1** proved to be superior to the other ligands, as it exhibited impressive conversion across all solvents and the highest enantioselectivities in MTBE, THF, DCE, toluene, and acetonitrile. Ligands **L2** and **L6** also showed good reactivity and high enantioselectivity in a variety of solvents. Ligand **L4** showed little to no reactivity in any solvent, which is likely due to palladium coordination

to a pyridyl nitrogen instead of a phosphine. Overall, the reactivity and selectivity observed from pairing ligand **L1** with **E2** is much greater than any ligand pairing with **E1**.

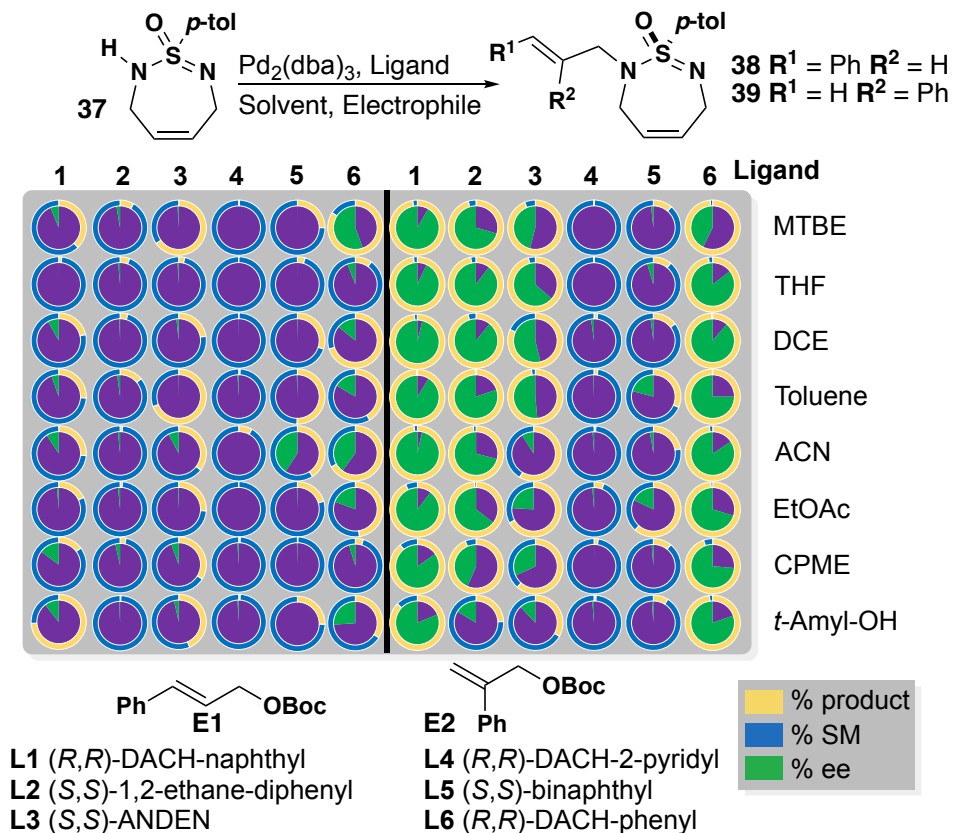


Figure 2.18: Heat map for high throughput screening and solvent optimization;

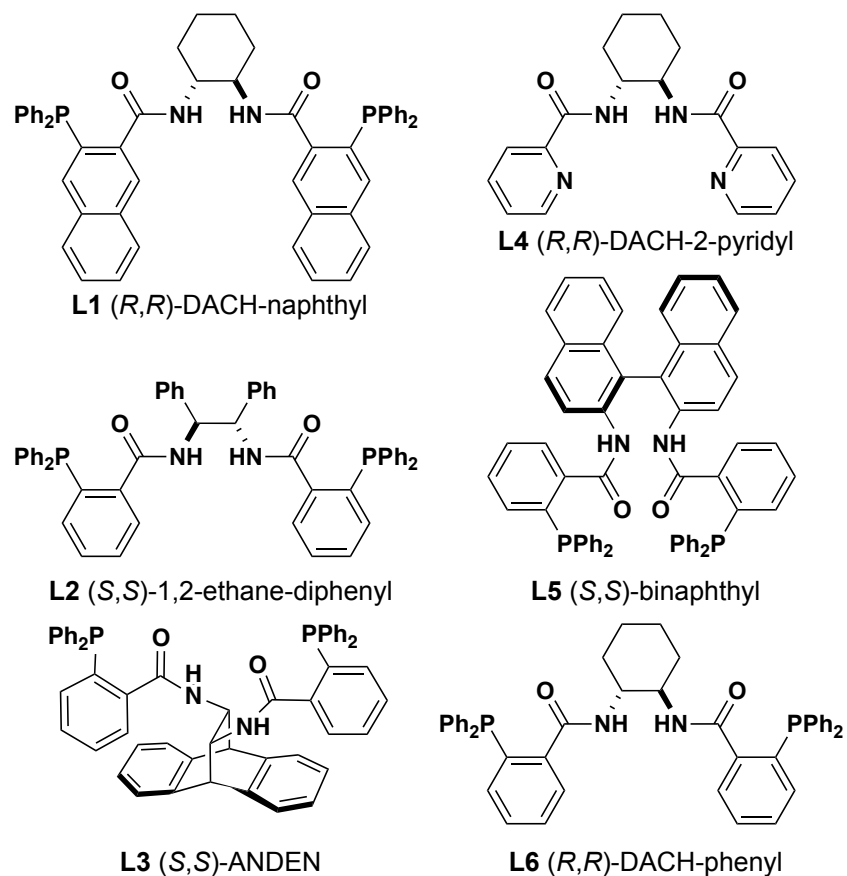


Figure 2.19: Ligand structures

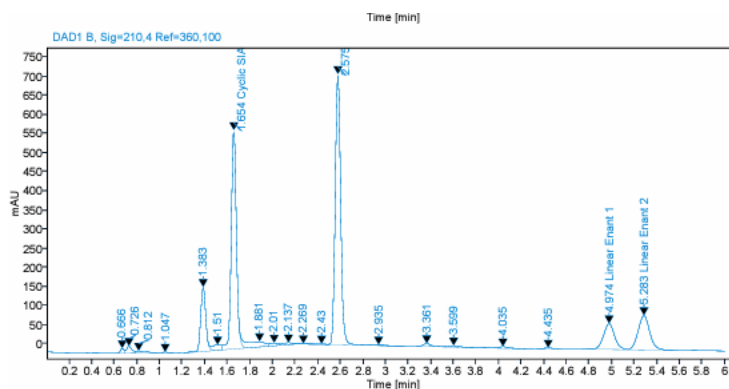


Figure 2.20: Representative Chiral HPLC trace for reaction of **SIA 37** and **E1** to yield **38**. Labeled cyclic **SIA 37**, and enantiomers of **38**.

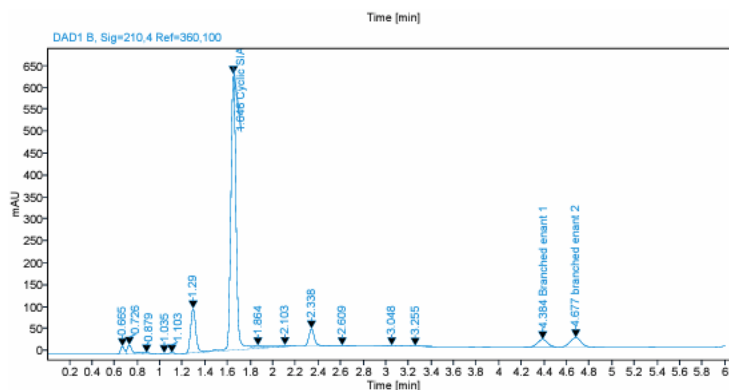
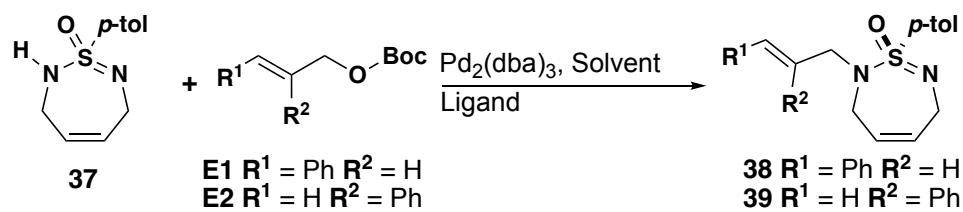


Figure 2.21: Representative Chiral HPLC trace for reaction of **SIA 37** and **E2** to yield **39**. Labeled cyclic **SIA 37**, and enantiomers of **39**.

Following the HTS, the most successful conditions for electrophiles **E1** and **E2** were scaled up to 0.1 mmol scale to obtain isolated yields (**Table 2.4**). For electrophile **E1**, the **L6** ligand in MTBE was the only set of conditions that resulted in any considerable enantioselectivity; upon scale up, the product was obtained in moderate yield, while the enantiomeric ratio (er) remained only modest. For **E2** with ligand **L1**, MTBE gave both the highest er and the highest isolated yield across the solvent range. Although ACN and toluene gave poor yields, the er of the products remained high. To our surprise, even though the HTS indicated DCE and THF were viable solvents for this reaction, neither of them led to a productive reaction and only starting material was recovered. From these data, we concluded that utilizing **L1** with 2-substituted allyl carbonates in MTBE represented the optimal conditions to achieve high er and modest yields.



Ligand	Solvent	R ¹ ,R ²	ER	Yield
(<i>R,R</i>)-DACH-Ph	MTBE	Ph,H	75:25	48%
(<i>R,R</i>)-DACH-NAP	MTBE	H,Ph	99:1	36%
<i>R,R</i>)-DACH-NAP	ACN	H,Ph	99:1	3%
<i>R,R</i>)-DACH-NAP	Toluene	H,Ph	99:5	Trace
<i>R,R</i>)-DACH-NAP	DCE	H,Ph	--	NR
<i>R,R</i>)-DACH-NAP	THF	H,Ph	--	NR

Table 2.4: Scale up of best reactions from HTS

2.2.2 Electrophile Substrate Scope

Once I identified optimal conditions, a variety of sterically and electronically differentiated electrophiles were evaluated using SIA **37** (**Figure 2.22**). On one mmol scale, product **39** was isolated in a significantly higher yield when compared to the 0.1 mmol scale while still maintaining excellent enantioselectivity 99%. Despite the drastic decrease in steric bulk, the smaller methyl substituted allyl carbonate **E3** also exhibited high enantioselectivity and yield. Remarkably, removing substitution at the 2 position altogether with the unsubstituted allyl carbonate **E4** still produced good enantioselectivity (90:10) with **L1**. To investigate the role of carbonate electronics, the electron rich PMP substituted allyl carbonate was utilized, leading to product **42** with high er and yield. Moving the steric component one carbon further from the allyl system with benzyl substituted allyl carbonate led to product **43**, while maintaining high er and yield. Unfortunately, the aza-Baylis Hillman adducts **44** and **45**, derived from ethyl acrylate **E7**

and *t*-butyl acrylate **E8**, gave lower enantioselectivities, albeit with synthetically useful yields.⁹⁸ Increasing the steric demand at the 2 position of the carbonate led to products **46** and **47**. Product **46**, derived from the 1-naphthyl allyl carbonate **E9**, gave very high er (99:1) and yield when compared to its 2-naphthyl substituted counterpart, **47**, indicating that achieving enantioselectivity in the desymmetrization using 2-substituted allyl carbonates is not a simple result of increasing steric bulk at the 2 position.

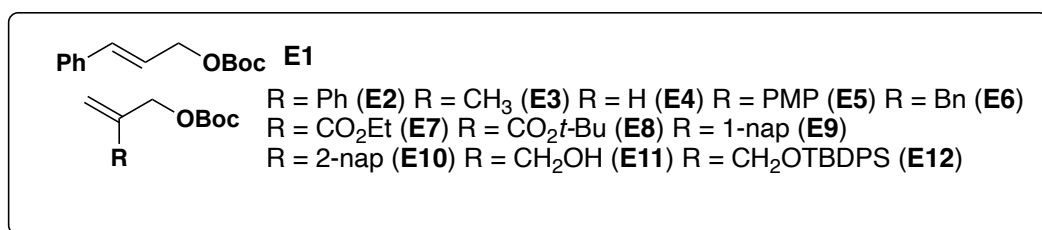
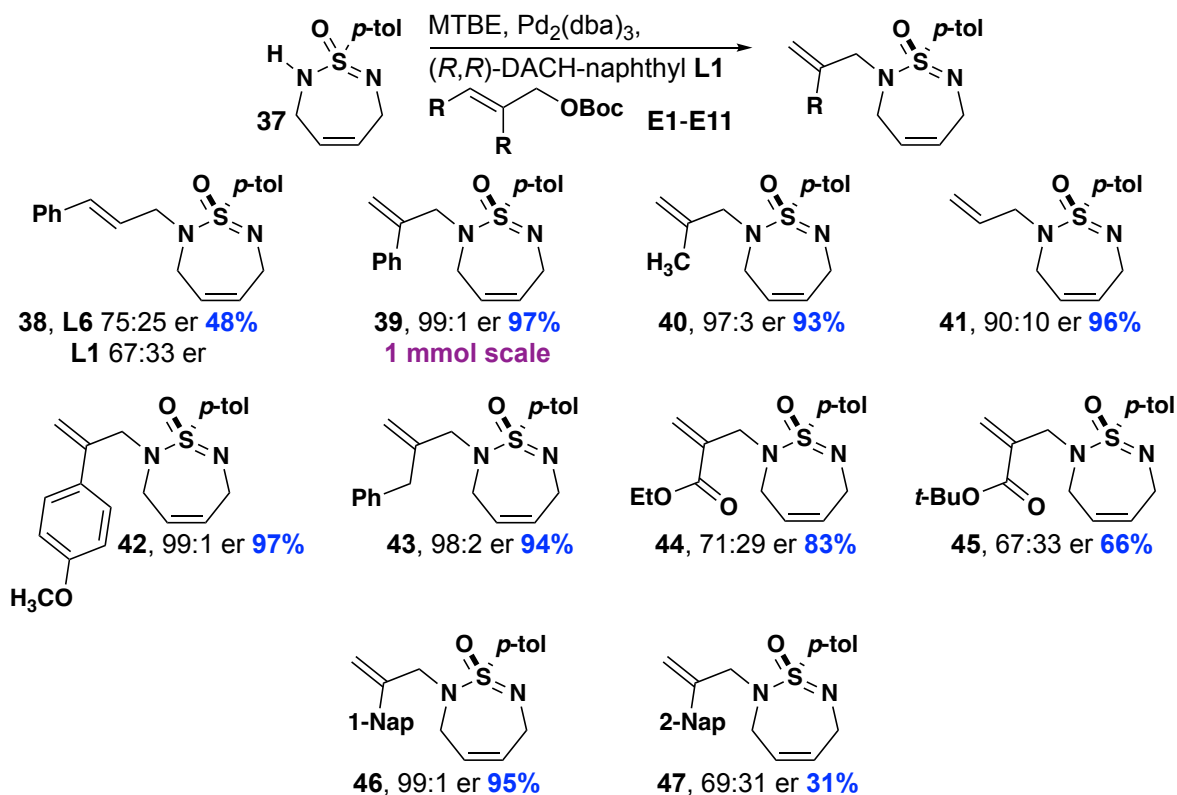


Figure 2.22: Substrate scope of SIA heterocycles in desymmetrization reaction. Reactions run at 0.1 mmol of SIA. Conditions: SIA (0.1 mmol), Pd₂dba₃ (0.005 mmol), (*R,R*)-DACH-naphthyl (0.012 mmol), allylic carbonate (0.15 mmol), methyl tert-butyl ether (1 mL).

2.2.3 Heterocyclic Sulfonimiamide Substrate Scope

To investigate the role of the nucleophile in imparting enantioselectivity, a series of SIA heterocycles were screened using electrophile **E2** and **E4** (Figure 2.23). The enantioselectivity of the products from the fully saturated SIA gave ers that are comparable to the saturated counter parts. The saturated SIA gave desymmetrized

products **48**, **49**, and **50** with nearly comparable enantioselectivity. Indicating any functional group manipulation of the double bond is inconsequential to enantioselectivity. To test this hypothesis SIA **1** was dihydroxylated and the diol was protected as the dimethyl acetal, yielding a 70:30 mixture of inseparable diastereomers which was subjected to the desymmetrization reaction. Both diastereomers of the acetone SIA gave high enantioselectivities with **E2** and comparable enantioselectivity with **E4**, products **59**, **60**, and **61**. The absolute stereochemistry was established by the X-ray crystal structures of **50** and **59**. The results indicate the steric influence of the bottom of the ring does not significantly impact the enantioselectivity.

A series of **R**¹ substituted SIA heterocycles were screened to investigate the role of the substitution in imparting enantioselectivity. Electrophiles **E2** and **E4** were selected to probe the selectivity. In general all the **R**¹ substituted SIAs reacting with **E2** are extremely enantiomerically enriched, yielding products 97:3 er or greater.

However **R**¹ substituted SIA heterocycles reacting with **E4** show either comparable selectivity to **41** or worse. The selectivity of the alkyl isopropyl SIA gave lower selectivity (75:25 er) **52**. For *m*-fluoro-*o*-methyl substituted SIA, with **E4** showed a mild decrease in enantioselectivity **54** (84:16 er) compared to **41**. The *o*-brosyl SIA reacting with **E4** gave the lowest enantioselectivity, **58**, of all the SIAs screened (69:31 er). It is clear that *ortho* bromine substitution has a more significant steric penalty on the desymmetrization process compared to *ortho* methyl substitution. Amazingly the reaction is highly functional group tolerant giving no detectable protodehalogenation products. The *p*-biphenyl substituted SIA gave essentially the same with **E4** (88:12 er) compared to **41**. Thus

highlighting that *para* substitution does not significantly impact the enantioselectivity of reaction.

SIA heterocycles possessing different ring sizes were explored too. The 9-membered SIA reacted with **E2** was highly enantioselective giving product **64** in 99:1 er, compared to the 6-membered SIA with **E2**, product **70** (91:9). The reaction of **E4** with either the 9-membered or the 6-membered SIA showed significantly diminished selectivity compared to product **41**. Surprisingly, the 5-membered SIA heterocycle led to no reaction with either electrophile, instead proving to be prone to decomposition; no starting material was recovered in either reaction. These results indicate that ring size has a significant effect on enantioselectivity, with 7-membered SIAs representing the ideal ring size for enantioselectivity.

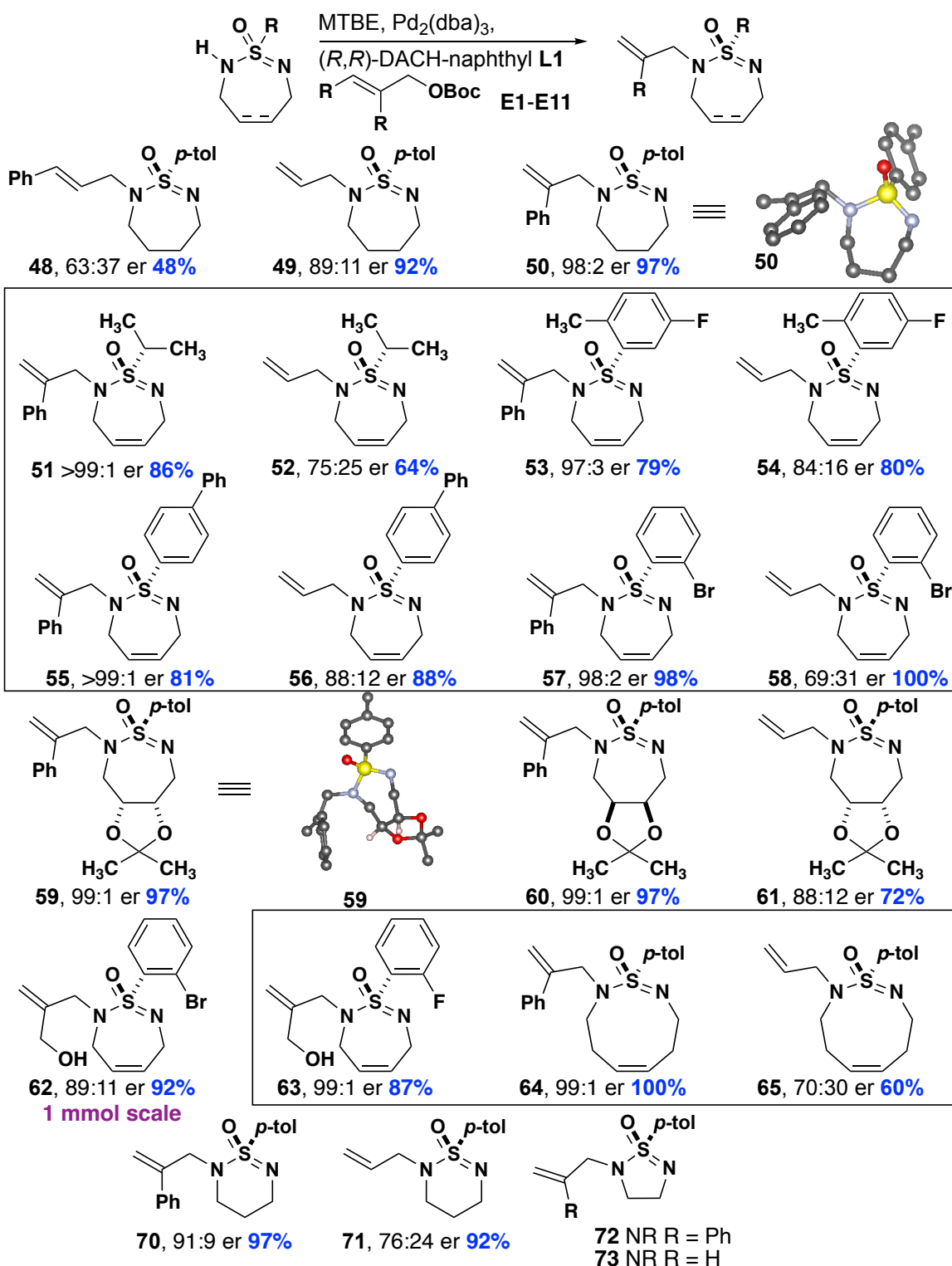


Figure 2.23: Substrate scope of SIA heterocycles in desymmetrization reaction. Reactions run at 0.1 mmol of SIA. Conditions: SIA (0.1 mmol), Pd₂dba₃ (0.005 mmol), (*R,R*)-DACH-naphthyl (0.012 mmol), allylic carbonate (0.15 mmol), methyl tert-butyl ether (1 mL). Boxed compounds were synthesized by labmate Garrett Toth-Williams

2.2.4 Stereochemical model for Enantioselectivity

The catalytic cycle for the desymmetrization is consistent with the prototypical catalytic cycle for palladium catalyzed allylation reactions (**Figure 2.24**).⁹¹ The ionization event releasing CO₂ and *t*-butoxide is essential in the desymmetrization reaction.⁹⁹ The liberated *t*-butoxide deprotonates the SIA, generating a prochiral anion nucleophile which can then attack the chiral π -allyl complex. The initial investigation into allyl leaving groups revealed that the initial deprotonation event is essential for the reaction as indicated via the use of different acetate leaving groups. Only starting material is recovered in these cases as the various acetates are not basic enough to deprotonate the SIA, shutting down the reaction. The transition state model for the desymmetrization is based on the model proposed by Trost.^{89–91} Analyzing the model accurately accounts for the desymmetrized selectivity.^{97,100} In the disfavored conformation, the **R** (Ph) group clashes with the aryl phosphine wall and the R group of the 2-substituted allyl. In the favored conformation, the **R** group is pointed away from phosphine wall and positioned in the flap portion of the ligand. The cyclic portion of the SIA is pointed downwards away from the ligand, highlighting why double bond functionalization has no effect on selectivity. Overall, the steric profile of **L1** and conformation of the SIA substrate in the catalyst pocket determines the high enantioselectivity. The stereoselectivity is accurately predicted using the Trost quadrant model.⁹¹

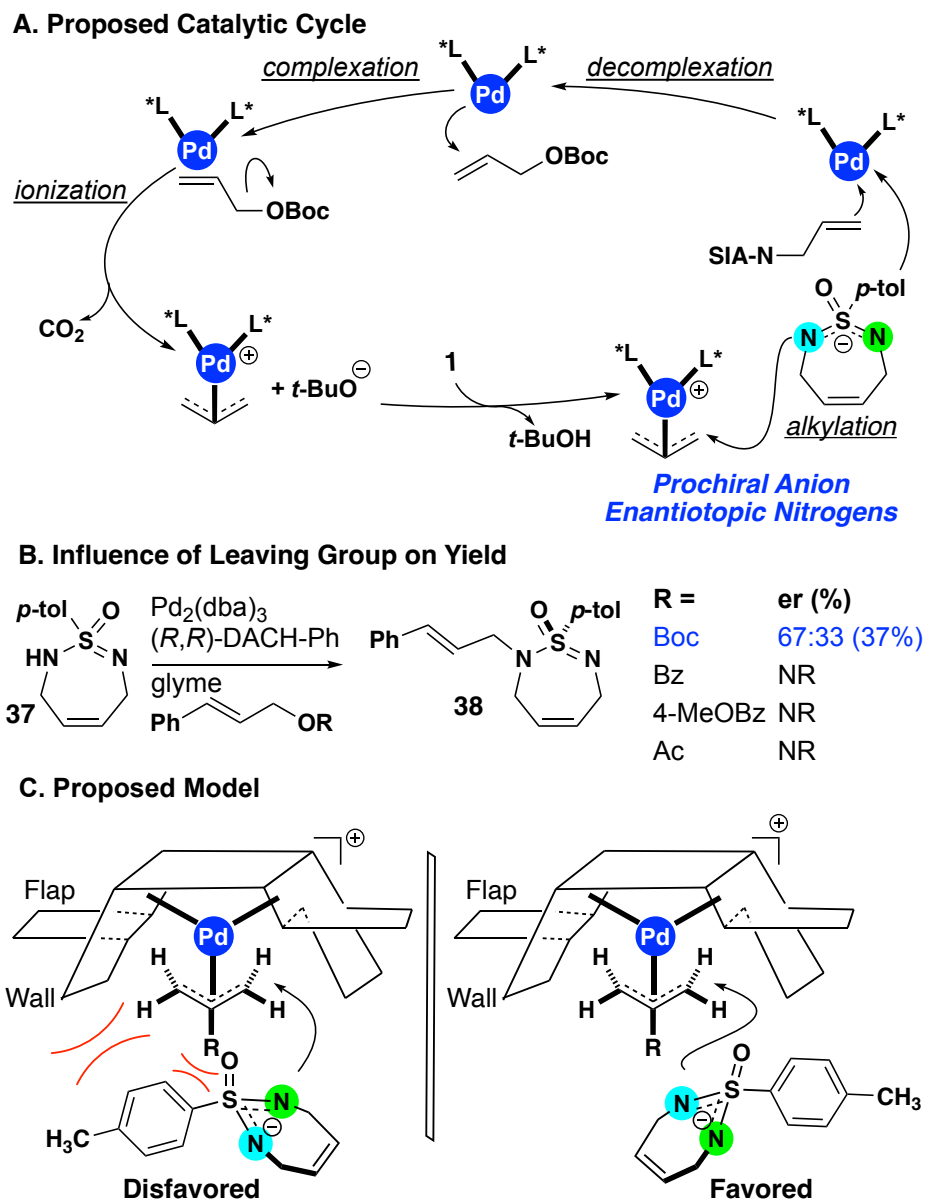


Figure 2.24: A) Catalytic cycle of allylation; B) influence of the leaving group on reactivity; C) stereochemical model for desymmetrization of SIA heterocycles with L1

2.2.5 Functionalization Reactions of Enantioenriched Sulfonimidamides

The enantioenriched Pd heterocycle SIAs can be further functionalized to either incorporate the SIA into other molecular scaffolds or cyclized to give a novel tricyclic chemical scaffold (**Figure 2.25**). The aryl bromide was coupled to PMP boronic acid and a Suzuki reaction, producing product **74** in high yield. The free alcohol in compound **62**

functions as a synthetic handle for building a novel class of hetero-tricyclic SIAs. Acetoxylation of the alcohol followed by an intramolecular palladium-catalyzed cyclization forges a new C-C bond, generating tricycle **74** in high yield. The enantioenriched heterocyclic SIAs can easily be functionalized using palladium catalyzed cross coupling reactions, or they can be cyclized to yield to yield tricyclic SIA heterocycles.

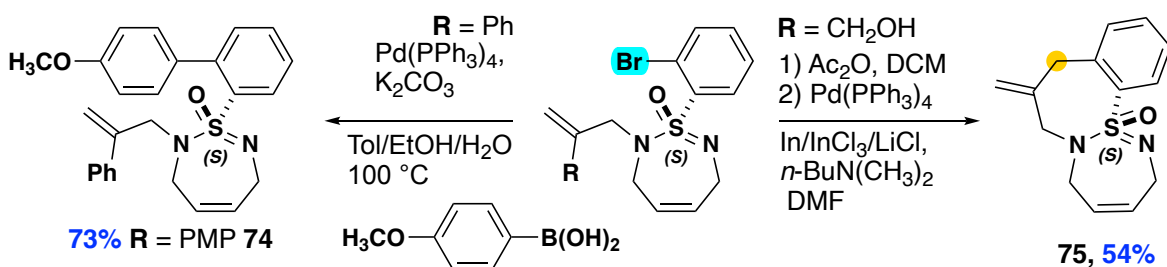


Figure 2.25: Functionalization of enantioenriched sulfonimidamides

The aryl bromide of **57** was carbonylated and yielded an interesting imide product **76** (Figure 2.26). The reaction did not yield the expected amide **78**. At the time this result was very exciting because in an ideal case the allyl acts as a protecting group and then deprotected in a cyclization. However, the product had a significant erosion of enantiopurity 70:30 er from 98:2. Thus modified reaction conditions were screened to see if the erosion could be negated.

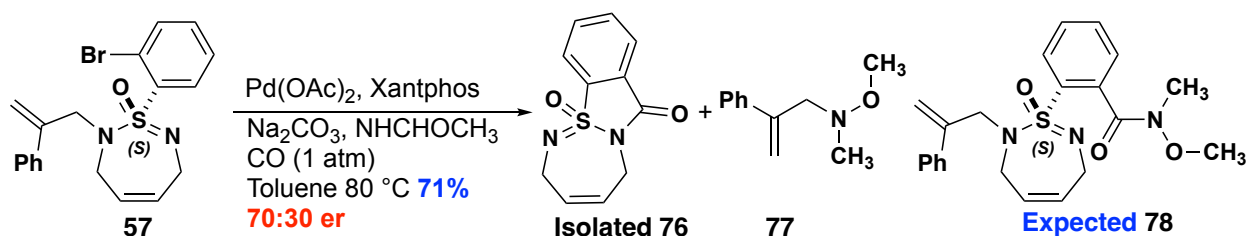
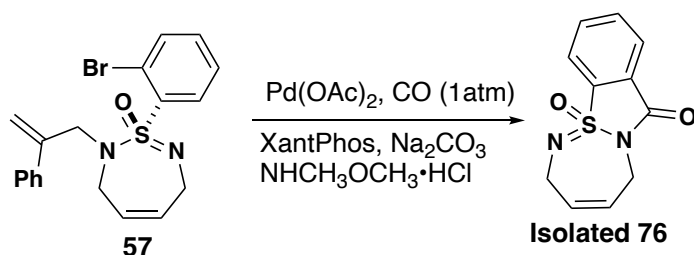


Figure 2.26: Carbonylation of aryl bromide

First part of the optimization was omitting the nucleophile NHCH₃OCH₃ and this yielded no reaction. Then under the same conditions but at higher temperature 100 °C

the product was virtually racemic. Switching to Pd₂dba₃ deallylates the starting material. Any attempts to lower the temperature and isolate product was fruitless and gave no conversion to product. Overall many attempts were made to optimize this reaction but none of them were able to quell the problem of erosion.



Solvent	Pd	Nucleophile	Temp	ER
Toluene	Pd(OAc) ₂	NHCH ₃ OCH ₃	80 °C	70:30
Toluene	Pd(OAc) ₂	none	100 °C	NR
Toluene	Pd(OAc) ₂	NHCH ₃ OCH ₃	100 °C	50:50
Toluene	Pd ₂ dba ₃	NHCH ₃ OCH ₃	50 °C	NR
THF	Pd ₂ dba ₃	NHCH ₃ OCH ₃	50 °C	NR
Toluene	Pd(OAc) ₂	NHCH ₃ OCH ₃	50 °C	NR
THF	Pd(OAc) ₂	NHCH ₃ OCH ₃	50 °C	NR
Toluene	Pd(OAc) ₂	DMAP	80 °C	NR
Toluene	Pd(OAc) ₂	Morpholine	50 °C	NR
DMF	Pd(OAc) ₂	NHCH ₃ OCH ₃	50 °C	NR
Toluene	PdCl ₂	NHCH ₃ OCH ₃	50 °C	NR

Table 2.5: Optimization attempt of intramolecular cyclization to imide.

Based on the reaction conditions above a mechanism for the cyclization de-allylation and racemization has been proposed. After oxidative addition and CO insertion the acyl palladium species can be attacked by either nitrogen. The nitrogen in blue would give a net inversion of absolute configuration and the purple would have net retention. One of the nitrogens is more nucleophilic than the other at 80 °C. However, at 100 °C

they both attack the acyl palladium at the same rate and lead to complete racemization. The mixture of enantiomers could not be separated and thus it is inconclusive which process takes place at 80 °C.

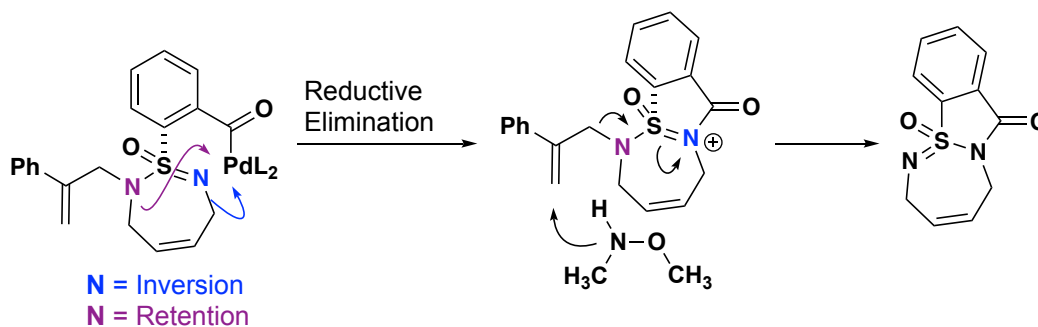


Figure 2.27: Proposed mechanism for cyclization and de-allylation

2.3 Conclusion

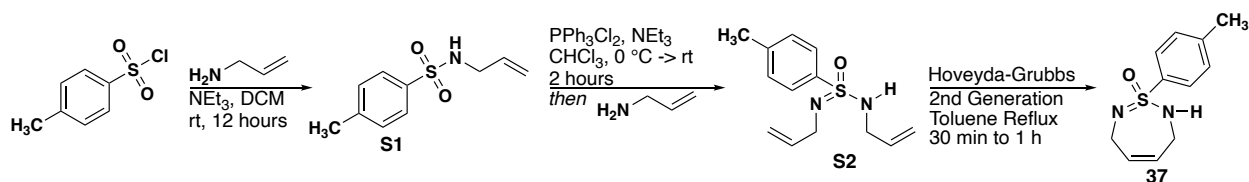
In summary, I have developed the first transition metal catalyzed desymmetrization of enantioenriched SIA heterocycles via a Tsuji-Trost asymmetric allylation. The optimal ligand and solvent were identified using high throughput screening techniques. The catalyst and ligand are commercially available and the desymmetrization is run under mild reaction conditions. A variety of sterically differentiated and electron rich electrophiles give high enantiomeric ratios and yields. Furthermore, a series of heterocyclic SIA substrates lead to high enantioselectivities and yields. A stereochemical model is presented to rationalize the observed selectivity. Finally, the products obtained following desymmetrization can be further functionalized to give a new class of tricyclic sulfonimidamide heterocycles possessing an enantioenriched stereogenic sulfur.

2.4 Experimental Section

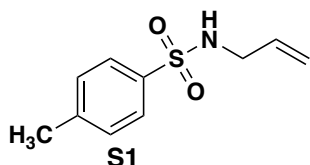
2.4.1 Materials and Instrumentation.

Unless otherwise specified, all commercially available reagents were used as received. All reactions using dried solvents were carried out under an atmosphere of argon in oven-dried glassware with magnetic stirring. Dry solvent was dispensed from a solvent purification system that passes solvent through two columns of dry neutral alumina. ^1H and ^{13}C NMR spectra were acquired at ambient temperature using Varian-600 (600 and 151 MHz, respectively), or Bruker-400 (400 and 101 MHz, respectively) spectrometers, as indicated. The data are reported as follows: chemical shift in ppm from internal tetramethylsilane = 0 ppm or referenced to residual solvent (^1H NMR: CDCl_3 δ 7.26. ^{13}C NMR: CDCl_3 δ 77.16) on the δ scale, multiplicity (appar = apparent, br = broad, s = singlet, d = doublet, t = triplet, q = quartet, quint = quintet, sext = sextet, m = multiplet), coupling constants (Hz), and integration. High-resolution mass spectra (HRMS) were acquired on a Thermo Electron LTQ-Orbitrap XL Hybrid mass spectrometer on positive ESI mode. Melting points were obtained on an EZ-melting apparatus and were uncorrected. Chiral HPLC solvent system is a revisor of Hexane and a 90:10 mixture of hexane and isopropanol. Solvent system ratio are that of hexane and the 90:10 mixture. Liquid chromatography was performed using forced flow (flash chromatography) of the indicated solvent system silica gel (Fisher, 40-63 μm) packed in glass columns.

2.4.2 Synthesis of thiadiazepine Sulfonimidamides



Step 1: To a flame dried round bottom flask allyl amine (1.90 g 0.033 mol) triethylamine (6.66 g 9.5 mL 0.066 mol) in 165 mL of dichloromethane. The solution was cooled to 0 °C and tosyl-chloride (7 g 0.0368 mol) was added dropwise via addition funnel. The ice bath was removed, and the reaction was warmed to room temperature and stirred overnight. Then the reaction mixture was diluted with water and dichloromethane. The organic layer was separated then washed 3 times with brine dried over Na₂SO₄. Filtered and concentrated. The crude residue was purified by flash column chromatography 30% ethyl acetate/hexanes to yield compound **S1** as a white amorphous solid (6.89 g 99%).



N-Allyl-4-methylbenzenesulfonamide (**S1**)

Yield: 6.890 g (99%)

Physical Description: White Amorphous Solid

Column Conditions: SiO₂, (10% to 50% EtOAc/Hexanes)

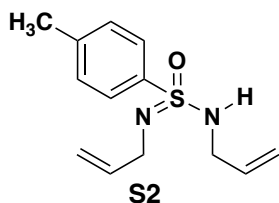
¹H NMR: (400 MHz, CDCl₃) δ 7.75 (d, *J* = 8.1 Hz, 2H), 7.32 (d, *J* = 8.1 Hz, 2H), 5.73 (ddt, *J* = 17.0, 10.2, 5.8 Hz, 1H), 5.22 – 5.06 (m, 2H), 4.41 (s, 1H), 3.59 (tt, *J* = 6.0, 1.5 Hz, 2H), 2.43 (s, 3H).

IR (neat): (3387-3190, bs), 1598, 1480, 1331, 1161.

Compound is in agreement with literature values.¹⁰¹

Step 2: Sulfonimidamides were synthesized according to a procedure developed by Chen.¹⁰² An oven dried round bottom flask was charged with triphenyl phosphine (14.803

g 0.0565 mol) and C_2Cl_6 (13.33 g 0.0565 mol). The flask was then evacuated and purged with argon. Chloroform (113 mL) that had been passed through basic alumina and sparged with argon was added to the flask and the reaction was stirred at 70 °C for 12 hours, or until a white suspension formed. Then the solution was cooled to 0 °C and then triethylamine (7.625 g 10.8 mL 0.0755 mol) was added. Then in one portion **S1** in a 120 mL solution of chloroform was added to the reaction and then warmed to room temperature and stirred for 2 hours. Then allyl amine (4.303 g 0.0755 mol) was slowly added to the mixture. The solution was stirred for 2 additional hours. Then the reaction mixture concentrated dissolved in ethyl acetate and filtered. The filtrate was concentrated and then purified by flash column chromatography 50% ethyl acetate/hexanes. The impure fractions were collected and then repurified by flash chromatography in successive column volumes of dichloromethane before transitioning to 10%, 30% then 50% ethyl acetate/Hexanes.



N,N'-Diallyl-4-methylbenzenesulfonimidamide (**S2**)

Yield: 8.725 g (92%)

Physical Description: Yellow Oil

Column Conditions: SiO_2 , (10% to 50% EtOAc/Hexanes)

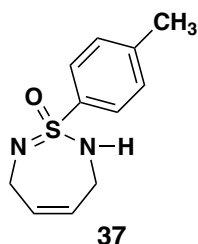
1H NMR: (400 MHz, $CDCl_3$) δ 7.85 (d, $J = 8.4$ Hz, 2H), 7.28 (d, $J = 8.4$ Hz, 2H), 5.85 (ddt, $J = 17.1, 10.2, 5.6$ Hz, 2H), 5.23 (dq, $J = 17.0, 1.7$ Hz, 2H), 5.07 (dq, $J = 10.2, 1.5$ Hz, 2H), 3.73 – 3.58 (m, 4H), 2.42 (s, 3H).

¹³C NMR: (101 MHz, CDCl₃) δ 142.7, 137.3, 135.8, 129.5, 127.5, 115.7, 45.5, 21.5.

IR (neat): (3390-3180, bs), 2841, 1643, 1273, 1148.

AMM: (ESI) *m/z* calcd for C₁₃H₁₉N₂OS⁺ [M+H]⁺ 251.1213, found 251.1214.

Step 3: A flame dried round bottom flask under argon was charged with toluene (133 mL) then heated to reflux. Then a 3 mL toluene solution of **S2** (0.500 g 0.002 mol) was added to refluxing solution dropwise. The refluxing solution was stirred for 30 min and then cooled to room temperature then filtered over a pad of silica gel using ethyl acetate to wash the silica gel pad. The solution was concentrated and then purified by flash column to yield the cyclized sulfonimidamides.



1-(*p*-Tolyl)-3,6-dihydro-2*H*-1,2,7-thiadiazepine 1-oxide (**37**)

Yield: 0.526 g (59%)

Physical Description: Brown Amorphous Solid

Column Conditions: SiO₂, (10% to 50% EtOAc/Hexanes)

¹H NMR: (400 MHz, CDCl₃) δ 7.98 – 7.82 (m, 2H), 7.29 – 7.18 (m, 2H), 5.86 (s, 1H), 5.63 (s, 2H), 4.33 (s, 1H), 3.71 (d, *J* = 17.4 Hz, 2H), 3.55 (s, 1H), 2.39 (s, 3H).

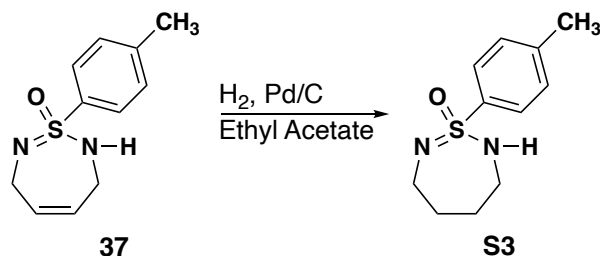
¹³C NMR: (101 MHz, CD₂Cl₂) δ 143.0, 136.8, 129.4, 129.0, 127.2, 41.8, 21.2.

IR (neat): 2837, 1635, 1450, 1269, 1136.

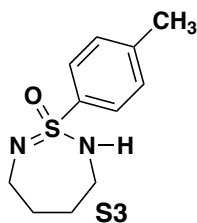
AMM: (ESI) *m/z* calcd for C₁₁H₁₅N₂OS⁺ [M+H]⁺ 223.0900, found 223.0903.

The following Sulfonimidamides were synthesized in a similar manner.

2.4.3 Hydrogenation of 37 to yield S3



To a round bottom flask was added palladium on carbon (0.010 g 0.094 mmol) then the vial was evacuated and backfilled with argon. Then 1-(*p*-tolyl)-3,6-dihydro-2*H*-1,2,7-thiadiazepine 1-oxide (0.032 g 0.14 mmol) in a 1.4 mL solution of Ethyl acetate was added to the vial. The reaction was then evacuated and backfilled with a balloon of hydrogen. The reaction stirred for 24 hours. Then the vial was evacuated and backfilled with argon and the solution was filtered over celite. The filtrate was concentrated to yield compound 1-(*p*-tolyl)-3,4,5,6-tetrahydro-2*H*-1,2,7-thiadiazepine 1-oxide with no further purification.



1-(*p*-Tolyl)-3,4,5,6-tetrahydro-2*H*-1,2,7-thiadiazepine 1-oxide (**S3**)

Yield: 27 mg (86%)

Physical Description: White Amorphous powder

Column Conditions: SiO₂, (10% to 50% EtOAc/Hexanes)

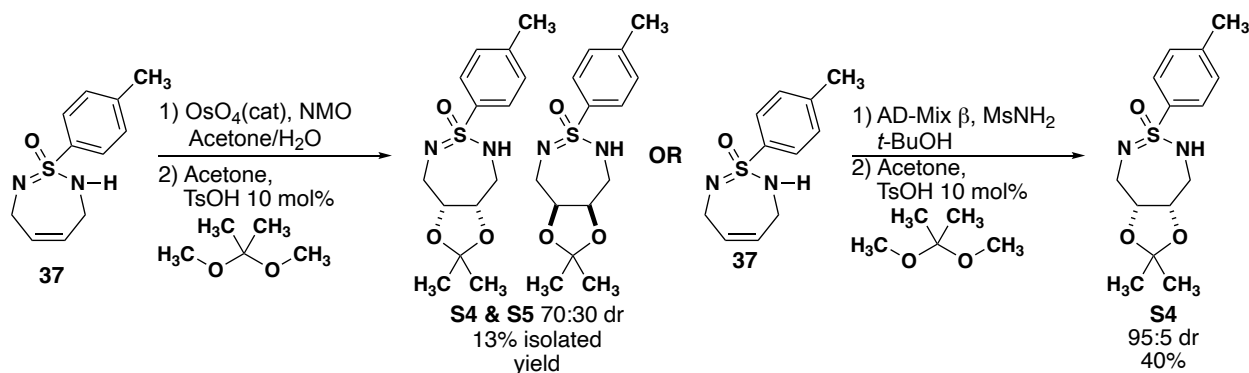
¹H NMR: (400 MHz, CDCl₃) δ 7.88 (d, *J* = 8.4 Hz, 2H), 7.25 (d, *J* = 8.1 Hz, 2H), 4.48 (s, 1H), 3.33 – 3.23 (m, 2H), 3.18 – 3.08 (m, 2H), 2.40 (s, 3H), 1.81 – 1.69 (m, 4H).

¹³C NMR: (101 MHz, CDCl₃) δ 142.5, 138.4, 129.4, 127.0, 43.0, 31.4, 21.4.

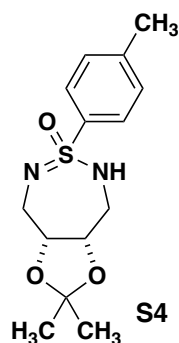
IR (neat): 2928, 2850, 1598, 1446, 1239.

AMM: (ESI) *m/z* calcd for C₁₁H₁₇N₂OS⁺ [M+H]⁺ 225.1056, found 225.1056.

2.4.4 Synthesis of Dimethyl Acetonide SIA's



1-(*p*-Tolyl)-3,4,5,6-tetrahydro-2*H*-1,2,7-thiadiazepine 1-oxide (0.290 g 1.3 mmol) was dissolved in a solution of 9/1 acetone water (1.3 mL). Then a 50 wt% aqueous solution of *N*-methylmorpholine *N*-oxide (0.229 grams 1.96 mmol of NMO) was added to the solution. Then a solid crystal 2 wt% solution of OsO₄ in tert-butanol was added to the solution and stirred for 24 hours or until consumption of starting material as monitored by TLC (1/1 EtOAc/Hexane). A saturated solution of sodium sulfite was added to the reaction and stirred for 1h then the organics were extracted 3x with DCM and washed with brine. The DCM layer was then dried with Na₂SO₄, filtered and concentrated to yield an off yellow amorphous solid. To this solid was added acetone (13 mL), tosic acid monohydrate (22 mg, 0.13 mmol) and 2,2-dimethoxypropane (468 mg, 4.5 mmol). The solution was refluxed for 24 hours then concentrated and purified by flash chromatography 10% → 30% → 50% → 60 % → 80% EtOAc/Hexane to yield a 70:30 mixture of inseparable diastereomeric acetonides (62 mg 16%).



Major Diastereomer (3a*S*,8a*R*)-2,2-dimethyl-6-(*p*-tolyl)-3a,5,8,8a-tetrahydro-4*H*-[1,3]dioxolo[4,5-*d*][1,2,7]thiadiazepine 6-oxide (**S4**)

Yield: 62 mg (16%) 70:30 mixture of diastereomers

Physical Description: White Amorphous powder

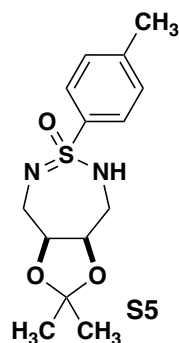
Column Conditions: SiO₂, (10% to 70% EtOAc/Hexanes)

¹H NMR: (400 MHz, CDCl₃) δ 7.94 (d, *J* = 8.3 Hz, 2H), 7.31 (d, *J* = 8.0 Hz, 2H), 4.18 (s, 3H), 3.22 (dd, *J* = 14.5, 3.3 Hz, 1H), 2.44 (s, 3H), 1.54 (s, 3H), 1.40 (s, 3H).

¹³C NMR: (101 MHz, CDCl₃) δ 143.2, 136.9, 129.6, 127.4, 108.4, 76.4, 28.8, 25.9, 21.5.

IR (neat): 2986, 2928, 2360, 1290, 1224.

AMM: (ESI) *m/z* calcd for C₁₄H₂₁N₂O₃S⁺ [M+H]⁺ 297.1267, found 297.1272.



Minor Diastereomer (3a*R*,8a*S*)-2,2-dimethyl-6-(*p*-tolyl)-3a,5,8,8a-tetrahydro-4*H*-[1,3]dioxolo[4,5-*d*][1,2,7]thiadiazepine 6-oxide (**S5**)

Physical Description: White Amorphous powder

Column Conditions: SiO₂, (10% to 70% EtOAc/Hexanes)

¹H NMR: (400 MHz, CDCl₃) δ 7.93 (d, *J* = 7.9 Hz, 2H), 7.32 (d, *J* = 7.9 Hz, 2H), 3.50 (s, 4H), 2.45 (s, 3H), 1.57 (s, 3H), 1.39 (s, 3H).

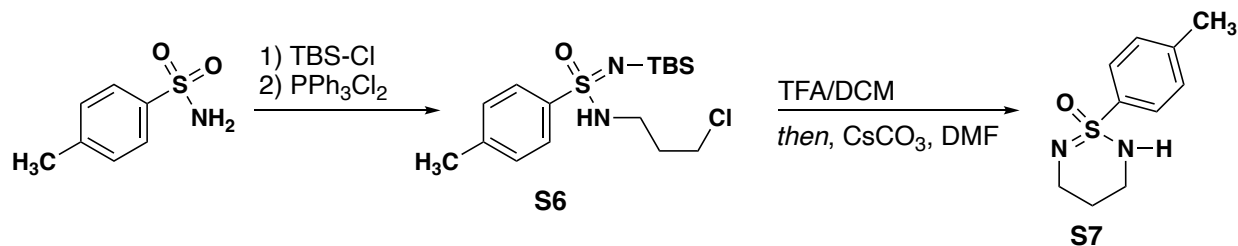
¹³C NMR: (101 MHz, CDCl₃) δ 143.4, 135.6, 129.6, 127.7, 108.2, 29.7, 28.6, 26.2. **IR (neat):** 2984, 2858, 1373, 1252, 1244.

IR (neat): 2986, 2928, 2360, 1290, 1224.

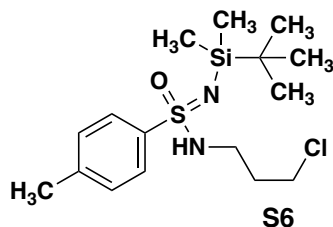
AMM: (ESI) *m/z* calcd for C₁₄H₂₁N₂O₃S⁺ [M+H]⁺ 297.1267, found 297.1272.

Complementary, the use of AD-Mix b gave a single diastereomer of acetonide. Methane sulfonamide (0.009 g 0.01 mmol) and AD-Mix b (0.140 g 1.4 g/mmol alkene) was stirred in tert-butanol (1 mL) for 30 min. Then 1-(*p*-tolyl)-3,4,5,6-tetrahydro-2*H*-1,2,7-thiadiazepine 1-oxide (0.022 g 0.1 mmol) was added and stirred for 36 hours. Then a saturated solution of sodium sulfite was added to the reaction and stirred for 1h then the organics were extracted 3x with DCM and washed with brine. The DCM layer was then dried with Na₂SO₄, filtered and concentrated to yield an off yellow amorphous solid. To this solid was added acetone (2mL), tosic acid monohydrate (2 mg, 0.01 mmol) and 2,2-dimethoxypropane (0.036 mg, 0.35 mmol). The solution was refluxed for 24 hours then concentrated and purified by flash chromatography 10% → 30% → 50% → 60 % → 80% EtOAc/Hexane to yield acetonide (3*a*S,8*a*R)-2,2-dimethyl-6-(*p*-tolyl)-3*a*,5,8,8*a*-tetrahydro-4*H*-[1,3]dioxolo[4,5-*d*][1,2,7]thiadiazepine 6-oxide (12 mg 40%).

2.4.5 Synthesis of 5 and 6 membered -thiadiazine 1-oxides



The TBS protected sulfonamide was protected via literature procedures.¹⁰³ The sulfonimidamides were synthesized using the general method above. The *N*-(*tert*-butyldimethylsilyl)-*N*-(3-chloropropyl)-4-methylbenzenesulfonimidamide (0.720 g 2 mmol) was dissolved in DCM/TFA 1:1 [0.2] 10 mL. The reaction was stirred at room temperature for 1 hour. Once the starting material was consumed (TLC monitoring) the reaction was concentrated on the rotovap and then rotovaped 3x with benzene. Then DMF 50 mL [0.004] was added to the reaction followed by Cs₂CO₃ (1.30 g 4mmol). The reaction was heated to 50 °C for 12 hours and then the reaction was cooled to room temperature diluted with brine and EtOAc and organic layer was separated. The aqueous layer was extracted 3x with EtOAc. The combined organics were then dried with Na₂SO₄ filtered, concentrated, and then purified by flash chromatography to yield the title compound.



N-(*Tert*-butyldimethylsilyl)-*N*-(3-chloropropyl)-4-methylbenzenesulfonimidamide (**S6**)

Yield: 1.221 g (61%)

Physical Description: yellow amorphous solid

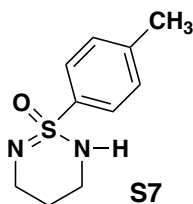
Column Conditions: SiO₂, (10% to 30% EtOAc/Hexanes)

¹H NMR: (400 MHz, CDCl₃) δ 7.77 (d, *J* = 8.7 Hz, 2H), 7.27 (d, *J* = 8.2 Hz, 2H), 4.20 (t, *J* = 6.5 Hz, 1H), 3.64 – 3.47 (m, 2H), 3.01 (qd, *J* = 6.5, 5.0 Hz, 2H), 2.43 (s, 3H), 1.90 (pd, *J* = 6.5, 2.8 Hz, 2H), 0.94 (s, 9H), 0.12 (d, *J* = 2.6 Hz, 5H).

¹³C NMR: (101 MHz, CDCl₃) δ 142.1, 141.2, 129.4, 126.8, 45.2, 43.9, 26.0, 21.4, 18.0, -2.6, -2.7.

IR (neat): 2951, 2933, 2855, 1598, 1325.

AMM: (ESI) *m/z* calcd for C₁₆H₃₀ClN₂OSSi⁺ [M+H]⁺ 361.1531, found 361.1534.



1-(*p*-Tolyl)-2,3,4,5-tetrahydro-1,2,6-thiadiazine 1-oxide (**S7**)

Yield: 65 mg (10%)

Physical Description: off white amorphous solid

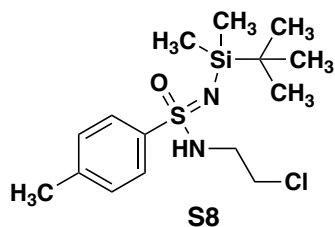
Column Conditions: SiO₂, (10% to 60% EtOAc/Hexanes)

¹H NMR: (400 MHz, CDCl₃) δ 7.91 – 7.83 (m, 2H), 7.33 – 7.25 (m, 2H), 3.57 (ddd, *J* = 12.7, 6.6, 3.6 Hz, 2H), 3.39 (dtt, *J* = 13.3, 8.8, 4.1 Hz, 2H), 2.42 (d, *J* = 2.9 Hz, 3H), 2.04 – 1.91 (m, 1H), 1.78 (tt, *J* = 8.2, 4.8 Hz, 1H).

¹³C NMR: (101 MHz, CDCl₃) δ 143.0, 138.6, 129.5, 127.4, 42.5, 23.9, 21.5.

IR (neat): 2933, 2802, 1290, 1242, 1222.

AMM: (ESI) *m/z* calcd for C₁₀H₁₅N₂OS⁺ [M+H]⁺ 211.0900, found 211.0901.



N'-(*Tert*-butyldimethylsilyl)-*N*-(2-chloroethyl)-4-methylbenzenesulfonimidamide (**S8**)

Yield: 1.231 g (65%)

Physical Description: yellow amorphous solid

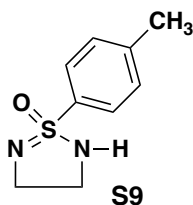
Column Conditions: SiO₂, (10% to 30% EtOAc/Hexanes)

¹H NMR: (400 MHz, CDCl₃) δ 7.77 (d, *J* = 8.3 Hz, 2H), 7.28 (d, *J* = 8.3 Hz, 3H), 4.53 (t, *J* = 6.6 Hz, 1H), 3.56 – 3.45 (m, 2H), 3.32 – 3.11 (m, 2H), 2.43 (s, 3H), 0.95 (s, 9H), 0.13 (d, *J* = 1.5 Hz, 6H).

¹³C NMR: (101 MHz, CDCl₃) δ 142.1, 141.2, 129.4, 126.8, 45.2, 43.9, 26.0, 21.4, 18.0, -2.6, -2.7.

IR (neat): 3221, 2956, 2926, 2855, 1297.

AMM: (ESI) *m/z* calcd for C₁₅H₂₈N₂O₃SSi⁺ [M+H]⁺ 347.1375, found 347.1379.



1-(*p*-Tolyl)-3,4-dihydro-2*H*-1,2,5-thiadiazole 1-oxide (**S9**)

Yield: 34 mg (25%)

Physical Description: off white amorphous solid

Column Conditions: SiO₂, (10% to 90% EtOAc/Hexanes)

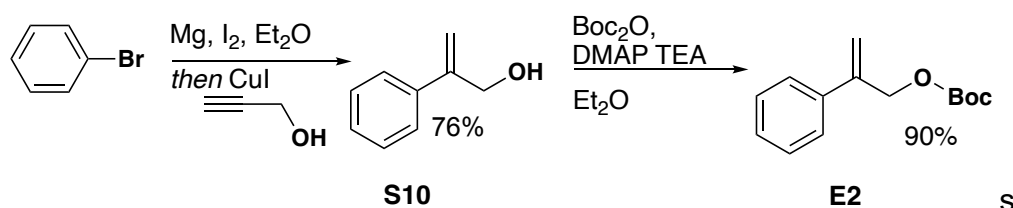
¹H NMR: (400 MHz, CDCl₃) δ 7.93 (d, *J* = 8.3 Hz, 2H), 7.35 (d, *J* = 8.0 Hz, 2H), 2.70 (s, 1H), 2.46 (s, 3H), 2.27 (s, 4H).

¹³C NMR: (101 MHz, CDCl₃) δ 143.9, 137.1, 129.6, 127.8, 26.8, 21.6.

IR (neat): 2931, 2873, 1600, 1398, 1222.

AMM: (ESI) *m/z* calcd for C₉H₁₂N₂OS⁺ [M+H]⁺, 197.0743 found 197.0746.

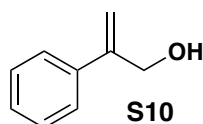
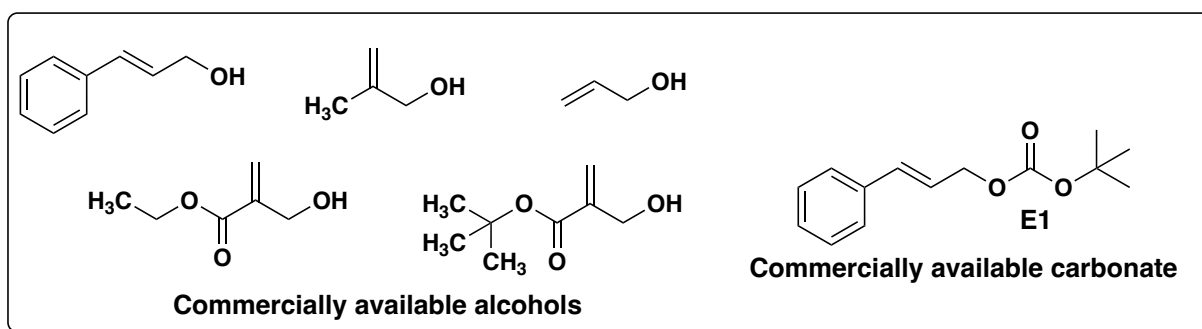
2.4.6 Synthesis of 2-allyl Substituted Carbonates



To an oven dried round bottom flask was added magnesium turnings (0.792 g 0.033 mol) and a small iodine chip, and then diethyl ether (100 mL) was added. The reaction was cooled to 0 °C and then phenyl bromide was added (4.71 g 0.030 mol). The solution was then warmed to 30 °C for 3 hours and then cooled to room temperature and then under a stream of argon CuI (0.286 g 0.015 mol) was added in one portion. The reaction was stirred for an additional hour then propargyl alcohol (0.6 ml 0.0105 mmol) was added drop wise. (Caution evolution of gas). The reaction was stirred for 12 hours. Then the solution was cooled to 0 °C and saturated ammonium chloride 50 mL was added drop wise. The biphasic mixture was stirred for 2 hours. The organics were extracted with diethyl ether and then the organic layer was washed 3x with ammonium chloride and 3x with brine then dried over Na₂SO₄ filtered and concentrated. The crude mixture was purified by flash chromatography 50% Et₂O/Hexane to yield 2-phenylprop-2-en-1-ol as a yellow oil.

Representative procedure for Boc protection of allylic alcohols

The 2-phenylprop-2-en-1-ol (1.530 g 0.012 mol) was dissolved in diethyl ether (60 mL) and then triethyl amine (2.88 g 0.028 mol) and DMAP (0.141 g 0.0012 mol) was added. To this solution was added Boc anhydride (2.98 grams 0.0137 mol) and stirred for 2 hours. Then the reaction was concentrated to a viscous oil adsorbed onto silica gel and purified by flash chromatography isocratic 10% Et₂O/Hexane to yield *tert*-butyl (2-phenylallyl) carbonate as a clear oil.



2-Phenylprop-2-en-1-ol (**S10**)

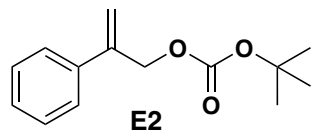
Yield: 1.530 g (76%)

Physical Description: Clear Oil

Column Conditions: SiO₂, (10% to 30% EtOAc/Hexanes)

¹H NMR: (400 MHz, CDCl₃) δ 7.48 (dd, J = 8.0, 1.6 Hz, 2H), 7.43 – 7.29 (m, 4H), 5.50 (s, 1H), 5.38 (d, J = 1.5 Hz, 1H), 4.58 (d, J = 5.9 Hz, 2H), 4.15 (q, J = 7.1 Hz, 1H), 2.07 (s, 1H), 1.60 (s, 3H), 1.28 (t, J = 7.1 Hz, 1H).

Compound is in agreement with literature values¹⁰⁴



Tert-butyl (2-phenylallyl) carbonate (**E2**)

Yield: 2.53 g (90%)

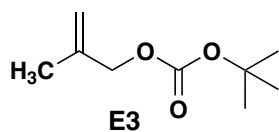
Physical Description: Clear Oil

Column Conditions: SiO₂, (10% Et₂O/Hexanes)

¹H NMR: (400 MHz, CDCl₃) δ 7.50 – 7.42 (m, 2H), 7.42 – 7.33 (m, 2H), 7.37 – 7.28 (m, 1H), 5.57 (q, *J* = 0.8 Hz, 1H), 5.42 (q, *J* = 1.2 Hz, 1H), 4.99 (dd, *J* = 1.4, 0.7 Hz, 2H), 1.50 (s, 2H).

¹³C NMR: (101 MHz, CDCl₃) δ 153.4, 142.4, 138.0, 128.5, 128.1, 126.1, 115.3, 82.3, 68.1, 27.9, 27.8.

Compound is in agreement with literature values¹⁰⁵



Tert-butyl (2-methylallyl) carbonate (**E3**)

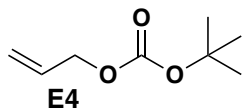
Yield: 0.834 g (97%) *Compound is prone to hydrolysis on Silica isolated and used as a mixture of alcohol and carbonate

Physical Description: Clear Oil

Column Conditions: SiO₂, (10% Et₂O/Hexanes)

¹H NMR: (400 MHz, CDCl₃) δ 4.99 (p, *J* = 1.2 Hz, 1H), 4.93 (dp, *J* = 2.5, 0.8 Hz, 1H), 4.58 – 4.54 (m, 1H), 4.50 – 4.44 (m, 2H), 1.76 (dd, *J* = 1.5, 0.9 Hz, 3H), 1.49 (s, 10H).

Compound is in agreement with literature values¹⁰⁶



Allyl *tert*-butyl carbonate (**E4**)

Yield: 0.718 g (91%)

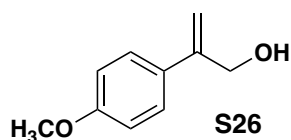
Physical Description: Clear Oil

Column Conditions: SiO₂, (10% Et₂O/Hexanes)

¹H NMR: (400 MHz, CDCl₃) δ 6.02 – 5.87 (m, 1H), 5.42 – 5.21 (m, 2H), 4.57 (dq, *J* = 5.7, 1.5 Hz, 2H), 1.50 (d, *J* = 1.4 Hz, 9H). 4.99 (p, *J* = 1.2 Hz, 1H), 4.93 (dp, *J* = 2.5, 0.8 Hz, 1H), 4.58 – 4.54 (m, 1H), 4.50 – 4.44 (m, 2H), 1.76 (dd, *J* = 1.5, 0.9 Hz, 3H), 1.49 (s, 10H).

¹³C NMR: (101 MHz, CDCl₃) δ 153.3, 132.0, 118.5, 82.1, 67.6, 27.8.

Compound is in agreement with literature values¹⁰⁷



2-(4-Methoxyphenyl)prop-2-en-1-ol (**S26**)

Yield: 4.182 g (85%)

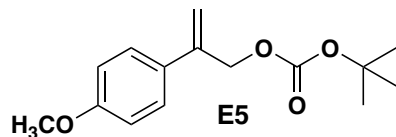
Physical Description: Clear Oil

Column Conditions: SiO₂, (10% to 30% EtOAc/Hexanes)

¹H NMR: (400 MHz, CDCl₃) δ 7.47 – 7.39 (m, 2H), 6.98 – 6.86 (m, 2H), 5.42 (q, *J* = 0.9 Hz, 1H), 5.28 (q, *J* = 1.3 Hz, 1H), 4.55 (d, *J* = 3.2 Hz, 2H), 3.84 (s, 3H), 1.58 (s, 1H).

¹³C NMR: (101 MHz, CDCl₃) δ 159.5, 146.6, 130.9, 127.2, 113.9, 111.1, 65.2, 55.3.

Compound is in agreement with literature values¹⁰⁸



Tert-butyl (2-(4-methoxyphenyl)allyl) carbonate (**E5**)

Yield: 2.91 g (92%)

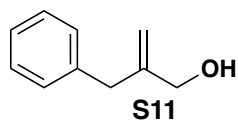
Physical Description: Clear Oil

Column Conditions: SiO₂, (10% Et₂O/Hexanes)

¹H NMR: (400 MHz, CDCl₃) δ 7.42 – 7.38 (m, 2H), 6.93 – 6.87 (m, 2H), 5.51 – 5.46 (m, 1H), 5.32 (q, *J* = 1.2 Hz, 1H), 4.96 (dd, *J* = 1.3, 0.6 Hz, 2H), 3.84 (s, 3H), 1.50 (s, 9H).

¹³C NMR: (101 MHz, CDCl₃) δ 159.5, 153.4, 141.7, 130.5, 127.2, 122.1, 113.9, 113.7, 82.2, 68.2, 55.3, 27.8.

Compound is in agreement with literature values ¹⁰⁹



2-Benzylprop-2-en-1-ol (**S11**)

Yield: 3.19 g (72%)

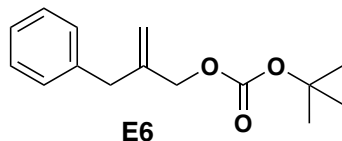
Physical Description: Clear Oil

Column Conditions: SiO₂, (10% to 30% EtOAc/Hexanes)

¹H NMR: (400 MHz, CDCl₃) δ 7.42 – 7.19 (m, 6H), 5.15 (dq, *J* = 1.6, 0.8 Hz, 1H), 4.93 (h, *J* = 1.2 Hz, 1H), 4.07 (t, *J* = 1.3 Hz, 2H), 3.44 (s, 2H).

¹³C NMR: (101 MHz, CDCl₃) δ 148.2, 139.0, 128.9, 128.4, 126.3, 111.5, 65.3, 39.9.

Compound is in agreement with literature values ¹¹⁰



2-Benzylallyl *tert*-butyl carbonate (**E6**)

Yield: 1.14 g (92%)

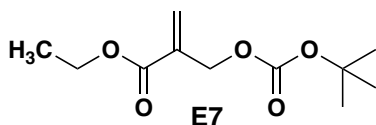
Physical Description: Clear Oil

Column Conditions: SiO₂, (10% Et₂O/Hexanes)

¹H NMR: (400 MHz, CDCl₃) δ 7.32 (dd, *J* = 7.9, 6.5 Hz, 2H), 7.23 (ddd, *J* = 8.5, 7.0, 1.5 Hz, 3H), 5.22 – 5.15 (m, 1H), 5.04 – 4.95 (m, 1H), 4.49 (d, *J* = 1.3 Hz, 2H), 3.44 (s, 2H), 1.52 (d, *J* = 2.7 Hz, 9H).

¹³C NMR: (101 MHz, CDCl₃) δ 153.4, 143.1, 138.4, 129.0, 128.5, 126.4, 114.5, 82.1, 68.7, 39.9, 27.8.

Compound is in agreement with literature values¹¹¹



Ethyl 2-(((*tert*-butoxycarbonyl)oxy)methyl)acrylate (**E7**)

Yield: 0.131 g (57%)

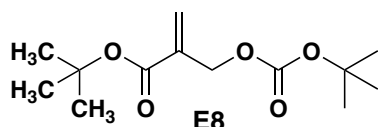
Physical Description: Clear Oil

Column Conditions: SiO₂, (10% Et₂O/Hexanes)

¹H NMR: (400 MHz, CDCl₃) δ 6.38 (q, *J* = 1.0 Hz, 1H), 5.88 (q, *J* = 1.4 Hz, 1H), 4.82 (t, *J* = 1.2 Hz, 2H), 4.25 (q, *J* = 7.1 Hz, 2H), 1.51 (s, 9H), 1.32 (t, *J* = 7.1 Hz, 3H).

¹³C NMR: (101 MHz, CDCl₃) δ 165.1, 153.1, 135.3, 127.2, 82.5, 64.7, 61.0, 27.8, 14.1.

Compound is in agreement with literature values¹¹²



Tert-butyl 2-(((*tert*-butoxycarbonyl)oxy)methyl)acrylate *Compound is prone to hydrolysis on silica isolated and used as a mixture of alcohol and carbonate (**E8**)

Yield: 125 mg (11%)

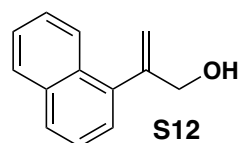
Physical Description: Clear Oil

Column Conditions: SiO₂, (10% Et₂O/Hexanes)

¹H NMR: (400 MHz, CDCl₃) δ 6.20 (q, *J* = 1.7 Hz, 1H), 5.77 (q, *J* = 1.6 Hz, 1H), 4.78 – 4.73 (m, 2H), 4.20 (t, *J* = 1.7 Hz, 2H), 1.49 (s, 18H).

Low Res: (ESI) *m/z* calcd for C₁₅H₂₂O₅⁺ [M]⁺ 258.1467, found 258.15.

Compound is in agreement with literature values¹¹²



2-(Naphthalen-1-yl)prop-2-en-1-ol (**S12**)

Yield: 3.31 g (61%)

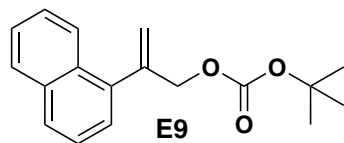
Physical Description: Orange Oil

Column Conditions: SiO₂, (10% to 30% EtOAc/Hexanes)

¹H NMR: (400 MHz, CDCl₃) δ 8.10 – 8.01 (m, 1H), 7.94 – 7.86 (m, 1H), 7.84 (dd, *J* = 8.3, 1.1 Hz, 1H), 7.52 (d, *J* = 3.3 Hz, 1H), 7.52 – 7.44 (m, 2H), 7.35 (dd, *J* = 7.0, 1.3 Hz, 1H), 5.74 (q, *J* = 1.7 Hz, 1H), 5.30 (q, *J* = 1.4 Hz, 1H), 4.50 (t, *J* = 1.5 Hz, 2H).

¹³C NMR: (101 MHz, CDCl₃) δ 147.8, 137.9, 133.7, 131.5, 128.4, 127.9, 126.1, 125.9, 125.7, 125.4, 125.2, 114.9, 66.8.

Compound is in agreement with literature values¹⁰⁴



Tert-butyl (2-(naphthalen-1-yl)allyl) carbonate (**E9**)

Yield: 0.691 g (93%)

Physical Description: Clear Oil

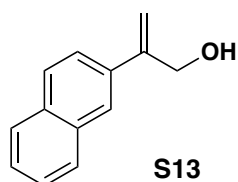
Column Conditions: SiO₂, (10% Et₂O/Hexanes)

¹H NMR: (400 MHz, CDCl₃) δ 8.13 – 8.05 (m, 1H), 7.94 – 7.80 (m, 2H), 7.57 – 7.48 (m, 2H), 7.48 (dd, *J* = 8.2, 7.0 Hz, 1H), 7.39 (dd, *J* = 7.1, 1.3 Hz, 1H), 5.72 (dd, *J* = 2.0, 1.1 Hz, 1H), 5.34 (t, *J* = 1.1 Hz, 1H), 4.92 (q, *J* = 1.2 Hz, 2H), 1.50 (d, *J* = 0.8 Hz, 9H).

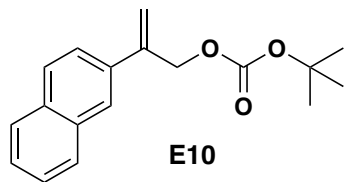
¹³C NMR: (101 MHz, CDCl₃) δ 153.3, 142.9, 137.2, 133.7, 131.5, 128.3, 128.0, 126.2, 125.9, 125.9, 125.4, 125.2, 116.9, 82.3, 69.4, 27.8.

IR (neat):

Low Res: (ESI) *m/z* calcd for C₁₈H₂₀O₃⁺ [M]⁺ 284.14, found 281.14.



Grignard formation was very poor for the 2-bromo-naphthyl substrate (**S13**). Thus after quenching and work up the crude reaction mixture was subjected to Boc protection without any further purification



Tert-butyl (2-(naphthalen-2-yl)allyl) carbonate (**E10**)

Yield: 0.68 g (8%)

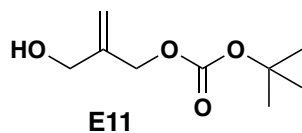
Physical Description: Clear Oil

Column Conditions: SiO₂, (10% Et₂O/Hexanes)

¹H NMR: (400 MHz, CDCl₃) δ 7.88 – 7.83 (m, 5H), 7.63 (dd, *J* = 8.7, 1.9 Hz, 1H), 7.52 – 7.48 (m, 3H), 5.73 (s, 1H), 5.53 (t, *J* = 1.2 Hz, 1H), 5.12 (d, *J* = 1.4 Hz, 2H), 1.60 – 1.49 (m, 14H), 1.49 – 1.46 (m, 1H), 1.46 – 1.27 (m, 2H).

¹³C NMR: (101 MHz, CDCl₃) δ 153.5, 142.2, 135.2, 133.3, 133.1, 128.3, 128.1, 127.6, 126.3, 126.2, 126.2, 124.9, 124.2, 115.8, 82.4, 68.1, 27.8, 27.8.

Low Res: (ESI) *m/z* calcd for C₁₈H₁₉O₃⁺ [M]⁺ 284.14, found.



Tert-butyl (2-(hydroxymethyl)allyl) carbonate (**E11**)

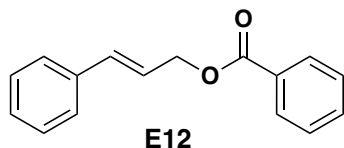
Yield: 468 mg (72%)

Physical Description: Clear Oil

Column Conditions: SiO₂, (10% Et₂O/Hexanes)

¹H NMR: (400 MHz, CDCl₃) δ 5.25 (d, *J* = 1.6 Hz, 1H), 5.20 (t, *J* = 1.2 Hz, 1H), 4.63 (s, 2H), 4.16 (d, *J* = 5.1 Hz, 2H).

Compound is in agreement with literature values^{113,114}



Cinnamyl benzoate (**E12**)

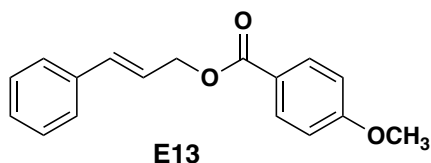
Yield: 124 mg (91%)

Physical Description: Clear Oil

Column Conditions: SiO₂, (10% Et₂O/Hexanes)

¹H NMR: (400 MHz, CDCl₃) δ 8.12 – 8.05 (m, 2H), 7.61 – 7.52 (m, 1H), 7.49 – 7.39 (m, 4H), 7.38 – 7.22 (m, 3H), 6.79 – 6.70 (m, 1H), 6.41 (dt, *J* = 15.9, 6.4 Hz, 1H), 4.99 (dd, *J* = 6.5, 1.4 Hz, 2H).

Compound is in agreement with literature values^{113,114}



Cinnamyl 4-methoxybenzoate (**E13**)

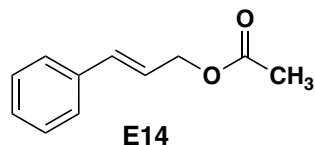
Yield: 89 mg (89%)

Physical Description: White Solid

Column Conditions: SiO₂, (10% Et₂O/Hexanes)

¹H NMR: (400 MHz, CDCl₃) δ 8.08 – 8.00 (m, 2H), 7.45 – 7.38 (m, 2H), 7.37 – 7.22 (m, 3H), 6.97 – 6.89 (m, 2H), 6.73 (d, *J* = 15.9 Hz, 1H), 6.41 (dt, *J* = 15.9, 6.4 Hz, 1H), 4.96 (dd, *J* = 6.4, 1.4 Hz, 2H), 3.87 (s, 3H).

Compound is in agreement with literature values¹¹⁶



Cinnamyl acetate (**E14**)

Yield: 103 mg (93%)

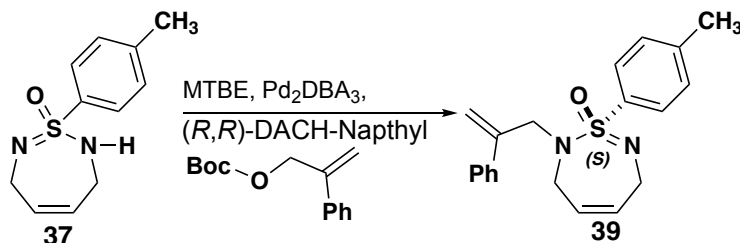
Physical Description: Clear Oil

Column Conditions: SiO₂, (10% Et₂O/Hexanes)

¹H NMR: (400 MHz, CDCl₃) δ 7.43 – 7.36 (m, 2H), 7.33 (ddd, J = 7.5, 6.6, 1.3 Hz, 2H), 7.33 – 7.22 (m, 1H), 6.66 (dt, J = 15.8, 1.5 Hz, 1H), 6.29 (dt, J = 15.9, 6.5 Hz, 1H), 4.73 (dd, J = 6.5, 1.4 Hz, 2H), 2.10 (s, 3H).

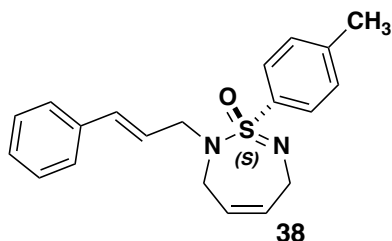
Compound is in agreement with literature values¹¹⁶

2.4.7 General Procedure of Tsuji-Trost Asymmetric Allylation



To a flame dried 7 mL dram vial is added **1** (0.022 g 0.1 mmol) Pd₂DBA₃ (0.0045 g 0.005 mmol) (*R,R*)-DACH-Naphthyl (0.0095 g 0.012 mmol) and *tert*-butyl (2-phenylallyl) carbonate (0.035 g 0.15 mmol) and a stir bar. The vial is then sealed with a rubber septum and then evacuated and backfilled with argon. Then 1 mL of methyl *tert*-butyl ether is added. (**Note:** MTBE is refluxed over sodium and benzophenone and then distilled and purged with argon prior to use) The reaction is then stirred overnight. The septum is then removed, and the stir bar rinsed with 0.25 mL dichloromethane and then silica gel is added to the crude reaction mixture and directly columned.

Racemic standards were synthesized in a similar manner except equal portions of (*R,R*)-DACH-naphthyl (0.0042 g) of (*S,S*)-DACH-naphthyl (and 0.0042 g) were added to the reaction.



(*S*)-2-Cinnamyl-1-(*p*-tolyl)-3,6-dihydro-2*H*-1,2,7-thiadiazepine 1-oxide (**38**)

Yield: 16 mg (48%)

Physical Description: Yellow Oil

Column Conditions: SiO₂, (10% to 50% EtOAc/Hexanes)

¹H NMR: (400 MHz, CDCl₃) δ 7.91 (d, *J* = 8.0 Hz, 2H), 7.33 – 7.18 (m, 7H), 6.40 (d, *J* = 15.9 Hz, 1H), 6.01 (ddd, *J* = 15.8, 7.2, 5.4 Hz, 1H), 5.78 (ddt, *J* = 10.5, 5.1, 2.3 Hz, 1H), 5.64 (tt, *J* = 7.9, 3.2 Hz, 1H), 4.44 (ddq, *J* = 18.0, 4.5, 2.2 Hz, 1H), 4.18 (ddd, *J* = 15.3, 5.5, 1.7 Hz, 1H), 4.00 – 3.88 (m, 1H), 3.80 (dd, *J* = 18.1, 5.5 Hz, 1H), 3.59 (dd, *J* = 15.3, 7.2 Hz, 1H), 3.22 (dd, *J* = 18.2, 6.8 Hz, 1H), 2.42 (s, 3H).

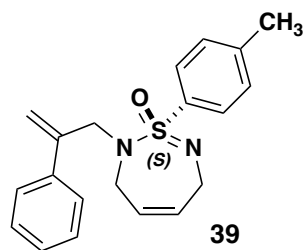
¹³C NMR: (101 MHz, CD₂Cl₂) δ 143.1, 136.6, 135.0, 132.7, 131.6, 129.5, 128.5, 127.76, 127.67, 126.3, 125.7, 125.3, 45.7, 42.7, 29.7, 21.1.

IR (neat): 2836, 1597, 1494, 1275, 1147.

AMM: (ESI) *m/z* calcd for C₂₀H₂₃N₂OS⁺ [M+H]⁺ 339.1526, found 339.1529.

ER: 75:25

Optical Rotation: -51 degrees c 0.32 at 21.6 °C.



(S)-2-(2-Phenylallyl)-1-(p-tolyl)-3,6-dihydro-2H-1,2,7-thiadiazepine 1-oxide (**39**)

Yield: 327 mg (97%)

Physical Description: Yellow Oil

Column Conditions: SiO₂, (10% to 50% EtOAc/Hexanes)

¹H NMR: (400 MHz, CDCl₃) δ 7.88 (d, *J* = 8.2 Hz, 2H), 7.51 – 7.43 (m, 2H), 7.38 – 7.24 (m, 5H), 5.62 (ddt, *J* = 10.6, 5.1, 2.3 Hz, 1H), 5.49 (td, *J* = 7.7, 3.5 Hz, 1H), 5.45 (s, 1H), 5.20 (d, *J* = 1.6 Hz, 1H), 4.63 (dt, *J* = 15.1, 1.6 Hz, 1H), 4.24 (ddd, *J* = 17.9, 4.7, 2.4 Hz, 1H), 3.92 – 3.80 (m, 1H), 3.76 – 3.64 (m, 2H), 3.20 (ddd, *J* = 17.5, 7.0, 2.0 Hz, 1H), 2.44 (s, 3H).

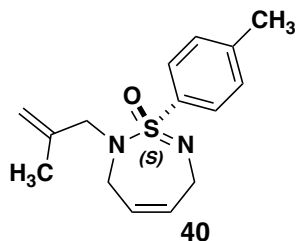
¹³C NMR: (101 MHz, CDCl₃) δ 144.0, 142.9, 138.6, 134.4, 131.4, 129.5, 128.2, 127.8, 127.8, 126.6, 125.2, 115.3, 54.5, 45.1, 42.6, 21.5.

IR (neat): 2839, 1597, 1494, 1276, 1148.

AMM: (ESI) *m/z* calcd for C₂₀H₂₃N₂OS⁺ [M+H]⁺ 339.1526, found 339.1529.

ER: 99:1

Optical Rotation: 82 degrees *c* 0.24 at 19.8 °C.



(S)-2-(2-Methylallyl)-1-(*p*-tolyl)-3,6-dihydro-2*H*-1,2,7-thiadiazepine 1-oxide (**40**)

Yield: 25 mg (93%)

Physical Description: Clear Oil

Column Conditions: SiO₂, (10% to 30% EtOAc/Hexanes)

¹H NMR: (400 MHz, CDCl₃) δ 7.89 (d, *J* = 8.4 Hz, 2H), 7.31 (d, *J* = 8.1 Hz, 2H), 5.78 (ddt, *J* = 10.3, 4.9, 2.2 Hz, 1H), 5.64 (dddd, *J* = 11.1, 7.1, 3.6, 1.8 Hz, 1H), 4.86 (q, *J* = 1.6 Hz, 1H), 4.82 (s, 1H), 4.43 (ddq, *J* = 18.0, 4.6, 2.0 Hz, 1H), 4.02 (d, *J* = 14.4 Hz, 1H), 3.92 – 3.74 (m, 2H), 3.19 – 3.06 (m, 2H), 2.43 (s, 3H), 1.74 (s, 3H).

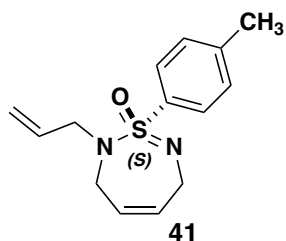
¹³C NMR: (101 MHz, CDCl₃) δ 142.9, 141.6, 134.4, 131.5, 129.5, 127.8, 125.6, 113.6, 57.2, 45.2, 42.7, 21.5, 19.8.

IR (neat): 3024, 2971, 2921, 1659, 1595.

AMM: (ESI) *m/z* calcd for C₁₅H₂₁N₂OS + [M+H]⁺ 277.1369, found 277.1368.

ER: 97:3

Optical Rotation: 129 degrees c 0.43 at 18.2 °C.



(S)-2-Allyl-1-(*p*-tolyl)-3,6-dihydro-2*H*-1,2,7-thiadiazepine 1-oxide (**41**)

Yield: 25 mg (96%)

Physical Description: Clear Oil

Column Conditions: SiO₂, (10% to 30% EtOAc/Hexanes)

¹H NMR: (400 MHz, CDCl₃) δ 7.89 (d, *J* = 8.3 Hz, 2H), 7.31 (d, *J* = 8.1 Hz, 2H), 5.79 (ddt, *J* = 10.5, 5.1, 2.3 Hz, 1H), 5.75 – 5.60 (m, 2H), 5.19 – 5.07 (m, 2H), 4.42 (ddt, *J* = 18.0, 4.5, 2.2 Hz, 1H), 4.04 (ddt, *J* = 15.3, 5.2, 1.7 Hz, 1H), 3.91 (ddq, *J* = 17.5, 4.8, 2.5 Hz, 1H), 3.79 (ddt, *J* = 18.0, 5.4, 1.7 Hz, 1H), 3.43 (ddd, *J* = 15.2, 6.7, 1.4 Hz, 1H), 3.17 (ddd, *J* = 17.5, 7.0, 2.0 Hz, 1H), 2.44 (s, 3H).

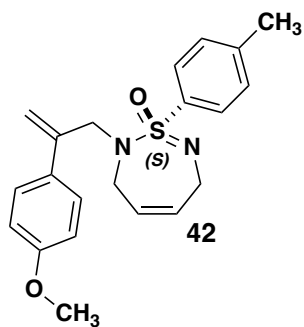
¹³C NMR: (101 MHz, CDCl₃) δ 142.9, 134.8, 133.9, 131.8, 129.5, 127.7, 125.5, 117.9, 53.8, 45.5, 42.8, 21.5.

IR (neat): 3017, 2921, 2835, 1600, 1280.

AMM: (ESI) *m/z* calcd for C₁₄H₂₀N₂OS⁺ [M+H]⁺ 263.1213, found 263.1212.

ER: 90:10

Optical Rotation: 106 degrees *c* 0.56 at 18.5 °C.



(*S*)-2-(2-(4-Methoxyphenyl)allyl)-1-(*p*-tolyl)-3,6-dihydro-2*H*-1,2,7-thiadiazepine 1-oxide
(42)

Yield: 35 mg (97%)

Physical Description: Clear Oil

Column Conditions: SiO₂, (10% to 30% EtOAc/Hexanes)

¹H NMR: (400 MHz, CDCl₃) δ 7.86 (d, *J* = 8.2 Hz, 2H), 7.41 (d, *J* = 8.5 Hz, 2H), 7.28 (d, *J* = 8.1 Hz, 2H), 6.84 (d, *J* = 8.5 Hz, 2H), 5.59 (ddt, *J* = 10.6, 5.2, 2.3 Hz, 1H), 5.46 (ddd,

$J = 10.7, 6.4, 3.1$ Hz, 1H), 5.35 (s, 1H), 5.07 (d, $J = 1.6$ Hz, 1H), 4.59 (dt, $J = 15.0, 1.5$ Hz, 1H), 4.22 (ddt, $J = 17.8, 4.6, 2.2$ Hz, 1H), 3.85 – 3.81 (m, 1H), 3.80 (s, 3H), 3.73 – 3.62 (m, 1H), 3.59 (d, $J = 14.9$ Hz, 1H), 3.18 (ddd, $J = 17.4, 7.0, 1.9$ Hz, 1H), 2.42 (s, 3H).

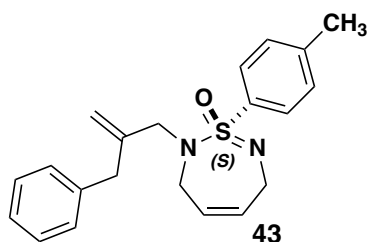
^{13}C NMR: (101 MHz, CDCl_3) δ 159.4, 143.2, 142.9, 134.3, 131.3, 130.9, 129.5, 127.8, 127.8, 125.2, 113.8, 113.5, 55.3, 54.6, 45.0, 42.6, 21.5.

IR (neat): 2837, 2358, 2340, 1608, 1515.

AMM: (ESI) m/z calcd for $\text{C}_{16}\text{H}_{23}\text{N}_2\text{O}_2\text{S}^+$ $[\text{M}+\text{H}]^+$, found.

ER: 99:1

Optical Rotation: 34 degrees c 0.74 at 20.6 $^\circ\text{C}$.



(S)-2-(2-Benzylallyl)-1-(p-tolyl)-3,6-dihydro-2H-1,2,7-thiadiazepine 1-oxide (**43**)

Yield: 33 mg (94%)

Physical Description: Clear Oil

Column Conditions: SiO_2 , (10% to 30% EtOAc/Hexanes)

^1H NMR: (400 MHz, CDCl_3) δ 7.86 (d, $J = 8.6$ Hz, 2H), 7.31 – 7.25 (m, 4H), 7.23 – 7.16 (m, 3H), 5.84 – 5.76 (m, 1H), 5.70 – 5.60 (m, 1H), 4.94 (s, 1H), 4.79 (s, 1H), 4.45 (ddd, $J = 17.8, 4.4, 2.4$ Hz, 1H), 4.06 (d, $J = 14.5$ Hz, 1H), 3.83 (tqd, $J = 18.1, 3.3, 2.2$ Hz, 2H), 3.41 (d, $J = 15.4$ Hz, 1H), 3.33 (d, $J = 15.4$ Hz, 1H), 3.16 – 3.05 (m, 2H), 2.41 (s, 3H).

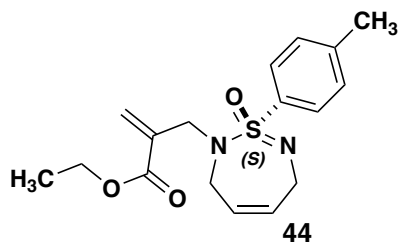
^{13}C NMR: (101 MHz, CDCl_3) δ 145.1, 142.9, 138.9, 134.2, 131.7, 129.5, 129.2, 128.4, 127.8, 126.3, 125.7, 114.9, 55.8, 45.4, 42.8, 39.7, 21.5.

IR (neat): 2923, 2363, 2338, 1454, 1277.

AMM: (ESI) m/z calcd for $C_{21}H_{25}N_2OS^+$ $[M+H]^+$ 353.1682, found 353.1691.

ER: 98:2

Optical Rotation: 29 degrees c 0.74 at 21 °C.



Ethyl (S)-2-(((1-oxido-1-(*p*-tolyl)-3,6-dihydro-2H-1 λ^6 ,2,7-thiadiazepin-2-yl)methyl)acrylate
(44)

Yield: 28 mg (83%)

Physical Description: Clear Oil

Column Conditions: SiO_2 , (10% to 30% EtOAc/Hexanes)

1H NMR: (400 MHz, $CDCl_3$) δ 7.89 (d, J = 8.4 Hz, 2H), 7.30 (d, J = 8.0 Hz, 2H), 6.29 (q, J = 1.1 Hz, 1H), 5.81 (dq, J = 13.7, 3.0, 2.3 Hz, 2H), 5.65 (ddtd, J = 10.7, 6.7, 2.7, 1.1 Hz, 1H), 4.42 (ddd, J = 18.1, 4.7, 2.4 Hz, 1H), 4.27 – 4.14 (m, 3H), 4.04 (ddq, J = 17.6, 4.9, 2.5 Hz, 1H), 3.81 (ddt, J = 18.0, 5.6, 1.7 Hz, 1H), 3.68 (dt, J = 17.1, 1.4 Hz, 1H), 3.08 (ddd, J = 17.6, 7.0, 1.9 Hz, 1H), 2.42 (s, 3H), 1.28 (t, J = 7.1 Hz, 3H).

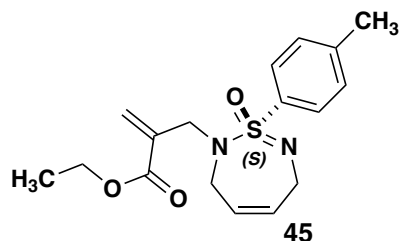
^{13}C NMR: (101 MHz, $CDCl_3$) δ 166.0, 143.1, 136.6, 134.7, 131.9, 129.6, 127.7, 126.4, 125.7, 60.9, 51.6, 47.4, 42.8, 21.5, 14.2.

IR (neat): 2921, 2358, 2343, 1719, 1277.

AMM: (ESI) m/z calcd for $C_{17}H_{23}N_2O_3S^+$ $[M+H]^+$ 335.1424, found 335.1423.

ER: 71:29

Optical Rotation: 43 degrees *c* 0.16 at 19.6 °C.



Ethyl (S)-2-((1-oxido-1-(*p*-tolyl)-3,6-dihydro-2*H*-1 λ^6 ,2,7-thiadiazepin-2-yl)methyl)acrylate
(45)

Yield: 24 mg (66%)

Physical Description: Clear Oil

Column Conditions: SiO₂, (10% to 30% EtOAc/Hexanes)

¹H NMR: (400 MHz, CDCl₃) δ 7.89 (d, *J* = 8.3 Hz, 2H), 7.30 (d, 2H), 6.18 (q, *J* = 1.4 Hz, 1H), 5.80 (ddt, *J* = 10.4, 5.1, 2.2 Hz, 1H), 5.74 (q, *J* = 1.7 Hz, 1H), 5.65 (ddtd, *J* = 10.7, 6.6, 2.5, 1.0 Hz, 1H), 4.42 (ddd, *J* = 18.1, 4.6, 2.4 Hz, 1H), 4.21 (dt, *J* = 17.1, 1.9 Hz, 1H), 4.01 (ddq, *J* = 17.5, 4.8, 2.5 Hz, 1H), 3.80 (ddt, *J* = 18.0, 5.7, 1.7 Hz, 1H), 3.61 (dt, *J* = 17.0, 1.4 Hz, 1H), 3.09 (ddd, *J* = 17.5, 7.0, 1.9 Hz, 1H), 2.42 (s, 3H), 1.46 (s, 9H).

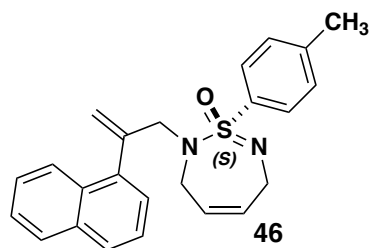
¹³C NMR: (101 MHz, CDCl₃) δ 165.3, 143.0, 137.8, 134.6, 131.9, 129.6, 127.8, 125.7, 125.5, 81.2, 51.8, 47.2, 42.8, 28.0, 21.5.

IR (neat): 2976, 2926, 2365, 1706, 1280.

AMM: (ESI) *m/z* calcd for C₁₉H₂₇N₂O₃S⁺ [M+H]⁺ 363.1737, found 363.1730.

ER: 67:33

Optical Rotation: 20 degrees *c* 0.17 at 21.6 °C.



(S)-2-(2-(Naphthalen-1-yl)allyl)-1-(*p*-tolyl)-3,6-dihydro-2*H*-1,2,7-thiadiazepine 1-oxide (**46**)

Yield: 37 mg (95%)

Physical Description: Clear Oil

Column Conditions: SiO₂, (10% to 30% EtOAc/Hexanes)

¹H NMR: (400 MHz, CDCl₃) δ 7.99 – 7.92 (m, 1H), 7.89 – 7.78 (m, 1H), 7.79 – 7.68 (m, 3H), 7.46 (dt, *J* = 6.3, 3.4 Hz, 2H), 7.37 (dd, *J* = 8.2, 7.0 Hz, 1H), 7.28 – 7.18 (m, 1H), 7.15 (d, *J* = 8.1 Hz, 2H), 5.73 (ddt, *J* = 10.2, 5.2, 2.2 Hz, 1H), 5.68 – 5.57 (m, 2H), 5.24 (q, *J* = 1.4 Hz, 1H), 4.39 (dt, *J* = 16.4, 1.6 Hz, 1H), 4.31 (ddd, *J* = 18.0, 4.6, 2.3 Hz, 1H), 4.01 (ddq, *J* = 17.5, 4.8, 2.5 Hz, 1H), 3.81 (d, *J* = 16.5 Hz, 1H), 3.74 (ddt, *J* = 18.0, 5.4, 1.7 Hz, 1H), 3.30 (ddd, *J* = 17.4, 6.9, 1.9 Hz, 1H), 2.36 (s, 3H).

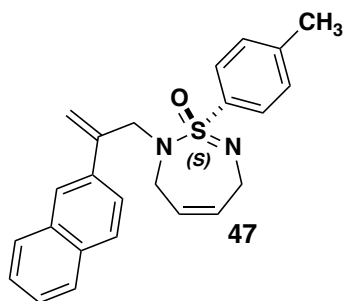
¹³C NMR: (101 MHz, CDCl₃) δ 144.0, 142.7, 138.2, 134.8, 133.7, 131.9, 131.3, 129.4, 128.3, 127.8, 127.6, 126.1, 125.8, 125.7, 125.5, 125.3, 125.1, 117.5, 56.9, 46.7, 42.8, 21.4.

IR (neat): 2921, 2835, 2363, 1277, 1149.

AMM: (ESI) *m/z* calcd for C₂₄H₂₅N₂OS⁺ [M+H]⁺ 389.1682, found 389.1700.

ER: 99:1

Optical Rotation: 33 degrees c 0.86 at 18.3 °C.



(S)-2-(2-(Naphthalen-2-yl)allyl)-1-(*p*-tolyl)-3,6-dihydro-2*H*-1,2,7-thiadiazepine 1-oxide (**47**)

Yield: 12 mg (31%)

Physical Description: Clear Oil

Column Conditions: SiO₂, (10% to 30% EtOAc/Hexanes)

¹H NMR: (400 MHz, CDCl₃) δ 7.93 (d, *J* = 1.8 Hz, 1H), 7.87 – 7.84 (m, 2H), 7.80 (ddd, *J* = 8.0, 4.9, 2.2 Hz, 2H), 7.76 (d, *J* = 8.6 Hz, 1H), 7.58 (dd, *J* = 8.6, 1.9 Hz, 1H), 7.47 – 7.44 (m, 2H), 7.23 (d, *J* = 8.0 Hz, 2H), 5.57 (s, 1H), 5.53 (ddt, *J* = 9.7, 4.9, 2.1 Hz, 1H), 5.49 – 5.42 (m, 1H), 5.27 (s, 1H), 4.71 (dt, *J* = 15.1, 1.5 Hz, 1H), 4.20 (ddd, *J* = 18.0, 4.6, 2.3 Hz, 1H), 3.95 – 3.77 (m, 2H), 3.65 (ddd, *J* = 18.3, 5.4, 2.0 Hz, 1H), 3.23 (ddd, *J* = 17.4, 6.7, 1.9 Hz, 1H), 2.39 (s, 3H).

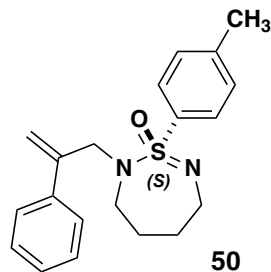
¹³C NMR: (101 MHz, CDCl₃) δ 143.8, 142.9, 135.7, 134.5, 133.2, 133.0, 131.5, 129.5, 128.3, 127.8, 127.7, 127.5, 126.1, 126.0, 125.7, 125.2, 124.7, 115.9, 54.6, 45.1, 42.7, 21.4.

IR (neat): 2918, 2358, 1595, 1275, 1232.

AMM: (ESI) *m/z* calcd for C₂₄H₂₅N₂OS⁺ [M+H]⁺ 389.1682, found 389.1688.

ER: 69:31

Optical Rotation: 17 degrees *c* 0.42 at 18.9 °C.



(S)-2-(2-Phenylallyl)-1-(p-tolyl)-3,4,5,6-tetrahydro-2H-1,2,7-thiadiazepine 1-oxide (**50**)

Yield: 33 mg (97%)

Physical Description: Off White Crystal

Melting Point: 175-176 °C

Column Conditions: SiO₂, (10% to 30% EtOAc/Hexanes)

¹H NMR: (400 MHz, CDCl₃) δ 7.86 (d, *J* = 8.3 Hz, 2H), 7.61 – 7.54 (m, 2H), 7.41 – 7.26 (m, 5H), 5.45 (d, *J* = 1.2 Hz, 1H), 5.06 (d, *J* = 1.5 Hz, 1H), 4.73 (dt, *J* = 14.6, 1.4 Hz, 1H), 3.68 (d, *J* = 14.7 Hz, 1H), 3.36 – 3.18 (m, 2H), 3.11 (dd, *J* = 14.8, 11.8 Hz, 1H), 2.91 (dt, *J* = 14.8, 3.4 Hz, 1H), 2.44 (s, 3H), 1.68 – 1.39 (m, 4H).

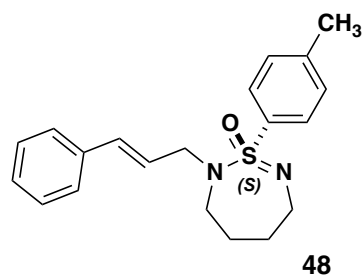
¹³C NMR: (101 MHz, CDCl₃) δ 144.1, 142.5, 138.2, 135.7, 129.4, 128.3, 128.0, 127.9, 126.7, 115.7, 54.6, 46.9, 42.5, 29.9, 28.7, 21.4.

IR (neat): 3042, 2959, 2908, 2843, 1244.

AMM: (ESI) *m/z* calcd for C₂₀H₂₅N₂OS⁺ [M+H]⁺ 341.1682, found 341.1684.

ER: 98:2

Optical Rotation: 40 degrees *c* 0.10 at 20.2 °C.



(S)-2-Cinnamyl-1-(*p*-tolyl)-3,4,5,6-tetrahydro-2*H*-1,2,7-thiadiazepine 1-oxide (**48**)

Yield: 18 mg (54%)

Physical Description: Yellow Oil

Column Conditions: SiO₂, (10% to 30% EtOAc/Hexanes)

¹H NMR: (400 MHz, CDCl₃) δ 7.87 (d, *J* = 9.0 Hz, 2H), 7.34 – 7.25 (m, 4H), 7.23 (d, *J* = 7.2 Hz, 3H), 6.38 – 6.28 (m, 1H), 6.02 (ddd, *J* = 15.8, 7.4, 5.7 Hz, 1H), 4.13 (ddd, *J* = 15.2, 5.8, 1.6 Hz, 1H), 3.75 (dd, *J* = 15.2, 7.4 Hz, 1H), 3.57 (ddd, *J* = 13.3, 11.8, 1.7 Hz, 1H), 3.40 – 3.30 (m, 1H), 3.25 (dd, *J* = 14.9, 11.3 Hz, 1H), 2.95 (dq, *J* = 15.2, 2.2 Hz, 1H), 2.41 (s, 3H), 1.81 – 1.66 (m, 2H), 1.66 – 1.47 (m, 2H).

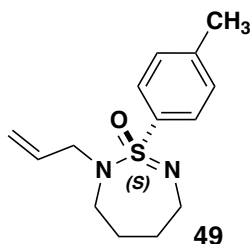
¹³C NMR: (101 MHz, CDCl₃) δ 142.5, 136.9, 136.5, 132.9, 129.5, 128.6, 127.8, 127.6, 126.4, 125.5, 53.3, 48.0, 42.7, 30.0, 29.7, 21.4.

IR (neat): 3043, 2962, 2911, 2847, 1240.

AMM: (ESI) *m/z* calcd for C₂₀H₂₅N₂OS⁺ [M+H]⁺ 341.1682, found 341.1681.

ER: 63:37

Optical Rotation: 20 degrees c 0.10 at 20.2 °C



(S)-2-Allyl-1-(*p*-tolyl)-3,4,5,6-tetrahydro-2*H*-1,2,7-thiadiazepine 1-oxide (**49**)

Yield: 25 mg (92%)

Physical Description: Yellow Oil

Column Conditions: SiO₂, (10% to 30% EtOAc/Hexanes)

¹H NMR: (400 MHz, CDCl₃) δ 7.84 (d, *J* = 8.3 Hz, 2H), 7.26 (d, *J* = 8.1 Hz, 2H), 5.68 (dddd, *J* = 16.3, 10.7, 7.0, 5.6 Hz, 1H), 5.07 (s, 1H), 5.04 (dq, *J* = 8.2, 1.4 Hz, 1H), 3.97 (ddt, *J* = 15.1, 5.6, 1.6 Hz, 1H), 3.63 – 3.48 (m, 2H), 3.38 – 3.28 (m, 1H), 3.21 (dd, *J* = 14.9, 11.4 Hz, 1H), 2.90 (dq, *J* = 15.1, 2.2 Hz, 1H), 2.41 (s, 3H), 1.86 – 1.71 (m, 2H), 1.70 – 1.47 (m, 2H).

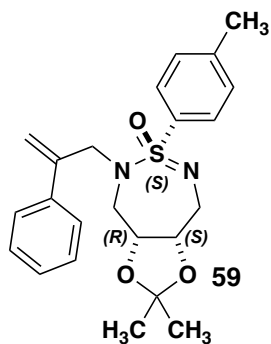
¹³C NMR: (101 MHz, CDCl₃) δ 142.4, 136.8, 134.3, 129.4, 127.6, 117.9, 53.8, 47.7, 42.6, 30.0, 29.5, 21.4.

IR (neat): 2928, 2855, 1287, 1252, 1141.

AMM: (ESI) *m/z* calcd for C₁₄H₂₁N₂OS⁺ [M+H]⁺ 265.1369, found 265.1370.

ER: 89:11

Optical Rotation: 106 degrees c 0.12 at 21.4 °C.



(3a*R*,6*S*,8a*S*)-2,2-Dimethyl-5-(2-phenylallyl)-6-(*p*-tolyl)-3a,5,8,8a-tetrahydro-4*H*-[1,3]dioxolo[4,5-*d*][1,2,7]thiadiazepine 6-oxide (**59**)

Yield: 28 mg (97%)

Physical Description: Colorless Crystal

Melting Point: 179-181 °C

Column Conditions: SiO₂, (1% to 30% EtOAc/Hexanes)

¹H NMR: (400 MHz, CDCl₃) δ 7.92 (d, *J* = 8.2 Hz, 2H), 7.67 – 7.63 (m, 2H), 7.43 – 7.37 (m, 2H), 7.37 – 7.31 (m, 3H), 5.55 (s, 1H), 5.15 (s, 1H), 4.93 (d, *J* = 13.8 Hz, 1H), 3.82 (dt, *J* = 4.9, 2.3 Hz, 1H), 3.56 (t, *J* = 2.1 Hz, 2H), 3.46 – 3.34 (m, 2H), 3.24 (dd, *J* = 14.3, 11.3 Hz, 1H), 2.67 (dd, *J* = 14.3, 4.9 Hz, 1H), 2.46 (s, 3H), 1.49 (s, 3H), 1.29 (s, 3H).

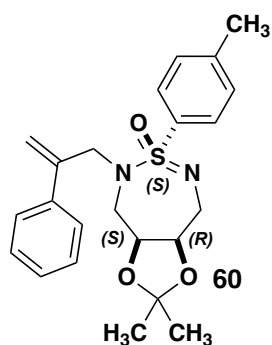
¹³C NMR: (101 MHz, CDCl₃) δ 143.3, 143.2, 137.3, 134.0, 129.6, 128.5, 128.2, 126.7, 116.8, 108.1, 75.5, 74.9, 54.5, 46.3, 39.3, 28.8, 25.9, 21.5.

IR (neat): 2986, 2931, 2860, 1449, 1295.

AMM: (ESI) *m/z* calcd for C₂₃H₂₉N₂O₃S⁺ [M+H]⁺ 413.1893, found 413.1897.

ER: 99:1

Optical Rotation: 91 degrees *c* 0.16 at 20.9 °C.



(3*a*S,6*S*,8*a*R)-2,2-Dimethyl-5-(2-phenylallyl)-6-(*p*-tolyl)-3*a*,5,8,8*a*-tetrahydro-4*H*-[1,3]dioxolo[4,5-*d*][1,2,7]thiadiazepine 6-oxide (**22**)

Yield: 12 mg (97%)

Physical Description: Clear Oil

Column Conditions: SiO₂, (10% to 30% EtOAc/Hexanes)

¹H NMR: (400 MHz, CDCl₃) δ 7.79 (d, *J* = 8.3 Hz, 2H), 7.51 – 7.46 (m, 2H), 7.34 – 7.23 (m, 5H), 5.41 (s, 1H), 4.95 (q, *J* = 1.3 Hz, 1H), 4.66 (d, *J* = 15.3 Hz, 1H), 4.17 (dt, *J* = 10.8,

5.1 Hz, 1H), 4.10 – 3.98 (m, 2H), 3.58 (t, $J = 12.1$ Hz, 1H), 3.34 (d, $J = 2.4$ Hz, 2H), 3.10 (d, $J = 12.2$ Hz, 1H), 2.42 (s, 3H), 1.26 (s, 3H), 1.17 (s, 3H).

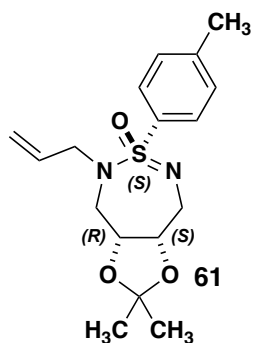
^{13}C NMR: (101 MHz, CDCl_3) δ 143.3, 143.2, 138.6, 133.6, 129.5, 128.4, 128.3, 127.8, 126.5, 115.8, 108.2, 76.3, 75.0, 55.0, 44.7, 28.1, 26.1, 21.5.

IR (neat): 2928, 2873, 1282, 1214, 1146.

AMM: (ESI) m/z calcd for $\text{C}_{23}\text{H}_{29}\text{N}_2\text{O}_3\text{S}^+$ $[\text{M}+\text{H}]^+$ 413.1893, found 413.1896.

ER: 99:1

Optical Rotation: 33 degrees c 0.86 at 18.3 °C.



(3a*S*,6*S*,8a*R*)-5-Allyl-2,2-dimethyl-6-(*p*-tolyl)-3a,5,8,8a-tetrahydro-4*H*-[1,3]dioxolo[4,5-*d*][1,2,7]thiadiazepine 6-oxide (**61**)

Yield: 24 mg (72%)

Physical Description: Clear Oil

Column Conditions: SiO_2 , (10% to 30% EtOAc/Hexanes)

^1H NMR: (400 MHz, CDCl_3) δ 7.87 (d, $J = 8.1$ Hz, 2H), 7.29 (d, $J = 8.1$ Hz, 2H), 5.67 (dddd, $J = 16.7, 10.3, 7.9, 5.4$ Hz, 1H), 5.14 (q, $J = 1.4$ Hz, 1H), 5.10 (dq, $J = 9.6, 1.3$ Hz, 1H), 4.19 (dt, $J = 4.8, 2.3$ Hz, 1H), 4.16 – 4.00 (m, 2H), 3.91 (dd, $J = 15.2, 1.9$ Hz, 1H), 3.72 (dd, $J = 15.2, 2.7$ Hz, 1H), 3.38 (dt, $J = 14.4, 9.9$ Hz, 2H), 2.65 (dd, $J = 14.5, 4.7$ Hz, 1H), 2.42 (s, 3H), 1.52 (s, 3H), 1.38 (s, 3H).

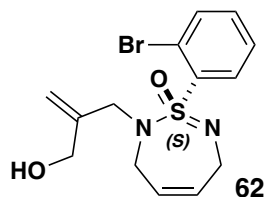
¹³C NMR: (101 MHz, CDCl₃) δ 143.2, 135.1, 133.4, 129.6, 127.9, 119.3, 108.2, 75.7, 75.4, 53.6, 47.0, 39.4, 28.8, 25.9, 21.5.

IR (neat): 2986, 2928, 2860, 1295, 1242.

AMM: (ESI) *m/z* calcd for C₁₇H₂₅N₂O₃S⁺ [M+H]⁺ 337.1580, found 337.1591.

ER: 88:12

Optical Rotation: 18 degrees c 0.06 at 19.5°C.



(*S*)-1-(2-Bromophenyl)-2-(2-(hydroxymethyl)allyl)-3,6-dihydro-2*H*-1,2,7-thiadiazepine 1-oxide (**62**)

Yield: 225 mg (92%)

Physical Description: Amorphous Solid

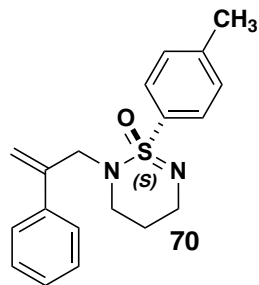
Column Conditions: SiO₂, (10% to 80% EtOAc/Hexanes)

¹H NMR: (400 MHz, CDCl₃) δ 7.95 (dd, *J* = 7.9, 1.8 Hz, 1H), 7.80 (dd, *J* = 7.8, 1.4 Hz, 1H), 7.47 – 7.34 (m, 2H), 5.72 – 5.66 (m, 2H), 5.24 – 5.00 (m, 2H), 4.55 – 4.35 (m, 4H), 4.10 – 3.90 (m, 3H), 3.58 (d, *J* = 14.8 Hz, 1H), 3.35 (ddd, *J* = 17.7, 4.4, 1.7 Hz, 1H), 2.87 (s, 1H).

¹³C NMR: (101 MHz, CDCl₃) δ 145.2, 139.1, 136.5, 132.9, 131.2, 129.0, 127.4, 125.5, 120.4, 115.2, 63.4, 54.1, 46.5, 43.9.

IR (neat):

ER: 89:11



(S)-2-(2-Phenylallyl)-1-(*p*-tolyl)-2,3,4,5-tetrahydro-1,2,6-thiadiazine 1-oxide (**70**)

Yield: 31 mg (97%)

Physical Description: Clear Oil

Column Conditions: SiO₂, (10% to 30% EtOAc/Hexanes)

¹H NMR: (400 MHz, CDCl₃) δ 7.83 (d, *J* = 8.1 Hz, 2H), 7.30 – 7.20 (m, 7H), 5.45 (d, *J* = 1.2 Hz, 1H), 5.20 (d, *J* = 1.3 Hz, 1H), 4.08 (d, *J* = 14.5 Hz, 1H), 3.66 (d, *J* = 14.5 Hz, 1H), 3.57 (ddd, *J* = 12.7, 9.1, 5.0 Hz, 1H), 3.43 (ddd, *J* = 12.7, 5.8, 4.3 Hz, 1H), 3.18 (ddd, *J* = 12.4, 6.9, 5.5 Hz, 1H), 3.08 (ddd, *J* = 12.3, 7.2, 5.1 Hz, 1H), 2.43 (s, 3H), 1.99 – 1.74 (m, 2H).

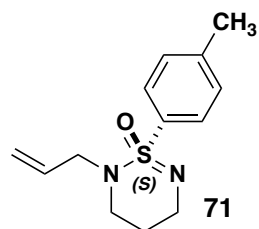
¹³C NMR: (101 MHz, CDCl₃) δ 143.3, 142.5, 138.2, 135.7, 129.4, 129.0, 128.2, 127.9, 126.3, 116.4, 52.9, 45.4, 41.9, 25.5, 21.5.

IR (neat): 2933, 2848, 1345, 1292, 1257.

AMM: (ESI) *m/z* calcd for C₁₉H₂₃N₂OS⁺ [M+H]⁺, found.

ER: 91:9

Optical Rotation: 32 degrees *c* 0.04 at 21.6 °C.



(S)-2-Allyl-1-(*p*-tolyl)-2,3,4,5-tetrahydro-1,2,6-thiadiazine 1-oxide (**71**)

Yield: 23 mg (92%)

Physical Description: Clear Oil

Column Conditions: SiO₂, (10% to 30% EtOAc/Hexanes)

¹H NMR: (400 MHz, CDCl₃) δ 7.87 (d, *J* = 8.0 Hz, 2H), 7.30 (d, *J* = 8.0 Hz, 2H), 5.62 (ddt, *J* = 16.6, 10.1, 6.3 Hz, 1H), 5.20 – 5.11 (m, 2H), 3.75 – 3.59 (m, 2H), 3.52 (dt, *J* = 12.7, 5.2 Hz, 1H), 3.32 (dd, *J* = 14.9, 6.4 Hz, 1H), 3.29 – 3.11 (m, 2H), 2.43 (s, 3H), 2.15 – 1.95 (m, 2H).

¹³C NMR: (101 MHz, CDCl₃) δ 143.2, 136.5, 132.9, 129.4, 128.6, 118.9, 52.0, 46.0, 42.0, 25.7, 21.5.

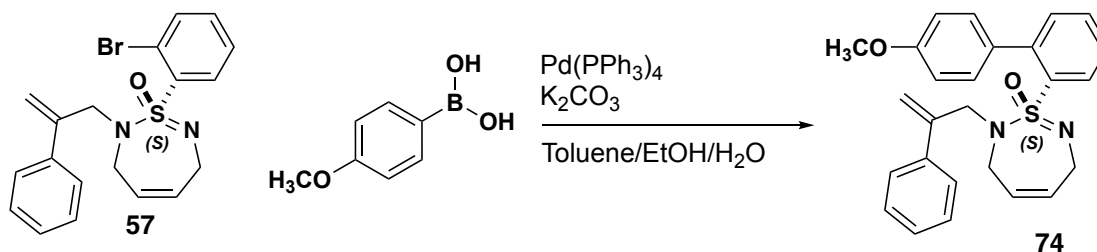
IR (neat): 2921, 2848, 1595, 1267, 1138.

AMM: (ESI) *m/z* calcd for C₁₃H₁₉N₂OS⁺ [M+H]⁺ 251.1213, found 251.1213.

ER: 76:24

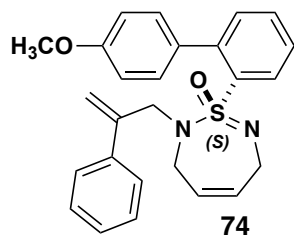
Optical Rotation: 11 degrees *c* 0.5 at 20.5 °C.

8. Functionalization of Enantioenriched SIAs



To a microwave vial was added compound **24** (0.040 g 0.1 mmol) Pd(PPh₃)₄ (0.010 g 0.01 mmol) K₂CO₃ (0.055 g 0.4 mmol) and boronic acid (29 mg 0.15 mmol) then sealed. The vial was evacuated and backfilled with argon then a 0.8 mL of a 5/2/1 mixture of toluene, ethanol, water was added to the vial and then heated to 100 °C for 12 hours. The

reaction was then cooled to room temperature and was adsorbed to silica gel and then purified by flash chromatography 30% EtOAc/Hexanes to isolate the title compound (31 mg 73%).



(S)-1-(4'-Methoxy-[1,1'-biphenyl]-2-yl)-2-(2-phenylallyl)-3,6-dihydro-2H-1,2,7-thiadiazepine 1-oxide (**74**)

Yield: 31 mg (73%)

Physical Description: Clear Oil

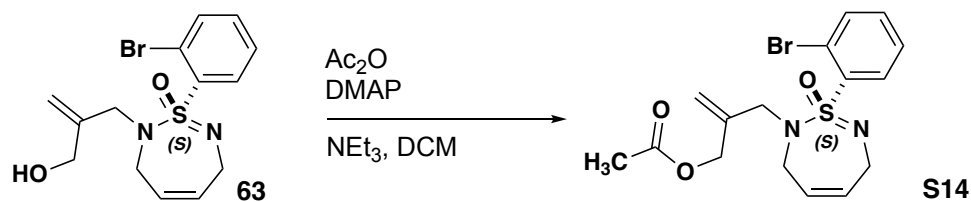
Column Conditions: SiO₂, (10% to 30% EtOAc/Hexanes)

¹H NMR: (400 MHz, CDCl₃) δ 7.94 (dd, J = 8.0, 1.3 Hz, 1H), 7.45 (td, J = 7.5, 1.4 Hz, 1H), 7.34 – 7.28 (m, 5H), 7.25 – 7.22 (m, 4H), 6.94 – 6.86 (m, 2H), 5.49 – 5.40 (m, 2H), 5.37 (d, J = 1.2 Hz, 1H), 5.18 (q, J = 1.3 Hz, 1H), 4.15 (dt, J = 15.3, 1.2 Hz, 1H), 3.96 – 3.78 (m, 5H), 3.74 (d, J = 15.4 Hz, 1H), 3.57 (ddd, J = 18.1, 3.4, 2.2 Hz, 1H), 3.20 – 3.08 (m, 1H).

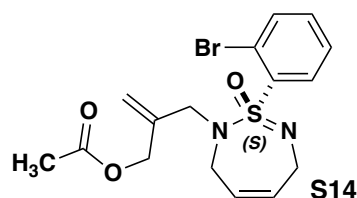
¹³C NMR: (101 MHz, CDCl₃) δ 159.1, 144.8, 141.2, 138.6, 138.6, 133.6, 132.7, 131.7, 131.3, 131.1, 128.2, 128.1, 127.8, 126.9, 126.8, 125.3, 115.8, 112.7, 55.3, 53.9, 45.1, 43.5.

IR (neat): 3057, 3019, 2923, 2835, 1611.

AMM: (ESI) m/z calcd for C₂₆H₂₇N₂O₂S⁺ [M+H]⁺ 431.1788, found 431.17909.



Compound **26** (0.035 g 0.1 mmol) was dissolved in DCM (1mL) and then triethylamine (0.020 g 0.02 mmol) and DMAP (0.001 g 0.01 mmol) was added and then acetic anhydride (0.015 g 0.15 mmol) was added and stirred for 2 hours. The reaction was adsorbed directly to silica gel and then columned 50% EtOAc/Hexanes to yield the title compound (37mg 95%).



(S)-2-((1-(2-Bromophenyl)-1-oxido-3,6-dihydro-2H-1λ⁶,2,7-thiadiazepin-2-yl)methyl)allyl acetate (**S14**)

Yield: 37 mg (95%)

Physical Description: Sticky Oil

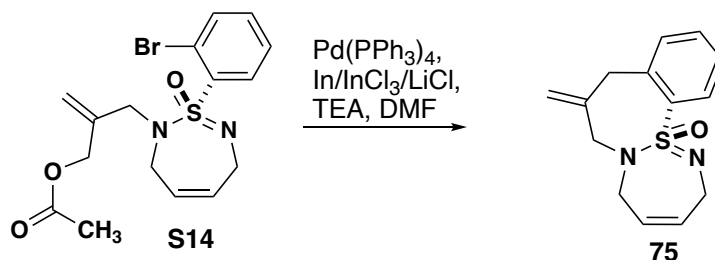
Column Conditions: SiO₂, (10% to 50% EtOAc/Hexanes)

¹H NMR: (400 MHz, CDCl₃) δ 8.06 (dd, *J* = 7.9, 1.8 Hz, 1H), 7.75 (dd, *J* = 7.8, 1.4 Hz, 1H), 7.36 (dtd, *J* = 26.2, 7.5, 1.6 Hz, 2H), 5.77 – 5.60 (m, 2H), 5.24 – 5.18 (m, 2H), 4.67 (d, *J* = 13.5 Hz, 1H), 4.53 (d, *J* = 13.5 Hz, 1H), 4.39 (s, 1H), 4.37 – 4.26 (m, 2H), 3.95 – 3.85 (m, 1H), 3.79 (d, *J* = 14.8 Hz, 1H), 3.34 – 3.23 (m, 1H), 2.06 (s, 3H).

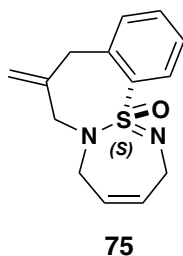
¹³C NMR: (101 MHz, CDCl₃) δ 170.6, 140.3, 139.0, 136.4, 132.7, 131.8, 129.9, 127.2, 125.3, 120.3, 116.9, 64.4, 53.6, 45.7, 43.7, 20.9..

IR (neat): 2837, 2017, 1739, 1272, 1234

AMM: (ESI) *m/z* calcd for C₁₆H₂₀ BrN₂O₃S⁺ [M+H]⁺ 399.0373, found 399.0375.



N,N-Dimethylbutylamine (20 mg, 0.2 mmol) and allyl acetate (40 mg, 0.1 mmol) were added under nitrogen to a suspension of indium (3 mg, 0.05 mmol), indium (III) chloride (11 mg, 0.05 mmol), lithium chloride (12 mg, 0.3 mmol), and [Pd (PPh₃)₄] (11 mg, 0.01 mmol) in DMF (1 mL) was added and stirred at 100 for 9 h and then quenched with Na₂S₂O₃ (saturated aqueous). The aqueous layer was extracted with ether and the combined organics were washed with water and brine, dried with MgSO₄, filtered, and concentrated under reduced pressure. The residue was purified by silica gel column chromatography.



(S)-8-Methylene-2,7,8,9-tetrahydro-5H

benzo[6,7][1,2]thiazepino[1,2a][1,2,7]thiadiazepine 14-oxide (**75**)

Yield: 14 mg (54%)

Physical Description: Amorphous Solid

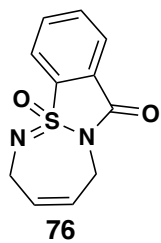
Column Conditions: SiO₂, (100% DCM to 10% to 30% EtOAc/Hexanes)

¹H NMR: (400 MHz, CDCl₃) δ 8.30 (d, *J* = 7.7 Hz, 1H), 7.44 – 7.36 (m, 1H), 7.30 (d, *J* = 7.6 Hz, 2H), 5.77 (ddt, *J* = 10.8, 5.3, 2.3 Hz, 1H), 5.59 (ddd, *J* = 10.7, 6.8, 2.9 Hz, 1H), 5.03 (s, 1H), 4.89 (s, 1H), 4.62 (d, *J* = 14.6 Hz, 1H), 4.44 (ddd, *J* = 17.5, 4.9, 2.5 Hz, 1H), 4.31 (d, *J* = 13.7 Hz, 1H), 3.77 (ddd, *J* = 17.5, 6.0, 2.1 Hz, 1H), 3.56 – 3.42 (m, 3H), 3.09 (ddd, *J* = 17.8, 7.0, 2.3 Hz, 1H).

¹³C NMR: (101 MHz, CDCl₃) δ 139.2, 138.5, 136.7, 132.1, 131.3, 130.8, 130.4, 126.2, 125.6, 116.3, 60.0, 47.6, 43.5, 41.9.

IR (neat): 2931, 1597, 1491, 1269, 1148.

AMM: (ESI) *m/z* calcd for C₁₄H₁₇N₂OS⁺ [M+H]⁺ 261.1056, found 261.1055.



2,5-Dihydro-7H-12λ⁴-benzo[4,5]isothiazolo[1,2-a][1,2,7]thiadiazepin-7-one 12-oxide

Yield: 16 mg (71%)

Physical Description: Yellow Film

Column Conditions: SiO₂, (100% DCM to 10% to 30% EtOAc/Hexanes)

¹H NMR: (400 MHz, CDCl₃) δ 8.06 (dt, *J* = 7.4, 1.0 Hz, 1H), 7.96 – 7.86 (m, 2H), 7.83 (td, *J* = 7.2, 1.7 Hz, 1H), 5.77 – 5.62 (m, 2H), 4.58 (ddd, *J* = 17.7, 5.4, 1.6 Hz, 1H), 4.36 (ddd, *J* = 18.2, 4.0, 2.2 Hz, 1H), 3.74 (ddd, *J* = 17.9, 5.4, 1.8 Hz, 1H), 3.48 – 3.37 (m, 1H).

^{13}C NMR: (101 MHz, CDCl_3) δ 159.4, 137.7, 135.1, 134.1, 130.4, 128.7, 124.9, 124.5, 121.9, 43.3, 37.5.

2.4.8 High Throughput screening

Working inside a glove box a 20 mL scintillation vial was charged with Pd_2dba_3 (8.78 mg 0.0096 mmol) and ligand (0.024 mmol) and 5.4 mL of DCE was added to the vial. Once the solids were completely dissolve the solution 0.3 mL of the stock solution was dispensed into its designated well. The plate was then left in the glove box to evaporate overnight. Then in a 7 ml scintillation vial SIA **37** (17.784 mg 0.080 mmol) and either **E1** or **E2** (28.115 mg 0.120 mmol) was added, then 4.8 mL of the appropriate solvent was added to make a stock solution. Then inside the glove box 0.6 mL of the stock solution was dispensed into the appropriate well. The 96 well was then sealed with a plastic covering and vibrated for 24 hours. Then the wells were diluted with 0.3 mL 90/10 acetonitrile water and then analyzed via chiral UHPLC.

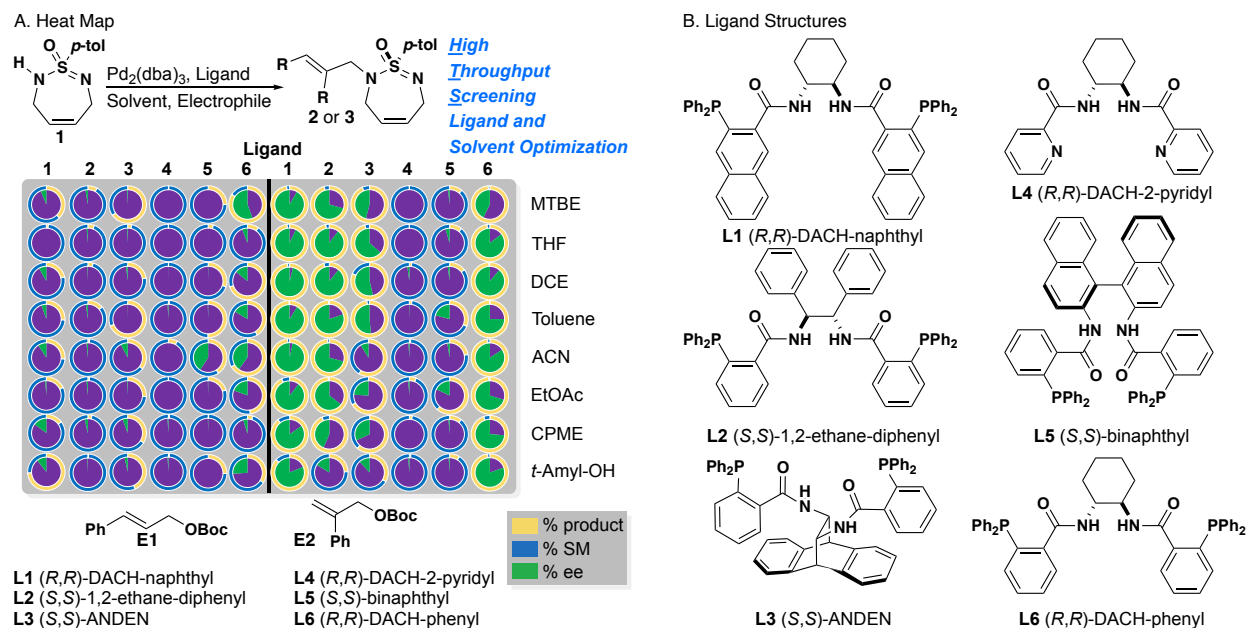


Table Chiral HPLC results of SIA **37** with **E1** to yield **38**

SM Area	Ent1 Area	Ent2 Area	SM% area	Ent1 % Area	Ent2 % Area	%ee	%convert	Ligand	Solvent
1816.15	460.62	641.90	62.23	15.78	21.99	6.21	37.77	L1	MTBE
1722.74	51.84	102.50	91.78	2.76	5.46	2.70	8.22	L2	MTBE
2242.96	611.11	581.57	65.29	17.79	16.93	0.86	34.71	L3	MTBE
6833.94	14.48	15.39	99.56	0.21	0.22	0.01	0.44	L4	MTBE
2805.49	469.25	468.01	74.96	12.54	12.50	0.03	25.04	L5	MTBE
841.69	3710.56	758.92	15.85	69.86	14.29	55.57	84.15	L6	MTBE
3630.67	32.84	34.44	98.18	0.89	0.93	0.04	1.82	L1	THF
2833.36	64.10	105.71	94.35	2.13	3.52	1.39	5.65	L2	THF
5796.64	133.12	81.19	96.43	2.21	1.35	0.86	3.57	L3	THF
6997.64	0.00	0.00	100.00	0.00	0.00	0.00	0.00	L4	THF
6203.97	149.43	146.47	95.45	2.30	2.25	0.05	4.55	L5	THF
3924.97	344.76	85.55	90.12	7.92	1.96	5.95	9.88	L6	THF
4303.38	367.88	817.53	78.40	6.70	14.89	8.19	21.60	L1	DCE
3735.00	101.70	80.28	95.35	2.60	2.05	0.55	4.65	L2	DCE
3384.15	454.04	529.97	77.47	10.39	12.13	1.74	22.53	L3	DCE
6604.46	0.00	8.85	99.87	0.00	0.13	0.13	0.13	L4	DCE
3500.68	758.87	743.53	69.97	15.17	14.86	0.31	30.03	L5	DCE
487.54	684.75	454.56	29.97	42.09	27.94	14.15	70.03	L6	DCE
3636.57	503.62	769.59	74.07	10.26	15.67	5.42	25.93	L1	Toluene
3677.80	249.16	341.28	86.17	5.84	8.00	2.16	13.83	L2	Toluene
2594.53	2913.48	2896.29	30.87	34.67	34.46	0.20	69.13	L3	Toluene
3684.19	0.00	33.63	99.10	0.00	0.90	0.90	0.90	L4	Toluene
2901.80	1454.08	1481.31	49.71	24.91	25.38	0.47	50.29	L5	Toluene
2520.64	1242.65	531.93	58.68	28.93	12.38	16.55	41.32	L6	Toluene
4223.28	488.10	1019.94	73.69	8.52	17.80	9.28	26.31	L1	ACN
5436.50	0.00	86.65	98.43	0.00	1.57	1.57	1.57	L2	ACN
4214.86	1405.11	899.56	64.65	21.55	13.80	7.75	35.35	L3	ACN

6616.01	284.96	286.68	92.05	3.96	3.99	0.02	7.95	L4	ACN
117.28	0.00	80.93	59.17	0.00	40.83	40.83	40.83	L5	ACN
3583.94	5752.87	1442.63	33.25	53.37	13.38	39.99	66.75	L6	ACN
4361.65	446.32	514.51	81.95	8.39	9.67	1.28	18.05	L1	EOAc
5165.93	0.00	78.35	98.51	0.00	1.49	1.49	1.49	L2	EOAc
3648.97	627.11	659.20	73.94	12.71	13.36	0.65	26.06	L3	EOAc
6035.38	0.00	0.00	100.00	0.00	0.00	0.00	0.00	L4	EOAc
4057.05	529.48	509.19	79.62	10.39	9.99	0.40	20.38	L5	EOAc
2066.08	1323.74	558.18	52.33	33.53	14.14	19.39	47.67	L6	EOAc
3772.74	0.00	658.39	85.14	0.00	14.86	14.86	14.86	L1	CPME
6151.31	0.00	226.57	96.45	0.00	3.55	3.55	3.55	L2	CPME
4371.74	931.79	1302.79	66.18	14.10	19.72	5.62	33.82	L3	CPME
5968.90	0.00	59.13	99.02	0.00	0.98	0.98	0.98	L4	CPME
7238.23	0.00	27.80	99.62	0.00	0.38	0.38	0.38	L5	CPME
3810.48	0.00	188.65	95.28	0.00	4.72	4.72	4.72	L6	CPME
1686.07	2065.87	2760.99	25.89	31.72	42.39	10.67	74.11	L1	T-Amyl-OH
6918.69	0.00	37.50	99.46	0.00	0.54	0.54	0.54	L2	T-Amyl-OH
4046.25	1433.79	1684.25	56.48	20.01	23.51	3.50	43.52	L3	T-Amyl-OH
6719.79	0.00	63.60	99.06	0.00	0.94	0.94	0.94	L4	T-Amyl-OH
5735.76	969.87	969.56	74.73	12.64	12.63	0.00	25.27	L5	T-Amyl-OH
1839.28	832.45	108.21	66.16	29.94	3.89	26.05	33.84	L6	T-Amyl-OH

Table Chiral HPLC results of SIA37 with E2 to yield 39

SM Area	Ent1 Area	Ent2 Area	SM% area	Ent1 % Area	Ent2 % Area	%ee	%convert	Ligand	Solvent
148.14	158.69	5256.61	2.66	2.85	94.48	91.63	97.34	L1	MTBE
202.18	3720.63	558.62	4.51	83.02	12.47	70.56	95.49	L2	MTBE
256.80	969.95	2845.43	6.31	23.82	69.87	46.06	93.69	L3	MTBE

3869.33	0.00	0.00	100.00	0.00	0.00	0.00	0.00	L4	MTBE
2039.67	111.21	150.15	88.64	4.83	6.53	1.69	11.36	L5	MTBE
65.53	1284.34	3252.68	1.42	27.90	70.67	42.77	98.58	L6	MTBE
109.18	118.62	4684.94	2.22	2.41	95.36	92.95	97.78	L1	THF
164.22	5082.78	200.04	3.01	93.31	3.67	89.64	96.99	L2	THF
198.20	794.04	3915.20	4.04	16.18	79.78	63.60	95.96	L3	THF
5640.26	0.00	0.00	100.00	0.00	0.00	0.00	0.00	L4	THF
3055.14	109.43	266.05	89.05	3.19	7.76	4.57	10.95	L5	THF
93.82	232.27	3523.66	2.44	6.03	91.53	85.50	97.56	L6	THF
98.72	53.93	5395.93	1.78	0.97	97.25	96.28	98.22	L1	DCE
137.98	2684.38	88.77	4.74	92.21	3.05	89.16	95.26	L2	DCE
540.37	408.70	1991.07	18.38	13.90	67.72	53.82	81.62	L3	DCE
4094.00	0.00	90.99	97.83	0.00	2.17	2.17	2.17	L4	DCE
3365.58	246.39	325.88	85.47	6.26	8.28	2.02	14.53	L5	DCE
170.71	1257.80	22511.79	0.71	5.25	94.03	88.78	99.29	L6	DCE
54.54	740.31	16815.81	0.31	4.20	95.49	91.28	99.69	L1	Toluene
71.59	7060.42	743.13	0.91	89.65	9.44	80.22	99.09	L2	Toluene
252.29	2603.27	8409.75	2.24	23.11	74.65	51.54	97.76	L3	Toluene
3638.18	36.42	51.23	97.65	0.98	1.37	0.40	2.35	L4	Toluene
3812.81	293.33	1451.76	68.60	5.28	26.12	20.84	31.40	L5	Toluene
16.35	1495.39	10517.68	0.14	12.43	87.43	75.00	99.86	L6	Toluene
95.12	37.42	4773.87	1.94	0.76	97.30	96.54	98.06	L1	Acetonitrile
68.78	3556.09	576.65	1.64	84.64	13.72	70.91	98.36	L2	Acetonitrile
2574.05	1540.17	2089.51	41.49	24.83	33.68	8.86	58.51	L3	Acetonitrile
5954.29	0.00	67.18	98.88	0.00	1.12	1.12	1.12	L4	Acetonitrile
2814.08	358.33	452.59	77.63	9.88	12.49	2.60	22.37	L5	Acetonitrile
87.97	302.58	4027.09	1.99	6.85	91.16	84.31	98.01	L6	Acetonitrile
221.85	54.09	2897.82	6.99	1.70	91.31	89.60	93.01	L1	EOAc

66.67	5477.38	1154.04	1.00	81.78	17.23	64.55	99.00	L2	EOAc
1380.24	892.45	1894.79	33.12	21.41	45.47	24.05	66.88	L3	EOAc
5802.63	140.88	222.49	94.11	2.28	3.61	1.32	5.89	L4	EOAc
91.28	52.02	94.49	38.39	21.88	39.74	17.86	61.61	L5	EOAc
57.46	782.50	4624.26	1.05	14.32	84.63	70.31	98.95	L6	EOAc
317.03	66.27	2579.32	10.70	2.24	87.06	84.83	89.30	L1	CPME
193.09	2067.03	755.63	6.40	68.54	25.06	43.49	93.60	L2	CPME
1476.51	566.84	1790.18	38.52	14.79	46.70	31.91	61.48	L3	CPME
7353.54	97.39	93.26	97.47	1.29	1.24	0.05	2.53	L4	CPME
4534.59	242.35	306.88	89.20	4.77	6.04	1.27	10.80	L5	CPME
126.45	247.79	1992.08	5.34	10.47	84.18	73.71	94.66	L6	CPME
215.58	49.01	1416.50	12.82	2.92	84.26	81.35	87.18	L1	T-Amyl-OH
3094.08	829.60	163.38	75.70	20.30	4.00	16.30	24.30	L2	T-Amyl-OH
2826.66	449.63	953.78	66.82	10.63	22.55	11.92	33.18	L3	T-Amyl-OH
8343.49	0.00	110.62	98.69	0.00	1.31	1.31	1.31	L4	T-Amyl-OH
4731.75	200.09	255.76	91.21	3.86	4.93	1.07	8.79	L5	T-Amyl-OH
146.61	657.84	6654.06	1.97	8.82	89.21	80.39	98.03	L6	T-Amyl-OH

2.5 References

- (67) Chinthakindi, P. K.; Naicker, T.; Thota, N.; Govender, T.; Kruger, H. G.; Arvidsson, P. I. Sulfonimidamides in Medicinal and Agricultural Chemistry. *Angew. Chemie Int. Ed.* **2017**, *56* (15), 4100–4109.
- (68) Nandi, G. C.; Arvidsson, P. I. Sulfonimidamides: Synthesis and Applications in Preparative Organic Chemistry. *Adv. Synth. Catal.* **2018**, *360* (16), 2976–3001.
- (69) Okazaki, Y.; Ishizuka, A.; Ishihara, A.; Nishioka, T.; Iwamura, H. New Dimeric Compounds of Avenanthramide Phytoalexin in Oats. *J. Org. Chem.* **2007**, *72* (10),

3830–3839.

- (70) Davies, T. Q.; Willis, M. C. Rediscovering Sulfinylamines as Reagents for Organic Synthesis. *Chem. - A Eur. J.* **2021**, *27* (35), 8918–8927.
- (71) Chinthakindi, P. K.; Benediktsdottir, A.; Ibrahim, A.; Wared, A.; Aurell, C.-J.; Pettersen, A.; Zamaratski, E.; Arvidsson, P. I.; Chen, Y.; Sandstroem, A. Synthesis of Sulfonimidamide-Based Amino Acid Building Blocks with Orthogonal Protecting Groups. *European J. Org. Chem.* **2019**, *2019* (5), 1045–1057.
- (72) Nandi, G. C.; Jesin, I. Direct Synthesis of N-Acyl Sulfonimidamides and N-Sulfonimidoyl Amidines from Sulfonimidoyl Azides. *Adv. Synth. Catal.* **2018**, *360* (13), 2465–2469.
- (73) Pemberton, N.; Graden, H.; Evertsson, E.; Bratt, E.; Lepistö, M.; Johannesson, P.; Svensson, P. H. Synthesis and Functionalization of Cyclic Sulfonimidamides: A Novel Chiral Heterocyclic Carboxylic Acid Bioisostere. *ACS Med. Chem. Lett.* **2012**, *3* (7), 574–578.
- (74) Ballatore, C.; Huryn, D. M.; Smith, A. B. Carboxylic Acid (Bio)Isosteres in Drug Design. *ChemMedChem* **2013**, *8* (3), 385–395.
- (75) Schöbel, J. H.; Passia, M. T.; Wolter, N. A.; Puttreddy, R.; Rissanen, K.; Bolm, C. 1,2,6-Thiadiazine 1-Oxides: Unsaturated Three-Dimensional S,N-Heterocycles from Sulfonimidamides. *Org. Lett.* **2020**, *22* (7), 2702–2706.
- (76) Schöbel, J.-H.; Liang, W.; Wöll, D.; Bolm, C. Mechanochemical Synthesis of 1,2,6-Thiadiazine 1-Oxides from Sulfonimidamides and the Fluorescence Properties of the Products. *J. Org. Chem.* **2020**, *85* (23), 15760–15766.

- (77) Fruit, C.; Robert-Peillard, F.; Bernardinelli, G.; Müller, P.; Dodd, R. H.; Dauban, P. Diastereoselective Rhodium-Catalyzed Nitrene Transfer Starting from Chiral Sulfonimidamide-Derived Iminoiodanes. *Tetrahedron Asymmetry* **2005**, *16* (21), 3484–3487.
- (78) Jones, M. R.; Cram, D. J. Stereochemistry of Sulfur Compounds. VII. Course of Substitution at Sulfur Attached to Four Different Ligands. *J. Am. Chem. Soc.* **1974**, *96* (7), 2183–2190.
- (79) Feng, J.; Liu, H.; Yao, Y.; Lu, C. D. Synthesis of Enantioenriched Primary Tert-Butanesulfonimidamides via Imination-Hydrazinolysis of N'-Tert-Butanesulfinyl Amidines. *J. Org. Chem.* **2022**, *87* (7), 5005–5016.
- (80) Johnson, C. R.; Jonsson, E. U.; Bacon, C. C. Preparation and Reactions of Sulfonimidoyl Chlorides. *J. Org. Chem.* **1979**, *44* (13), 2055.
- (81) Regan, S. L.; Maggs, J. L.; Hammond, T. G.; Lambert, C.; Williams, D. P.; Park, B. K. Acyl Glucuronides: The Good, the Bad and the Ugly. *Biopharm. Drug Dispos.* **2010**, *31* (7), 367–395.
- (82) Borhade, S. R.; Svensson, R.; Brandt, P.; Artursson, P.; Arvidsson, P. I.; Sandström, A. Preclinical Characterization of Acyl Sulfonimidamides: Potential Carboxylic Acid Bioisosteres with Tunable Properties. *ChemMedChem* **2015**, *10* (3), 455–460.
- (83) Wolfgang, Guba. Wolfgang, Haap. Andreas, Kuglstatter. Jens-Uwe, Peters. Ulrike, Obst Sander. Christian, Schnider. Roger, WERMUTH. Thomas, W. Preparation of 5-Aryl-1-Imino-1-Oxo-[1,2,4]Thiadiazines as Anti-Alzheimer Agents, WO2015091595A1, 2015.

- (84) Katz, J.; Roush, W.; Seidel, H. M.; Shen, D.-M.; Venkatraman, S. Preparation of Benzothiazolylideneureas and Related Compounds and Compositions for Treating Conditions Associated with NLRP Activity, May 22, 2020.
- (85) Paulini, Ralph. Wolfgang, Von Deyn. Bastiaans, Henricus Maria Martinus. Beyer, C. Sulfonimidamide Compounds for Combating Animal Pests. *WO201106995A1* **2010**.
- (86) Yang, G.; Yuan, Y.; Tian, Y.; Zhang, S.; Cui, X.; Xia, B.; Li, G.; Tang, Z. Synthesis of Chiral Sulfonimidoyl Chloride via Desymmetrizing Enantioselective Hydrolysis. *J. Am. Chem. Soc.* **2023**, *145* (9), 5439–5446.
- (87) Tilby, M. J.; Dewez, D. F.; Hall, A.; Martínez Lamencá, C.; Willis, M. C. Exploiting Configurational Lability in Aza-Sulfur Compounds for the Organocatalytic Enantioselective Synthesis of Sulfonimidamides. *Angew. Chemie - Int. Ed.* **2021**, *60* (49), 25680–25687.
- (88) Trost, B. M.; Strege, P. E. Asymmetric Induction in Catalytic Allylic Alkylation. *J. Am. Chem. Soc.* **1977**, *99* (5), 1649–1651.
- (89) Trost, B. M.; Van Vranken, D. L. Asymmetric Transition Metal-Catalyzed Allylic Alkylations. *Chem. Rev.* **1996**, *96* (1), 395–422.
- (90) Trost, B. M.; Toste, F. D. Regio- and Enantioselective Allylic Alkylation of an Unsymmetrical Substrate: A Working Model. *J. Am. Chem. Soc.* **1999**, *121* (19), 4545–4554.
- (91) Trost, B. M.; Vranken, D. L. Van; Bingel, C. A Modular Approach for Ligand Design for Asymmetric Allylic Alkylations via Enantioselective Palladium-Catalyzed

- Ionizations. **1992**, *25* (39), 9327–9343.
- (92) Glatz, F.; Petrone, D. A.; Carreira, E. M. Ir-Catalyzed Enantioconvergent Synthesis of Diversely Protected Allenylic Amines Employing Ammonia Surrogates. *Angew. Chemie - Int. Ed.* **2020**, *59* (38), 16404–16408.
- (93) Bauer, J. M.; Frey, W.; Peters, R. Dual Palladium(II)/Tertiary Amine Catalysis for Asymmetric Regioselective Rearrangements of Allylic Carbamates. *Chem. - A Eur. J.* **2016**, *22* (16), 5767–5777.
- (94) Lynch, C. C.; Balaraman, K.; Wolf, C. Catalytic Asymmetric Allylic Amination with Isatins, Sulfonamides, Imides, Amines, and N-Heterocycles. *Org. Lett.* **2020**, *22* (8), 3180–3184.
- (95) Biosca, M.; Salto, J.; Magre, M.; Norrby, P. O.; Pamies, O.; Dieguez, M. An Improved Class of Phosphite-Oxazoline Ligands for Pd-Catalyzed Allylic Substitution Reactions. *ACS Catal.* **2019**, *9* (7), 6033–6048.
- (96) Xu, W. Bin; Ghorai, S.; Huang, W.; Li, C. Rh(I)/Bisoxazolinephosphine-Catalyzed Regio- And Enantioselective Allylic Substitutions. *ACS Catal.* **2020**, *10* (8), 4491–4496.
- (97) Liu, L. X.; Huang, W. J.; Xie, Q. X.; Wu, B.; Yu, C. Bin; Zhou, Y. G. Dynamic Kinetic Resolution of Flavonoids via Asymmetric Allylic Alkylation: Construction of Two Contiguous Stereogenic Centers on Nucleophiles. *ACS Catal.* **2021**, *11* (21), 12859–12863.
- (98) Zhang, Q. X.; Gu, Q.; You, S. L. Palladium(0)-Catalyzed Intermolecular Asymmetric Allylic Dearomatization of Substituted β -Naphthols with Morita-Baylis-Hillman

- (MBH) Adducts. *Org. Lett.* **2022**, *24* (43), 8031–8035.
- (99) Bhat, V.; Welin, E. R.; Guo, X.; Stoltz, B. M. Advances in Stereoconvergent Catalysis from 2005 to 2015: Transition-Metal-Mediated Stereoablative Reactions, Dynamic Kinetic Resolutions, and Dynamic Kinetic Asymmetric Transformations. *Chem. Rev.* **2017**, *117* (5), 4528–4561.
- (100) Song, T.; Arseniyadis, S.; Cossy, J. Asymmetric Synthesis of α -Quaternary Gamma;-Lactams through Palladium-Catalyzed Asymmetric Allylic Alkylation. *Org. Lett.* **2019**, *21* (3), 603–607.
- (101) Gibson, S. E.; Kaufmann, K. A. C.; Haycock, P. R.; White, A. J. P.; Hardick, D. J.; Tozer, M. J. Pendant Alkenes Promote Cobalt–Cobalt Bond Cleavage in (Alkyne)(Binap)Tetracarbonyldicobalt(0) Complexes. *Organometallics* **2007**, *26* (7), 1578–1580.
- (102) Chen, Y.; Gibson, J. A Convenient Synthetic Route to Sulfonimidamides from Sulfonamides. *RSC Adv.* **2015**, *5* (6), 4171–4174.
- (103) Chen, Y.; Gibson, J. A Convenient Synthetic Route to Sulfonimidamides from Sulfonamides. *RSC Adv.* **2015**, *5* (6), 4171–4174.
- (104) Loison, A.; Hanquet, G.; Toulgoat, F.; Billard, T.; Panossian, A.; Leroux, F. R. Ketenimines as Intermediates To Access Difluoromethoxylated Scaffolds. *Org. Lett.* **2022**, *24* (45), 8316–8321.
- (105) Hayashi, M.; Brown, L. E.; Porco Jr., J. A. Asymmetric Dearomatization/Cyclization Enables Access to Polycyclic Chemotypes. *European J. Org. Chem.* **2016**, *2016* (28), 4800–4804.

- (106) Pham, Q. H.; Tague, A. J.; Richardson, C.; Hyland, C. J. T.; Pyne, S. G. The Pd-Catalysed Asymmetric Allylic Alkylation Reactions of Sulfamidate Imines. *Chem. Sci.* **2021**, *12* (38), 12695–12703.
- (107) Kraus, J. M.; Gits, H. C.; Silverman, R. B. High Yielding Allylation of a Chiral Secondary Alcohol Containing Base Sensitive Functional Groups. *Tetrahedron Lett.* **2012**, *53* (11), 1319–1322.
- (108) Harada, S.; Masuda, R.; Morikawa, T.; Nishida, A. Trichloromethylative Olefin Cycloamination by Photoredox Catalysis. *European J. Org. Chem.* **2021**, *2021* (32), 4531–4535.
- (109) Takemoto, S.; Ishii, T.; Yasuda, S.; Ohmiya, H. Synergistic N-Heterocyclic Carbene/Palladium-Catalyzed Allylation of Aldehydes with Allylic Carbonates. *Bull. Chem. Soc. Jpn.* **2019**, *92* (5), 937–940.
- (110) Faulkner, A.; Scott, J. S.; Bower, J. F. An Umpolung Approach to Alkene Carboamination: Palladium Catalyzed 1,2-Amino-Acylation, -Carboxylation, -Arylation, -Vinylolation, and -Alkynylation. *J. Am. Chem. Soc.* **2015**, *137* (22), 7224–7230.
- (111) Kim, M.; Park, B.; Shin, M.; Kim, S.; Kim, J.; Baik, M.-H.; Cho, S. H. Copper-Catalyzed Enantiotopic-Group-Selective Allylation of Gem-Diborylalkanes. *J. Am. Chem. Soc.* **2021**, *143* (2), 1069–1077.
- (112) Meng, L.; Liu, H.; Lin, Z.; Wang, J. Synthetic and Computational Study of the Enantioselective [3+2]-Cycloaddition of Chromones with MBH Carbonates. *Org. Lett.* **2022**, *24* (32), 5890–5895.

- (113) Trost, B. M.; Mata, G. Enantioselective Palladium-Catalyzed [3+2] Cycloaddition of Trimethylenemethane and Fluorinated Ketones. *Angew. Chemie Int. Ed.* **2018**, *57* (38), 12333–12337.
- (114) Yuan, S.-P.; Bao, Q.; Sun, T.-J.; Zhao, J.-Q.; Wang, Z.-H.; You, Y.; Zhang, Y.-P.; Zhou, M.-Q.; Yuan, W.-C. Catalytic Enantioselective α -Allylation of Deconjugated Butenolides with Aza- π -Allylpalladium 1,4-Dipoles: Access to Optically Pure 2-Piperidones Bearing an All-Carbon Quaternary Stereocenter. *Org. Lett.* **2022**, *24* (45), 8348–8353.